THE NON-STRUCTURAL ROLES OF DENGUE VIRUS STRUCTURAL CAPSID PROTEIN

CHONG MUN KEAT
B. Sci (Hons),
National University of Singapore

A THESIS SUBMITTED

FOR THE DEGREE OF DOCTOR OF PHILOSOPHY

DEPARTMENT OF MICROBIOLOGY

NATIONAL UNIVERSITY OF SINGAPORE

2013

DECLARATION

I hereby declare that the thesis is my original work and it has been written by me in its entirety. I have duly acknowledged all the sources of information which have been used in the thesis.
This thesis has also not been submitted for any degree in any university previously.

_____

Chong Mun Keat
16 May 2013

Publications and Presentations Generated

Publications:

Chong, M.K., Parthasarathy, K., Yeo, H.Y., and Ng, M.L. (2013) Optimized Sequential Purification Protocol for in vivo Site-Specific Biotinylated Full-Length Dengue Virus Capsid Protein. Protein Eng. Des. Sel. 26(5):377-387.

Bhuvanakantham, R., **Chong, M.K.**, and Ng, M.L. (2009) Specific Interaction of Capsid Protein and Importin-Alpha/Beta Influences West Nile Virus Production. Biochem. Biophys. Res. Commun. 389(1):63-9.

Manuscript In Preparation:

Chong, M.K., Parthasarathy, K., and Ng, M.L. High-Throughput ProtoaArray Screening of Dengue Virus Capsid Protein. (Journal: Molecular and Cellular Proteomics)

Book Chapter

Chong, M.K., Chua, A.J.S., Tan, T.T.T., Tan, S.H., and Ng, M.L. (2013) Microscopy Techniques in Flavivirus Research. Micron (Under Review)

Patent:

Title of Invention: **Biotinylated Protein**

Inventors: Ng, M.L., Parthasarathy, K., **Chong, M.K.**, and Yeo, H.Y.

Singapore patent application number: 201208602-1

Filing date: 22nd November 2012

Conference Presentations (Oral):

Chong, M.K. and Ng, M.L. (30th January 2013) Deciphering the Roles of Multifunctional Dengue Virus Capsid Protein in the Nucleus. *3rd Yong Loo Lin School of Medicine-Annual Graduate Scientific Congress, National University of Singapore, Singapore*. Paper Number: O02

Chong, M.K. and Ng, M.L. (14-15th January 2013) Dengue Virus Capsid Protein – A Structural Protein with Non-Structural Roles. *The Inaugural Microbiology Students' Symposium, National University of Singapore, Singapore*.

Chong, M.K. and Ng, M.L. (5-9th February 2012) Microscopic Study of Dengue Virus Capsid Protein: Nuclear Translocation. *10th Asia-Pacific Microscopy Conference (APMC 10), 22nd Australian Conference on Microscopy and Microanalysis (ACMM22) and the 2012 International Conference on Nanoscience and Nanotechnology (ICONN 2012), Perth, Australia*. Paper Number: 344.00

Bhuvanakantham, R., **Chong, M.K.**, and Ng, M.L. (25-28th February 2009) Flavivirus Capsid Protein and Importin-α Interaction Influences Virus Replication. *8th Asia Pacific Congress of Medical Virology, Hong Kong*.

Conference Presentations (Poster):

Chong, M.K., Krupakar, P., Yeo, H.Y., and Ng, M.L. (22-25th March 2013) Full-length Dengue Virus Capsid Protein – Protein Design, Engineering, Expression and Purification. *BioPharma Asia Convention 2013, Singapore.*

Chong, M.K., and Ng, M.L. (21-23rd November 2012) Multifunctional Dengue Virus Capsid Protein – Role in the Nucleus? *Singapore International Conference on Dengue and Emerging Infections, Singapore*. Poster Number: PP-6-049-03.

Chong, M.K., Krupakar, P., and Ng, M.L. (15-16th November 2011) Identification of Dengue Virus Capsid Protein Interacting Partners. *Singapore-Japan Joint Forum 'Emerging Concepts in Microbiology', Singapore*.

Chong, M.K. and Ng, M.L. (12-13th November 2010) Cell Cycle Arrest upon Dengue Virus Infection Is a Host Antiviral Response. *1st Singapore Health & Biomedical Congress, Singapore*.

Awards and Achievements:

1. **Winner** of the Best Oral Presentation Award at the 3rd Yong Loo Lin School of Medicine-Annual Graduate Scientific Congress (AGSC), National University of Singapore, Singapore (30th January 2013)

2. **Winner** of The Yakult 1st Prize for Oral Presentation at The Inaugural Microbiology Students' Symposium in National University of Singapore, Singapore (14-15th January 2013)

3. Recipient of IFSM **Bursary** for Oral Presentation in 10th Asia-Pacific Microscopy Conference (APMC 10), 22nd Australian Conference on Microscopy and Microanalysis (ACMM22) and the 2012 International Conference on Nanoscience and Nanotechnology (ICONN 2012) in Perth, Australia (5-9th February 2012)

4. Selected participant for **EMBO Course**, "FRET, FCS, FLIM, and FRAP and 3D Imaging: Application to Cell and Development Biology" in Biopolis, Singapore (13-24th April, 2009)

Acknowledgements

I would like to express my sincere gratitude to my supervisor, Professor Mary Ng Mah Lee for the immense amount of guidance and support given throughout the whole course of this study. Professor Ng's advices and insights in this project have been a true blessing. This dissertation would not have been possible without Professor Ng's continuous encouragement, patience and guidance.

I sincerely thank all the members of the Flavilaboratory: Madam Loy Boon Pheng, Dr. Raghavan Bhuvanakantham, Dr. Krupakar Parthasarathy, Mr. Samuel Chiang Cern Cher, Dr. Edwin Liu Wei Yang, Mr. Anthony Chua Jin Shun, Dr. Terence Tan Tze Tong, Dr. Melvin Tan Lik Chern, Dr. Adrian Cheong Yuen Kuen, Ms. Netto Patricia Annabelle, Ms. Guan Chin Huey, Mr. Yeo Kim Long, Mr. Yap Han, Ms. Bi Xiao Ling, Ms. Goh Li Shan, Ms. Pua Shu Min, Ms. Audrey Ngo Mei Li, Mr. Lim Han Fui, Ms. Hayden Yeo Hui Yu, Mr. Steven Ong Kia Kian, Mr. Vincent Pang Junxiong, Ms Fiona Chin and Mr. Wu Haowei for their friendship and kind assistance in one way or another. Technical advices on various techniques and constructive suggestions from them have indeed helped me a lot in this project.

I would also like to thank Mr. Clement Khaw and Ms. Joleen Lim for their kind assistance on various microscopic techniques at the Nikon Imaging Centre (Singapore Bio-imaging Consortium), Biopolis. I am also grateful for the kind technical assistance given by Ms. Saw Marlar and Ms. Wang Xiaoning at the Flowcytometry Laboratory Unit, Clinical Research Centre, NUS.

Last but not least, I would like to extend my gratitude to my family, relatives and best friends who always support and encourage me during the entire course of this study. I would love to dedicate this work to my beloved girl friend, Ms. Amber Guan, for always being there for me, loving me and supporting me.

Thank you.

Table of Contents

	Page Number
Publications and Presentations Generated	i
Acknowledgements	iv
Table of Contents	v
Summary	xiii
List of Tables	xv
List of Figures	xvii
Abbreviations	xxiii
1. LITERATURE REVIEW	
1.1. Dengue Virus	1
1.1.1. Epidemiology of dengue virus infection	3
1.1.2. Mosquito vector of dengue virus	7
1.1.3. Clinical manifestations of dengue virus infection	8
1.2. Dengue Virus Genome and Proteins	9
1.3. Replication Cycle of Dengue Virus	12
1.4. Dengue Virus Capsid Protein	16
1.4.1. Structure of dengue virus capsid protein	19
1.4.2. Structural functions of capsid protein	22
1.5. Non-Structural Roles of Capsid Protein in the Cytoplasm	23
1.6. Nuclear Phase of Capsid (C) Protein	24
1.6.1. Roles of nuclear localization signal	24
1.6.2. Roles of importin-α/β proteins and phosphorylation	26
1.6.3. Possible non-structural roles of capsid (C) protein in the nucleus	27
1.7. Objectives	28

Page Number

2. MATERIALS AND METHODS

2.1. Cell Culture Techniques 29

2.1.1. Cell lines 29

2.1.2. Propagation of cell lines 30

2.1.3. Cultivation of cells in 24-well and 6-well tissue culture plates 30

2.1.4. Cultivation of cells on coverslips in 24-well tissue culture plates 31

2.2. Virus Works 31

2.2.1. Preparation of virus stock 31

2.2.2. Plaque assay 32

2.2.3. Infection of cell monolayer for virus study 32

2.3. Molecular Techniques 33

2.3.1. Construction of green fluorescent protein (GFP)-tagged Dengue virus (DENV)-2 capsid (C) protein and nuclear localization signal (NLS) motif plasmids 33

2.3.2. Site-directed mutagenesis 35

2.3.3. Generation of FLAG-tagged Dengue virus (DENV)-2 capsid (C) protein plasmid 36

2.3.4. Construction of biotinylated Dengue virus (DENV)-2 capsid (C) protein (pET28aDENVBioCap) plasmid 37

2.3.5. Cloning of Dengue virus (DENV)-2 capsid protein tagged with activation domain (DENVC-AD) and importin alpha protein tagged with DNA-binding domain (Impα-DBD) for mammalian-2-hybrid (M2H) assay 38

2.3.6. Transfection 39

2.3.7. Mammalian-2-hybrid (M2H) Assay 40

2.3.8. Real-time polymerase chain reaction (PCR) 40

2.3.9. Mutagenesis of Dengue virus (DENV) infectious clone 41

2.3.10. In vitro synthesis of infectious RNA 42

Page Number

2.4. Microscopic Techniques 42

2.4.1. Direct immuno-fluorescence microscopy of fixed cells 42

2.4.2. Indirect immuno-fluorescence microscopy of fixed cells 43

2.4.3. Live cell imaging 44

2.4.4. Effect of leptomycin B, H-89 dihydrochloride, and bisindolylmaleimide on Dengue virus (DENV) capsid (C) protein localization 45

2.4.5. Co-localization analysis 45

2.5. Protein Techniques 46

2.5.1. Protein expression 45

2.5.1.1. Competent cell strains screening for optimal protein expression 46

2.5.1.2. Protein extraction 47

2.5.2. Protein purification 47

2.5.2.1. His-tag affinity purification 47

2.5.2.2. Ion exchange chromatography 48

2.5.2.3. Size-exclusion chromatography 48

2.5.3. Protein analysis 49

2.5.3.1. Sodium dodecyl sulphate-polyacrylamide gel (SDS-PAGE) 49

2.5.3.2. Western-blotting 50

2.5.3.3. Coomassie blue staining 50

2.5.3.4. Silver staining 51

2.5.3.5. Sample preparation for mass spectrometry 51

2.5.3.6. Enzyme-linked immunosorbent assay (ELISA) 52

2.5.3.7. Enzyme-linked immunosorbent assay (ELISA)-based binding assay 52

2.5.3.8. Functional binding assay for purified Dengue virus (DENV) capsid (C) protein with human Sec3 53

Page Number

protein

2.5.3.9. Co-immunoprecipiation 53

2.6. Protoarray Screening 54

2.7. Cell Cycle Analysis 55

2.7.1. Fluorescence-activated cell sorting (FACS) 55

2.7.2. Effect of cell cycle synchronization on Dengue virus (DENV) replication 56

2.7.3. Cell cycle-polymerase chain reaction (PCR) array 57

2.8. Effect of Signal Recognition Particle (SRP19) and DIM1 Dimethyladenosine Transferase 1 Homolog (DIMT1) Genes Over-Expression on Dengue Virus (DENV) Replication 58

2.9. Effect of Signal Recognition Particle (SRP19) and DIM1 Dimethyladenosine Transferase 1 Homolog (DIMT1) Genes Knock-Down on Dengue Virus (DENV) Replication 58

2.10. Software used in this study 59

2.11. Statistical Analyses 59

RESULTS

3. DELINEATING THE NUCLEAR TRANSPORT MECHANISM OF DENGUE VIRUS (DENV) CAPSID (C) PROTEIN

3.1. Introduction 60

3.2. Cloning of Green Fluorescent Protein (GFP)-Tagged Full-Length Dengue Virus (DENV) Capsid (C) Protein 60

3.3. Nuclear Localization of Green Fluorescent Protein (GFP)-Tagged Dengue Virus (DENV) Capsid (C) Protein 61

3.3.1. Not all Dengue virus (DENV) capsid (C) proteins are in the nuclei 67

3.3.2. Dengue virus (DENV) capsid (C) protein is not exported out from the nucleus 69

3.3.3. Nuclear localization of Dengue virus (DENV) (C) protein 70

Page Number

is not cell type-specific

3.3.4. Live cell imaging of the localization of DENV C protein in the cell 71

3.4. Role of Nuclear Localization Signal (NLS) 78

3.4.1. Prediction of functional nuclear localization signal (NLS) motifs 78

3.4.2. Cloning of green fluorescent protein (GFP)-tagged nuclear localization signal (NLS) motif plasmids 80

3.4.3. Immuno-fluorescence microscopy study on NLS clones 81

3.5. Delineating Pivotal Amino Acid Residues for Nuclear Localization of Dengue Virus (DENV) Capsid (C) Protein 84

3.5.1. Single site-directed mutagenesis of capsid (C) protein 84

3.5.2. Multiple site-directed mutagenesis of C protein 88

3.6. Effect of R(97-100)A Mutations on Dengue Virus (DENV) Replication 92

3.7. Importins-α/β Imports Dengue Virus (DENV) Capsid (C) Protein into Nucleus 94

3.7.1. Identifying nuclear transporting partner of Dengue virus (DENV) capsid (C) protein 94

3.7.2. Determining binding strength of DENV C protein and importin-α 98

3.8. Role of Phosphorylation in Nuclear Localization of Dengue Virus (DENV) Capsid (C) Protein 101

4. EXPRESSION AND PURIFICATION OF DENGUE VIRUS (DENV) CAPSID (C) PROTEIN

4.1. Introduction 108

4.2. Expression and Purification of Dengue Virus (DENV) Capsid (C) Protein in Mammalian System 108

4.2.1. Molecular cloning of FLAG-tagged dengue virus (DENV) capsid (C) protein 108

Page Number

4.2.2. Pilot screening of FLAG-tagged full-length dengue virus (DENV) capsid (C) protein expression 110

4.2.3. Immunoprecipitation of FLAG-tagged dengue virus (DENV) capsid (C) protein in the cell lysates 112

4.3. Expression and Purification of Dengue Virus (DENV) Capsid (C) Protein in Bacterial System 115

4.3.1. Engineering of biotin acceptor peptide (BAP) into dengue virus (DENV) capsid (C) plasmid, pET28aDENVBioCap 115

4.3.2. Pilot screening of Dengue virus (DENV) capsid (C) protein expression 117

4.3.3. Optimization of Western-blot for biotinylated protein 121

4.3.4. Discovery of endogenous biotinylation in BL-21-CodonPlus competent cells 122

4.3.5. Purification of biotinylated Dengue virus (DENV) capsid (C) protein 124

4.3.5.1. Extraction of Dengue virus (DENV) capsid (C) protein under denaturing condition 124

4.3.5.2. Purification of Dengue virus (DENV) capsid (C) protein via affinity chromatography 125

4.3.5.3. Aggregation issue during stepwise dialysis and concurrent refolding of partially purified Dengue virus (DENV) capsid (C) protein 126

4.3.5.4. Second purification of full-length Dengue virus (DENV) capsid (C) protein via ion exchange chromatography 130

4.3.5.5. Third purification of biotinylated full-length Dengue virus (DENV) capsid (C) protein via size-exclusion chromatography 132

4.4. Functional Study of Purified Biotinylated Full-Length Dengue Virus (DENV) Capsid (C) Protein 135

4.4.1. High in vivo biotinylation efficiency in BL-21-CodonPlus competent cells 135

4.4.2. Purified full-length Dengue virus (DENV) capsid (C) 137

Page Number

protein is functional

5. HIGH-THROUGHPUT PROTOARRAY SCREENING FOR NOVEL INTERACTING PARTNERS OF DENGUE VIRUS CAPSID PROTEIN

5.1. Introduction 139

5.2. Description of ProtoArray® Technology-Based Protein Microarray 139

5.3. Screening of Novel Interacting Partners for Dengue Virus (DENV) Capsid (C) Protein via ProtoArray® Technology-Based Protein Microarray 143

5.3.1. Functional classification of the interacting partners 148

5.3.2. Compartmentalization of the interacting partners 150

5.4. Non-Structural Role of Dengue Virus (DENV) Capsid (C) Protein in the Nucleus 151

5.4.1. Role of Dengue virus (DENV) capsid (C) protein in cell cycle arrest 152

5.4.1.1. Validation of the binding between Dengue virus (DENV) capsid (C) protein and identified interacting partners 152

5.4.1.2. Dengue virus (DENV) capsid (C) protein arrested cell cycle at S-phase 154

5.4.1.3. Cell cycle arrest during wild type flavivirus infection 157

5.4.1.4. Flavivirus-induced cell cycle arrest is cell-type specific 161

5.4.1.5. Effect of cell cycle arrest upon Dengue virus (DENV) infection 168

5.4.1.6. Effect of DENV infection on cell cycle-related genes 170

5.4.2. Role of Dengue virus (DENV) capsid (C) protein in regulating host transcriptional and translational activity 173

5.4.2.1. Validation of the binding between Dengue virus 173

Page Number

(DENV) capsid (C) protein and identified interacting partners

5.4.2.2. Effect of signal recognition particle 19 (SRP19) and dimethyladenosine transferase 1 homolog (DIMT1) gene over-expression and knock-down upon Dengue virus (DENV) replication 177

5.4.2.3. Role of signal recognition particle 19 (SRP19) during Dengue virus (DENV) infection 182

6. DISCUSSIONS 188

CONCLUSION 208

FUTURE DIRECTION 209

REFERENCES 212

APPENDIX 1: MEDIA FOR TISSUE CULTURE 230

APPENDIX 2: MEDIA FOR VIRUS INFECTION AND PLAQUE ASSAY 233

APPENDIX 3: MATERIALS FOR MOLECULAR TECHNIQUES 235

APPENDIX 4: MATERIALS FOR PROTEIN EXPRESSION AND PURIFICATION 239

APPENDIX 5: MATERIALS FOR PROTEIN ANALYSIS 244

APPENDIX 6: MATERIALS FOR FLUORESCENCE-ACTIVATED CELL SORTING (FACS) ANALYSIS 253

APPENDIX 7: SOFTWARE USED FOR THIS PROJECT 254

APPENDIX 8: DNA SEQUENCES AND CONCEPTUAL TRANLSATION OF DNA INSERTIONS 255

Summary

Dengue virus (DENV) is the most important mosquito-borne viral disease, affecting millions of people in tropical and subtropical countries annually. However, antiviral drugs and vaccines are still not available in the market yet. This is mainly due to the incomplete understanding of the viral and host factors in the pathogenesis of DENV. Dengue capsid (C) protein was known to localize in both the cytoplasm and nucleus during infection but the significance of nuclear phase for a positive-stranded RNA virus is still shrouded in mystery. In this study, the underlying molecular mechanism of nuclear translocation of DENV C protein and its non-structural roles in the nucleus is elucidated.

Two functional bipartite nuclear localization signal (NLS) motifs were detected in DENVC protein and site-directed mutagenesis studies confirmed that second bipartite NLS2 motif (85-100 amino acids) was the most crucial part for nuclear translocation of DENV C protein. The first NLS motif (NLS1) was found to enhance the nuclear translocation ability of DENV C protein. The transporting partner of DENV C protein was also identified in this study. It was shown that DENVC protein interacted with importin-α protein allowing importin-β protein to bring the whole complex into the nucleus. Co-immunoprecipitation and mammalian-2-hybrid assays corroborated that the main binding site of DENV C protein to the importin-α protein was the whole NLS2 motif while NLS1 motif enhanced the binding of DENV C protein to importin-α protein. In addition, this transportation process was regulated by phosphorylation. Inhibition of the activity of protein kinase C (PKC) retarded the nuclear translocation of DENV C protein. Further investigation revealed that amino acid residue 71 was the phosphorylation site responsible for nuclear translocation of DENV C protein.

To decipher non-structural roles of DENVC protein in the nucleus, an optimized platform was developed to engineer, express and purify biotinylated full-length DENVC protein for high-throughput screening of novel interacting partners via ProtoArray® platform. Thirty-one protein interactors were identified and 50 % of them were nuclear proteins. One of the main categories in the list of identified interacting partners is related to cell cycle control. Cell cycle analyses demonstrated that DENV arrested infected cells at S- and G2- / M-phases during infection. It was also shown that virus production was greatly reduced when host cells were arrested at G1-phase during infection. Hence, DENV C protein translocated into nucleus and interacted with cyclin B3 (CCNB3), GADD45A, and CHES1 proteins to promote cell cycle progression from G1- to S-phase and from S- to G2- / M-phase. Another identified non-structural role of DENV C protein in the nucleus is to manipulate host transcriptional and translational activities. SRP19 protein which is involved in protein biogenesis was found to reduce DENV viral RNA replication resulting in lower virus production. To counter this effect, DENV C protein translocated into nucleus and degraded SRP19 protien via direct interaction.

In summary, this study deciphered the molecular mechanism of the nuclear transportation of DENV C protein and unravelled the non-structural roles of DENV C protein in the nucleus. This allowed for better understanding on the ability of flavivirus in overcoming the limited genomic information constraint by having multifunctional viral proteins.

List of Tables

Page Number

Table 1.1: Classification and level of severity of dengue infection 8

Table 1.2: Properties and functions of non-structural (NS) proteins 11

Table 2.1: Cell lines and media used in this project 29

Table 2.2: Primers used for generation of GFP-tagged DENV C protein and NLS motifs 35

Table 2.3: Primers used for site-directed mutagenesis 36

Table 2.4: Primers used for cloning of FLAG-tagged DENV C protein 37

Table 2.5: List of primers used for pET28aDENVBioCap plasmid construction 38

Table 2.6: Primers used for generating DENVC-AD and Impα-DBD plasmids 39

Table 2.7: Primers used for real-time PCR 41

Table 2.8: Primers used for mutagenesis of DENV infectious clone 42

Table 3.1: Putative bipartite NLS motifs of C protein in all four DENV serotypes 79

Table 3.2: Putative phosphorylation sites on DENV C protein 102

Table 4.1: Rare codon analysis of full-length DENV C protein 119

Table 4.2: Competent cells identified through BLAST analysis of BirA gene 124

Table 4.3: MALDI-TOF mass spectrometry analysis of purified DENV C protein 134

Table 5.1: Content and classifications of human proteins coated on ProtoArray glass slide 140

Table 5.2: Significant interacting partners of DENV C protein identified using z-score cut-off value of 3 144

Table 5.3: Putative cyclin binding sites of Dengue virus capsid proteins identified via eukaryotic linear motif (ELM) analysis 153

Page Number

Table 5.4: Cell cycle-related genes that are up-regulated during DENV infection 170

List of Figures

Page Number

Figure 1.1: Taxonomy of family *Flaviviridae* 2

Figure 1.2: The global DENV risk in various countries 4

Figure 1.3: Distribution of DENV serotypes in the world between the Year 1970 and 2011 5

Figure 1.4: The average number of DENV cases in the 30 most highly endemic countries 6

Figure 1.5: Schematic representation of polypeptide encoded by flavivirus genomic RNA 9

Figure 1.6: Schematic diagram of single polyprotein synthesized in the endoplasmic reticulum (ER) 10

Figure 1.7: Schematic diagram depicting the replication cycle of flavivirus 14

Figure 1.8: Multiple sequence alignment of mosquito-borne flaviviral C protein sequences 18

Figure 1.9: Sequence distances analysis of flaviviral C proteins 19

Figure 1.10: Structure of flaviviral C protein 21

Figure 1.11: Proposed model of C protein interaction with viral RNA and nucleocapsid assembly 22

Figure 2.1: Plasmid map of GFP-tagged DENV C gene 34

Figure 3.1: Cloning of full-length DENV C protein tagged with GFP 61

Figure 3.2: Immuno-fluorescence microscopic images of GFP-tagged DENV C protein 63

Figure 3.3: Verification of green fluorescence detected in the transfected cell nucleus 64

Figure 3.4: Three-dimensional images of DENV C-transfected cells showing the nuclear localization of C protein 66

Figure 3.5: Localization of DENV C proteins in the nuclei and perinuclear regions 67

Figure 3.6: Percentage of DENV C protein-transfected cells showing different localization patterns of C protein in 68

Page Number

the cells at two different time points

Figure 3.7: Percentage of DENV C protein-transfected cells showing different localization patterns of C protein in the cells with or without the presence of leptomycin (LMB) inhibitor 70

Figure 3.8: Nuclear localization of GFP-tagged DENV C protein in HEK293 (A) and HeLa (B) cells 71

Figure 3.9: Time-lapse experiment showing the localization of DENV C proteins in BHK cells 73

Figure 3.10: Nuclear staining of living BHK cells with Hoescht 33258 75

Figure 3.11: Time-lapsed imaging of the nuclear localization of recombinant DENV C protein in Hoescht-stained BHK cells 77

Figure 3.12: Schematic diagram of full-length DENV C protein and putative NLS motifs 80

Figure 3.13: Gel electrophoresis image of NLS1 and NLS2 fragments 81

Figure 3.14: Immuno-fluorescence images of GFP-tagged putative NLS motifs 82

Figure 3.15: Percentage of NLS motif-transfected cells showing different localization patterns in the cells 83

Figure 3.16: Schematic diagram showing the positions of mutation on different mutated clones 85

Figure 3.17: Determination of the key amino acid residues responsible for nuclear localization of C protein 86

Figure 3.18: Percentage of transfected cells showing different localization of GFP fusion proteins for different clones 88

Figure 3.19: Schematic diagram of clones with multiple mutations 89

Figure 3.20: Immuno-fluorescence images of clones with multiple mutations 90

Figure 3.21: Percentage of transfected cells showing different localization patterns of mutated C proteins 91

Page Number

Figure 3.22: Effect of R(97-100)A mutations on DENV replication 93

Figure 3.23: Interaction between C protein and importin-α/β proteins 96

Figure 3.24: Co-immunoprecipitation study on various NLS mutants and importin-α protein 98

Figure 3.25: Illustration of mammalian-2-hybrid concept 99

Figure 3.26: Cloning of importin-α (A) and full-length DENV C (B) genes into mammalian-2-hybrid vectors 100

Figure 3.27: Mammalian-2-hybrid assay on the binding strength of importin-α protein with full-length DENV C and mutated proteins 101

Figure 3.28: Schematic diagram of clones with mutation on putative phosphorylation site 103

Figure 3.29: Effect of mutations on the putative phosphorylation sites of DENV C protein 104

Figure 3.30: Role of protein kinase C on nuclear localization of DENV C protein 105

Figure 3.31: Proposed model of nuclear transportation of DENV C protein 106

Figure 4.1: Cloning of FLAG-tagged full-length DENV C protein 109

Figure 4.2: Pilot screening of FLAG-tagged DENV C protein expression in 293FT cells 110

Figure 4.3: Detection of FLAG-tagged DENV C protein in the 293FT cell lysates and culture media 112

Figure 4.4: Immunoprecipitation of FLAG-tagged DENV C proteins in 293FT cell lysates 113

Figure 4.5: Secondary structure prediction of biotinylated DENV C protein (BNC) and unbiotinylated C protein (UBNC) 116

Figure 4.6: Cloning of pET28aDENVBioCap plasmid via overlapping extension PCR (OE-PCR) technique 117

Figure 4.7: Schematic representation of pET28aDENVBioCap construct 118

Figure 4.8: Pilot expression screening of DENV C protein 120

Page Number

Figure 4.9: Expression of DENV C protein with and without BAP 121

Figure 4.10: Optimization of Western-blot protocol for biotinylated proteins 122

Figure 4.11: DENV C protein with biotin acceptor peptide (BAP) is biotinylated endogenously 123

Figure 4.12: Extraction of DENV C protein under non-denaturing and denaturing conditions 125

Figure 4.13: Purification of DENV C protein via affinity chromatography under denaturing condition 127

Figure 4.14: Resolubilization of DENV C protein aggregate using various detergents 128

Figure 4.15: Resolubilization of DENV C protein aggregate using different pH 129

Figure 4.16: Cation exchange chromatography purification of DENV C protein using Resource MonoS column 131

Figure 4.17: Anion exchange chromatography purification of DENV C protein using Resource MonoQ column 133

Figure 4.18: Size exclusion chromatography purification of DENV C protein using Superdex 75 column 135

Figure 4.19: Biotinylation efficiency of purified full-length DENV C protein 137

Figure 4.20: Functional assay of purified biotinylated full-length DENV C protein 138

Figure 5.1: Image of scanned ProtoArray glass slide 141

Figure 5.2: Workflow of ProtoArray screening 142

Figure 5.3: Number of identified protein interactors with z-score value of 1 and greater than 1 143

Figure 5.4: Functional classification of the interacting partners of DENV C protein 149

Figure 5.5: Localization of DENV C protein-interacting partners identified via ProtoArray® platform 151

Figure 5.6: Verification of the binding between identified interacting partners and DENV C protein via ELISA 154

Page Number

Figure 5.7: Cell cycle profile of DENV C protein-transfected and GFP control-transfected HEK293 cells 156

Figure 5.8: Cell cycle arrest induced by DENV C protein on HEK293 cells 157

Figure 5.9: Cell cycle arrest induced by DENV on HEK293 cells 159

Figure 5.10: Growth curve of DENV-2 in C6/36 cells 160

Figure 5.11: S-phase cell cycle arrest induced by WNV on HEK293 cells 161

Figure 5.12: Cell cycle arrest induced by DENV on BHK cells 163

Figure 5.13: Cell cycle arrest induced by WNV on BHK cells 164

Figure 5.14: Cell cycle arrest induced by DENV on C6/36 cells 166

Figure 5.15: Cell cycle arrest induced by WNV on C6/36 cells 167

Figure 5.16: Effect of cell cycle arrest on DENV infection 169

Figure 5.17: PCR array analysis of DENV-infected cells 171

Figure 5.18: Gene expression level of identified interacting partners of DENV C protein during DENV infection 172

Figure 5.19: Validation of the binding between DENV C protein and interacting partners identified via ProtoArray® platform 174

Figure 5.20: Reciprocal binding assay to confirm the interaction between DENV C protein and SRP19 / DIMT1 proteins 175

Figure 5.21: Protein binding assay with increasing amount of SRP19 / DIMT1 proteins 175

Figure 5.22: Co-localization between DENV C protein and SRP19 / DIMT1 proteins in the nucleolus 176

Figure 5.23: Over-expression of SRP19 and DIMT1 proteins in HEK293 cells 178

Figure 5.24: Effect of SRP19 and DIMT1 proteins over-expression on DENV infection 179

Figure 5.25: Knock-down of SRP19 and DIMT1 genes 181

Figure 5.26: Effect of SRP19 and DIMT1 genes knock-down upon 182

Page Number

DENV infection

Figure 5.27: Expression of SRP19 protein during DENV infection 184

Figure 5.28: DENV RNA level in the SRP19 gene over-expressed and knock-downed HEK293 cells 185

Figure 5.29: Degradation of SRP19 protein by DENV C protein 187

Figure 6.1: Positions of NLS1, NLS2 motifs, residues S71 and G42&P43 in DENV C protein 190

Figure 6.2: Model of transportation mechanism of DENV C protein into nucleus 192

Figure 6.3: Model depicting the role of SRP19 and DENV C proteins during DENV replication 198

Figure 6.4: The role of DENV C protein in cell cycle control and apoptosis 201

Figure 6.5: Model depicting the nuclear translocation mechanism of DENV C protein and its non-structural roles in the nucleus 204

Abbreviations

AD	Activation domain
ASXL1	Additional sex combs like 1 (Drosophila)
AFF4	AF4/FMR2 family, member 4
αvβ3	Alpha V beta 3 integrin
N-terminus/terminal	Amino-terminus/terminal
APS	Ammonium persulfate
anchC	Anchored capsid protein
Ab	Antibody
AURKA	Aurora kinase A
BHK	Baby Hamster Kidney cell
bp	Base pair (s)
BAP	Biotin acceptor peptide
BCIP/NBT	5-bromo-4-chloro-3-indolylphosphate/ p-nitro blue tetrazolium
BN	Biotinylated protein
Bis	Bisindolylmaleimide
BSA	Bovine serum albumin
CAMK2A	Calcium / calmodulin-dependent protein kinase II alpha
CACNB1	Calcium channel, voltage-dependent, beta 1 subunit
C	Capsid protein
CO_2	Carbon dioxide
C-terminus/terminal	Carboxyl-terminus/terminal
CMC	Carboxymethylcellulose
CDKN2AIP / CARF	CDKN2A interacting protein
CHAPS	3-[(3-cholamidopropyl)dimethylammonio]-1-propanesulfonate
CHES1 / FOXN3	Checkpoint suppressor 1 / Forkhead box N3
CHKA	Choline kinase alpha
CRM1	Chromosomal region maintenance 1
CV	Coefficient of variation
Co-IP	Co-immuno precipitation
cDNA	Complementary DNA
Ctrl	Control
CTTN	Cortactin
CM	Culture media
CCNB3	Cyclin B3
CDK	Cyclin dependent kinase
CAML	Cyclophilin-binding ligand
Da	Dalton
DAPI	4',6'-diamidino-2-phenylindole
˚C	Degree Celsius
DC-SIGN	Dendritic cell-specific ICAM grabbing non-integrin
DF	Dengue Fever

DHF	Dengue Haemorrhagic Fever
DSS	Dengue Shock Syndrome
DENV	Dengue virus
DENV-1	Dengue virus serotype 1
DENV-2	Dengue virus serotype 2
DENV-3	Dengue virus serotype 3
DENV-4	Dengue virus serotype 4
DEPC	Diethylpyrocarbonate
DIMT1	DIM1 dimethyladenosine transferase 1 homolog (S. cerevisiae)
Na_2HPO_4	Disodium phosphate
DBD	DNA-binding domain
DIII	Domain III
DMEM	Dulbecco's modified eagle's medium
EF1α	Elongation factor 1 alpha
ELOF1	Elongation factor 1 homolog (ELF1, S. cerevisiae)
E	Eluate
ER	Endoplasmic reticulum
E	Envelope protein
ELISA	Enzyme-linked immunosorbent assay
EDTA	Ethylenediaminetetraacetic acid
ELM	Eukaryotic linear motif
EIF1AX	Eukaryotic translation initiation factor 1A, X-linked
EIF1AY	Eukaryotic translation initiation factor 1A, Y-linked
FPLC	Fast protein liquid chromatography
FcγR	Fc gamma receptor
FT	Flow-through
FACS	Fluorescence-activated cell sorting
FCS	Foetal calf serum
F	Forward primer
IC	Full-length infectious clone
GRP18/BiP	Glucose-regulating protein 78
GST	Glutathione S transferase
GAPDH	Glyceraldehyde 3-phosphate
GFP	Green fluorescent protein
GTP	Guanosine triphosphate
HSP70	Heat shock protein 70
α1-4	Helices 1-4
HBV	Hepatitis B virus
HCV	Hepatitis C virus
HTS	High-throughput screening
HRP	Horseradish peroxidase
hr	Hour(s)
HEK	Human Embryonic Kidney cell
hSec3p	Human Sec3 exocyst protein
HCl	Hydrochloric acid

IGBP1	Immunoglobulin (CD79A) binding protein 1
Impα	Importin-α protein
INF	Infected
IBV	Infectious bronchitis virus
IC97	Infectious clone with mutations at residues 97-100
ICAM	Intercellular adhesion molecule
IRES	Internal ribosome entry sites
IEX	Ion-exchange chromatography
IPTG	Isopropyl β-D-thiogalactoside
JEV	Japanese Encephalitis virus
LMB	Leptomycin B
L	Liter
LAR II	Luciferase assay reagent II
LB	Luria-Bertani
LY	Cell lysate
MBP	Maltose-binding protein
M2H	Mammalian 2-hybrid
MALDI-TOF	Matrix-assisted laser desorption / ionization-time of flight
MES	2-[N-morpholino]ethanesulphonic acid
µg	Microgram
µl	Microliter
MAP2	Microtubule-associated protein 2
mM	Milli Molar
mg	Milligram
ml	Milliliter
min	Minute(s)
Hg	Mmercury
UI	Mock-infected
M	Molar
KH_2PO_4	Monopotassium phosphate
M.O.I.	Multiplicity of infection
MVEV	Murray Valley Encephalitis virus
mt	Mutation
TEMED	N,N,N',N'-tetramethylethylenediamine
nm	Nano meter
ng	Nanogram
NKp44	Natural killer-activating receptor
NGC	New Guinea C
Ni-NTA	Nickel-nitrilotriacetic acid
NEK7	NIMA (never in mitosis gene a)-related kinase 7
Noco	Nocodazole
NS	Non-structural protein
NLS	Nuclear localization signal
NPC	Nuclear pore complex
NSRP1	Nuclear speckle splicing regulatory protein 1

NP	Nucleoprotein
NTPase	Nucleoside triphosphatase
ORF	Open reading frame
OD	Optical density
OE-PCR	Overlap extension-PCR
PSRC1	p53-regulated DDA3 (DDA3) / proline/serine-rich coiled-coil 1
PLB	Passive lysis buffer
PBST	PBS with Tween-20
PBS	Phosphate buffered saline
PMT4	Photomultiplier tube four
PCLO	Piccolo (presynaptic cytomatrix protein)
PCR	Polymerase chain reaction
PVDF	Polyvinylidene difluoride
p.i.	Post-infection
KCTD18	Potassium channel tetramerisation domain containing 18
KCl	Potassium chloride
prM	Precursor membrane protein
PIC	Pre-integration complex
PPT	Preprotrypsin
PKA	Protein kinase A
PKB	Protein kinase B
PKC	Protein kinase C
PRKCI	Protein kinase C, iota
PPI	Protein-protein interaction
RAD51AP1	RAD51 associated protein 1
Rab5	Ras-related protein 5
g (rcf)	Relative centrifugal force
RF	Replicative form
RCSB	Research Collaboratory for Structural Bioinformatics
RO	Reverse osmosis
R	Reverse primer
RT	Reverse transcription
rpm	Revolutions per minute
rRNA	Ribosomal RNA
RTPase	RNA triphosphatase
RT	Room temperature
RTF1	Rtf1, Paf1/RNA polymerase II complex component, homolog (S. cerevisiae)
sec	Second(s)
SRP19	Signal recognition particle 19kDa
SIV	Simian immunodeficiency virus
SV40	Simian Vacuolating virus 40
SEC	Size-exclusion chromatography
SLAIN2	SLAIN motif family, member 2

snoRNA	Small nucleolar RNA
$NaHCO_3$	Sodium bicarbonate
NaCl	Sodium chloride
SDS	Sodium dodecyl sulphate
SDS-PAGE	Sodium dodecyl sulphate polyacrylamide gel electrophoresis
SAT2	Spermidine / spermine N1-acetyltransferase family member 2
H_2SO_4	Sulfuric acid
TBST	TBS with Tween-20
TMB	Tetramethyl benzidine
Thy	Thymidine
TBEV	Tick-Borne Encephalitis virus
TGN	Trans-Golgi network
TBE	Tris/Borate/EDTA
TBS	Tris-buffered saline
UBE2S	Ubiquitin-conjugating enzyme E2S
UBN	Unbiotinyalted protein
UTR	Untranslated region
UBF	Upstream binding factor
UV	Usutu virus
VRK1	Vaccinia related kinase 1
WIPF1	WAS / WASL interacting protein family, member 1
W	Wash
WDR5	WD repeat domain 5
WNV	West Nile virus
WHO	World Health Organization
YFV	Yellow Fever virus

1. Literature Review

1.1. Dengue Virus

Dengue Fever epidemics were first recorded in 1779 in Batavia (Indonesia) and Cairo (Egypt) (Gubler, 1998). The disease is caused by an arthropod-borne virus or arbovirus called Dengue Virus (DENV), and is transmitted to its human host by mosquito vectors. This virus belongs to the family *Flaviviridae*, genus Flavivirus. In Latin, "Flavi" means "Yellow". This name was derived from one of the greatest plagues which occurred hundreds of years ago, namely Yellow Fever. Other members of the Flavivirus genus include Yellow Fever virus (YFV), West Nile virus (WNV), Japanese Encephalitis virus (JEV), and Tick-Borne Encephalitis virus (TBEV). Figure 1.1 shows the taxonomy of family *Flaviviridae*.

There are four known DENV serotypes designated as DENV-1, DENV-2, DENV-3 and DENV-4 which are genetically and antigenically distinct. DENV infection encompasses a wide spectrum of severity ranging from a mild febrile illness known as Dengue Fever (DF) to a more critical and fatal illness known as Dengue Haemorrhagic Fever (DHF) / Dengue Shock Syndrome (DSS). It is one of the most medically important arboviral diseases in terms of human morbidity and mortality. More than 3.6 billion people are at risk of DENV infection in more than 100 countries (Gubler, 2011). There are approximately 390 million Dengue cases reported annually, of which 96 million are DHF / DSS cases (Bhatt *et al.*, 2013). Hence, great endeavour has been put together by the government and scientists to fight against this emerging and re-emerging infectious disease.

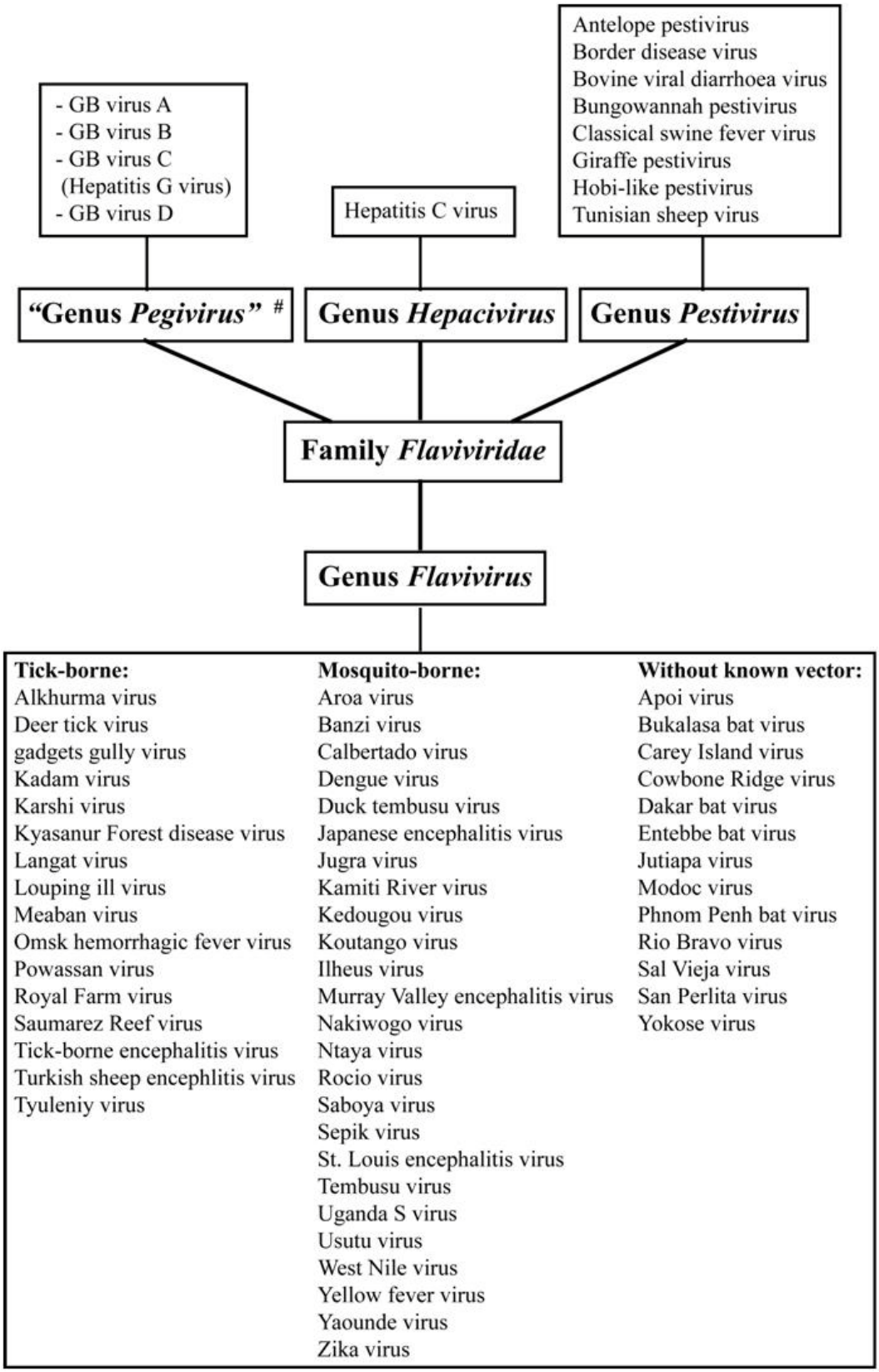

Figure 1.1: Taxonomy of family *Flaviviridae* (Calisher & Gould, 2003; Lindenbach *et al.*, 2007; Stapleton *et al.*, 2011). There are three known genara (Flavivirus, Pestivirus and Hepacivirus) under the family *Flaviviridae*. Dengue virus is in the Flavivirus genus which contains the most number of viruses. # Pegivirus is not formally endorsed by The International Committee on Taxonomy of Viruses yet.

1.1.1. Epidemiology of dengue virus infection

The transmission of DENV increased dramatically after World War II and it marked the onset of global DENV pandemic (Gubler, 1997). As shown in Figure 1.2, almost all the tropical and sub-tropical countries are susceptible to DENV infection to date. With increase of epidemic transmission, many countries have evolved from non endemic to hypoendemicity (one serotype present) or from hypoendemicity to hyperendemicity (multiple serotypes present) as indicated in Figure 1.3 (Gubler, 1998; 2011). Since epidemic of DHF was first recognized in Manila, Philippines in 1953, cases of DHF were also recorded in other Southeast Asia (SEA) countries such as Malaysia, Singapore, Myanmar, Thailand, Vietnam and Indonesia (Gubler, 1997). Figure 1.4 showed that SEA countries are still among the top 30 most highly dengue endemic countries in the world for the past eight years. Other countries such as Brazil, Mexico, India, Sri Lanka, and Paraguay are also badly affected. Hence, DENV infection indeed poses a major global health issue resulting in significant social and economic burden to the countries.

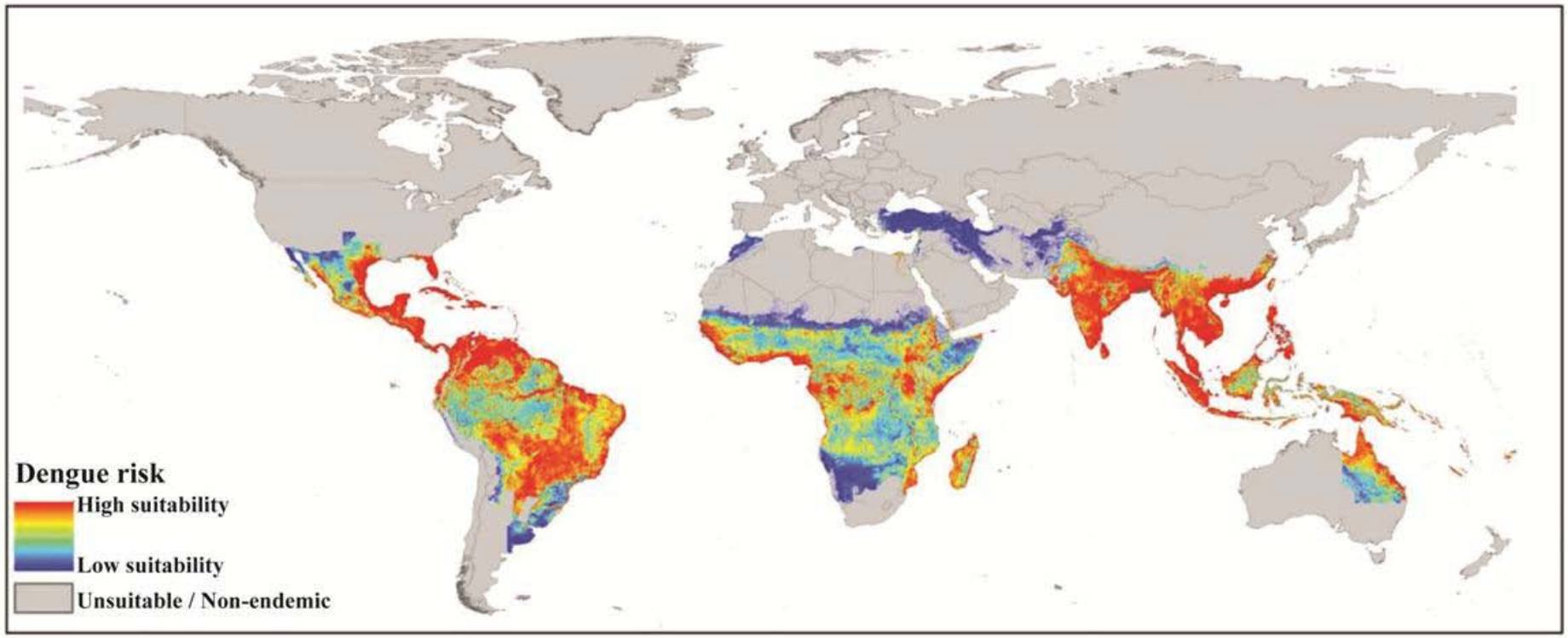

Figure 1.2: The global DENV risk in various countries (Simmons *et al.*, 2012)**.** Tropical and sub-tropical countries are at greater risk of contracting DENV infection.

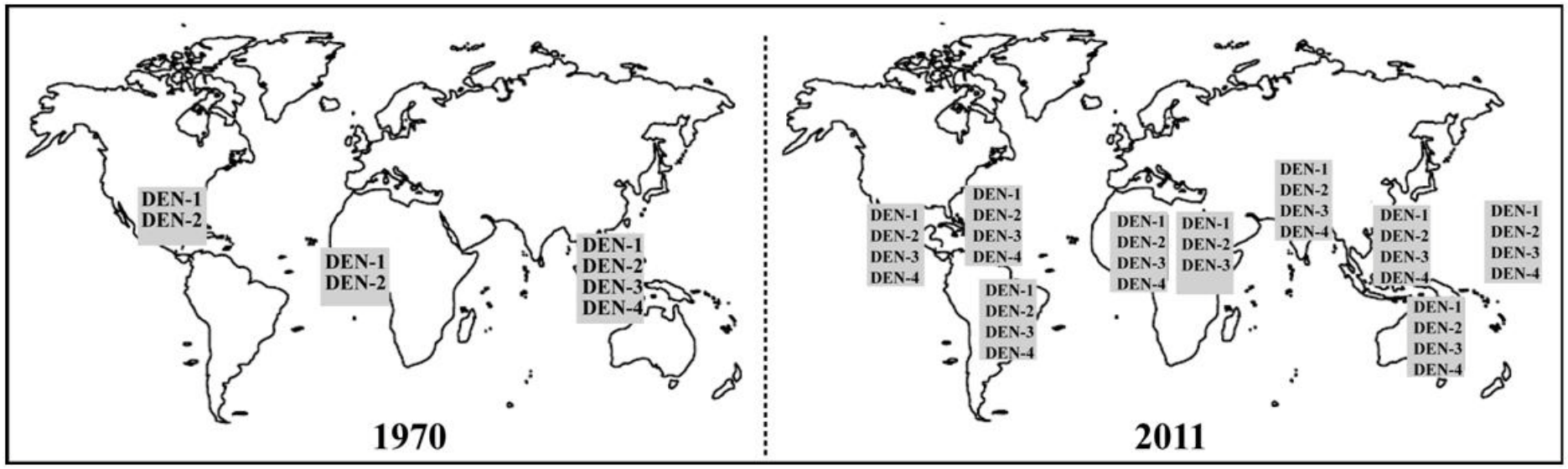

Figure 1.3: Distribution of DENV serotypes in the world between the Year 1970 and 2011 (Gubler, 2011)**.** To date, almost all DENV serotypes can be found in the affected countries.

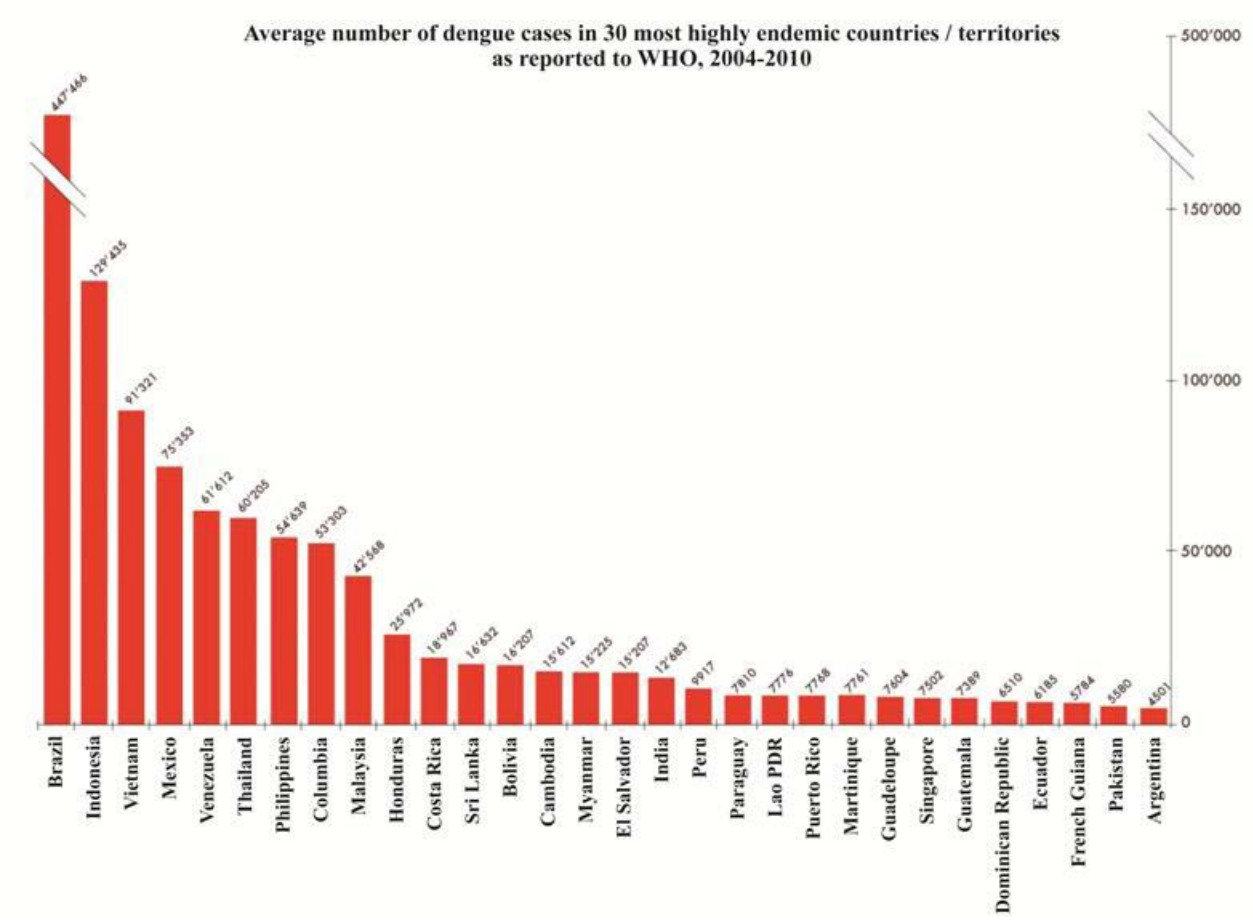

Figure 1.4: The average number of DENV cases in the 30 most highly endemic countries (WHO, 2012)**.** Southeast Asia countries are at the top 30 most affected countries.

1.1.2. Mosquito vector of dengue virus

One of the strategies to prevent DENV infection is to eradicate the vector that carries the virus, namely mosquito vector. DENV is predominantly transmitted by *Aedes* mosquitoes such as *Aedes aegypti*, *Aedes albopictus*, *Aedes polynesiensis*, and *Aedes scutellaris* (Holtzclaw, 2002). Generally, *A. aegypti* is the main vector in urban transmission but *A. albopictus* is shown to be more competent and more susceptible to experimental infection (Kramer & Ebel, 2003). *A. albopictus* is a less selective feeder so it becomes less epidemiological significance.

Aedes aegypti is an efficient vector for DENV transmission. Its eggs could remain viable even in dry condition for months. However, they are not able to survive in cool temperature. As such, the distribution of *A. aegypti* is confined to warmer latitude and lower altitudes nearest to the equator, explaining the high susceptibility of tropical and sub-tropical countries to DENV infection as indicated in Figure 1.2.

Female mosquito is a nervous feeder. Any disruption like a slight movement during the feeding will alert it to fly away. Therefore, it usually feeds on few persons for a single blood meal. If the female mosquito feeds on an infected person, the DENV would be transmitted to several persons in a short time. This explains why *A. aegypti* can transmit DENV so efficiently. After a person is bitten by an infected *A. aegypti*, the virus needs 3-14 days to incubate before the person experiences the acute fever with a variety of nonspecific symptoms (Gubler, 1998). During the febrile period, the viruses are circulated in human peripheral blood. If a female mosquito bites on this infected person, it will become infected and the cycle continues.

1.1.3. Clinical manifestations of dengue virus infection

DENV infection causes a wide spectrum of severity ranging from an asymptomatic, mild febrile illness to more critical and fatal hemorrhagic manifestations. The incubation period of DENV is approximately 3 to 15 days with an average of 5 to 8 days. World Health Organization (WHO) 1997 classification and 2009 classification define the criteria for classification of DF, DHF and DSS patients and guidance for diagnosis (Table 1.1).

Table 1.1: Classification and level of severity of dengue infection (WHO, 1997; 2009)

WHO 1997 Dengue Classification	
Grade of disease	**Signs and Symptoms**
I	Fever with mild non-specific symptoms with a positive tourniquet test (inflating a blood pressure cuff midway between systolic and diastolic pressure for 5 minutes and then counting the number of petechia appears below the cuff).
II	Similar to Grade I but accompanied by spontaneous hemorrhagic manifestation, usually skin or other hemorrhages.
III	Circulatory failure manifested by rapid, weak pulse and narrow pulse pressure (<20mmHg) or hypotension with the presence of cold, clammy skin.
IV	Profound shock with undetectable pulse and blood pressure.
WHO 2009 Dengue Classification	
Grade of disease	**Signs and Symptoms**
Dengue ± Warning Sign	Fever with two of the following criteria: nausea, vomiting, rash, aches and pains, tourniquet test positive, leukopenia, and any warning signs such as abdominal pain or tenderness, persistent vomiting, clinical fluid accumulation, mucosal bleed, lethargy or restlessness, liver enlargement more than 2 cm, and increase in hematocrit concurrent with rapid decrease in platelet count.
Severe Dengue	Severe plasma leakage (lead to shock and accumulation of fluid with respiratory distress), severe bleeding and severe organ involvement (Liver: aspartate aminotransferase or alanine aminotransferase ≥ 1000 unit/liter; Central Nervous System: impaired consciousness; Heart and other organs)

However, all the symptoms described above are not constant findings in all the patients. It varies from individual to individual and from different geographic regions.

For example, hepatomegaly is common in Bangkok but gastrointestinal bleeding is common in Indonesia (Henchal & Putnak, 1990). Therefore, there is still a dire need to investigate and understand the pathogenesis mechanism of DENV infection.

1.2. Dengue Virus Genome and Proteins

To study the pathogenesis of DENV infection, we must first understand the genome of the virus. DENV contains a single-stranded plus-sense RNA that has type-I 5′-cap of m7GpppA but lacks a 3′-end poly(A) tail (Chambers *et al.*, 1990). Its genomic RNA is directly infectious (Ada & Anderson, 1959). It mimics cellular mRNA and exploits cellular apparatus to synthesize its proteins during replication. The genomic RNA is about 11 kb and has an uninterrupted open reading frame (ORF) flanked by non-coding regions at both the 5′ and 3′ ends. The ORFs of DENV-1, DENV-2, DENV-3 and DENV-4 are 10188, 10173, 10170 and 10158 nucleotides in length, respectively (Chang, 1997).

DENV genome encodes three structural proteins, namely capsid protein (C), precursor membrane protein (prM) and envelope glycoprotein (E), and five non-structural (NS) proteins, namely NS1, NS2A, NS2B, NS3, NS4A, NS4B, and NS5, as shown in Figure 1.5.

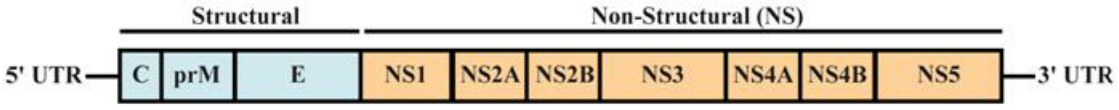

Figure 1.5: Schematic representation of polypeptide encoded by flavivirus genomic RNA (Chang, 1997)**.** C, prM and E denote capsid protein, precursor membrane protein and envelope protein, respectively. NS is non-structural protein while 5′ UTR and 3′ UTR are the 5′ and 3′ untranslated region.

The currently accepted model of DENV protein synthesis is that the full-length ORF of DENV genome is translated into a single polyprotein. The polyprotein precursor of DENV-1, DENV-2, DENV-3 and DENV-4 are 3396, 3391, 3390 and 3386 amino acids, respectively (Chang, 1997). The translated polyprotein is then cleaved by viral serine protease, host signalase, and other cellular proteases to yield individual viral proteins (Perera & Kuhn, 2008). Figure 1.6 shows the localization of each viral protein in the cytoplasm, endoplasmic reticular lumen and space between membranes.

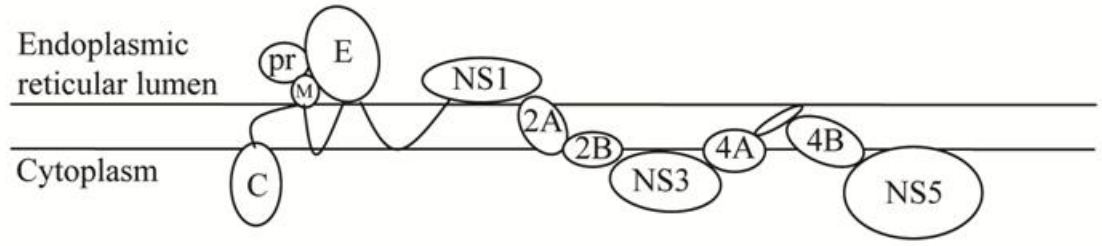

Figure 1.6: Schematic diagram of single polyprotein synthesized in the endoplasmic reticulum (ER) (Chang, 1997)**.** This single polypeptide is cleaved by viral protease, host signalase and other cellular proteases to release single viral proteins.

The first structural protein encoded at the 5′ end of flavivirus genome is capsid (C) protein which is the main focus of this study. The properties and functions of C protein will be discussed in more details in Section 1.4. The next encoded structural protein is pre-membrane (prM) protein. It is a glycoprotein that is synthesized as a precursor and will undergo proteolytic cleavage when the virus matures and exits from the host cell. It is suggested that prM protein helps to protect the envelope (E) protein, the third encoded structural protein, from misfolding or conformational change prior to maturation (Chambers *et al.*, 1990; Chang, 1997). The E protein is the major virion surface glycoprotein involved in a number of biological activities such as viral attachment, membrane fusion, hemagglutination of erythrocytes, induction of

neutralizing antibodies and virus assembly (Chambers *et al.*, 1990; Heinz & Allison, 2000; Modis *et al.*, 2004; Roehrig, 1997). It consists of three structural domains, Domain I, II, and III. Domain III (DIII) is located at the C-terminus of E protein and it is deemed to be the receptor binding domain (Kuhn *et al.*, 2002).

Non-structural 1 (NS1) protein is another glycoprotein that is synthesized in rough endoplasmic reticulum before it is transported to Golgi for glycosylation (Chang, 1997). This protein is an important pathogenic factor that has been used as a diagnostic marker for DENV infection (Alcon *et al.*, 2002). Non-structural 3 (NS3) protein is a hydrophilic protein that functions as serine protease and helicase (Li *et al.*, 1999) while non-structural 5 (NS5) protein is an RNA-dependent RNA polymerase (Khromykh *et al.*, 1998). Non-structural 2B (NS2B) protein together with NS3 protein acts as an important protease to cleave the single polyprotein at the C/anchor C, NS2A/NS2B, NS2B/3, NS3/NS4A, and NS4B/5 junctions to generate individual viral proteins (Falgout *et al.*, 1991). The functions of non-structural 2A (NS2A), non-structural 4A (NS4A), and non-structural 4B (NS4B) proteins are still unclear. Table 1.2 summarizes the known functions of each non-structural (NS) proteins.

Table 1.2: Properties and functions of non-structural (NS) proteins

Protein	Properties & Functions	References
NS1	❖ 42 kDa glycoprotein ❖ Exists in three forms: cytosolic, membrane-associated, secreted ❖ Antigen and antibody against NS1 can be found in the patients' sera ❖ Closely associated with viral double-stranded RNA in the replication complex ❖ Involved in complement pathway	(Alcon *et al.*, 2002; Avirutnan *et al.*, 2010; Mackenzie *et al.*, 1996; Noisakran *et al.*, 2007)
NS2A	❖ 23 kDa hydrophobic protein ❖ Co-localizes with viral double-stranded RNA ❖ Important for virus packaging ❖ Involved in interferon-α/β innate immune signalling	(Jones *et al.*, 2005; Liu *et al.*, 2003; Mackenzie *et al.*, 1998)
NS2B	❖ 14 kDa hydrophobic protein ❖ Co-factor for NS3 serine protease	(Chang *et al.*, 1999; Falgout *et*

Protein	Properties & Functions	References
	❖ NS2B/NS3 complex is involved in type I interferon-α/β signalling ❖ May involve in membrane permeability	*al.*, 1991; Rodriguez-Madoz *et al.*, 2010)
NS3	❖ 70 kDa hydrophilic protein ❖ Serine protease activity ❖ RNA helicase activity ❖ RNA-stimulated nucleoside triphosphatase (NTPase) activity ❖ RNA triphosphatase (RTPase) activity ❖ NS2B/NS3 complex is involved in type I interferon-α/β signalling	(Amberg & Rice, 1999b; Benarroch *et al.*, 2004; Li *et al.*, 1999; Rodriguez-Madoz *et al.*, 2010; Wengler & Wengler, 1993)
NS4A	❖ 16 kDa hydrophobic protein ❖ Involved in membrane modification ❖ Involved in interferon-α/β signalling ❖ Co-localizes with replication complex	(Jones *et al.*, 2005; Mackenzie *et al.*, 1998; Miller *et al.*, 2007)
NS4B	❖ 27 kDa hydrophobic protein ❖ Mediates the dissociation of NS3 protein from single-stranded viral RNA ❖ Stimulates helicase activity of NS3 protein ❖ Involved in interferon-α/β signalling	(Jones *et al.*, 2005; Umareddy *et al.*, 2006)
NS5	❖ 104 kDa hydrophilic protein ❖ RNA-dependent RNA polymerase ❖ Methyl-transferase activity ❖ Involved in STAT2 and interferon-α/β signalling	(Khromykh *et al.*, 1998; Mazzon *et al.*, 2009; Ray *et al.*, 2006)

1.3. Replication Cycle of Dengue Virus

Understanding the life cycle of DENV is of paramount importance in the development of anti-viral strategies. Nonetheless, many gaps still remain in the knowledge of establishment of DENV infection in various cell types. The susceptibility of various cell types to DENV infection is different. Monocytes and macrophages are recognized as the primary target cells for DENV (Kou *et al.*, 2008). However, DENV antigens and RNA can also be detected in the hepatocytes of infected patient's liver (Couvelard *et al.*, 1999; Kangwanpong *et al.*, 1995; Suksanpaisan *et al.*, 2007).

Despite the different infectivity of DENV in various cell types, the basic replication cycle of flavivirus is illustrated in Figure 1.7. Flavivirus binds to target cells via the interaction of E protein with primary receptor and probably together with

a low-affinity co-receptor. Several primary receptors and co-receptors for flavivirus have been identified such as C-type lectin dendritic cell-specific ICAM (intercellular adhesion molecule) grabbing non-integrin (DC-SIGN), alpha V beta 3 (αvβ3) integrin, glucose-regulating protein78 (GRP18/BiP), CD14-associated molecules, Fc gamma receptor (FcγR), Ras-related protein 5 (Rab5), heat shock protein 70 (HSP70), Natural killer-activating receptor (NKp44), glycosaminoglycan and heparin sulphate (Cabrera-Hernandez *et al.*, 2007; Chen *et al.*, 1997; Chen *et al.*, 1999; Chu & Ng, 2004b; Hershkovitz *et al.*, 2009; Hilgard & Stockert, 2000; Jindadamrongwech *et al.*, 2004; Krishnan *et al.*, 2007; Lee & Lobigs, 2000; Navarro-Sanchez *et al.*, 2003; Tassaneetrithep *et al.*, 2003). It is still controversial which receptor(s) is/are the main attachment molecule(s) for flavivirus. It is possible that different combination of primary receptor and co-receptor is required for different flaviviruses. Besides, one of the reasons for different susceptibility of DENV infection on various cell types could be due to the types of receptor(s) present and their prevalence on the cell surface.

Upon binding of E protein with cell surface receptor, the virion is internalized into host cells via clathrin-mediated endocytosis (Acosta *et al.*, 2008; Chu & Ng, 2004a). The acidic environment of the endosome triggers conformational change of E proteins from homodimers into homotrimers resulting in exposure of E protein fusion peptide which facilitates viral membrane-endosome fusion (Bressanelli *et al.*, 2004; Heinz & Allison, 2000; Mukhopadhyay *et al.*, 2005). After membrane fusion, the nucleocapsid is released into the cytosol and disassociates spontaneously into C proteins and viral genome (Heinz & Allison, 2000). The dissociation of WNV nucleocapsid upon the release from endocytic vesicles has been documented by Chu and Ng (2004a). However, the contributing factor for this spontaneous dissociation is still unknown. It could be due to the membrane fusion that disrupts the association

between the viral membrane and the hydrophobic regions of C proteins resulting in morphological instability of C protein homo-oligomer. Besides, there is also no publication thus far reporting the fate of the dissociated C proteins. These virus-originated C proteins could be degraded by the host cell or they may have significant roles in the establishment of infection.

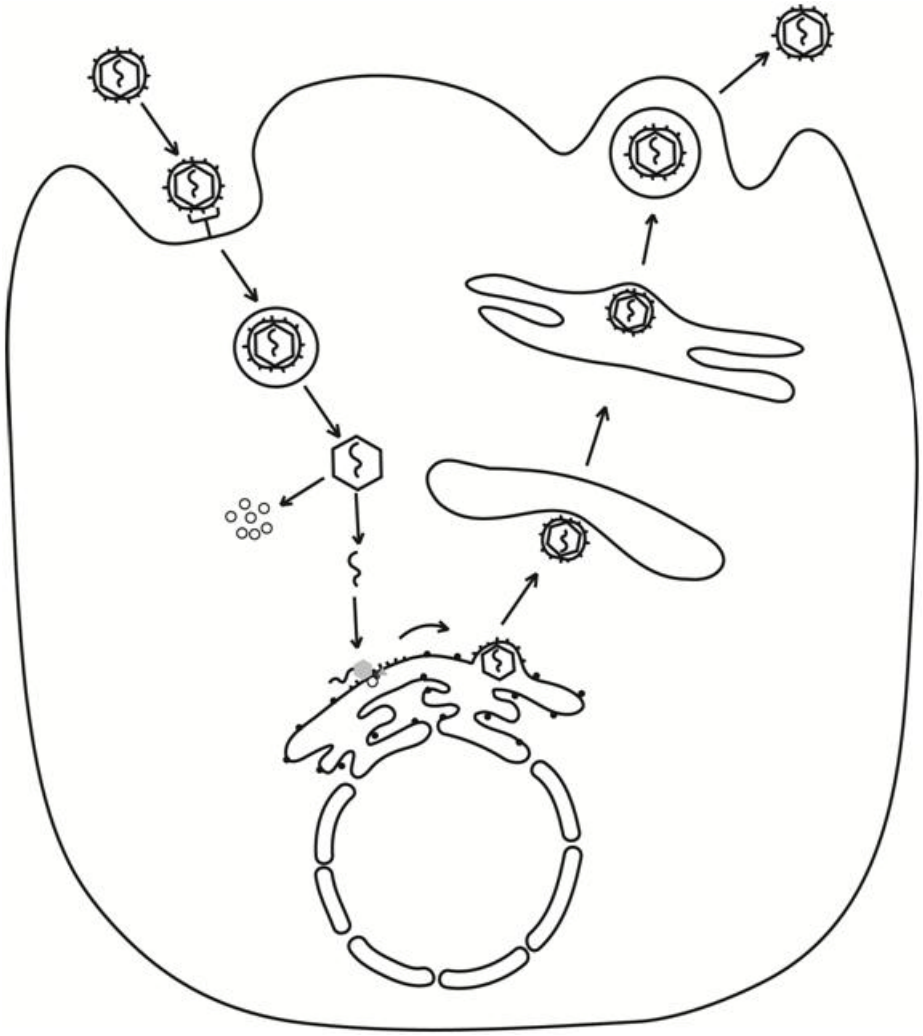

Figure 1.7: Schematic diagram depicting the replication cycle of flavivirus (Lindenbach *et al.*, 2007; Mukhopadhyay *et al.*, 2005). Virus binds to the host cell surface receptor and enters the cell via endocytosis pathway. Nucleocapsid is released to the cytosol after low-pH membrane fusion of viral membrane and endosome. Nucleocapsid dissociates and viral genome is free for translation into a single polyprotein at the endoplasmic reticulum (ER). Viral RNA replication occurs on the ER membrane and buds into ER lumen during assembly. The immature virus is transported to the Trans-Golgi network (TGN) for further post-translational modification. After cleavage by host protease furin, mature virus egresses from the cell via exocytosis.

The released viral genome is translated by host cell machinery at the ER into a single polyprotein. Together with host proteases, NS2B-NS3 protein cleaves the polyprotein into individual viral components. After cleavage, C protein remains anchored on the cytoplasmic side of ER while prM and E proteins are on the luminal side. Non-structural 1 (NS1) protein is released into the ER lumen and continues further post-translational modification. Non-structural 5 (NS5) protein with RNA-dependent RNA polymerase activity binds to positive-stranded viral genome and synthesizes the minus-strand RNA, forming the double-stranded RNA replicative form (RF). This RF then serves as template for new RNA synthesis in a replication complex composed of NS3-NS5 proteins, host proteins and other NS proteins (Uchil & Satchidanandam, 2003; Westaway *et al.*, 1997b). During flavivirus replication, extensive membrane rearrangement forming membranous structures such as vesicle pockets, convoluted membranes, and paracrystalline arrays are observed (Ng, 1987; Welsch *et al.*, 2009). It is believed that this extensive virus-induced membranous structure at the perinuclear region facilitates efficient synthesis, processing and assembly of virus particles (Mackenzie & Westaway, 2001; Ng, 1987).

During maturation, C proteins oligomerize, bind to viral genome and assemble into nucleocapsids in the cytoplasm (Khromykh & Westaway, 1996; Ma *et al.*, 2004). Physical nucleocapsid particles of WNV were first visualized accumulating in the infected Vero cells at 8 hr post-infection using cryo-immunoelectron microscope (Ng *et al.*, 2001). However, the exact mechanism of encapsidation and nucleocapsid formation is still unclear. It is still shrouded in mystery whether C protein-RNA binding, homo-oligomerization of C protein, and nucleocapsid formation are well-controlled sequential events or just spontaneous concurrent occurrence.

From the cytoplasm, nucleocapsid buds into ER lumen and is then surrounded by a 10 nm-thick host cell-derived lipid bilayer membrane anchored with 180 prM and E proteins each (Zhang *et al.*, 2003). This immature form of virion is transported via kinesin along microtubules towards plasma membrane via Trans-Golgi network (TGN) where host protease furin cleaves prM protein to produce mature virion (Chambers *et al.*, 1990; Chu & Ng, 2002; Stadler *et al.*, 1997). The mature viruses egress from the cells via exocytosis with the help of actin filaments (Chu *et al.*, 2003; Ng *et al.*, 1994).

1.4. Dengue Virus Capsid Protein

DENV capsid (C) protein is the focus of this project. This protein is the first structural protein found in the ORF of flaviviral genome. The C-terminal hydrophobic signal sequence of full-length C protein is cleaved by its NS2B-NS3 proteins at the anchC/prM cleavage site to generate mature DENV C protein (Amberg & Rice, 1999a; Markoff, 1989). However, the binding of NS2B-NS3 protein with C protein and how it cleaves polyprotein at anchC/prM site is unclear.

Capsid (C) protein has a molecular weight of about 12 kDa and it is a highly basic protein containing about 25 % of lysine and arginine residues (Henchal & Putnak, 1990). The high basic-residue content confers its RNA binding property to neutralize the negatively-charged viral RNA (Lindenbach *et al.*, 2007). It is believed that C protein interacts with the 3 end of the viral RNA to prevent recognition by RNA polymerase whereas 5 end is still able to bind to ribosome to start translation continuously (Westaway, 1987). Capsid (C) proteins encapsidate its viral RNA and form a spherical cage-like structure called nucleocapsid or core. The core is

approximately 30 nm in diameter which can be seen as a dense particle under electron microscope (Hase *et al.*, 1987).

The sequence homology of C proteins among other flaviviruses is poorly conserved. As shown in Figure 1.8, only eleven amino acids are conserved among the nine mosquito-borne flaviviral C proteins. According to the sequence distance analysis using ClustalV method (Higgins *et al.*, 1992; Higgins & Sharp, 1989) in the MegAlign, DNASTAR Lasergene 7.2 software, the sequence similarity among the nine flaviviral C proteins is mostly lower than 50 % and the sequence divergence is more than 100 % (Figure 1.9). The C proteins of all DENV serotypes share approximately 55-80 % amino acid sequence identity but diverge greatly (120-200 %) from other flaviviruses. The C proteins of JEV, MVEV (Murray Valley encephalitis virus), UV (Usutu virus) and WNV shares about 60 % amino sequence identity, implicating that they are more closely related to each other as compared to DENV. Nonetheless, the flaviviruses C protein is structurally and functionally similar throughout the genus.

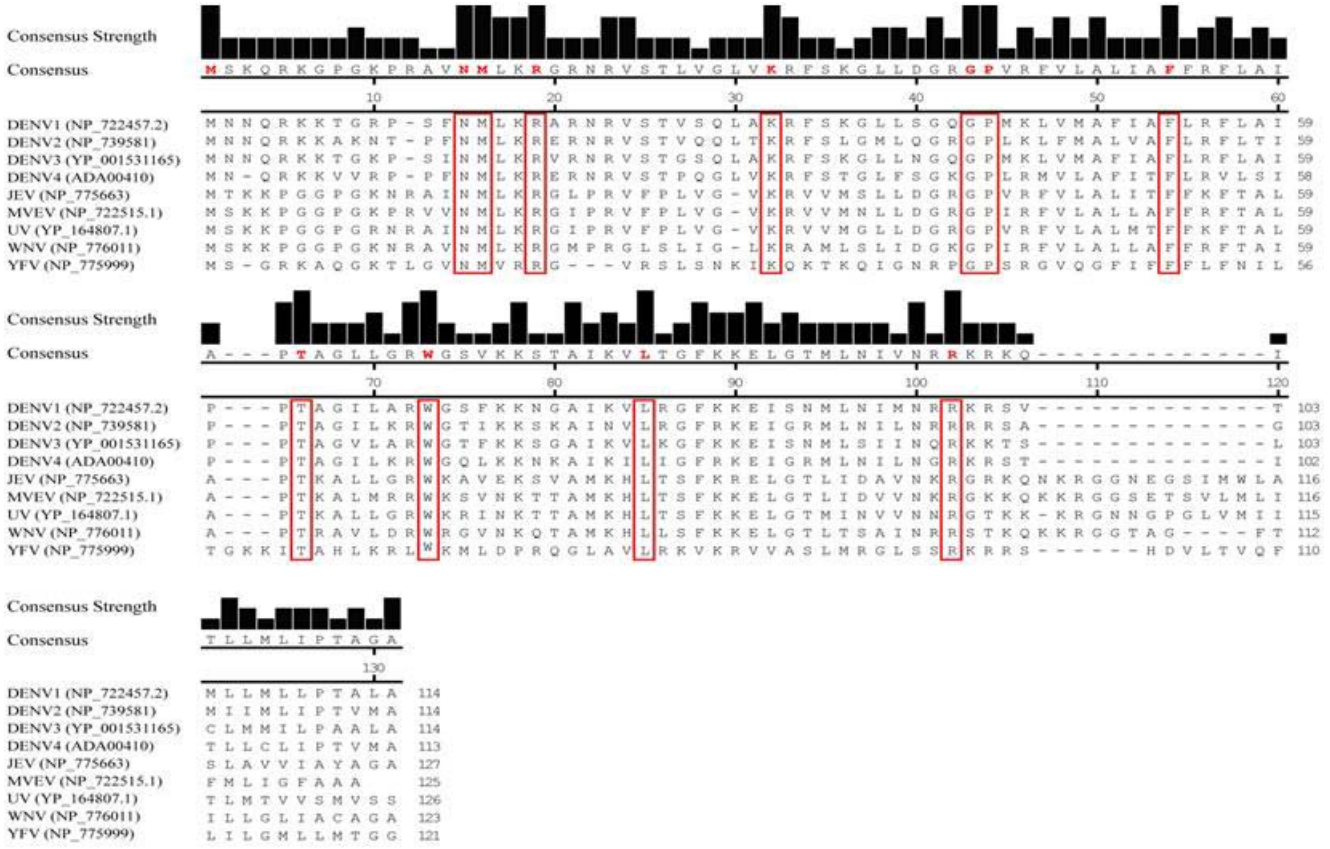

Figure 1.8: Multiple sequence alignment of mosquito-borne flaviviral C protein sequences. ClustalW method in MegAlign, DNASTAR Lasergene 7.2 software is used to perform multiple sequence alignment. Sequences with the highest consensus strength among the nine flavivirus C proteins are highlighted. (DENV1-4 – Dengue virus serotype 1-4; JEV – Japanese Encephalitis virus; MVEV – Murray Valley encephalitis virus; UV – Usutu virus; WNV – West Nile virus; YFV – Yellow Fever virus; Accession number of the protein sequence is shown in the bracket.)

Percent Identity

	1	2	3	4	5	6	7	8	9		
1		69.3	82.5	68.1	35.4	36.9	36.3	38.9	27.3	1	DENV1 (NP_722457.2)
2	39.4		61.4	69.0	31.9	30.6	33.6	33.6	20.9	2	DENV2 (NP_739581)
3	20.0	53.7		58.4	37.2	37.8	36.3	38.9	27.3	3	DENV3 (YP_001531165)
4	41.4	39.9	59.9		36.6	35.5	40.2	37.5	22.7	4	DENV4 (ADA00410)
5	130.7	148.8	122.9	125.3		73.6	72.2	64.2	25.6	5	JEV (NP_775663)
6	123.8	156.0	120.0	130.5	32.6		71.8	66.1	26.1	6	MVEV (NP_722515.1)
7	126.7	139.4	126.7	110.8	34.7	35.4		58.2	23.1	7	UV (YP_164807.1)
8	115.6	139.4	115.6	121.4	48.3	44.9	60.3		24.8	8	WNV (NP_776011)
9	179.0	234.0	179.0	215.0	192.5	188.6	212.0	197.0		9	YFV (NP_775999)
	1	2	3	4	5	6	7	8	9		

Divergence

Figure 1.9: Sequence distances analysis of flaviviral C proteins. Sequence distances analysis using ClustalV method shows that the protein sequence similarities among the nine flavivirus C proteins are mostly lower than 50 % and the sequence divergence is more than 100 %. The percent identity refers to the percentage of sequence similarity between two sequences whereas the divergence percentage is obtained by comparing two sequences in relation to their relative positions in the phylogenetic tree. (DENV1-4 – Dengue virus serotype 1-4; JEV – Japanese Encephalitis virus; MVEV – Murray Valley encephalitis virus; UV – Usutu virus; WNV – West Nile virus; YFV – Yellow Fever virus; Accession number of the protein sequence is shown in the bracket.)

1.4.1. Structure of dengue virus capsid protein

Although the structure for the whole nucleocapsid is not documented yet, nuclear magnetic resonance structural studies revealed that C protein is a dimeric alpha-helical protein (Jones *et al.*, 2003). As illustrated in Figure 1.10(A), the monomer of DENV C protein contains four α helices (α1-4) with an internal hydrophobic domain flanked by positively-charged residues. First helix (α1) includes amino acids from 26 to 31; second helix (α2) from amino acids 45 to 55; third helix (α3) from amino acids 63 to 69 whereas fourth helix (α4) is the longest helix from amino acids 74 to 96. Regions between helices are composed of short loops. The internal hydrophobic domain encompasses second and third helices (α2 & α3). Unfortunately, the N-terminus of C protein from amino acids 1 to 21 cannot be resolved due to its instability (Jones *et al.*, 2003).

According to the structure of DENV C protein, the second and fourth helices (α2 & α4) form most of the dimer contact surfaces [Figure 1.10(B)]. This dimer is stabilized by the extensive hydrophobic interactions on both the helices (α2 & α4) while major fraction of the hydrophilic regions are buried after dimerization. A conserved residue, W69, positions at the dimer interface is deemed to stabilize the dimeric α-helical structure. Bhuvanakantham and Ng (2005) also reported that internal hydrophobic segment between amino acid positions 26 and 69 is essential for the C-C homodimerization in WNV.

Crystal structure of WNV C protein revealed that C protein dimers organize into tetramers as shown in Figure 1.10(C) (Dokland *et al.*, 2004). Dokland and his colleagues (2004) suggested that C protein tetramers form the building blocks for nucleocapsid assembly as this structure shielded most of the hydrophobic regions, creating strongly positively-charged surfaces for RNA binding.

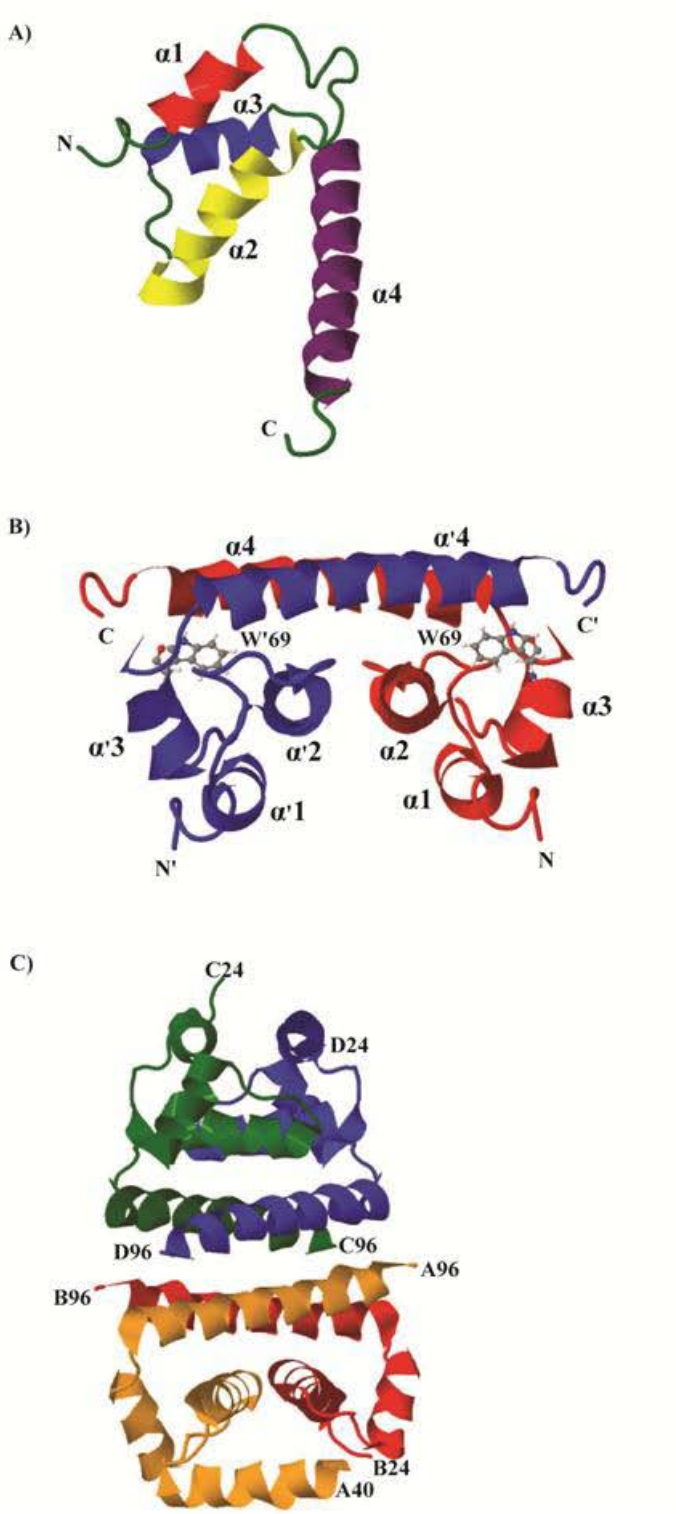

Figure 1.10: Structure of flaviviral C protein (Dokland *et al.*, 2004; Ma *et al.*, 2004). (A) Monomer of C protein contains four α-helices (α1, α2, α3 and α4) as indicated in four different colours. The C protein monomer shown only includes amino acid 21st to 100th. (B) Dimer of C protein is formed via the hydrophobic regions between second and forth helices (α2 - α′2 and α4 - α′4) stabilized residues W69. (C) Tetramer of C protein is formed by two dimers at the longest helix, α4. The images are reproduced by Jmol (http://www.jmol.org/) using RCSB (Research Collaboratory for Structural Bioinformatics) 1R6R.pdb and 1SFK.pdb files.

1.4.2. Structural functions of capsid protein

The main function of C protein is to encapsidate viral genomic RNA and form nucleocapsid during viral assembly. The RNA binding property of C protein was first reported for Kunjin strain of WNV (Khromykh & Westaway, 1996). They found that the positively-charged N-terminus and C-terminus of C protein were the RNA binding sites. This is further supported by Ma and colleagues' (2004) proposed model as shown in Figure 1.11. The hydrophilic surface formed by the fourth helices of the C protein dimer (α4 and α′4) interacts with viral RNA whereas the conserved hydrophobic cleft formed by the first and second helices (α1-α′1 and α2-α′2) interacts with viral membrane.

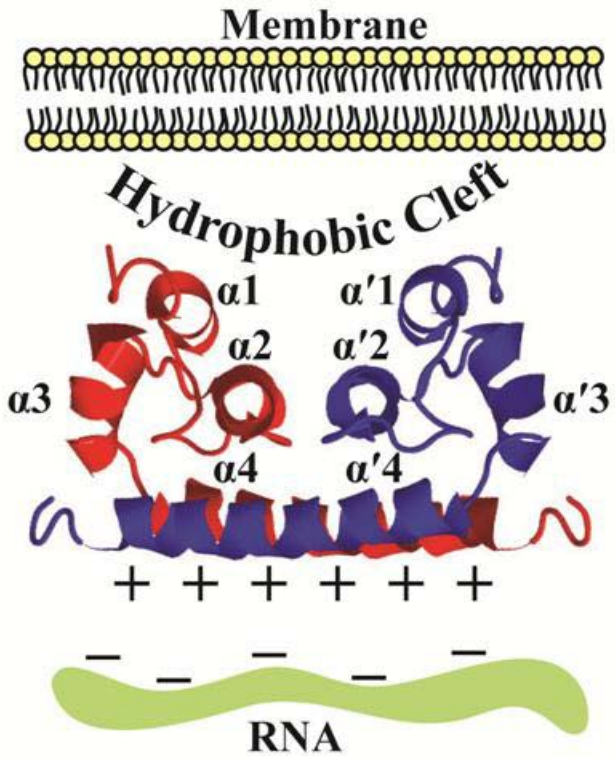

Figure 1.11: Proposed model of C protein interaction with viral RNA and nucleocapsid assembly. C protein dimer is shown in red and blue. The positively-charge surface formed by helices α4 - α′4 faces the negatively-charged viral RNA while the hydrophobic regions of C protein dimer face the lipid bilayer membrane. This diagram is modified from Ma and colleagues (2004).

Ivanyi-Nagy and colleagues (2008) demonstrated that C protein acted as RNA chaperone assisting in the proper folding of RNA by inducing RNA structural rearrangements via interaction with the N-terminal C protein. On the other hand, Zlotnick (2003) suggested that binding of RNA to C protein would elevate local C protein concentration and orientate C protein for proper dimerization. Hence, the interaction between C protein and RNA is essential for both components. This could be an evolution of symbiotic relationship between two viral components in flavivirus.

According to Sindbis virus nucleocapsid assembly model, viral RNA contains an encapsidation signal facilitating RNA-C protein interaction which results in dimerization of C protein (Geigenmuller-Gnirke *et al.*, 1993). Such encapsidation signal was also found in the viral RNA of Hantaan virus and coronavirus (Cologna *et al.*, 2000; Severson *et al.*, 2001). These encapsidation signals are complex secondary conformations such as stem loops and bulges (Khromykh & Westaway, 1996). Nevertheless, how exactly flaviviral RNA binds to C protein and induces nucleocapsid assembly is still elusive.

1.5. Non-Structural Roles of Capsid Protein in the Cytoplasm

It is widely accepted that flaviviral C protein is a multifunctional protein. It is not surprising since it will be beneficial for the virus to encode multifunctional proteins with its limited genomic content. Patkar and colleagues (2007) showed that C protein has a great functional flexibility although all the roles of C protein are not fully discovered yet. Studies are still on-going to uncover the non-structural roles of this multifunctional protein.

Recently, it was discovered that WNV and DENV C protein interact with human Sec3 exocyst protein (hSec3p) in the cytoplasm to antagonize the antiviral

effect caused by hSec3p (Bhuvanakantham *et al.*, 2010b). Human Sec3p is an exocyst component involved in the secretory pathways and exocytosis process. It was found that hSec3p affected flaviviral RNA transcription and translation via the sequestration of elongation factor 1 alpha (EF1α). Flaviviral C protein was able to antagonize this host-antiviral effect via direct binding to hSec3p and caused degradation of hSec3p, thereby releasing EF1α for viral RNA and protein synthesis.

1.6. Nuclear Phase of Capsid (C) Protein

Although positive-strand RNA viruses could exploit host cellular components to replicate in the cytoplasm, C proteins can also be visualized in the nucleus during replication (Tadano *et al.*, 1989; Yasui *et al.*, 1998). This observation implies that C protein might have potential non-structural roles in the nucleus. For other viruses such as HCV, C proteins were shown to localize in the nucleus / nucleolus of hepatocytes via immunoelectron microscopic study (Falcon *et al.*, 2003). Moreover, other non-structural proteins such as DENV NS5 (Kapoor *et al.*, 1995), Kunjin virus NS4B (Westaway *et al.*, 1997a), Semliki Forest virus nsP2 (Peranen *et al.*, 1990) and HCV NS3 (Muramatsu *et al.*, 1997) have been reported to localize in the nucleus / nucleolus of infected cells too.

1.6.1. Roles of nuclear localization signal

At least one putative nuclear localization signal (NLS) motif has been detected within all flaviviral C protein sequences but full characterization was not done (Chang, 1997). Nuclear localization signal was first discovered in Simian Vacuolating Virus 40 (SV40) Large Tumor Antigen (T-antigen). It is basically a stretch of protein sequence that is rich in basic residues, especially lysine and arginine. There are two

types of classical NLS – monopartite NLS, namely one short region of about four to five basic residues, and bipartite NLS which consists of two regions of basic residues separated by 10 to 12 random residues (Dingwall & Laskey, 1991).

Wang and co-workers (2002) discovered that a bipartite NLS motif, located at amino acids 85 to 100, was responsible for nuclear localization of DENV C protein. However, Mori and colleagues (2005) claimed that substitutions of Gly^{42} and Pro^{43} to alanine could also completely abolish the nuclear localization of DEVN C protein. This result contradicted with Wang and colleagues (2002) in which deletion of the first 45 amino acids at the N-terminus was reported to have no effects on the nuclear localization of DENV C protein. Another study using DENV infectious clones revealed that double alanine-substitutions mutation of residues (Lys^{73} and Lys^{74}) and (Arg^{85} and Arg^{86}) completely eliminate nuclear translocation ability of C protein while mutations on residues (Lys^{6} and Lys^{7}) and (Arg^{97} and Arg^{98}) reduced nuclear localization of C protein (Sangiambut *et al.*, 2008). Hence, residues (Lys^{6} and Lys^{7}) which are within the first 45 amino acids from the N-terminal C protein did play a role in the nuclear localization of C protein.

Other than the classical NLS, Suzuki and co-workers (2005) showed that HCV C protein contains non-classical NLS whereby at least two out of three basic-residue clusters are required for efficient nuclear localization. Although Sangiambut and his colleagues (2008) demonstrated that nuclear localization ability of C protein did not correlate with viral growth properties, Bhuvanakantham and co-workers (2009) showed that deletion of NLS from WNV C protein completely inhibited virus production. Thus, NLS indeed plays an essential role in nuclear localization of flaviviral C proteins which in turn is important for virus replication.

1.6.2. Roles of importin-α/β proteins and phosphorylation

It is widely accepted that NLS is important for nuclear protein import through the help of importin-α/β proteins (Friedrich *et al.*, 2006; Reguly & Wrana, 2003; Weis, 1998; Whittaker & Helenius, 1998). Karyopherins, including both importins and exportins, are responsible for majority of the nucleo-cytoplasmic trafficking in the cell. Importin-α protein binds to NLS-bearing protein and functions as an adapter to bind to importin-β protein. Importin-β protein docks the whole complex at the nuclear pore complex (NPC) and facilitates its translocation into the nucleus. Nuclear import of NLS-bearing proteins is an energy-dependent process (Gorlich & Mattaj, 1996).

It was shown that DENV NS5 protein contains two functional NLS motifs at the central region which were recognized by importin-α/β proteins (Brooks *et al.*, 2002; Pryor *et al.*, 2007). The NLS motifs of HCV C protein were shown to bind to importin-α protein (Suzuki *et al.*, 2005). Bhuvanakantham and colleagues (2009) also showed that there was a direct binding between WNV C protein and importin-α protein using mammalian 2-hybrid (M2H) assay. The binding efficiency of C protein to importin-α protein would affect nuclear translocation of C protein.

In addition, it was reported that phosphorylation also played an important role in the importins-mediated transportation of nuclear proteins. Phosphorylation was shown to enhance transportation of nuclear protein but the phosphorylated residues were not involved in the binding of importin-α protein (Fontes *et al.*, 2000). The C protein of HCV was also demonstrated to be phosphorylated. Mutation analyses showed that phosphorylation of HCV C protein at residue Ser 53 and Ser 116 was important to regulate nuclear localization of C protein (Lu & Ou, 2002). Bhuvanakantham and colleagues (2010a) also reported that nuclear localization of WNV (Sarafend) C protein was influenced by phosphorylation, which in turn affected

the virus replication. Other than nuclear localization, phosphorylation was also required to regulate nucleocapsid assembly by affecting the binding of C protein to the viral genomic RNA (Cheong & Ng, 2011; Law *et al.*, 2003). Hence, it will be interesting to investigate the role of phosphorylation and importins in transporting DENV C protein into nucleus.

1.6.3. Possible non-structural roles of capsid (C) protein in the nucleus

To date, the significance of nuclear localization of C proteins still remains a mystery. Several studies have demonstrated that positive-stranded RNA viruses disrupt nucleo-cytoplasmic trafficking by inhibiting nuclear import of some nuclear proteins during virus infection (Gustin & Sarnow, 2006; Hiscox, 2003). It is believed that this redistribution of nuclear protein into cytoplasm is to inhibit antiviral response. However, viral protein that is responsible for this nucleo-cytoplasmic disruption has not been found yet and the exact role of nuclear protein redistribution is unclear. Since Bhuvanakantham and colleagues (2009) reported that nuclear localization of WNV C protein was essential for the virus replication, it is important to unravel the non-structural roles of C protein in the nucleus for better understanding of the pathogenesis of flaviviruses.

1.7. Objectives

Dengue virus (DENV) is a positive-stranded RNA virus. Based on the current understanding of flaviviral replication cycle, host cell nucleus is not involved during the transcription, translation and assembly of virus. This traditional notion is challenged when capsid (C) protein is found to localize in the infected cell nucleus. Since then, the role of DENV C protein in the nucleus has been an intriguing mystery for researchers to unveil. Understanding the roles of C protein in the nucleus will not only completes the missing puzzle of flaviviral replication cycle, but also provides insights for novel anti-viral strategies development. This study aims to decipher the nuclear transportation mechanism of C protein and to discover novel non-structural roles of C protein in the nucleus.

The specific objectives of this study are as follows:

1. Determine the functional role of nuclear localization signal motif of DENV C protein
2. Identify the transporting partners of DENV C protein during nuclear translocation
3. Express and purify full-length DENV C protein for ProtoArray® screening
4. Perform high-throughput screening for novel interacting partners of DENV C protein via ProtoArray® technology-based platform
5. Validate and examine the roles of the identified interacting partners of DENV C protein in the nucleus

2. Materials and Methods

2.1. Cell Culture Techniques

All cell culture and media preparation works were performed in a Class II Type A2 Biosafety Cabinet (ESCO, Singapore) and cells were kept in a humidified 37 ^{o}C incubator (Thermo Fischer Scientific, USA) supplied with 5 % carbon dioxide.

2.1.1. Cell lines

Five cell lines were used in this project, namely Baby Hamster Kidney (BHK)-21 cells, mosquito C6/36 cells, Human Embryonic Kidney (HEK)-293 cells, 293FT cells and HeLa cells. Table 2.1 shows the origin, usage and the types of media used for each cell line. All media are supplemented with 10 % fetal calf serum [(FCS) (PAA Laboratories GmbH, Austria)].

Table 2.1: Cell lines and media used in this project

Cell line	Medium	Origin	Usage
Baby Hamster Kidney cells (BHK-21)	RPMI (Appendix 1a)	American Type Culture Collection, USA	• Plaque assay • Molecular studies • Imaging • Cell cycle analyses
Mosquito C6/36 cells derived from *Aedes albopictus*	L-15 (Appendix 1b)	Kind gift from late Emeritus Professor Edwin G. Westway, Australia	• Virus culture • Cell cycle analyses
Human Embryonic Kidney cells (HEK293)	DMEM (Appendix 1c)	American Type Culture Collection, USA	• Molecular studies • Cell cycle analyses
Human Embryonic Kidney FT cells (293FT)	DMEM-293FT (Appendix 1d)	Life Technologies (Catalog number: R700-07)	• Molecular studies • Protein expression
HeLa cells	DMEM (Appendix 1c)	American Type Culture Collection, USA	• Molecular studies • Imaging

2.1.2. Propagation of cell lines

Confluent flasks of the cell lines were sub-cultured into a new T-75 flask at a ratio of 1:3 for C6/36 cells or 1:10 for BHK-21, HEK293, 293FT and HeLa cells. Old growth medium [BHK-21 cells – RPMI growth medium (Appendix 1a); C6/36 cell – L-15 growth medium (Appendix 1b); HEK293 and HeLa cells – DMEM growth medium (Appendix 1c); 293FT cells – DMEM 293FT growth media (Appendix 1d)] was discarded and the cell monolayer was rinsed with 5 ml of phosphate-buffered saline [(PBS) (Appendix 1e)]. Two ml of trypsin (Appendix 1f) was added and the cell monolayer was incubated at 37 ^{o}C for 2 to 5 min to detach the cells. Cells were then dislodged by gentle tapping the flask. Eight ml of fresh growth medium (Appendices 1a – 1d) was added to the flasks to deactivate the enzymatic activities and the trypsinized cells were resuspended by pipetting up and down for a few times. Resuspended cells were aliquoted appropriately according to the required ratio and the final volume was topped up to 12 ml with respective fresh growth medium (Appendices 1a – 1d). C6/36 cells were grown at 28 ^{o}C while all other cell types were cultured at 37 ^{o}C.

2.1.3. Cultivation of cells in 24-well and 6-well tissue culture plates

Confluent monolayer of mammalian cells in a T-75 flask was used to seed on 24-well or 6-well tissue culture plates (Greiner Bio-One, St. Loius, USA). The monolayer cells were treated as previously described in Section 2.1.2 to obtain single-cell suspension. The number of viable cells in the suspension was determined using haemocytometer. Approximately 2 x 10^5 cells or 1 x 10^6 cells were pipetted into each well of the 24-well or 6-well plate, respectively. The plates were placed in a tray and

incubated at 37 ^{o}C in a humidified incubator with 5 % carbon dioxide. The cells were ready for use when they were about 80-90 % confluent.

2.1.4. Cultivation of cells on coverslips in 24-well tissue culture plates

Sterile coverslips (Marienfeld, Germany) were placed into the wells of a 24-well tissue culture plate using a sterile forceps. Coating of coverslip with poly-D-lysine was required for HEK293 cells. Single-cell suspension was prepared according to Section 2.1.2 and the number of viable cells was determined via haemocytometer. Approximately 2 x 10^5 cells were seeded onto one coverslip and the whole plate was incubated at 37 ^{o}C until they reached about 80-90 % confluency.

2.2. Virus Works

All virus works were performed in a Class II Type A2 Biosafety Cabinet (ESCO, Singapore) located in a dedicated virus culture room. Dengue virus (DENV) serotypes 1-4 were Singapore strains which were kind gifts from the Environmental Health Institute of Singapore (EHI). West Nile virus (WNV) was Sarafend strain, a generous gift from late Emeritus Professor Edwin George Westaway from Australia. Both DENV and WNV were propagated in C6/36 mosquito cell lines.

2.2.1. Preparation of virus stock

Monolayers of C6/36 cells with 90 % confluency were grown in T-75 flask prior to DENV or WNV infection. Old L-15 growth medium (Appendix 1b) was discarded and the cell monolayer was washed with virus diluent (Appendix 2a). One ml of virus suspension was added onto the cell monolayer and incubated at 37 ^{o}C for 1 hr with rocking at 15 min interval to ensure even infection. After 1 hr incubation,

15 ml of L-15 growth medium (Appendix 1b) supplemented with 2 % foetal calf serum (FCS) was added into the flask and incubated at 28 ^{o}C. WNV and DENV were harvested on Day 3 and Day 4 post-infection (p.i.), respectively. Syncytial was observed in DENV-2 infection on C6/36 cells. At the time of harvesting, the supernatant was adjusted to pH of 7.2 and aliquoted into sterile cryovials. All the cryovials were snap-freezed in cold ethanol and kept at -80 ^{o}C until further used.

2.2.2. Plaque assay

Monolayers of BHK cells were grown in 24-well plate until 80 % or 90 % confluency for DENV or WNV, respectively. Virus stock was thawed and 10-fold serial dilutions of the virus were made using virus diluent. Growth media in the plates were discarded and washed with virus diluent. One hundred µl of the diluted virus were added into triplicate wells and incubated at 37 ^{o}C for 1 hr with rocking at 15 min intervals. Virus diluent was used in control wells. After 1 hr absorption, excess viruses were removed and 1 ml of overlay medium (Appendix 2b) was added into each well. The plates were incubated at 37 ^{o}C for 3 (WNV) or 5 (DENV) days before they were stained with crystal violet (Appendix 2c) for at least 3 hr at room temperature. The plates were then washed thoroughly with water and dried before counting the plaques.

2.2.3. Infection of cell monolayer for virus study

Appropriate amount of BHK cells, HEK293 cells, 293FT cells or HeLa cells were seeded into T-25 flask according to Section 2.1.2. When the cells were ready for infection, cell culture supernatant was discarded and the monolayer was rinsed with 3 ml virus diluent (Appendix 2a). Five hundred µl of virus suspension was used to

infect the cell monolayer at multiplicity of infection (M.O.I.) of one. For mock-infected cells, 500 µl of virus diluent was used. During the incubation at 37 ^{o}C, flasks were rocked at every 15 min to ensure even infection. After 1 hr incubation, remaining viruses were removed and washed with PBS before topping up with 5 ml of growth media supplemented with 2 % FCS. The infected cells were incubated at 37 ^{o}C until the appropriate harvesting time.

2.3. Molecular Techniques

2.3.1. Construction of green fluorescent protein (GFP)-tagged Dengue virus (DENV)-2 capsid (C) protein and nuclear localization signal (NLS) motif plasmids

DENV-2 (accession number: M29095) RNA was extracted using QIAmp® Viral RNA Mini kit (Qiagen, Germany) and the first strand cDNA was synthesized using SuperScriptTM III reverse transcriptase (Life Technologies, USA). The DENV-2 capsid (C) protein cDNA coding sequence (nucleotide 100-438) was then amplified using Advantage 2 polymerase mix (Clontech, USA). The DNA sequences of primers used, DENV2C (F) and DENV2C (R), are listed in Table 2.2. The PCR cycling profile was 2 min of initial denaturing step at 94 ^{o}C followed by 29 cycles of denaturation at 94 ^{o}C for 1 min, annealing at 55 ^{o}C for 30 sec and extension at 72 ^{o}C for 1 min. After 29 cycles, a final extension step was carried out at 72 ^{o}C for 7 min.

The PCR products were separated using 2 % agarose gel (Appendix 3a) in Tris/Acetate/EDTA (TAE) buffer (Appendix 3b) and purified using QIAquick® gel extraction kit (Qiagen, Germany) according to the manufacturer's protocol. The purified PCR products were then ligated with GFP Fusion TOPO vector (Life Technologies, USA) and the ligated product was incubated with TOP10 competent

cells (Life Technologies, USA) on ice for 30 min. The plasmid map of GFP Fusion TOPO vector is shown in Figure 2.1. The expression of DENV C protein in mammalian cells is under the control of human cytomegalovirus (CMV) promoter. The cells were heat shocked at 42 ^{o}C for 45 sec and incubated on ice immediately for 2 min. Super optimal broth with catabolic repressor (SOC) medium (Life Technologies, USA) was added to the competent cells and incubated at 37 ^{o}C shaker for 1 hr. Recovered competent cells were spread on Luria-Bertani (LB) agar plate (Appendix 3c) containing ampicillin antibiotic and incubated overnight at 30 ^{o}C incubator. Colony PCR was carried out to identify positive clones. Positive clones were incubated overnight in 2 ml of LB broth (Appendix 3d) containing ampicillin and the plasmid DNA were isolated using QIAprep Spin Miniprep kit (Qiagen, Germany).

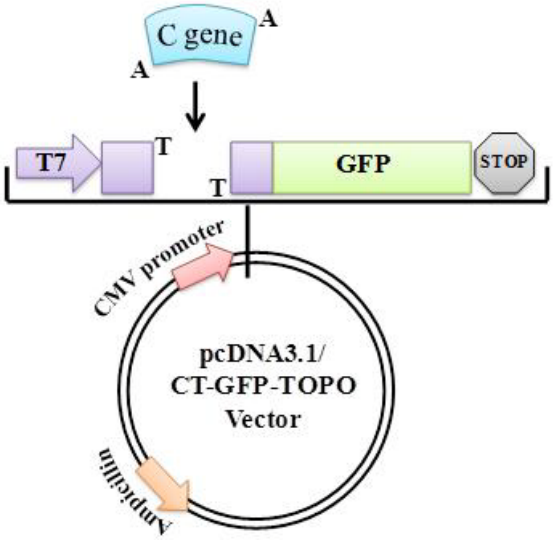

Figure 2.1: Plasmid map of GFP-tagged DENV C gene. DENV C gene is inserted into pcDNA3.1/CT-GFP-TOPO vector via TA cloning. The 3 -A overhang on the C gene is ligated with the 3 -T overhang on the linearized plasmid vector. Green fluorescent protein (GFP) is fused to the C protein at the C-terminus. The expression of this protein construct in mammalian cells is under the control of human cytomegalovirus (CMV) promoter. Bacteria transformed with this plasmid can be cultured in LB broth containing ampicillin antibiotic.

Nuclear localization signal (NLS) motifs of DENV C proteins were also cloned into GFP Fusion TOPO vector via the same protocol using the constructed DENV-2 C plasmid as template. The sequences of DENV2NLS primers are shown in Table 2.2. Since the PCR products for NLS motifs only contain approximately 60 nucleotides, the PCR products were used directly for ligation with the pcDNA3.1/CT-GFP-TOPO vector. To visualize the molecular size of the NLS motif PCR products, 8 % non-denaturing polyacrylamide gel (Appendix 3e) and Tris/Borate/EDTA (TBE) buffer (Appendix 3f) were used. Positive clones were sent for DNA sequencing to confirm the orientation of the insert and to check for mutation.

Table 2.2: Primers used for generation of GFP-tagged DENV C protein and NLS motifs. Kozak sequences (translational start site) are underlined. DENV2 denotes Dengue virus serotype-2 while C and NLS denote capsid and putative bipartite nuclear localization signal, respectively. The numbers behind NLS refer to the amino acid positions in the C protein. F denotes forward primer while R denotes reverse primer.

Name	Sequence (5′-3′)
DENV2C (F)	CACCATGGATGACCAACGGAAAAA
DENV2C (R)	CCGCCATCACTGTTGGAAT
DENV2NLS5-22 (F)	CACCATGGGGCGGAAAAAGGCGAGAAAC
DENV2NLS5-22 (R)	CGCGGTTTCTCTCGCGTTT
DENV2NLS85-101 (F)	CACCATGGGGAGGAAAGAGATTGGAAGGA
DENV2NLS85-101 (R)	CAGTTCTACGTCTCCTGTT

2.3.2. Site-directed mutagenesis

QuickChange® II Site-Directed Mutagenesis kit (Stratagene, USA) was used for mutagenesis on the full-length DENV-2 C vector constructs according to the manufacturer's protocol. Briefly, *PfuUltra* HF DNA polymerase was mixed with plasmid DNA template, forward primer, reverse primer, and dNTP mix. The sequences of forward and reverse primers for mutagenesis are listed in Table 2.3. The mixture was then subjected to mutagenesis cycling profile. An initial denaturing step was conducted at 95 ^{o}C for 30 sec, followed by 18 cycles of 30 sec of denaturing step

at 95 ^{o}C, 1 min of annealing at 55 ^{o}C and 7 min of extension at 68 ^{o}C. Subsequently, *DpnI* restriction enzyme was added to digest the parental methylated DNA template before the final product was transformed into the supercompetent cells provided in the kit. Positive clones on LB agar plate (Appendix 3c) containing ampicillin antibiotic were cultivated and the plasmid DNA was isolated using QIAprep Spin Miniprep kit (Qiagen, Germany). Extracted plasmids were sent for sequencing to check for correct mutation and no other additional unwanted mutations.

Table 2.3: Primers used for site-directed mutagenesis. mtC represents the mutation of putative NLS in the full-length capsid clone. The numbers stated denote the amino acid residue positions that were mutated to alanine. F denotes forward primer while R denotes reverse primer.

Name	Sequence (5′-3′)
mtC5/6F	ACCATGGATGACCAAGCGGCGAAGGCGAGAAACACG
mtC5/6R	CGTGTTTCTCGCCTTCGCCGCTTGGTCATCCATGGT
mtC17/18F	CCTTTCAATATGCTGGCGGCGGAGAGAAACCGCGTG
mtC17/18R	CACGCGGTTTCTCTCCGCCGCCAGCATATTGAAAGG
mtC42/43F	ATGCTGCAGGGACGAGCAGCATTAAAACTGTTCATG
mtC42/43R	CATGAACAGTTTTAATGCTGCTCGTCCCTGCAGCAT
mtC85/86F	GTTTTGAGAGGGTTCGCGGCGGAGATTGGAAGGATG
mtC85/86R	CATCCTTCCAATCTCCGCCGCGAACCCTCTCAAAAC
mtC97-100F	CTGAACATCTTGAACGCGGCAGCCGCAACTGCAGGCATG ATC
mtC97-100R	GATCATGCCTGCAGTTGCGGCTGCCGCGTTCAAGATGTTC

2.3.3. Generation of FLAG-tagged Dengue virus (DENV)-2 capsid (C) protein plasmid

To express FLAG-tagged C protein in mammalian system, DENV-2 C gene was cloned into pFLAG-CMV-3 mammalian expression vector (Sigma, USA). DENV-2 C gene was amplified from the DENV-2 cDNA obtained from Section 2.3.1 using FlagDENCF2 and FlagDENCR primers (Table 2.4). A thrombin cleavage site was included at the N-terminus of C protein. The PCR products were electrophoresed in a 2 % agarose gel (Appendix 3a) and the correct band was excised for gel purification. The purified PCR product was then used as template for overlap

extension-PCR to insert one more FLAG peptide at the N-terminus. FlagDENCF1 and FlagDENCR primers (Table 2.4) were used for this OE-PCR. Final PCR product was also purified via gel purification. Restriction enzymes *HindIII* and *BamHI* (New England Biolabs, USA) were used to cut the PCR product and pFLAG-CMV-3 vector at 37 ^{o}C for 4 hr. After PCR purification, ligation was performed using ligase (Promega, USA) according to the manufacturer's protocol. Positive colonies were inoculated into LB broth (Appendix 3d) containing ampicillin and extracted plasmids were sent for DNA sequencing.

Table 2.4: Primers used for cloning of FLAG-tagged DENV C protein. Restriction enzyme recognition sites are highlighted in **BOLD** and overlapping sites are underlined. F denotes forward primer while R denotes reverse primer.

Name	Description	Sequence (5′-3′)
FlagDENCF1	Forward primer with *HindIII* cut site at the 5′-end and an additional FLAG peptide	GACGAC**AAGCTT**GACTAC AAAGACGATGACGACAA GGGAC
FlagDENCF2	Forward primer for priming out DENV C protein from DENV-2 cDNA with thrombin cleavage site at the N-terminus and part of the FLAG peptide for OE-PCR	CGACAAGGGACTAGTACC GCGCGGCAGCATGAATAA CCAA
FlagDENCR	Reverse primer for priming out DENV C protein from DENV-2 cDNA with *BamHI* cut site	TCACCG**GGATCC**TCATTA CTACGCCATCACTGTT

2.3.4. Construction of biotinylated Dengue virus (DENV)-2 capsid (C) protein (pET28aDENVBioCap) plasmid

To express biotinylated DENV C protein in bacterial system, pET28aDENVBioCap plasmid was constructed. DENV C gene was amplified from cDNA synthesized from DENV-2 RNA using SuperScript^{TM} III First-Strand Synthesis System (Life Technologies, USA). Primers Biotin_F, Biotin_C_F, Biotin_C_R, and C_R (Table 2.5) were used to join signal peptide gene (Cull & Schatz, 2000) and an enterokinase cleavage site with DENV C gene via overlap

extension-PCR (OE-PCR). Gel-purified PCR products containing the joined fragments were subsequently ligated with expression vector, pET28a (Novagen, Germany) via *Nhe* I and *Xho* I cut sites. 6xHis tag and thrombin cleavage site were at the N-terminus of signal peptide followed by enterokinase cleavage site and DENV C protein was at the C-terminus. DNA sequencing was performed to verify the constructs.

Table 2.5: List of primers used for pET28aDENVBioCap plasmid construction. Letters in **BOLD** are restriction enzyme recognition sites while underlined letters are overlapping PCR sites. F denotes forward primer while R denotes reverse primer.

Primers	Description	Sequence (5′-3′)
Biotin_F	Forward primer for priming out signal peptide with *Nhe* I cut site	CTA**GCTAGC**TCCGGCCTGA ACGAC
Biotin_C_F	Forward primer for overlapping signal peptide and DENV C protein	GACGACGACAAGAGCATGA ATAACCAA
Biotin_C_R	Reverse primer for overlapping signal peptide and DENV C protein	TTGGTTATTCATGCTCTTGTC GTCGTC
C_R	Reverse primer for priming out DENV C protein from DENV cDNA with *Xho* I cut site	CCG**CTCGAG**TTACGCCATCA CTGT

2.3.5. Cloning of Dengue virus (DENV)-2 capsid protein tagged with activation domain (DENVC-AD) and importin alpha protein tagged with DNA-binding domain (Impα-DBD) for mammalian-2-hybrid (M2H) assay

To measure the binding efficiency between importin-α protein and various DENV C protein mutants, DENVC-AD and Impα-DBD plasmids were engineered. GFP-tagged DENV C proteins generated in Section 2.3.1 and mutants in Section 2.3.2 were used as templates whereas primers M2HDenCF and M2HDenCR (Table 2.6) were used to prime out DENV C genes. PCR products were gel purified, cut and ligated with pFN10A (ACT) vector (Promega, USA) via *Sgf* I (GCGATCGC) and

Pme I (GTTTAAAC) restriction enzyme sites. To obtain Impα-DBD, mRNA was first extracted from BHK cells using RNeasy® mini kit (Qiagen, Germany). cDNA was then synthesized using SuperScript™ III First-Strand Synthesis System (Life Technologies, USA) and oligo(dT) primers. M2HImpαF and M2HImpαR primers (Table 2.6) were used to amplify importin-α gene from the cDNA. PCR product was gel purified, cut, and ligated with pFN11A (BIND) vector (Promega, USA). Positives clones were sent for DNA sequencing to verify the constructs and correct orientation.

Table 2.6: Primers used for generating DENVC-AD and Impα-DBD plasmids. M2H denotes mammalian-2-hybrid while DenC and Impα represent DENV C protein and importin-α protein, respectively. F denotes forward primer while R denotes reverse primer. Restrictive enzyme sites are underlined.

Name	Sequence (5′-3′)
M2HDenCF	CGAAGCGATCGCCATGAATAACCAACGAAAAAAG
M2HDenCR	ATTAGTTTAAACCGCCATCACTGTTGGAATCA
M2HImpαF	CACCGCGATCGCCATGTCCACCAACGAGAATGC
M2HImpαR	TTGTGTTTAAACAAAGTTAAAGGTCCCAGGAGCC

2.3.6. Transfection

Baby Hamster Kidney (BHK) cells, Human Embryonic Kidney (HEK)-293 cells, 293FT cells or HeLa cells were seeded into 6-well plate according to Section 2.1.3 or onto coverslips in a 24-well plate according to Section 2.1.4 on the day before transfection. Vector constructs were transfected into the cells using Lipofectamine 2000 (Life Technologies, USA). A mixture of 0.8 µg of plasmid DNA and 2 µl of Lipofectamine reagent was incubated in 250 µl of Opti-MEM (Gibco BRL, USA) for 30 min at room temperature. Old media was discarded and the mixture was added into the wells for 5 hr incubation at 37 ^{o}C. After incubation, 1 ml of fresh RPMI-1640 growth medium (Appendix 1a) was added and incubated at 37 ^{o}C in 5 % CO_2 incubator (Nuaire, USA) for 24 hr.

2.3.7. Mammalian-2-hybrid (M2H) Assay

Baby Hamster Kidney (BHK) cells were seeded on 24-well plates as described in Section 2.1.4. DENVC-AD and Impα-DBD plasmids that were generated in Section 2.3.6 were co-transfected into BHK cells together with reporter vector [pGL4.31(*luc*2P/*GAL4U*AS/Hygro) (Promega, USA)] using Lipofectamine 2000 (Life Technologies, USA) as described in Section 2.3.6. Single transfection, positive controls (pACT-MyoD and pBIND-Id vectors) and negative controls (pACT and pBIND vectors) were also included. At 24 hr post-transfection, 5 x passive lysis buffer (PLB) provided in the dual-luciferase reporter assay kit (Promega, USA) was diluted and added into the wells to lyse the transfected cells. About 100 µl of Luciferase assay reagent II (LAR II) were mixed with 20 µl of cell lysates in a black flat-bottom 96-well plate. The firefly luciferase activity was measure using a luminometer (Promega, USA). Subsequently, 100 µl of Stop&Glo® reagent were added into the mixture. *Renilla* luciferase activity was measured. Mock-transfected cell lysates were used for measuring endogenous luminescence background, single-transfected cell lysates were used for respective luciferase activity baseline, and co-transfected cells were used to measure protein-protein binding efficiency. *Renilla* luciferase activity detected from the BIND-type vectors could be used to normalize transfection efficiency.

2.3.8. Real-time polymerase chain reaction (PCR)

Total RNA were isolated from transiently HEK293 transfected cells (Section 2.3.6) using RNeasy® mini kit (Qiagen, Germany). First strand cDNA was then synthesized from 2 µg of total RNA using SuperScript™ III First-Strand Synthesis System (Life Technologies, USA) and random hexamers. The first-strand cDNA was

diluted by a factor of 100 and mixed with Fast SYBR® Green master mix (Life Technologies, USA). Each reaction well consists of 10 µl of Fast SYBR® Green (2x), 1 µl of diluted cDNA, 0.4 µl of forward primer, 0.4 µl of reverse primer and 8.2 µl of diethylpyrocarbonate (DEPC)-treated water (Appendix 3g). The real-time PCR primers used in this project are listed in Table 2.7. Real-time PCR was carried out using ABI PRISM 7500 real-time PCR system (Applied Biosystems, USA). Glyceraldehyde 3-phosphate dehydrogenase (GAPDH) was used as housekeeping gene.

Table 2.7: Primers used for real-time PCR. F denotes forward primer while R denotes reverse primer.

Name	Sequence (5′-3′)
SRP19-F	GAAGGCGAATCCCCATAAGTAAG
SRP19-R	GCCTCTGTATTGGACATCACGA
DIMT1-F	GCTGGAGGACTCATGTTCAAC
DIMT1-R	CCTTGGGTCAAGTTCACAAGC
CDKN2AIP-F	CTTCCTCGGGTGCCGATAC
CDKN2AIP-R	ACCCCTTCATTGCTACTCGAT
FOXN3-F	TCGTTGTGGTGCATAGACCC
FOXN3-R	GTGGACCTGATGTGCTTTGATA
CCNB3-F	ATGAAGGCAGTATGCAAGAAGG
CCNB3-R	CATCCACACGAGGTGAGTTGT
VRK1-F	CTACCAACGAGCTGCAAAACC
VRK1-R	TCACTCCCAAAGCGATCCATTA
GADD45A-F	GAGAGCAGAAGACCGAAAGGA
GADD45A-R	CACAACACCACGTTATCGGG
DENV2-F	AAAAACTATGCTACCTGTGAG
DENV2-R	CATTTTCTGGCGTTCTGTG
GAPDH-F	CATGAGAAGTATGACAACAGCCT
GAPDH-R	AGTCCTTCCACGATACCAAAGT

2.3.9. Mutagenesis of Dengue virus (DENV) infectious clone

Dengue virus (DENV)-2 infectious clone, pDVWS601 (Gualano *et al.*, 1998; Pryor *et al.*, 2001), was a generous gift from Dr. Andrew Davidson, Bristol University, United Kingdom. Approximately 1.2 kb fragment containing C gene sequence was first cloned out from the infectious clone using DINBsrGIF and DINSphIR primers

(Table 2.8). *BsrG* I and *Sph* I restriction enzyme recognition cut sites were at the′5 and 3′ ends, respectively. This fragment was then ligated with pcDNA3.1/CT-GFP TOPO vector (Life Technologies, USA) to form a carrier plasmid. Mutations R(97-100)A were then introduced on the carrier plasmid as described in Section 2.3.2 using DIN97F and DIN97R primers (Table 2.8). After confirming the presence of introduced mutations on the carrier plasmid by sequencing, the 1.2 kb fragment was excised using restriction enzyme *BsrG* I and *Sph* I (Promega, USA) and ligated back to the original infectious clone backbone using T4 DNA ligase (Promega, USA). Positive clones were sent for full plasmid sequencing to ensure no additional mutations.

Table 2.8: Primers used for mutagenesis of DENV infectious clone. F denotes forward primer while R denotes reverse primer.

Name	Sequence (5′-3′)
DINBsrGIF	CCGCGTGTCGACTGTACAACAGCTGACAAA
DINSphIR	CATTTCCGACTGCATGCTCTTCCCCTGAGT
DIN97F	TGAACATCTTGAACGCGGCAGCCGCTACTGCAGGCATGAT
DIN97R	ATCATGCCTGCAGTAGCGGCTGCCGCGTTCAAGATGTTCA

2.3.10. *In vitro* synthesis of infectious RNA

About 5 μg of full-length / mutant infectious clone of DENV were linearized with *Xba I* restriction enzyme (Promega, USA). The linearized DNA was purified using QIAquick® PCR purification kit (Qiagen, Germany) according to the manufacturer's protocol. The purified linearized DNA was then used for *in vitro* synthesis of infectious RNA using T7 Ribomax™ large scale RNA production system (Promega, USA) and Ribo m^7G Cap Analogue (Promega, USA) according to the manufacturer's protocol. Briefly, the linearlized DNA was mixed with T7 reaction components and incubated at 37 ^oC for 4 hr. To obtain purified infectious RNA from the reaction, RNeasy® Mini kit (Qiagen, Germany) was employed. The infectious

RNA was then transfected into BHK cells according to Section 2.3.6 and virus progeny was harvested from the supernatant for growth kinetic analysis.

2.4. Microscopic Techniques

2.4.1. Direct immuno-fluorescence microscopy of fixed cells

Baby Hamster Kidney (BHK) cells were transfected with GFP-tagged vector constructs [full length C protein, NLS motifs and various NLS mutants] according to Section 2.3.6. At 24 hr post-transfection, the transfected cells were washed with 1 x PBS (Appendix 1e) and fixed with paraformaldehyde for 20 min at room temperature inside a fume hood. After fixation, 4',6'-diamidino-2-phenylindole [(DAPI) (Life Technologies, USA)] were used to stain the cell nuclei and the coverslips were mounted on glass slides using Prolong® Gold antifade reagent (Life Technologies, USA). The mounted samples were then viewed under an optical immunofluorescence microscope (IX-81, Olympus, Japan). A confocal microscope (C1si, Nikon, Japan) was used to analyze the z-axis planes and to obtain three-dimensional images of the transfected cells.

2.4.2. Indirect immuno-fluorescence microscopy of fixed cells

To study the localization of recombinant proteins, BHK cells or HeLa cells were transfected according to Section 2.3.6. For mock-transfected cells, only transfection reagent was added. At 24 hr post-transfection, transfected cells were fixed with 4 % paraformaldehyde for 20 min at room temperature. After permeabilization with 0.1 % Triton-X, 5 % skim milk or 1 % bovine serum albumin (BSA) in 1 x PBS (Appendix 1e) were used for blocking at 37 ^{o}C for 30 min. Primary antibody was diluted to 1.0 – 10 μg/ml in blocking buffer before it was used for

binding at 37 ^{o}C. After 1 hr incubation, primary antibody was decanted and the coverslips were washed thrice with 1 x PBS (Appendix 1e). Secondary antibody [Alexa Fluor-488 or Alexa Fluor-594 antibodies (Life Technologies, USA)] was also diluted to optimal concentration in blocking buffer and [(DAPI) (Life Technologies, USA)] was used for nuclear staining. After 1 hr incubation at 37 ^{o}C, the coverslips were washed with 1x PBS (Appendix 1e) and mounted on glass slides using Prolong® Gold antifade reagent (Life Technologies, USA). The slides were ready for viewing with confocal microscope (C1si, Nikon, Japan) after sealing the sides of coverslips with nail polish. [Mouse anti-DIMT1L (ab69434) and rabbit anti-SRP19 (ab131239) antibodies were purchased from Abcam, UK; mouse anti-FLAG (F3165) and rabbit anti-FLAG (F7425) antibodies were from Sigma, USA; mouse anti-Dengue 4G2 antibody (MAB10216) was purchased from Millipore, USA]

2.4.3. Live cell imaging

Time-lapse experiment was performed to visualize the localization of recombinant GFP-tagged DENV-2 C proteins in transfected BHK cells. Thirty-five-millimetre glass-bottom dish (WillCo Wells, Netherland) was used in this experiment. The BHK cells were transfected with 4 µg of plasmid DNA and 10 µl of Lipofectamine reagent according to Section 2.3.6. At 8 hr post-transfection, the glass-bottom dish was placed in Nikon Live Cell Imaging System (TE2000, Nikon, Japan) which contained a 37 ^{o}C incubation chamber with 5 % CO_2. After allowing the cells to equilibrate in the chamber for 1 hr, phase contrast and GFP fluorescence was captured at every half an hour interval for a total of 40 hr. A video was then produced using the images.

2.4.4. Effect of leptomycin B, H-89 dihydrochloride, and bisindolylmaleimide on Dengue virus (DENV) capsid (C) protein localization

Leptomycin B [(LMB) (Merck, Germany)], inhibitor of chromosomal region maintenance 1 (CRM1)-mediated export pathway, was used to inhibit the exportation of C proteins. H-89 dihydrochloride and bisindolylmaleimide (Bis) which are inhibitors of protein kinase A (PKA) and protein kinase C (PKC), respectively, were used to study the role of phosphorylation on nuclear localization of DENV C protein. Baby Hamster Kidney (BHK) cells were seeded on coverslips in a 24-well plate and were transfected with recombinant C-GFP plasmid according to Section 2.3.6. After transfection, LMB, H-89 dihydrochloride and Bis drugs was added to a final concentration of 1 nM, 10 µM and 10 nM, respectively. The transiently-transfected cells were incubated at 37 ^{o}C in 5 % CO_2 incubator for 24 hr. After 24 hr post-transfection, the cells were fixed with cold methanol, followed by nuclear staining with DAPI and the coverslips were then mounted on glass slides with Prolong® Gold antifade reagent. The localization of C proteins was examined under fluorescence microscope (IX-81, Olympus, Japan).

2.4.5. Co-localization analysis

The signal intensities of the fluorochromes were analyzed with ImageJ software (http://rsbweb.nih.gov/ij/). Images of Alexa Fluor-488 and Alexa Fluor-594 were cropped for co-localization analysis using the JACoP plugin (Bolte & Cordelieres, 2006). Cytofluorogram was generated and the post-thresholding Pearson's coefficient was obtained. The cytofluorogram indicated the correlation of the two fluorochromes and the spread of the dots distribution with respect to the fitted line refered to the Pearson's coefficient. Perfect co-localization yield a Pearson's

coefficient value of +1 while -1 showed a perfect inverse correlation. Zero Pearson's coefficient value meant that there was no correlation. At least 20 different images of each interactor were analyzed to obtain the average value of Pearson's coefficient and its standard deviation.

2.5. Protein Techniques

2.5.1. Protein expression

2.5.1.1. Competent cell strains screening for optimal protein expression

pET28aDENVBioCap plasmid that was engineered in Section 2.3.4 was transformed into two bacterial competent cell strains [BL-21 (DE3) and BL-21-CodonPlus] (Agilent Technologies, USA). Three colonies were picked and grown in 20 ml Luria-Bertani (LB) broth (Appendix 3d) with 30 μg/ml kanamycin antibiotic. When the bacteria absorbance OD_{600nm} reached 0.65, protein expression was induced with 1 mM isopropyl β-D-thiogalactoside (IPTG) overnight at 16 ^{o}C. On the following day, the bacteria absorbance OD_{600nm} was measured again and 200 μl of equal bacteria density for both strains were used for expression level screening. Bacterial cells were pelleted down with centrifugation at 8,000 rpm for 15 min at 4 ^{o}C and resuspended with 100 μl protein sample buffer (Bio-Rad, USA) containing β-mercaptoethanol. The samples were boiled for 10 min with constant vortexing at 1 min interval. Insoluble substances were pelleted down with centrifugation for 2 min at 13,500 rpm. About 20 μl of the supernatant was analyzed for protein expression level.

2.5.1.2. Protein extraction

pET28aDENVBioCap plasmid was transformed into BL-21-CodonPlus expression competent cells (Agilent Technologies, USA) and grown on LB agar (Appendix 3c) containing 30 μg/ml kanamycin. Selected clones were cultured in 1 L LB broth [(30 μg/ml kanamycin) (Appendix 3d)] at 30 ^{o}C until absorbance OD_{600nm} of 0.8. Expression of DENV C protein was induced with 1 mM isopropyl β-D-thiogalactoside (IPTG) overnight at 16 ^{o}C. Bacterial cells were pelleted down with centrifugation at 8,000 rpm for 15 min at 4 ^{o}C. Pellet was then resuspended in resuspension buffer (Appendix 4a) and the suspension was clarified by centrifugation at 8,000 rpm for 20 min. The pellet was re-solubilized in resuspension buffer with Triton-X (Appendix 4b) and incubated at room temperature for 30 min. The lysate was subsequently centrifuged at 8,000 rpm for 20 min and washed with resuspension buffer (Appendix 4a). The inclusion bodies were lysed with lysis buffer (Appendix 4c) containing 8 M urea and EDTA-free protease inhibitor (Roche, Switzerland). It was incubated at 4 ^{o}C for 4 hr with gentle agitation. The lysate was subsequently clarified by centrifugation at 13,500 rpm for 20 min. Lysates collected from each step were analyzed as described in Section 2.5.3.1-2.5.3.3 and the final cell lysates were subjected to His-tag affinity purification as described in Section 2.5.2.1.

2.5.2. Protein purification

2.5.2.1. His-tag affinity purification

Bacterial lysate containing DENV C protein from Section 2.5.1.2 was incubated with nickel-nitrilotriacetic acid (Ni-NTA) resin (Bio-Rad, USA) for binding in a chromatography column overnight at 4 ^{o}C. Ten column volume of wash buffer (Appendix 4d) was used to wash away non-specific binding proteins. DENV C

protein was eventually eluted out with elution buffer (Appendix 4e) in ten fractions. All the flowed-through, washed and eluted fractions were analyzed via SDS-PAGE (Section 2.5.3.1) stained with Coomassie-blue [Section 2.5.3.3 and Appendix 5d(i-iii)] and Western-blotting (Section 2.5.3.2).

Eluates with DENV C proteins were combined for dialysis and refolding. Briefly, all eluates were pooled into a SnakeSkin dialysis membrane tubing (Thermo Scientific, USA) and 0.5 % of Tween-20 was added into the samples. The dialysis tubing was incubated in 1 L of 6 M urea for 6-12 hr at 4 ^{o}C and 250 ml of refolding buffer (Appendix 4f) was added into the solution at every 6-12 hr interval. When the final volume reached 3 L, the dialysis tubing was transferred into 2 L of 25 mM Tris and 150 mM NaCl buffer (pH 8.0) for 6 hr. Refolded DENV C proteins were collected from the dialysis tubing. Second round of purification was carried out using ion-exchange chromatography as described in Section 2.5.2.2.

2.5.2.2. Ion exchange chromatography

Ion exchange chromatography column, Resource^{TM} Q/S 1 ml-packed size column (GE Healthcare, UK), was connected to fast protein liquid chromatography (FPLC) system (GE Healthcare, UK). For Resource^{TM} Q column, ten column volumes of Tris starting buffer (Appendix 4g) was used for equilibration until the UV baseline and conductivity were stable. Refolded DENV C protein was injected into the column and the flow rate was set to 0.5 ml/min. After the sample passed through the column, ten column volumes of 20 mM Tris (pH 8.0) was used to wash away all the unbound proteins. Ionically-bound proteins were eluted out with increasing concentration of sodium chloride to a final concentration of 1 M (100 %) using elution buffer (Appendix 4h). For Resource^{TM} S column, 2-[N-morpholino]ethanesulphonic acid

(MES) starting buffer (Appendix 4i) was used for equilibration while MES elution buffer (Appendix 4j) was used to elute out the bound protein. All the fractions were analyzed via ELISA (Section 2.5.3.6) to determine the presence of biotinylated C protein.

2.5.2.3. Size-exclusion chromatography

Superdex 75 10/300 GL chromatographic separation column (GE Healthcare, UK) was connected to FPLC system (GE Healthcare, UK). The column was washed with five column volumes of MilliQ^{TM} water to remove ethanol and equilibrated with two column volumes of filtered 1x PBS (Appendix 1e). When the UV baseline and conductivity were stable, samples with biotinylated DENV C protein from Section 2.5.2.2 were injected into the column and the flow rate was set to 0.25 ml/min. Buffer used for this purification is filtered PBS. All the eluates were analyzed via ELISA (Section 2.5.3.6) to determine the presence of biotinylated C protein.

2.5.3. Protein analysis

2.5.3.1. Sodium dodecyl sulphate-polyacrylamide gel (SDS-PAGE)

Glycine gel was used for normal and large protein size analysis whereas tricine gel was used for small protein size analysis during protein expression and purification. A Tris-glycine polyacrylamide denaturing gel containing 12 % separating glycine gel [Appendix 5a(i) and 5a(iii)] and 5 % staking gel [Appendix 5a(ii) and 5a(iv)] was cast. The comb was removed and the gel was placed into a tank with glycine running buffer [Appendix 5a(iv-v)]. For Tris-tricine gel [Appendix 5b(i-iii)], tricine-containing running buffers [Appendix 5b(iv-v)] were used. Samples were boiled for 5 min at 95 ^{o}C before loading into the wells. Electrophoresis of samples and

pre-stained molecular marker (Fermentas, USA) was carried out at constant 120 V for 1 ½ hr. The gel was then used for Western blot transfer [Section 2.5.3.2 and Appendix 5c(i-iv)] or stained with Coomassie blue [Section 2.5.3.3 and Appendix 5d(i-iii)] / Silver staining [Section 2.5.3.4 and Appendix 5e(i-ii)].

2.5.3.2. Western-blotting

Separated proteins in SDS-PAGE gels from Section 2.5.3.1 were transferred onto a polyvinylidene diflouride (PVDF) membrane using iBlot® Dry Blotting System (Life Technologies, USA) for 7 min. The membrane was then blocked with 5 % skim milk [Appendix 5c(i)] or 4 % bovine serum albumin (BSA) [Appendix 5c(ii)] at room temperature for 1 hr before incubating it with appropriate primary antibody at 4 ^{o}C overnight. After that, the membrane was washed with TBST [Appendix 5c(iii)] or PBST [Appendix 5c(iv)], followed by incubation with secondary antibody (conjugated with alkaline phosphatise or horseradish peroxidase) for 1 hr at room temperature. 5-bromo-4-chloro-3-indolylphosphate / p-nitro blue tetrazolium (BCIP/NBT) substrate (Chemicon, USA) or SuperSignal® West Pico chemiluminescent substrate (Thermo Scientific, USA) were added for bands visualization. For low concentration protein, SuperSignal® West Dura or Femto chemiluminescent substrate (Thermo Scientific, USA) were used.

2.5.3.3. Coomassie blue staining

Separated proteins in SDS-PAGE gels were stained with Coomassie blue staining solution [Appendix 5d(i)] overnight. To accelerate the staining, it could be heated up in a microwave for 30 sec. To destain the background, destaining solution I [Appendix 5d(ii)] was used. When the destaining solution became blue, it was

discarded and new destaining solution I was added. This process was repeated until the background was clear and the bands were obvious. At this stage, stained gel could be kept in destaining solution II [Appendix 5d(iii)] for photographing or dried using dual temperature SLAB 1125B gel dryer (Bio-Rad, USA).

2.5.3.4. Silver staining

For low concentration protein, SDS-PAGE gels were stained with silver stain plus kit (Bio-Rad, USA) according to the manufacturer's protocol. Briefly, gels were fixed with Fixative Enhancer solution [Appendix 5e(i)] with gentle agitation for 20 min. After fixing, gels were washed thrice with 400 ml distilled water for 10 min each. After the last washing, Development Accelerator Solution [Appendix 5e(ii)] was added and waited for the bands to appear. When the desired staining intensity was reached, Development Accelerator Solution was discarded and 5 % acetic acid was added to stop the staining reaction. The stained gels were photographed or dried using gel dryer (Bio-Rad, USA).

2.5.3.5. Sample preparation for mass spectrometry

Purified protein was electrophoresed through SDS-PAGE using 12 % Tris-tricine polyacrylamide denaturing gel (Section 2.5.3.1) and stained with Coomassie blue [Section 2.5.3.3 and Appendix 5d(i)]. After removing the background of Coomassie-stained gel with destaining solution I [Appendix 5d(ii)]. DENV C protein-corresponding band was excised from the gel and kept in eppendorf tube containing distilled water. Samples were submitted to Dr. Lim Yoon Pin, Department of Biochemistry, NUHS for mass spectrometry analysis.

2.5.3.6. Enzyme-linked immunosorbent assay (ELISA)

Samples and standards were added into the wells of MaxiSorp plate (eBioscience, USA) in triplicate. The plate was covered with aluminum foil and incubated for 2 hr. All incubating and washing steps were carried out at room temperature. After washing with 1x PBST [Appendix 5c(iv)], blocking buffer [Appendix 5c(ii)] was added into each well and incubated for another hour. Next, streptavidin-horseradish peroxidase (HRP) enzyme conjugates (Millipore, USA) was diluted 20,000 times with blocking buffer and added into each well for 1 hr incubation. The plate was washed with 1x PBST [Appendix 5c(iv)] thrice to remove unbound conjugates and then substrate solution, tetramethyl benzidine [(TMB) (Promega, USA)], was added for development for 15 – 30 min at room temperature. 0.5 M H_2SO_4 solution was added to stop the reaction. The absorbance was measured immediately at 450 nm.

2.5.3.7. Enzyme-linked immunosorbent assay (ELISA)-based binding assay

Pure proteins of the potential interacting partners were purchased from Abnova (USA) and 100 ng of the proteins were added into the wells of MaxiSorp plate (eBioscience, USA) in triplicates for coating overnight at 4 ^{o}C. After discarding the solution, 150 µl of blocking buffer [Appendix 5c(ii)] was added into each well and incubated for another hour at 37 ^{o}C. Next, 100 ng of purified biotinylated full-length DENV protein was added into the wells for binding and incubated for 1 hr at 37 ^{o}C. After washing with 1x PBST [Appendix 5c(iv)], 150 µl streptavidin-horseradish peroxidase (HRP) secondary antibodies (Millipore, USA) were added and incubated for 1 hr. The plate was washed with 1x PBST [Appendix 5c(iv)] to remove unbound conjugates and then 100 µl substrate solution, tetramethyl benzidine [(TMB)

(Promega, USA)], was added for colour development. When necessary, 50 µl of 0.5 M H_2SO_4 solution was added to stop the reaction. The absorbance was measured immediately at 450 nm. For reciprocal binding assay, DENV C protein was coated on the plates instead followed by the interacting partners. The bound proteins were detected by HRP-conjugated anti-glutathione S transferase (GST) antibody (Millipore, USA).

2.5.3.8. Functional binding assay for purified Dengue virus (DENV) capsid (C) protein with human Sec3 protein

Pure Sec3 protein [(Abnova, Taiwan) (known interacting partner of flavivirus C protein (Bhuvanakantham *et al.*, 2010))] was added into the wells of MaxiSorp plate (eBioscience, USA) for coating overnight at 4 ^{o}C. After washing with 1x PBST [Appendix 5c(iv)], blocking buffer [Appendix 5c(ii)] was added into each well and incubated for another hour. Purified DENV C protein was added into the well for binding at 37 ^{o}C for 1 hr. Next, streptavidin horseradish peroxidase (HRP) enzyme conjugates (Millipore, USA) was added and incubated for one more hour at 37 ^{o}C. After washing three times with 1x PBS (Appendix 1e), 100 µl TMB substrate (Promega, USA) was added for development and 50 µl of 0.5 M H_2SO_4 solution was added to stop the reaction when necessary. The absorbance was measured at 450 nm.

2.5.3.9. Co-immunoprecipiation

Co-immunoprecipitation was carried out to study the interaction between DENV C protein and importins. Baby Hamster Kidney cells were seeded onto a 6-well plate according to Section 2.1.3. When the cell confluency reached approximately 80-90 %, the cells were transfected with GFP-tagged C protein plasmid

according to Section 2.3.6. At 24 hr post-transfection, cells were washed with 1 x PBS (Appendix 1e) and lysed with ice-cold mild lysis buffer provided in the µMACS^{TM} GFP isolation kit (Miltenyi Biotec, Germany). The cell lysates were then incubated with anti-GFP magnetic microbeads overnight with constant rotation for enough binding before loading the mixture into µMACs separator column. After the cell lysates flowed through the column, Wash Buffer I and Wash Buffer II (Miltenyi Biotec, Germany) were used to rinse the column. Elution buffer was preheated to 95 ^{o}C before loading it into the column to eluate out the bound proteins as immunoprecipitates. The eluates were then analyzed through SDS-PAGE (Section 2.5.3.1) and Western-blotting (Section 2.5.3.2).

2.6. Protoarray Screening

ProtoArray® Human Protein Microarray PPI Complete Kit (Life Technologies, USA) was employed for protein-protein interaction study according to the manufacturer's protocol. Briefly, the protein microarray was blocked with 5 ml of Blocking Buffer provided in the kit for 1 hr. The whole experiment was performed at 4 ^{o}C. Six µg of purified biotinylated proteins (50 µg/ml) was used to probe the array and a LifterSlip^{TM} coverlip was placed over the array slowly. The array was incubated for 90 min to allow enough binding time. Next, 5 ml of diluted Alexa Fluor® 647-conjugated streptavidin secondary antibody (Life Technologies, USA) was added and incubated for another 90 min. After washing thoroughly with Wash Buffer provided in the kit, the array was dried via centrifugation at 200x g for 1-2 min at room temperature. Scanning of the array was done using GenePix® scanner (Molecular Devices Corporation, USA), a fluorescence microarray scanner, within 24 hr.

Images of the array were analyzed with GenePix® Pro software (Life Technologies, USA) using the specific ".GAL" file downloaded from ProtoArray® Central. The ".GAL" file contains information on the identity and location of each spot on the microarray. The software acquired data by analyzing the pixel intensity of each spot after adjusting the grid and aligning all the features based on the ".GAL" file. The data acquired from the image can be further analyzed using ProtoArray® Prospector software to identify statistically significant interactors. The functions and subcellular locations of the interactors were analyzed via GeneCards (http://www.genecards.org), UniProt (http://www.uniprot.org), and The Gene Ontology (http://www.geneontology.org). Classification of the interactors was then performed based on the obtained information.

2.7. Cell Cycle Analysis

2.7.1. Fluorescence-activated cell sorting (FACS)

Appropriate cell density of BHK, C6/36 and HEK293 cells were seeded in T-25 flask as described in Section 2.1.2. Two flasks (control and experiment) were used for each time-point. During virus infection as described in Section 2.2.3, 500 µl of virus [multiplicity of infection (M.O.I.) = one] was added into each experimental flask. To synchronize the infection, all flasks were incubated at 4 ^{o}C for 1 hr, followed by incubation at 37 ^{o}C for another 1 hr. During the incubation at 37 ^{o}C, flasks were rocked at every 15 min to ensure even infection. After 2-hr incubation, remaining viruses were removed and washed with 1 x PBS (Appendix 1e) before topping up with 5 ml of respective growth media supplemented with 2 % FCS. BHK and HEK293 cells were then incubated at 37 ^{o}C while C6/36 cells were incubated at 28 ^{o}C during the whole course of the experiment. Time course experiments for WNV

infections were 2 hr, 4 hr, 6 hr, 8 hr, 10 hr, 12 hr and 24 hr while for DENV infections were 12 hr, 24 hr, 36 hr and 48 hr p.i.

At each time point, supernatant for the infected cells were kept to determine virus titers. Cells for both control and experimental flasks were trypsinized and spun down in 15 ml falcon tubes at 250 x g for 5 min at 4 ^{o}C. The cells were then resuspended in 0.5 ml ice-cold 1 x PBS (Appendix 1e) and fixed with 4.5 ml 70 % ice-cold ethanol. For staining, fixed cells were spun down again at 250 x g for 5 min and washed with ice-cold 1 x PBS (Appendix 1e) to remove excess ethanol. Cell pellets were then resuspended with 1 ml of propidium iodide staining solution (Appendix 6a) and incubated at 37 ^{o}C for 15 min. After staining, the cells were filtered with 41 µm filter cloth into mini-glass vials for flow cytometry. Fluorescence activated cell sorting (FACS) analysis was performed using Beckman Coulter Epics Altra (FACScan) machine in Clinical Research Center (CRC), National University of Singapore (NUS). Stained cells were excited with 488 nm laser line and the emitted light was detected through photomultiplier tube four (PMT4). Ten thousands cells were analyzed for each sample to create a cell cycle profile using the software, EXPO32 Version 2.0. WinMDI version 2.8 was used to further analyze the data to obtain the percentage of cells at each cell cycle phase.

2.7.2. Effect of cell cycle synchronization on Dengue virus (DENV) replication

Human Embryonic Kidney (HEK)-293 cells were seeded in T-25 flask as described in Section 2.1.2 and infected with DENV at M.O.I. of one according to Section 2.2.3. To synchronize the infection, all flasks were incubated at 4 ^{o}C for 1 hr, followed by incubation at 37 ^{o}C for another 1 hr. After 2-hr incubation, remaining viruses were removed and washed with 1 x PBS (Appendix 1e) before adding 5 ml of

DMEM growth medium (Appendix 1c) supplemented with 2 % FCS and drugs. To arrest cell cycle at G1 phase, fresh growth media without FCS were used. Thymidine (4 mM) was used to synchronize host cell cycle at S-phase whereas nocodazole (100 ng/ml) was used to arrest cell cycle at G2- / M-phase. At 48 hr post-infection, supernatant of the infected cells were collected for virus titer quantitation whereas infected cells were harvested for FACS analysis according to Section 2.7.1.

2.7.3. Cell cycle-polymerase chain reaction (PCR) array

Human cell cycle RT^2 Profiler PCR array kit (SABiosciences, Qiagen, Germany) was employed to screen for the cell cycle-related genes that were affected during DENV and WNV infection on HEK-293 cells. The HEK293 cells were infected with virus at M.O.I. = 1 as described in Section 2.7.1 with synchronization. At various post-infection time points, the total RNAs were extracted with RNeasy® mini kit (Qiagen, Germany). The RNA of infected cells and mock infected cells were reverse-transcribed into cDNA with the RT^2 First-Strand kit provided. The synthesized cDNAs were then mixed with RT^2 qPCR master mix containing SYBR Green and reference dye. The mixture was aliquoted carefully into a 96-well plate containing pre-dispensed gene specific primer sets. All the aliquoting steps were carried out in a dedicated clean PCR hood. After that, the plates were sealed and analyzed using ABI PRISM 7500 real-time PCR system (Applied Biosystems, USA). The gene expression profiling of virus-infected cells were analyzed using a kit-specific Excel sheet template provided by SABiosciences, Germany.

2.8. Effect of Signal Recognition Particle (SRP19) and DIM1 Dimethyladenosine Transferase 1 Homolog (DIMT1) Genes Over-Expression on Dengue Virus (DENV) Replication

Both SRP19 (Accession number: NM_003135) and DIMT1 (Accession number: NM_014473) clones were purchased from OriGene, USA. DNA sequencing was carried out to confirm the identity of the clones. Human Embryonic Kidney (HEK)-293 cells were seeded onto 6-well plate according to Section 2.1.3 and transfected with the plasmids using TurboFectin transfection reagent (OriGene, USA) according to Section 2.3.6. At 24 hr post-transfection, transfected cells were infected with DENV at M.O.I. = 1 according to Section 2.2.3. After 1 hr incubation, remaining viruses were discarded and washed with 1 x PBS (Appendix 1e) before topping up with 2 ml of growth medium (Appendix 1c) supplemented with 2 % FCS. At 24 hr post-infection, medium was harvested for plaque assay (Section 2.2.2) while total RNA and proteins were extracted for real-time PCR (Section 2.3.8) and Western-blot (Section 2.5.3.2) analyses, respectively.

2.9. Effect of Signal Recognition Particle (SRP19) and DIM1 Dimethyladenosine Transferase 1 Homolog (DIMT1) Genes Knock-Down on Dengue Virus (DENV) Replication

Human shRNA constructs of SRP19 (Locus ID: 6728) and DIMT1 (Locus ID: 27292) were purchased from OriGene, USA. There were four unique shRNA constructs for each gene. All four shRNA constructs were combined during transfection to target multiple splice variants. Scrambled shRNA constructs were included for negative control. Human Embryonic Kidney (HEK)-293 cells were seeded onto 6-well plate according to Section 2.1.3 and transfected with the shRNA

constructs using TurboFectin transfection reagent (OriGene, USA) according to Section 2.3.6. At 24 hr post-transfection, transfected cells were infected with DENV at M.O.I. = 1 according to Section 2.2.3. At 24 hr post-infection, medium containing viruses was harvested for plaque assay (Section 2.2.2) whereas total RNA and proteins were extracted from the cells for real-time PCR (Section 2.3.8) and Western-blot (Section 2.5.3.2) analyses, respectively.

2.10. Software used in this study

Various bioinformatic software were used to: (1) check DNA sequences of the plasmid constructs; (2) predict putative binding domains with host proteins in C protein; and (3) analyze cell cycle data. The major software used were listed in Appendix 7.

2.11. Statistical Analyses

Means, standard deviations, *p*-values, and 95 % confidence intervals were obtained using Microsoft Office Excel 2007. Student's t test was performed to obtain *p*-values.

3. Delineating the Nuclear Transport Mechanism of Dengue Virus (DENV) Capsid (C) Protein

3.1. Introduction

The nuclear localization of Dengue virus (DENV) capsid (C) protein was first reported by Bulich and Aaskov (1992) using anti-DENV-2 C protein monoclonal antibodies. Following this discovery, attempts have been made to decipher the important regions responsible for the nuclear localization of DENV C protein (Sangiambut *et al.*, 2008; Wang *et al.*, 2002). The exact mechanism of nuclear translocation of DENV C protein is still unknown. The aim of this chapter is to delineate the underlying molecular mechanism of transporting DENV C protein into host cell nucleus.

3.2. Cloning of Green Fluorescent Protein (GFP)-Tagged Full-Length Dengue Virus (DENV) Capsid (C) Protein

To examine the nuclear translocation ability of DENV C protein alone without the presence of other viral proteins, recombinant full-length DENV-2 C protein was cloned as fusion protein with GFP tag to ease the visualization under fluorescent microscope. After harvesting the DENV-2 virus, viral RNA was extracted and reverse-transcribed to cDNA which served as a template to amplify the full-length C gene. Figure 3.1 showed the molecular size of the C gene to be about 350 bp as indicated by the arrow. The amplified full-length C gene was purified and inserted into pcDNA3.1/CT-GFP-TOPO vector (Invitrogen, USA) via TA cloning strategy. Ligated plasmids were transformed into One Shot® TOP 10 chemically competent *Escherichia coli* cells (Invitrogen, USA). Positive clones were sent for DNA

sequencing to ensure that there was no mutation and correct orientation. The DNA and amino acid sequences of the DENV-2 C protein were shown in Appendix 8a.

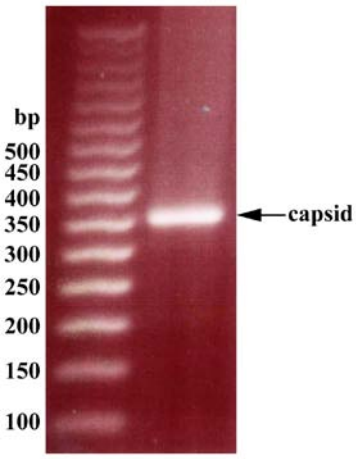

Figure 3.1: Cloning of full-length DENV C protein tagged with GFP. DENV C gene is primed out from the cDNA of DENV-2 (NGC) viral genome. The molecular size of DENV C gene is approximately 346 bp.

3.3. Nuclear Localization of Green Fluorescent Protein (GFP)-Tagged Dengue Virus (DENV) Capsid (C) Protein

Since C protein was cloned as GFP fusion protein, the localization of the proteins in the cells can be visualized directly under immuno-fluorescence microscope as green fluorescence. Plasmid DNAs were transfected into Baby Hamster Kidney (BHK)-21 cells (Section 2.3.6) on coverslips and fixed at 24 hr post-transfection before viewing under fluorescence microscope at 100 x magnification (Section 2.4.1).

As shown in Figure 3.2(A), DENV full-length C protein indeed localized into the cell nuclei / nucleoli as bright green fluorescence in the 4',6'-diamidino-2-phenylindole (DAPI)-stained regions indicating the position of nuclei. To ensure the nuclear translocation phenomenon was not due to the presence of GFP protein, GFP control plasmid was also transfected into BHK cells. Figure 3.2(B) demonstrated that GFP proteins were evenly distributed throughout the whole cells. Mock-transfected cells were also included as negative controls [Figure 3.2(C)]. To further confirm the

nuclear localization ability was attributed by DENV C protein, FLAG octapeptide which was a small tag was fused at the C-terminus of C protein and indirect immuno-fluorescence microscopy was carried out (Section 2.4.2). Likewise, bright green fluorescence was observed in the cell nuclei / nucleoli [Figure 3.2(D)]. To confirm the localization of DENV C protein is in the nucleoli, nucleolus marker, SYTO® RNASelect Green Fluorescence cell stain (Invitrogen, USA) was employed. DENV C protein indeed co-localized with nucleolus stain as indicated by Figure 3.2(E). Hence, these proved that nuclear localization of DENV C proteins was specific and it was purely caused by C protein itself, without the presence of other viral proteins.

Figure 3.3 illustrated two-dimensional images of transfected cells. These images could not differentiate whether the GFP-tagged DENV C proteins were inside the nuclei or resided at the top or at the bottom of the nuclei. To further corroborate that C protein indeed localized into the nuclei / nucleoli, three-dimensional images were obtained using confocal microscope A1R^{+}, in the SBIC-Nikon Imaging Centre, Biopolis, Singapore. Before constructing three-dimensional images, the emission spectrum of green fluorescence in the transfected samples was analyzed with NIS-Elements Imaging software. As shown in Figure 3.3, green fluorescence outside the blue region was chosen and marked with a green box (1) so that only the green fluorescence was analysed. A spectrum graph was plotted and a distinct peak was detected between 500 to 550 nm. This peak coincided with that of the GFP signal from the known database. Thus, the spectrum analysis reaffirmed that the green fluorescence detected from GFP-transfected cells was specific and reliable.

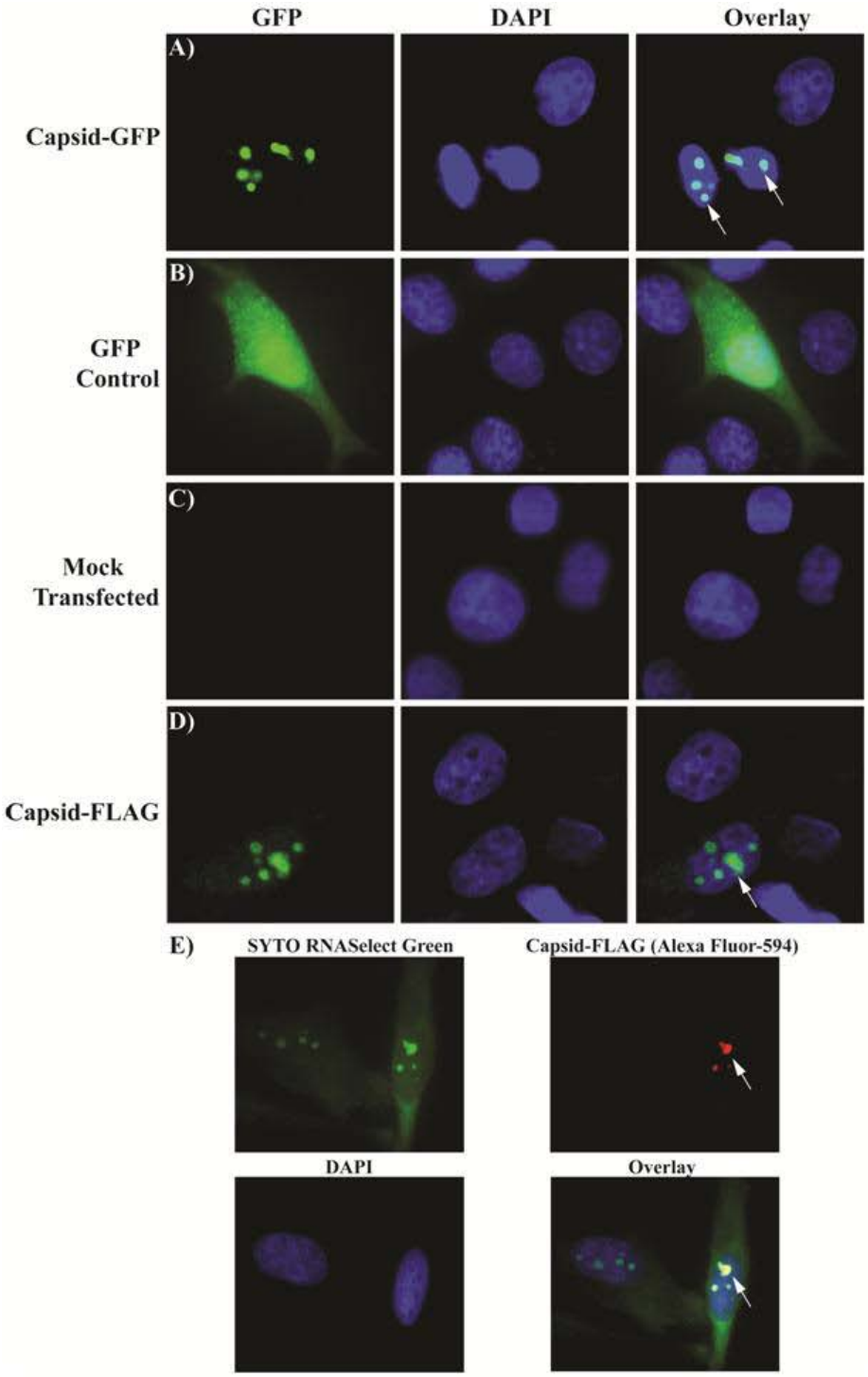

Figure 3.2: Immuno-fluorescence microscopic images of GFP-tagged DENV C protein. The localization of GFP fusion proteins is visualized under fluorescence microscope IX-81 (Olympus, Japan) using 100 x magnifications with oil immersion. DENV full-length C proteins (A) localize in the nuclei / nucleoli as indicated by the white arrows in the overlay image whereas GFP control (B) shows even distribution throughout the cytoplasm and nucleus. DAPI is used to stain the nuclei. Mock-transfected cells (C) serve as negative controls. DENV C protein tagged with FLAG octapeptide (D) also localizes in the nuclei / nucleoli as indicated by white arrow. To confirm the localization of DENV C protein is in the nucleoli, SYTO RNASelect Green (E) is used to stain the nucleoli. DENV C protein co-localizes with nucleoli stain as indicated by the white arrow.

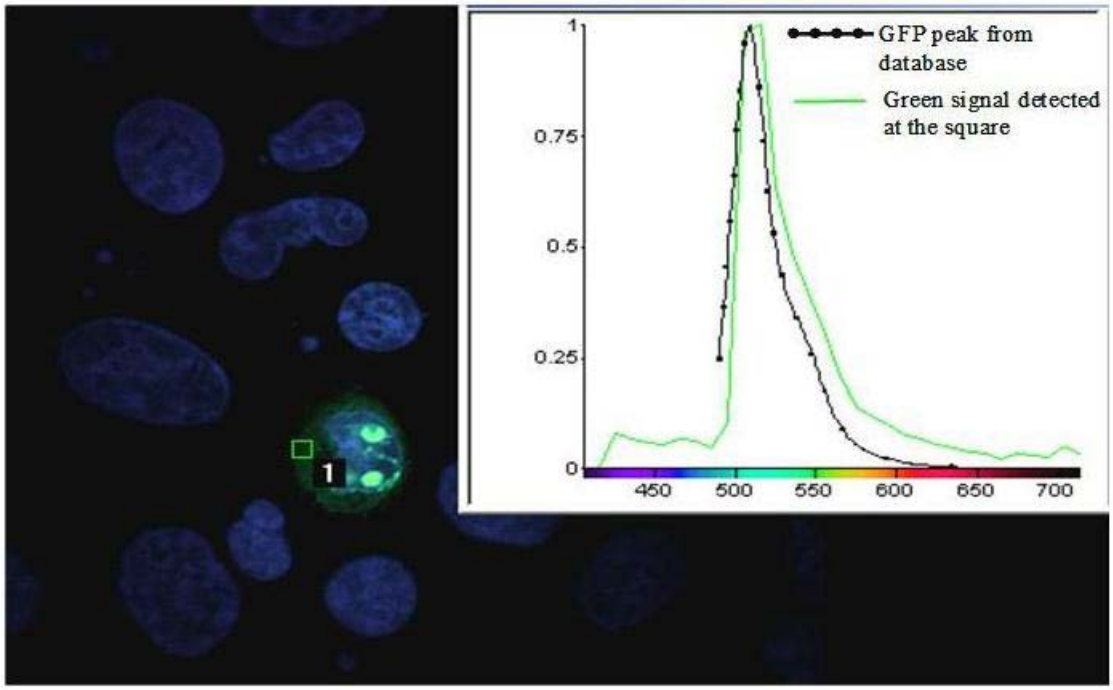

Figure 3.3: Verification of green fluorescence detected in the transfected cell nucleus. Green fluorescence signal detected outside the blue region (nuclei) is marked with a green square box (1) and analysed. A peak between 500 and 550 nm is detected and it matches with a known GFP peak stored in the database.

To construct three-dimensional images of the DENV C-transfected cells, z-stack programme was employed to acquire the z-axis planes from the top of the nuclei to the bottom whereby the x- and y-axes were fixed. Three-dimensional image was then generated using the obtained z-axis images. Figure 3.4 showed the three-dimensional volume views of the z-stacked images. A total of 105 planes was acquired with approximately 0.125 µm thickness for each plane. Both DAPI and green fluorescence channels were merged in the images.

When the three-dimensional volume image was viewed from the top or XY surface, green fluorescence signals detected from the two DENV C-transfected cells were co-localized with the blue DAPI staining which were the nuclei [Figure 3.4(A)]. Likewise, when the volume view was rotated to the side or XZ surface, the green fluorescence signals were still seen together with the DAPI staining [Figure 3.4(B)]. When the volume image was viewed from an angle where all three x-, y-, and z-axes

were visible, the green fluorescence was again detected in the nuclei [Figure 3.4(C)]. To further substantiate that the green fluorescence detected was inside the nuclei and not on top, at the sides or at the bottom of the nuclei, a slice view (slice 35 from the top) of the three-dimensional image was shown [Figure 3.4(D)]. As indicated by the white crosses in Figure 3.4(D), green fluorescence signals were detected inside the nucleus, predominantly nucleolus, in all three XY, XZ and YZ planes. By going through the whole 105 planes from the top to the bottom of the nuclei, green fluorescence signals were not only detected around the nuclei, but also in the nuclei especially the nucleoli. Therefore, this result clearly demonstrated that DENV C proteins indeed localized in the nuclei / nucleoli.

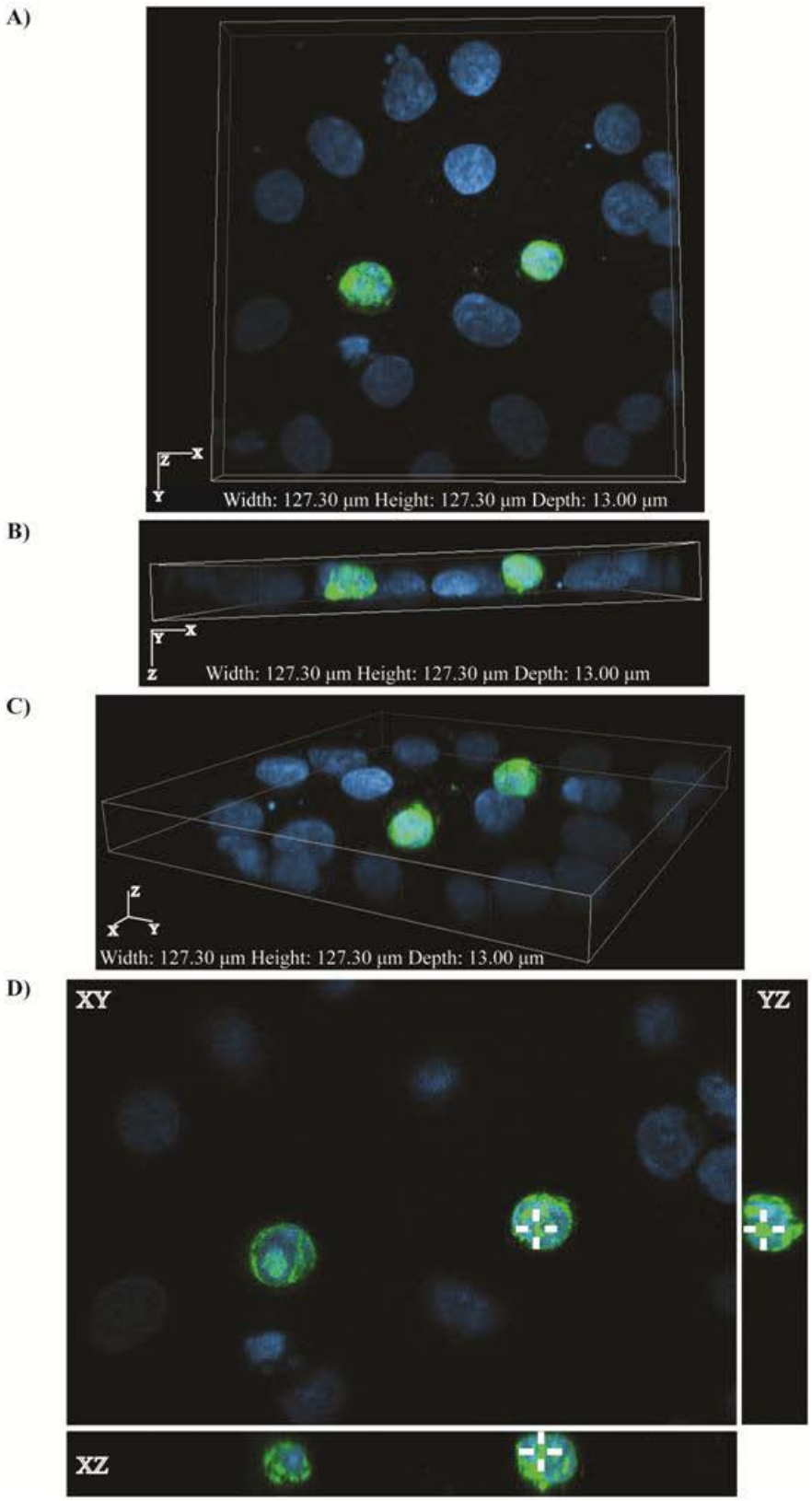

Figure 3.4: Three-dimensional images of DENV C-transfected cells showing the nuclear localization of C protein. Volume views of confocal microscopic images (105 planes; 13 µm depth) at XY plane (A), XZ plane (B), and XYZ angle show the co-localization of green fluorescence and blue DAPI staining. Slice view (D) of the three-dimensional image (slice 35 from the top) shows that DENV C protein indeed localizes in the nuclei / nucleoli as indicated by the white crosses.

3.3.1. Not all Dengue virus (DENV) capsid (C) proteins are in the nuclei

As observed in Figures 3.3 and 3.4, green fluorescence was not only detected in the nuclei / nucleoli, substantial amount of green fluorescence signals were also seen in the perinuclear regions and a minority in the cytoplasm. Figure 3.5 showed the different localization patterns of DENV C protein observed under one field of view. The overlay image in Figure 3.5 illustrated that one of transfected cells showed complete nuclear localization as indicated by a white arrow whereas the other cell retained some green fluorescence at the perinuclear region as indicated by a yellow arrow.

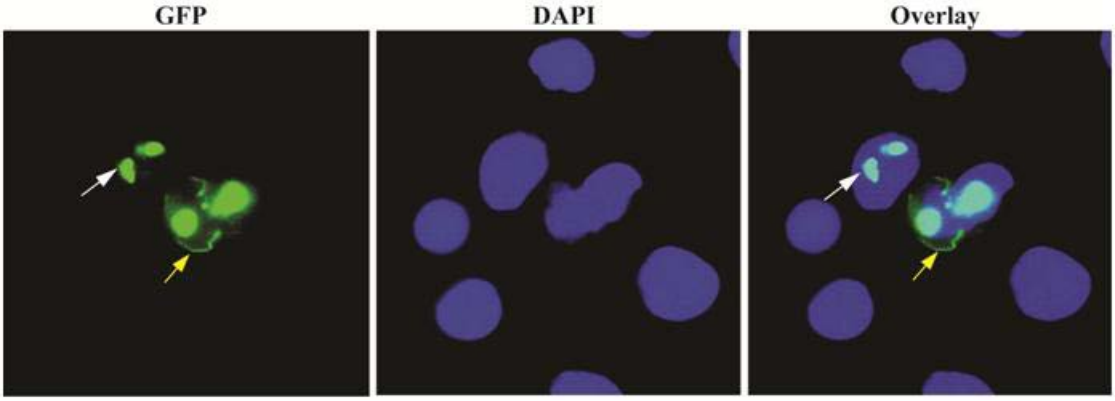

Figure 3.5: Localization of DENV C proteins in the nuclei and perinuclear regions. Immuno-fluorescence image shows two successfully GFP-tagged C protein-transfected cells in which one of them shows complete nuclear localization as indicated by white arrow while the other cell shows fluorescence at both nuclei and the perinuclear region as indicated by yellow arrow. DAPI is used to stain the nuclei.

This phenomenon raises a question as to whether all DENV C proteins are required to enter host cell nuclei during replication. It is possible that the C proteins detected at the perinuclear regions are newly-synthesized C proteins that are yet to be transported into the nuclei? To verify this, the same procedure of transfection (Section 2.3.6) was carried out and the transfected cells were fixed at 24 hr and 48 hr post-transfections. The number of cells showing green fluorescence in the nuclei only or all

other regions (nuclei, perinuclear regions, and cytoplasms) were tabulated and presented in Figure 3.6.

It was noticed that the number of fluorescing cells at 48 hr post-transfection was much lower than 24 hr post-transfection. This could be due to the transfected cells undergoing apoptosis caused by over-expression of DENV C proteins. About 100 transfected cells were counted and the percentage of cells showing nuclei localization only or all regions (nuclei, perinuclear regions and cytoplasms) were compared with that of 24 hr post-transfection. Figure 3.6 showed the percentage of cells demonstrating different localization patterns at 24 hr and 48 hr post-transfection. No significant difference was observed for both time points. Green fluorescence was still seen in the perinuclear regions and cytoplasms of transfected cells at 48 hr post-transfection. This result showed that the amount of C proteins localized in the nuclei was not time dependent. As such, 24 hr post-transfection was used for all subsequent experiments that involved transfection of DENV C protein.

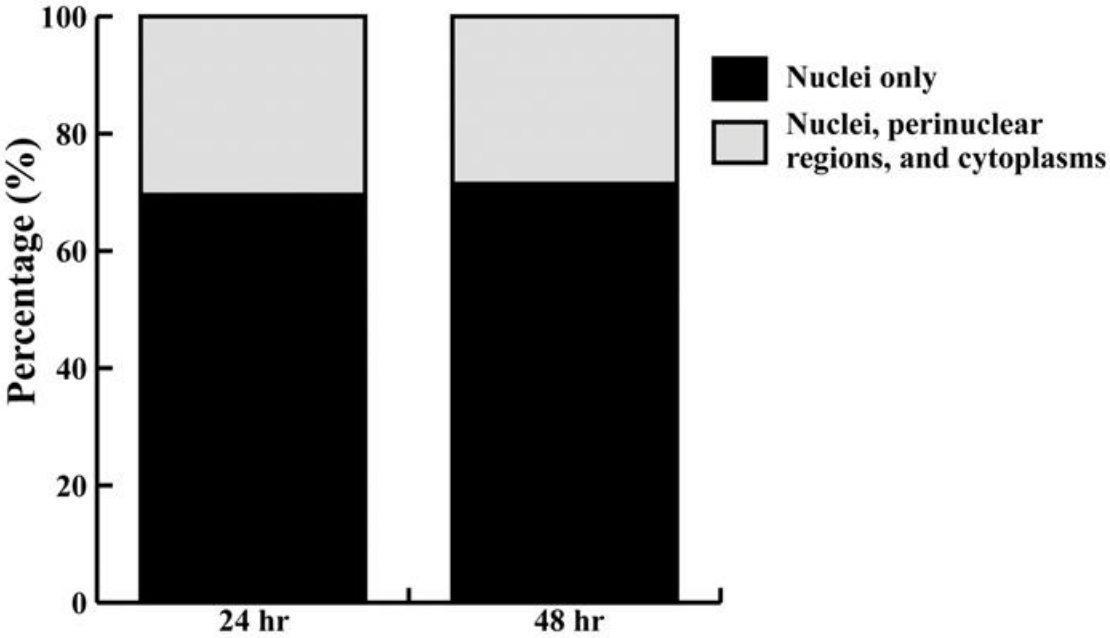

Figure 3.6: Percentage of DENV C protein-transfected cells showing different localization patterns of C protein in the cells at two different time points. The percentage of cells showing complete nuclear localization at 24 hr post-transfection is not significantly different from 48 hr post-transfection.

3.3.2. Dengue virus (DENV) capsid (C) protein is not exported out from the nucleus

It was recently reported that C proteins were exported out of nucleus via chromosomal region maintenance 1 (CRM1)-mediated pathway (Oh *et al.*, 2006). Hence, the fluorescence observed in the cytoplasm could be attributable to the exported C proteins from the nuclei. To examine this possibility, leptomycin B [(LMB) (Merck, Germany)], which is an inhibitor for CRM1-mediated export, was used to inhibit any possible exportation of recombinant C proteins.

After transfection, LMB was added to a final concentration of 1 nM (Oh *et al.*, 2006). A total of at least 100 cells showing fluorescence in the nuclei only or in both nuclei and cytoplasm were counted. As shown in Figure 3.7, the proportion of complete nuclear localization of C protein in the LMB-treated cells was not significantly different from LMB-untreated cells. Hence, the green fluorescence observed at the cytoplasm of some cells was not due to the exported recombinant C proteins from the nuclei but more likely were GFP-tagged C proteins that were translated by ribosomes and remained in the cytoplasm. Taken together, these results (Section 3.3.1 and Section 3.3.2) suggested that not all C proteins were needed to be localized in the nuclei. The perinuclear C proteins could eventually be used for encapsidation of the progeny viral RNA. Cytoplasmic C proteins might interact with host proteins carrying out other non-structural functions. This would be investigated in subsequent chapters.

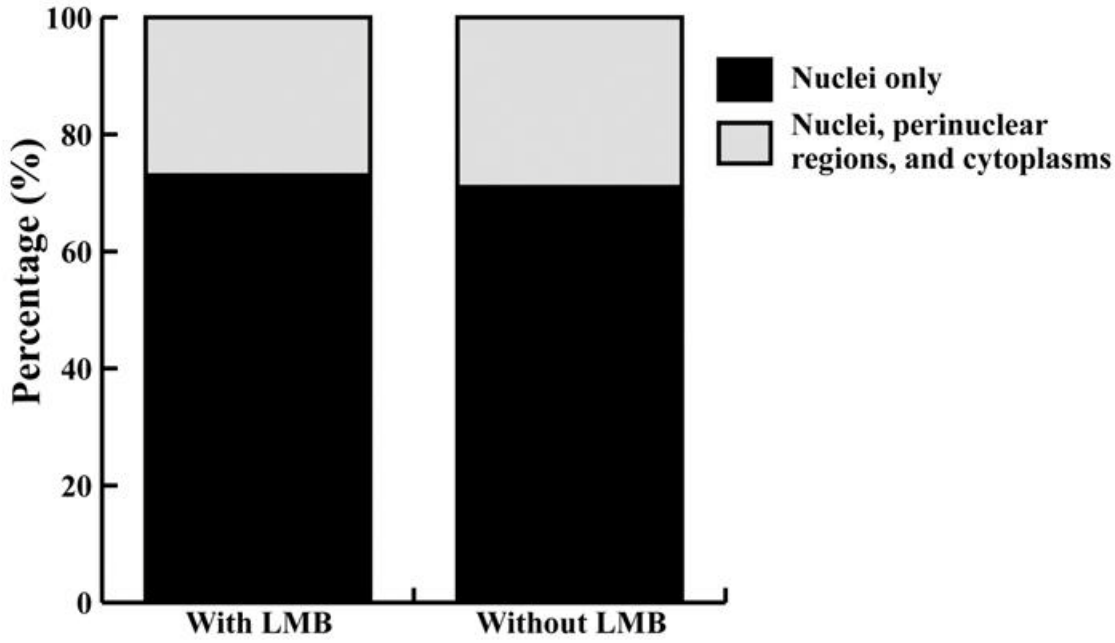

Figure 3.7: Percentage of DENV C protein-transfected cells showing different localization patterns of C protein in the cells with or without the presence of leptomycin (LMB) inhibitor. Leptomycin inhibitor is used to inhibit chromosomal region maintenance 1 (CRM1)-mediated export to examine the distribution of C proteins in the transfected cells after treatment. The percentages of cells with only nuclear localization of C proteins for both treated and untreated groups are not significantly different.

3.3.3. Nuclear localization of Dengue virus (DENV) (C) protein is not cell type-specific

The examination of DENV C protein localization so far was carried out in BHK cells. To investigate whether nuclear localization of DENV C protein is cell-type specific, similar direct immuno-fluorescence microscopic study protocol (Section 2.4.1) was performed on other cell lines, namely human embryonic kidney (HEK)-293 and HeLa cells. These two cell lines were used for other experiments throughout this project. Similar to BHK cells, nuclear localization of DENV C protein was also observed in human cell lines, namely HEK293 and HeLa cells. Distinct green fluorescence signals were still seen in the DAPI-stained nuclei, predominantly in the nucleoli. Hence, nuclear localization of DENV C protein was not cell type-specific and this observed phenomenon was in the absence of other viral factors.

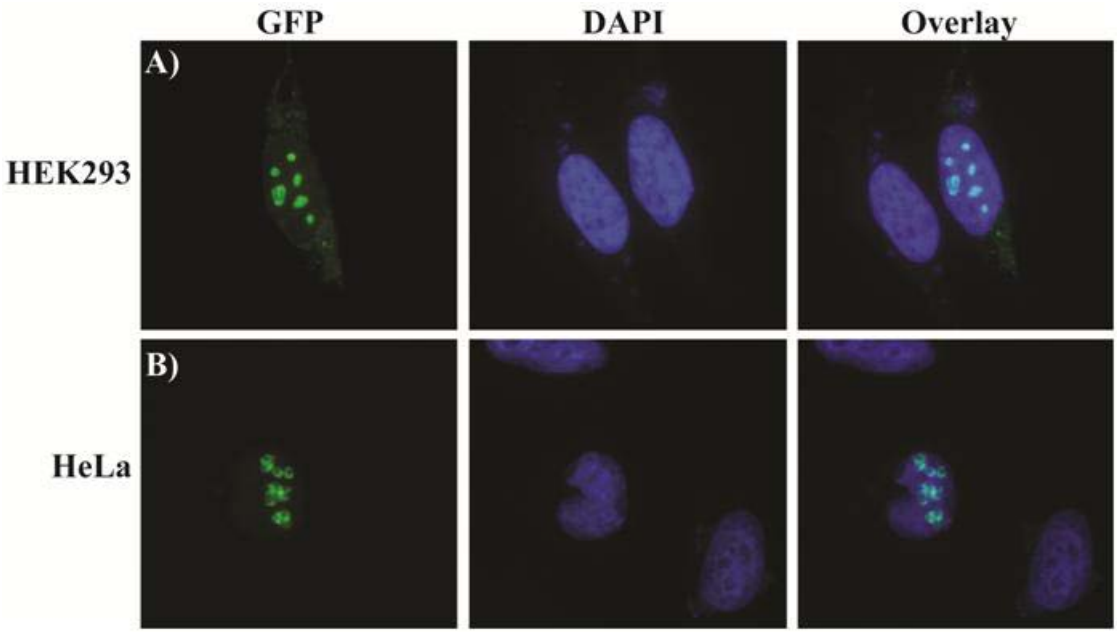

Figure 3.8: Nuclear localization of GFP-tagged DENV C protein in HEK293 (A) and HeLa (B) cells. The localization of DENV C protein is visualized under fluorescence microscope IX-81 (Olympus, Japan) using 100 x magnifications with oil immersion. Similar to BHK cells, DENV full-length C proteins also localize in the nuclei / nucleoli of HEK293 and HeLa cells.

3.3.4. Live cell imaging of the localization of DENV C protein in the cell

Nuclear localization of C protein was only captured at a fixed timing in other studies (Bulich & Aaskov, 1992; Tadano *et al.*, 1989; Wang *et al.*, 2002) so the whole process of nuclear translocation of C protein has not been fully described thus far. Therefore, it will be interesting to decipher the entire transportation process.

To capture the whole process of nuclear translocation of C proteins, time-lapsed live cell imaging technique (Section 2.4.3) was employed. BHK cells were transfected with full-length DENV C plasmid for 8 hr before the cell monolayer in the dish was viewed under Nikon Live Cell Imaging System (Nikon, Japan). Only one field of view was chosen to capture the time-lapsed images throughout the whole experiment. Green fluorescence and phase contrast images were acquired at every half an hour interval up to 40 hr post-transfections.

Figure 3.9 showed part of the overlay images of GFP fluorescence and phase contrast microscopy at every 1 hr interval from 21 hr post-transfection until 34 hr post-transfection. Localization of GFP-tagged C proteins was followed in one transfected cell as highlighted by the white arrows in Figure 3.9. Merged image at 29 hr post-transfection was enlarged to illustrate the localization of intense green fluorescence in the nucleus as indicated by the yellow arrow. GFP-tagged C protein was observed in the nucleus from 21 hr post-transfection onwards after the green fluorescence signals were detected in the cytoplasm at 16 hr post-transfection.

One interesting observation was that C protein-induced apoptosis was observed clearly at 32 hr post-transfection and the cell eventually rounded up at 34 hr post-transfection as highlighted by yellow circle in Figure 3.9. The blebbing appearance of the cell at 32 hr and 33 hr post-transfection was indicative of the occurrence of apoptosis (Majno & Joris, 1995). DENV C protein-induced apoptosis was captured live for the first time via time-lapsed live cell imaging. This result elucidated the observation in Figure 3.6 where lower number of transfected cells was observed at 48 hr post-transfection.

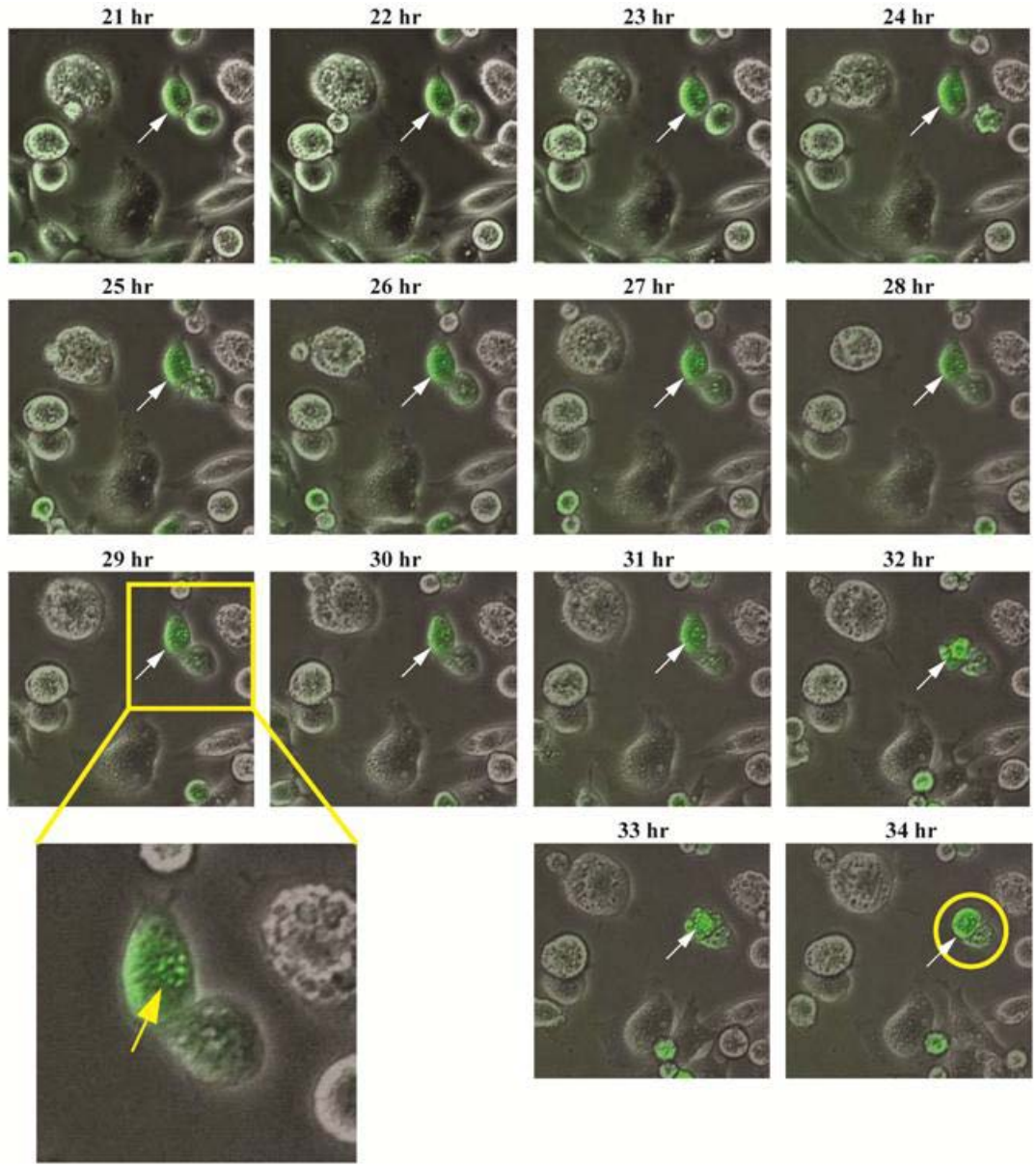

Figure 3.9: Time-lapse experiment showing the localization of DENV C proteins in BHK cells. BHK cells are transfected with GFP-tagged DENV C plasmid before viewing using Nikon Live Cell Imaging System (Nikon, Japan). Green fluorescence and phase contrast images of the cells were captured at every half an hour interval. Images shown here are the overlay images of GFP fluorescence and phase contrast microscopy at every one hour interval from 21 hr to 34 hr post-transfection. Nuclear localization of C protein is followed in one transfected cell as indicated by white arrows. Faint green fluorescence is observed in the nucleus of the cell from 21 hr post-transfection onwards. The image at 29 hr post-transfection is enlarged for better view of the nuclear localized DENV C protein. DENV C protein-induced apoptosis is observed at 32 hr and 33 hr post-transfection.

Nevertheless, one major drawback in Figure 3.9 was that the nuclei were not clearly distinguishable from the cytoplasm. As a result, it could not indicate conclusively that the C proteins were indeed in the nuclei of the transfected cells. To rectify this problem, Hoescht 33258 (Sigma, USA) was chosen to stain the nuclei. Cytotoxicity test of Hoescht 33258 was carried out to ensure that this stain will not affect the physiology of BHK cells. Hence, different concentration of Hoescht 33258 was added into 6-well plate to examine the effect of this stain on the living BHK cells. About 10^6 cells were seeded into each well and different amounts of Hoescht 33258 (2 μg to 10 μg) was added. To examine whether Hoescht could stain all cell nuclei, immuno-fluorescence images of each well were taken at 24 hr and 48 hr post-treatment.

Figure 3.10 showed that 6 μg of Hoescht 33258 was sufficient to stain all the cell nuclei consistently at 24 hr post-transfection. The same intensity of blue fluorescence was also detected in the wells of 8 μg and 10 μg of Hoescht. Besides, Hoescht staining did not affect cell proliferation since the cell density was higher at 48 hr post-transfection as compared to 24 hr post-transfection (Figure 3.10). Thus, Hoescht 33258 could be adopted as a suitable nuclear stain for live imaging in BHK cells.

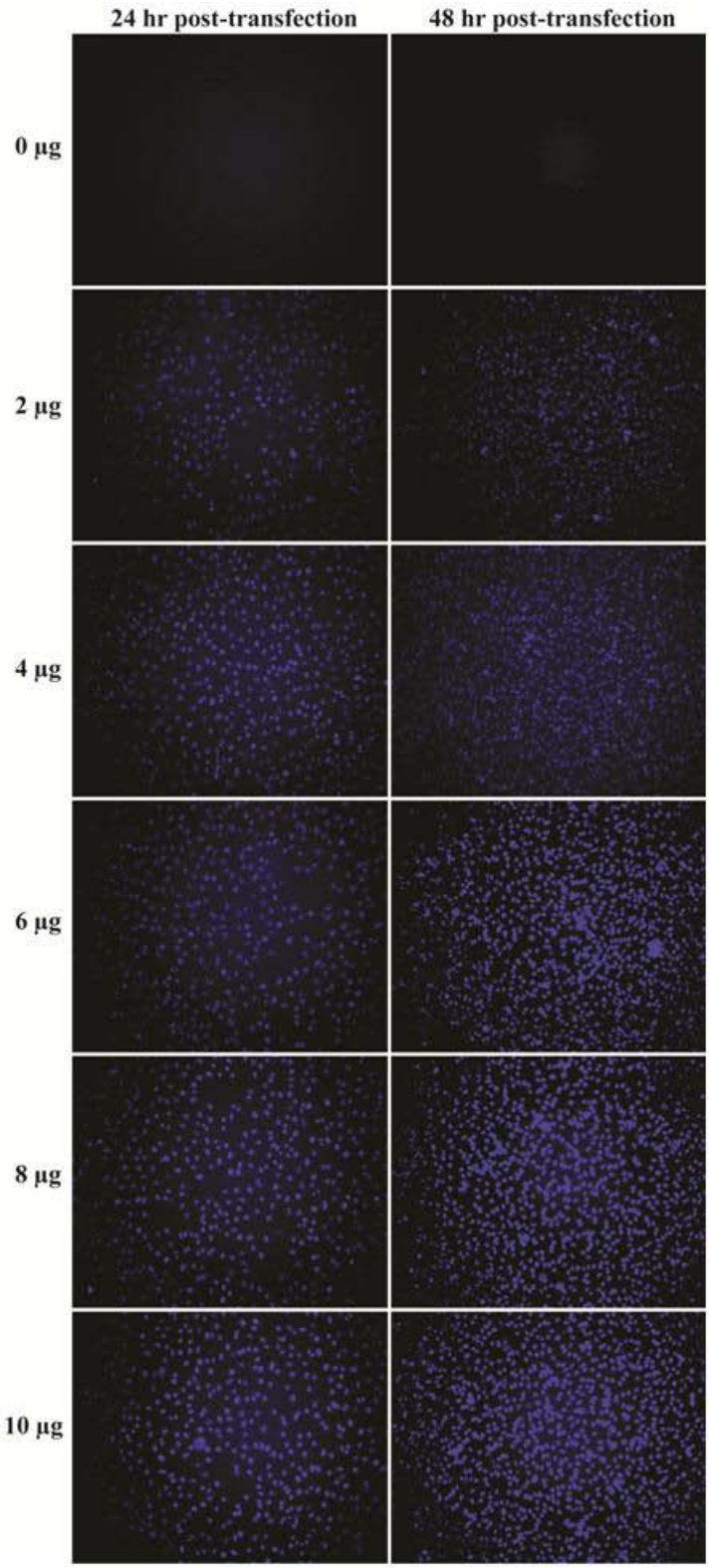

Figure 3.10: Nuclear staining of living BHK cells with Hoescht 33258. Immuno-fluorescence images showing the nuclei of living BHK cells stained with different amount of Hoescht 33258 – 0 µg to 10 µg at 24 hr and 48 hr post-transfection. The intensity of blue signal is weak for 2 µg and 4 µg on both days. Similar intensity of blue fluorescence can still be detected for 6 µg, 8 µg and 10 µg at both timings. The density of cells at 48 hr post-transfection is higher than 24 hr post-transfection, indicating that Hoescht does not affect cell proliferation.

After optimizing the amount of Hoescht 33258 used for nuclear staining, BHK cells were transfected with GFP-tagged DENV C plasmid and green fluorescence signals were tracked via time-lapsed fluorescence microscopy (Section 2.4.3). For this experiment, a new and more user-friendly microscope called BioStation (IM, Nikon, Japan) was used. Four different fields of view were chosen to capture the time-lapsed images throughout the whole experiment. Green fluorescence, Hoescht staining signal and phase contrast images were acquired at every half an hour interval up to 40 hr post-transfections.

As shown in Figure 3.11, cell nuclei were distinguishable from the cytoplasms in the merged images of phase contrast microscopy, Hoescht staining and GFP fluorescence microscopy. Faint green fluorescence signal was observed in the cytoplasm from 25 hr post-transfection onwards as highlighted by the white arrows. The green fluorescence accumulated gradually in the nucleus and concentrated in the nucleolus from 26.5 hr onwards. The entire nucleus fluoresced green with highest intensity at the nucleoli as highlighted by yellow arrows in the enlarged image (Figure 3.11). Likewise, similar apoptotic event as observed in Figure 3.9 was also seen here. The DENV C protein-transfected cell blebbed and rounded up after accumulation of C protein in the nucleoli.

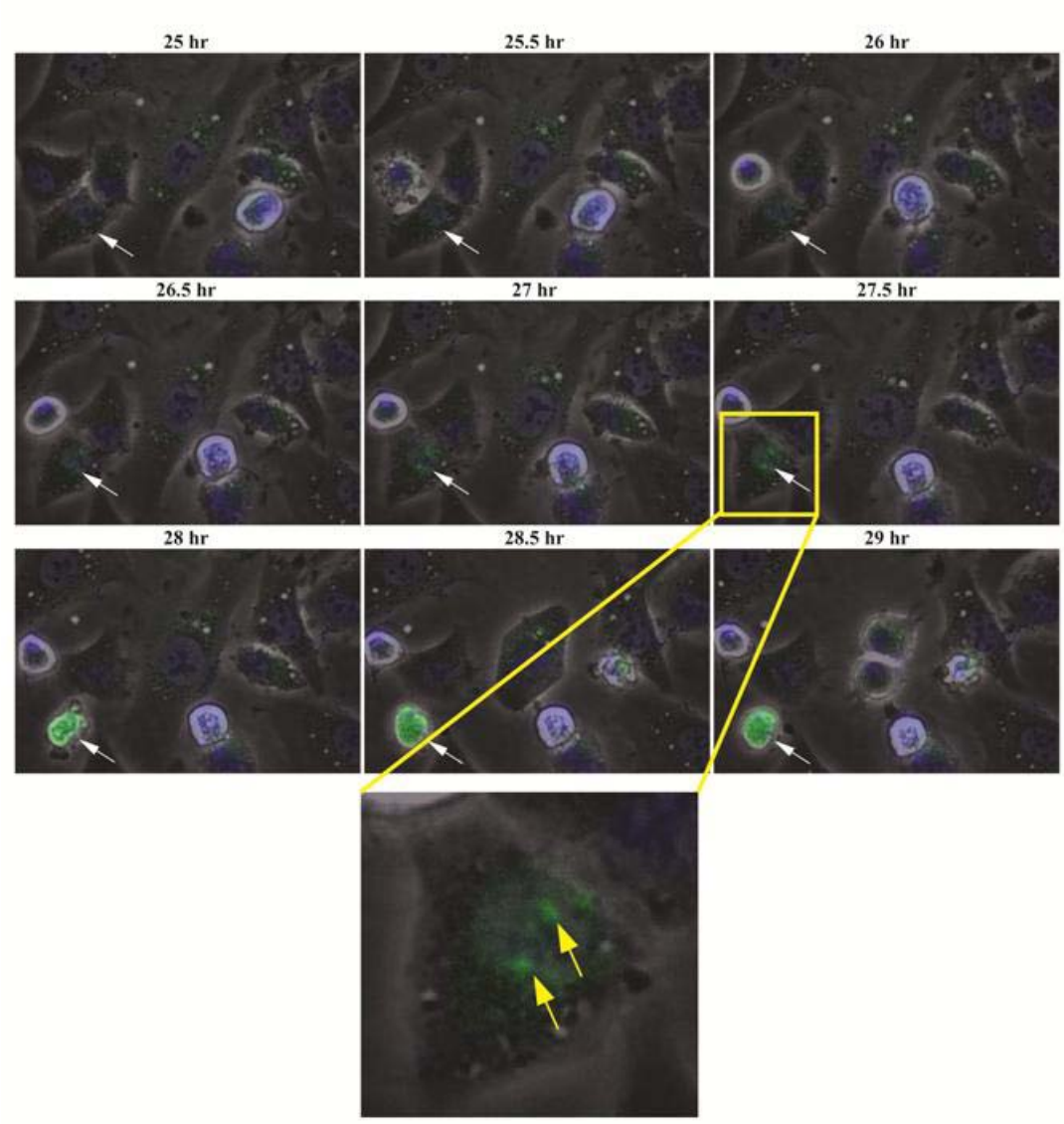

Figure 3.11: Time-lapsed imaging of the nuclear localization of recombinant DENV C protein in Hoescht-stained BHK cells. The fluorescence images shown here are merged images of phase contrast microscopy, Hoescht staining and GFP fluorescence microscopy from 25 hr post-transfection to 29 hr post-transfection at half an hour interval. The yellow arrows indicate one of the transfected cells in which GFP fluorescence is seen clearly in the nucleus / nucleolus from 26.5 hr to 27.5 hr post-transfection. The transfected cell at 27.5 hr post-transfection is enlarged and intense green fluorescence can be seen clearly in the nucleoli as indicated by white arrows. Cell blebbing occurs at 28 hr post-transfection and the cell is rounded up after that.

Figure 3.11 provided more convincing evidence that the GFP-tagged DENV C proteins were indeed transported into the nuclei / nucleoli as green fluorescence signals were co-localized with the blue fluorescence emitted from Hoescht 33258-stained nuclei in living cells. The entire transportation process of DENV C protein

from the cytoplasm into the nucleus followed by accumulation in the nucleoli was demonstrated successfully via this optimized live cell imaging technique in BHK cells. In addition, both Figure 3.9 and Figure 3.11 also illustrated that DENV C protein-transfected underwent apoptosis confirming the results reported by other studies (Limjindaporn *et al.*, 2007; Netsawang *et al.*, 2010; Oh *et al.*, 2006; Yang *et al.*, 2008).

3.4. Role of Nuclear Localization Signal (NLS)

3.4.1. Prediction of functional nuclear localization signal (NLS) motifs

After confirming the nuclear translocation ability of DENV C protein, the next objective of this study was to identify the essential amino acid residues responsible for the transportation. There were two contradicting evidences reported by Wang and colleagues (2002) and Mori and co-workers (2005). This discrepancy has not been resolved thus far. Hence, bioinformatics analysis of all four DENV serotypes was performed to screen for potential functional motifs involved in nuclear localization.

ScanProsite and MyHits were used to scan the full-length C proteins of all four DENV serotypes. Checking with two different bioinformatics software was to ensure that there was no discrepancy between software algorithms. Both software tools consistently predicted that there were two putative bipartite NLS motifs in all four DENV C proteins (Table 3.1). These two putative bipartite NLS motifs were located at the N-terminus (residues 5 to 22) and C-terminus (residues 85 to 100) of DENV C protein as shown in Figure 3.12 (A).

Table 3.1: Putative bipartite NLS motifs of C protein in all four DENV serotypes. Basic residues in the left and right regions in the putative bipartite NLS motifs are shown in upper case letters; others are shown in lower case letter. NLS1 denotes putative NLS motif at the N-terminus of DENV C protein while NLS2 denotes putative NLS motif at the C-terminus.

Serotypes	NLS1 (residue 5-22)			NLS2 (residue 85-100)		
	Left	**Middle**	**Right**	**Left**	**Middle**	**Right**
DENV-1	RKK	tgrpsfnml	KRaRnR	KK	eissmlnimn	RRKR
DENV-2	RKK	arntpfnml	KReRnR	RK	eigrmlniln	RRRR
DENV-3	RKK	tgkpsinml	KRvRnR	KK	eisnmlsiin	KRKK
DENV-4	RKK	vvrppfnml	KReRnR	RK	eigrmlnilng	RKR
Consensus	**RKK**	**9 residues**	**KR-RnR**	**$(R/K)_2$**	**10-11 residues**	**$(R/K)_{3-4}$**

This scanning result is different from the prediction of Wang and co-workers (2002) whereby three putative NLS motifs were predicted at positions 6-9, 73-76, and 85-100 as shown in Figure 3.12(B). They demonstrated that only putative bipartite NLS motif at position 85-100, which was also predicted by ScanProsite and MyHits, was important in nuclear localization. Deletion of the first 45 amino acids from the N-terminus of C protein and mutation of amino acids at position 73-76 did not affect the nuclear localization (Wang *et al.*, 2002). However, ScanProsite and MyHits predicted that there was another putative bipartite NLS motif from the amino acid residues 5-22, which was within the first 45 amino acids from the N-terminus of C protein.

Both predicted bipartite NLS motifs (Table 3.1) were well conserved in all four DENV serotypes. Conservation of amino acid sequences in both regions implied that NLS1 and NLS2 could be functionally important. Thus, experiment was carried out to examine the functionality of both putative NLS1 (residues 5 to 22) and NLS2 (residues 85 to 100) as predicted by the software.

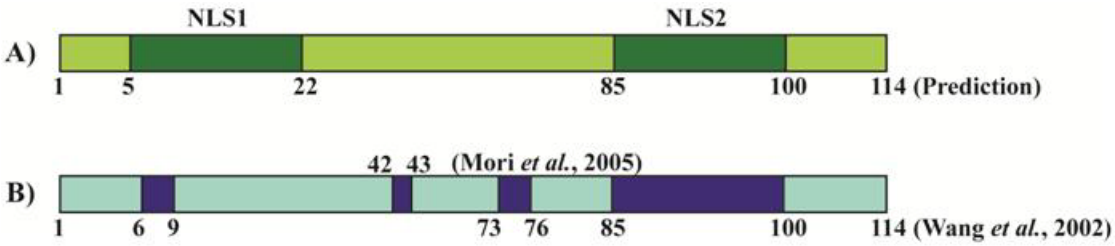

Figure 3.12: Schematic diagram of full-length DENV C protein and putative NLS motifs. (A) ScanProsite and MyHits predict that there are two putative bipartite NLS regions in the DENV C protein, namely NLS1 from residues 5 to 22 and NLS2 from residues 85 to 100. (B) NLS motifs predicted by Wang and colleagues (2002). There are two predicted monopartite NLS motifs located from residues 6 to 9 and from residues 73 to 76 while one bipartite NLS motif is located from residues 85 to 100. Residue 42 and 43 are also found to be essential amino acids for nuclear localization of C protein (Mori *et al.*, 2005).

3.4.2. Cloning of green fluorescent protein (GFP)-tagged nuclear localization signal (NLS) motif plasmids

To determine the nuclear translocation role of both putative bipartite NLS motifs, NLS1 (amino acid 5 to 22) and NLS2 (amino acid 85 to 100) fragments were cloned as fusion proteins with GFP as previously described in Section 3.2. The GFP-tagged full-length DENV C plasmid generated in Section 3.2 was used as template to amplify the two putative NLS fragments.

Since the size of both putative NLS motifs was too small (approximately 60 bp) to be eluted out during gel purification, this purification step was bypassed and the PCR products were used directly for ligation with the pcDNA3.1/CT-GFP-TOPO vector. To minimize the chances of ligating the vector with the full-length C template, the amount of template used to amplify NLS fragment was minimized to 30 ng. Ligated vectors were transformed into One Shot® TOP 10 chemically competent *Escherichia coli* cells and ten colonies were randomly picked for colony PCR.

Figure 3.13 shows the molecular sizes of the C gene, NLS1 and NLS2 fragments in 8 % non-denaturing polyacrylamide gel with Tris/Borate/EDTA (TBE)

buffer (Appendix 3e and 3f). The full-length C gene was about 350 bp while NLS1 and NLS2 were about 60 bp as indicated by the arrows.

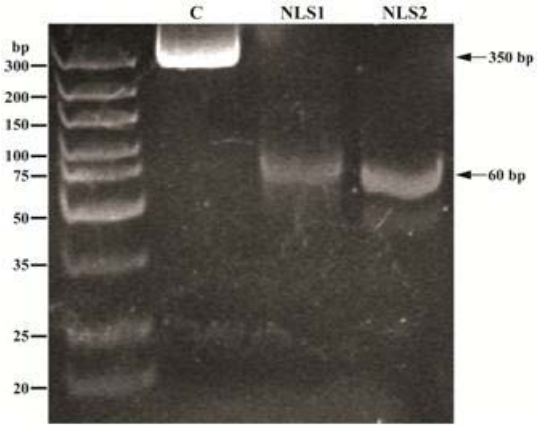

Figure 3.13: Gel electrophoresis image of NLS1 and NLS2 fragments. Eight percent non-denaturing polyacrylamide gel is used to resolve small NLS fragments which are about 60 bp as indicated by arrow. Full-length DENV C gene, which is approximately 350 bp, is also included for reference.

DNA sequencing was carried out to confirm the DNA insert and its orientation. The amino acid sequences for the insertion were checked with ExPASy (Expert Protein Analysis System) - Translate tool to confirm the insertion was in frame with the vector. Appendix 8 (b-c) showed the DNA sequences of NLS1 and NLS2 plasmids together with the conceptual translation of the DNA sequences.

3.4.3. Immuno-fluorescence microscopy study on NLS clones

Generated NLS1 and NLS2 plasmids were transfected into BHK cells (Section 2.3.6) on coverslips and fixed at 24 hr post-transfection (Section 2.4.1). The localization of GFP-tagged putative NLS motifs was visualized under fluorescence microscope IX-81 (Olympus, Japan) at 100 x magnification. As shown in Figure 3.14, both NLS 1 (A) and NLS2 (B) motifs were indeed functional as bright green fluorescence could be detected in the DAPI-stained nuclei. The pattern of localization observed for NLS motifs was similar to full-length C protein [Figure 3.2(A)]. This indicated that DENV C protein contained another functional bipartite NLS motif at

the N-terminus from residues 5 to 22 in addition to the reported NLS motif at the C-terminus from residues 85 to 100 (Wang *et al.*, 2002). Both functional NLS motifs were responsible for the nuclear localization of DENV C proteins.

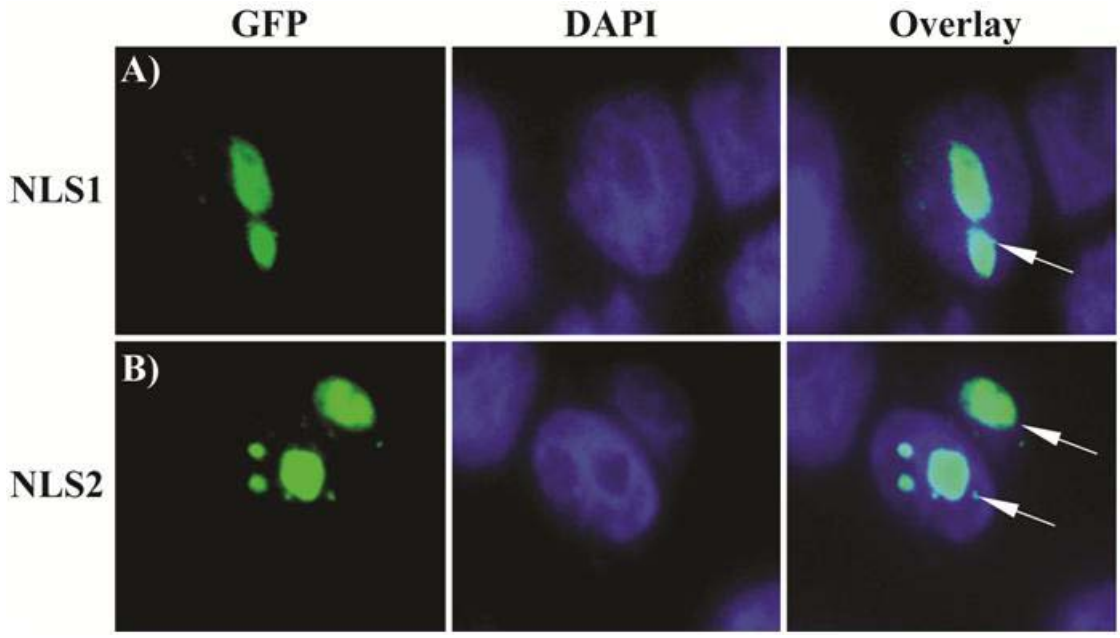

Figure 3.14: Immuno-fluorescence images of GFP-tagged putative NLS motifs. The localization of putative NLS motifs is visualized under fluorescent microscope using 100 x magnifications with oil immersion. DAPI is used to stain the nuclei. Both NLS1 (A) and NLS2 (B) motifs localize in the nucleoli as indicated by white arrows in the merged images.

The immuno-fluorescence images shown in Figure 3.14 were representatives of the majority population observed. As previously demonstrated in Section 3.3.1, not all C protein-transfected cells exhibited complete nuclear localization. To determine the role of NLS motifs in bringing GFP tag into nuclei / nucleoli, the number of cells showing complete or partial nuclear localization was counted manually under the microscope. At least 100 transfected cells were tabulated for each clone.

Figure 3.15 showed that there was approximately 70 % of the full-length C protein-transfected cells showed complete nuclear localization. However, less than 40 % of NLS1 motif-transfected cell and approximately 50 % NLS2 motif-transfected cells showed green fluorescence at the nuclei only. This result could possibly be explained

that NLS motif alone was not as effective in bringing GFP tags into the nuclei as compared to full-length C protein. Nonetheless, NLS2 motif was slightly more efficient in nuclear translocation compared to NLS1 motif.

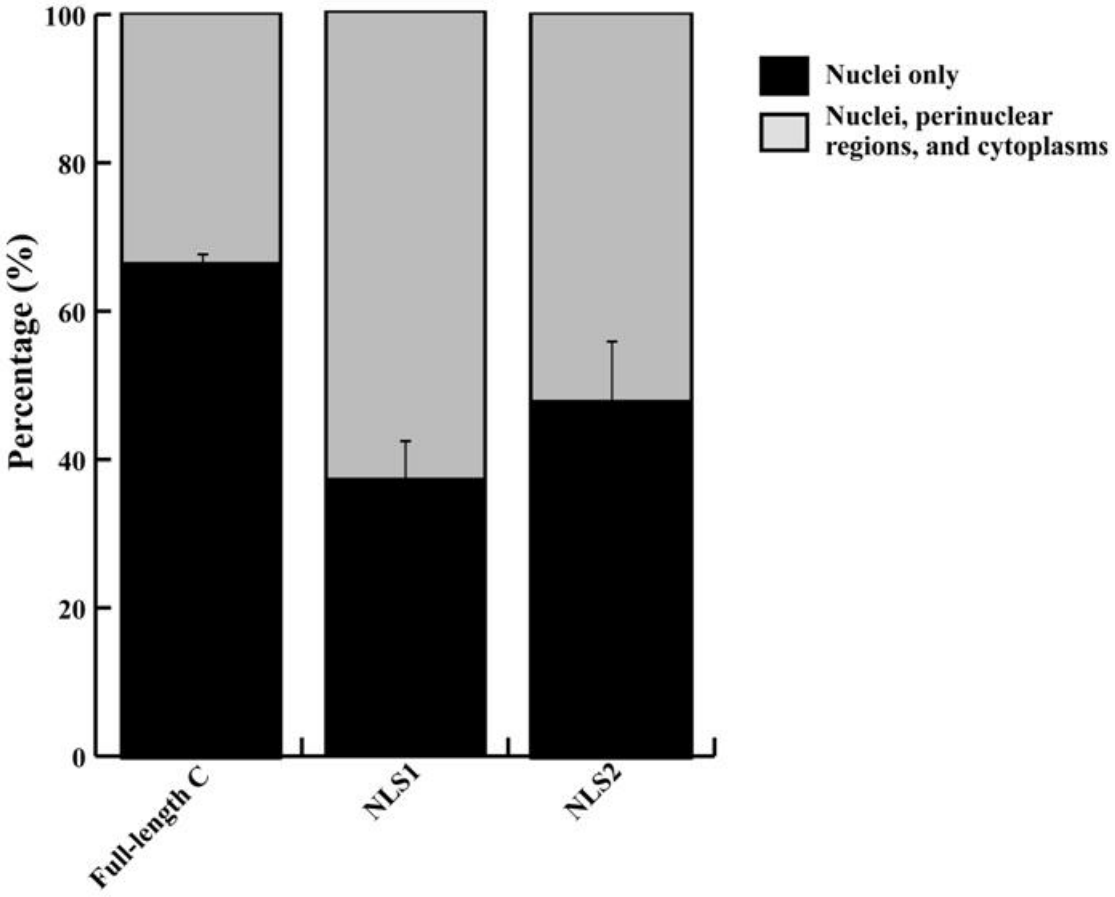

Figure 3.15: Percentage of NLS motif-transfected cells showing different localization patterns in the cells. Full-length C protein is also included for comparison. The percentage of NLS motif-transfected cells showing complete nuclear localization at 24 hr post-transfection is significantly lower than full-length C protein-transfected cells (P=0.001). Higher percentage of NLS2-transfected cells shows complete nuclear localization as compared to NLS1-transfected cells (P=0.023).

3.5. Delineating Pivotal Amino Acid Residues for Nuclear Localization of Dengue Virus (DENV) Capsid (C) Protein

3.5.1. Single site-directed mutagenesis of capsid (C) protein

Wang and co-workers (2002) demonstrated that NLS2 from residues 85 to 100 was crucial for nuclear localization of DENV C protein using truncated clones. However, deletion of amino acid domains may affect proper folding of C protein. To overcome this flaw, site-directed mutagenesis was performed in this study on selected amino acid residues to minimize the negative impact on protein folding.

It was demonstrated structurally that bipartite NLS bound to its receptor protein via its basic amino acid clusters (Fontes *et al.*, 2000). As such, the binding ability of NLS-containing proteins to its transporting proteins would be affected if the basic residue clusters were disrupted. With this information, basic residues of bipartite NLS1 (amino acids 5 to 22) and NLS2 (amino acids 85 to 100) on full-length recombinant C proteins were substituted with alanine residue. In addition, residues 42 and 43 were also mutated to alanine to examine whether these mutations would also abrogate the nuclear localization of DENV-2 C proteins as reported by Mori and colleagues (2005). The mutated amino acid sequences of all the mutants generated for this experiment were shown in Figure 3.16. DNA sequencing was carried out to ensure that there was no extra mutation. The DNA and protein sequences of all the mutated clones were included in Appendix 8 (d-h).

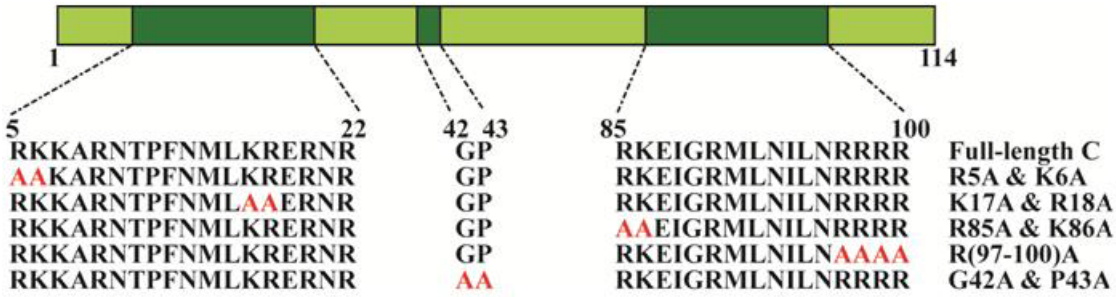

Figure 3.16: Schematic diagram showing the positions of mutation on different mutated clones. Basic residues of bipartite NLS and residues 42-43 on full-length C protein are mutated to alanine to examine the importance of the residues for nuclear localization of DENV C proteins.

As shown in Figure 3.17, different mutations on NLS affected the nuclear localization ability of C protein to varying degrees. Transfected cells with R5A & K6A mutant clearly showed higher cytoplasmic fluorescence as compared to normal C protein [Figure 3.2(A)]. The green fluorescence could be detected in the nuclei as well as the cytoplasm. Figure 3.17(B) showed that only sparse green fluorescence signals were detected in the nuclei for mutant K17A & R18A. Most of the C proteins were at the perinuclear region. Mutations on residues 42 and 43 did not completely abrogate the nuclear localization of C proteins as bright GFP fluorescence was still clearly observed in the nuclei / nucleoli with some green fluorescence at the perinuclear region [Figure 3.17(C)]. As for R85A & K86A mutant, intense GFP fluorescence was observed at the nuclei clusters and also well-defined perinuclear membrane region [Figure 3.17(D)]. Mutation on the second basic residue cluster at the C-terminus of NLS2, from residues 97 to 100, resulted in most severe outcome. Nuclear localization was abolished and transfected cells showed cytoplasmic localization of C proteins only [Figure 3.17(E)]. Therefore, not all four basic-residue clusters contributed equally to the translocation of C protein into the nucleus.

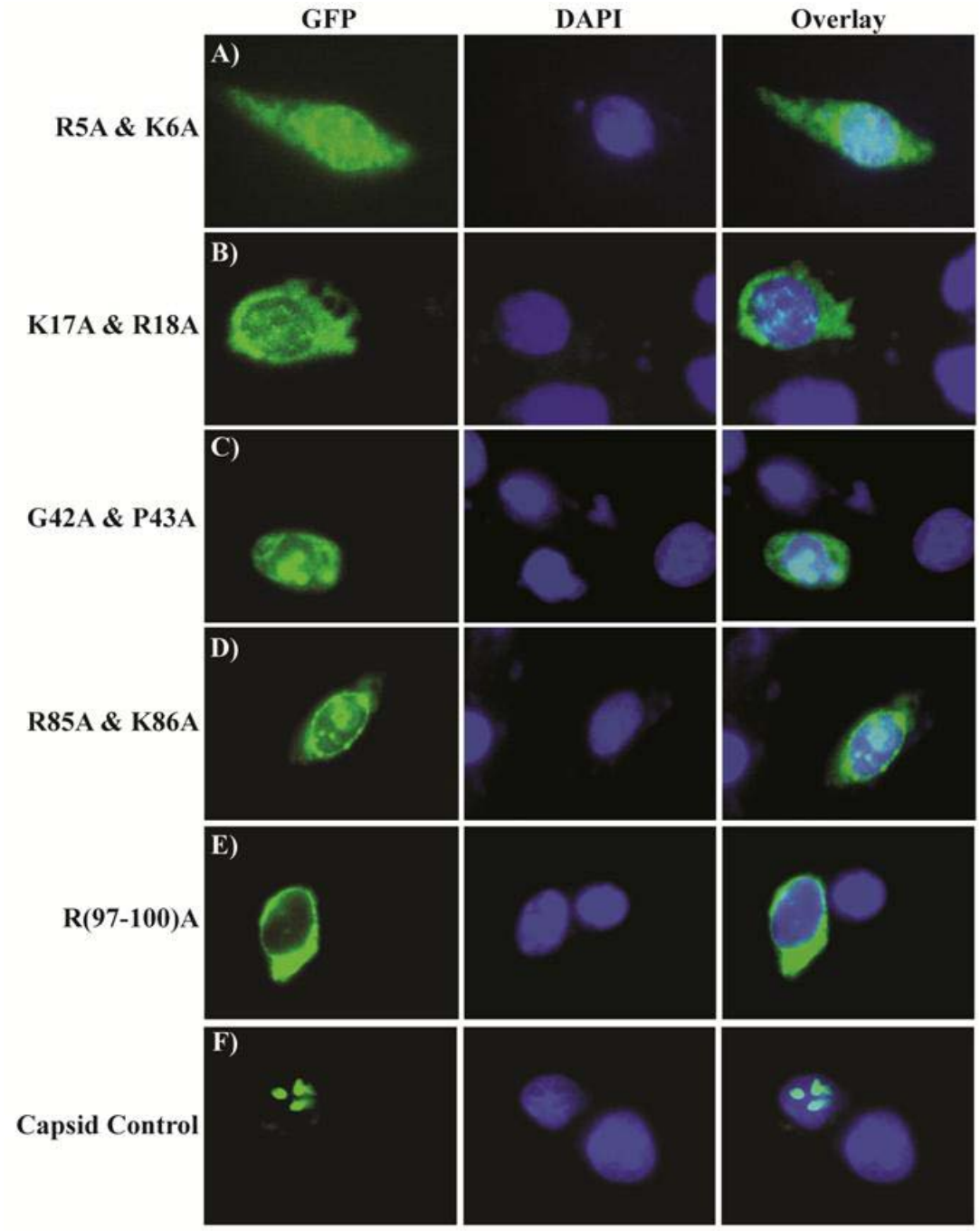

Figure 3.17: Determination of the key amino acid residues responsible for nuclear localization of C protein. The immuno-fluorescence images represent the majority localization pattern shown by the respective mutated clones. Green fluorescence is clearly visualized in the cytoplasm for R5A & K6A (A). K17A & R18A mutants (B) show intense GFP fluorescence in the perinuclear region with lower intensity of fluorescence in the nuclei. G42A & P43A (C) also show intense GFP fluorescence in the nuclei with low intensity of fluorescence in the cytoplasm. Whereas intense GFP fluorescence is observed in the nuclei clusters of R85A & K86A (D) transfected cells with weak cytoplasmic fluorescence but with well-defined nuclear membrane staining. R(97-100)A mutant (E) is the only clone that show no nuclear translocation of C proteins. The green fluorescence is observed at the perinuclear regions as well as the cytoplasm. Wild type C protein without mutation (F) is included as control.

To determine the degree of involvement of the amino acid residues in nuclear localization of DENV C protein, at least 100 transfected cells showing complete, partial or abolished nuclear localization were counted under the microscope. Figure 3.18 provided evidence that single-site mutations on the NLS motifs of full-length C protein negatively affected the nuclear translocation of C protein to different degrees. The percentages of R5A & K6A (42 %), K17A & R18A (38 %), G42A & P43A (45 %) and R85A & K86A (33 %) mutants showing complete nuclear localization were significantly lower than full-length C protein (70 %) in Figure 3.15. In other words, these mutations induced partial blockage to the nuclear localization of C proteins. In contrast, mutations at amino acid residues 97 to 100 resulted in complete abrogation of nuclear localization of C proteins as no green fluorescence was observed in the nuclei [Figure 3.17(E) and Figure 3.18].

Approximately 13 % of the cells exhibited localization of GFP-C protein in the nuclei and perinuclear regions. The fluorescence was markedly more pronounced in the perinuclear regions and cytoplasm. Besides, it was observed that the second basic-residue cluster in both bipartite NLS motifs appeared to be more important than the first basic-residue cluster [Figure 3.17(A, B, D and E) and Figure 3.18]. Taken together, it could be inferred that among four basic-residue clusters in bipartite NLS1 and NLS2 motif, amino acid residues 97 to 100 in NLS2 motif were the most pivotal residues responsible for nuclear translocation of DENV C protein.

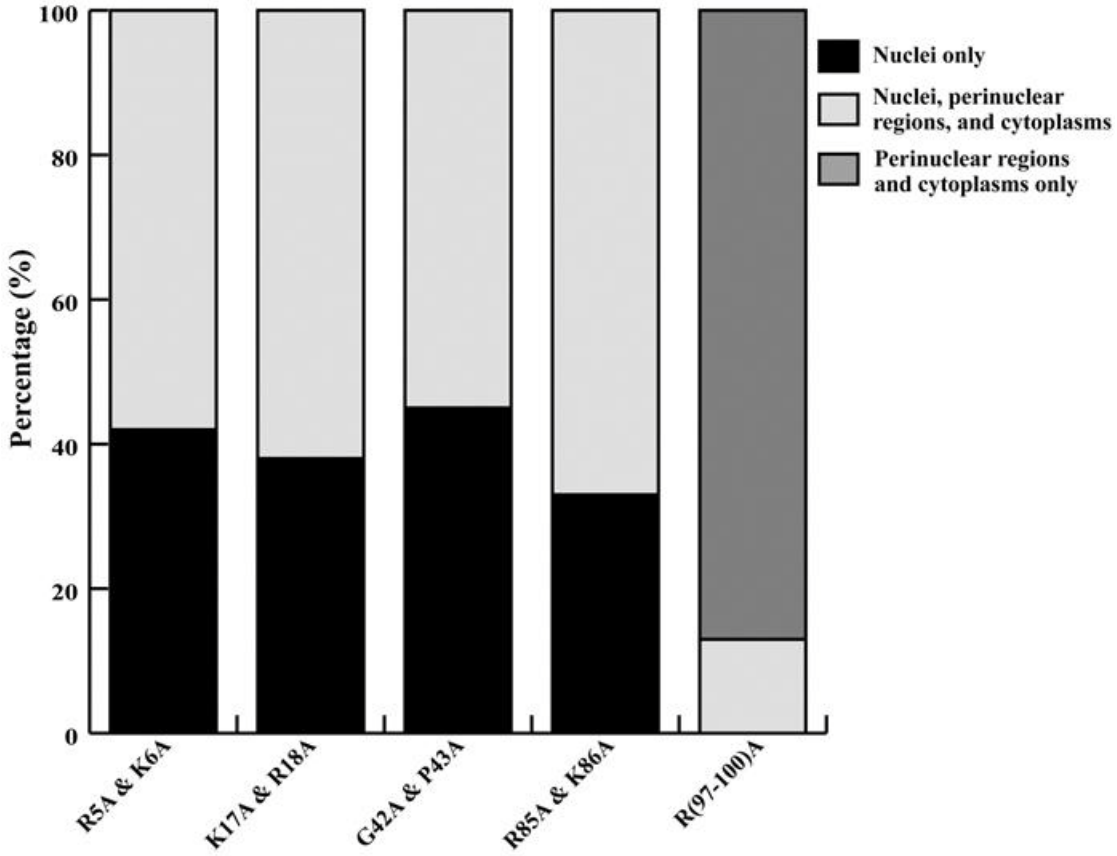

Figure 3.18: Percentage of transfected cells showing different localization of GFP fusion proteins for different clones. Mutants R5A & K6A, K17A & R18A, G42A & P43A and R85A & K86A show a mixture of complete and partial nuclear localization except mutant R(97-100)A exhibiting minority of partial and majority of non-nuclear localization.

3.5.2. Multiple site-directed mutagenesis of C protein

The results so far were not sufficient to justify the need and pre-existence of two bipartite NLS motifs if only amino acid residues 97 to 100 were needed for nuclear translocation. Thus, further characterization of the involvement of NLS1 and NLS2 motifs in the nuclear localization of C proteins was investigated. To further examine the role of NLS motifs, multiple site-directed mutagenesis were performed on double basic-residue clusters [R5A & K6A & K17A & R18A and R85A & K86A & R(97-100)A] and all four basic residue clusters simultaneously (4all) as shown in Figure 3.19.

To generate double mutation sites, single-site mutant clones generated in Section 3.5.1 were used as templates. Primers for mutation on residues 17 & 18 were used on R5A & K6A plasmid to produce R5A & K6A & K17A & R18A clone. While primers for mutation on residues 85 & 86 were used on R(97-100)A plasmid to generate R85A & K86A & R(97-100)A clone. This procedure was repeated until all four basic residues clusters were mutated to generate Δall clone [R5A & K6A & K17A & R18A & R85A & K86A & R(97-100)A]. The DNA sequences and the conceptual translation of these mutant sequences are included in Appendix 8 (i-k).

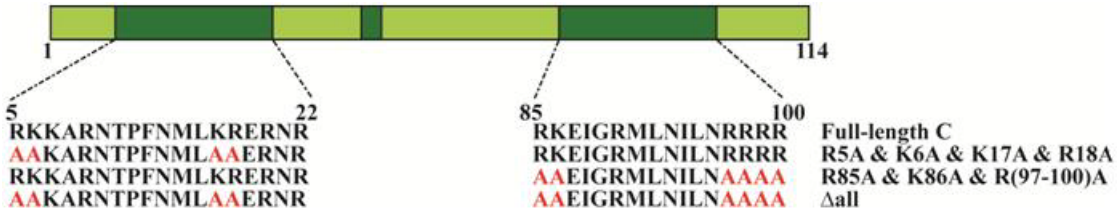

Figure 3.19: Schematic diagram of clones with multiple mutations. Both basic-residue clusters in each NLS motif are mutated to alanine to study the effect of NLS mutation on the full-length C protein.

Figure 3.20(A) indicated that double mutations on both the basic-residue clusters of NLS1 motif (R5A & K6A & K17A & R18A) did not abolish the nuclear localization of C proteins completely. Bright green fluorescence clusters were still seen in the nuclei / nucleoli of the transfected cells with more accumulation at the perinuclear regions. On the other hand, double-sites mutations on NLS2 motif [R85A & K86A & R(97-100)A] [Figure 3.20(B)] showed the same effect as with single-site mutation on the second basic-residue cluster [R(97-100)A] [Figure 3.17(E)]. The nuclear localization of C protein was completely absent in all the transfected cells. Likewise, no green fluorescence signal was detected in the nuclei / nucleoli of transfected cells when all the basic-residue clusters were mutated (Δall) [Figure 3.20(C)]. DENV C proteins were only seen in the perinuclear regions or cytoplasm.

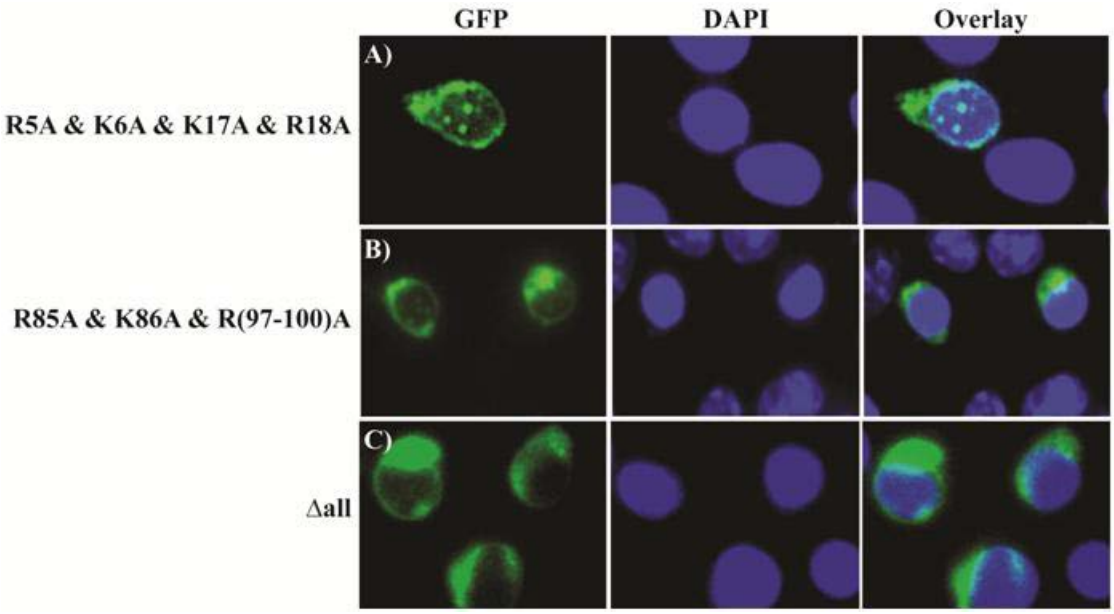

Figure 3.20: Immuno-fluorescence images of clones with multiple mutations. Both basic-residue clusters in each NLS motif are mutated to alanine. Green fluorescence clusters are still observed in the nuclei although NLS1 motif namely R5A & K6A & K17A & R18A (A) is mutated. Nuclear localization of C protein is completely abolished when NLS2 motif namely [R85A & K86A & R(97-100)A (B)] is mutated. No green fluorescence appears in the nuclei when all basic residue clusters of both NLS motifs are mutated in Δall (C).

Cell count was also performed to quantify the effect of mutations on nuclear translocation of C proteins. Alanine replacement on both basic-residue clusters of NLS1 motif (R5A & K6A & K17A & R18A) reduced the number of cells showing complete nuclear localization to about 40 % as shown in Figure 3.21. This percentage was not much different from the single-site mutation on the basic-residue cluster of NLS1 motif (Figure 3.18). On the other hand, the percentage of transfected cells showing partial nuclear localization of C protein was further reduced from approximately 13 % to 7 % when residues 85 & 86 were also mutated on R(97-100)A clone (Figure 3.21). The effect of nuclear import abrogation was even more pronounced when all basic-residue clusters of NLS1 and NLS2 motifs were mutated to alanine residues. None of the transfected cells (0 %) exhibited nuclear localization of C protein forΔall mutant [R5A & K6A & K17A & R18A & R85A & K86A & R(91-100)A] (Figure 3.21).

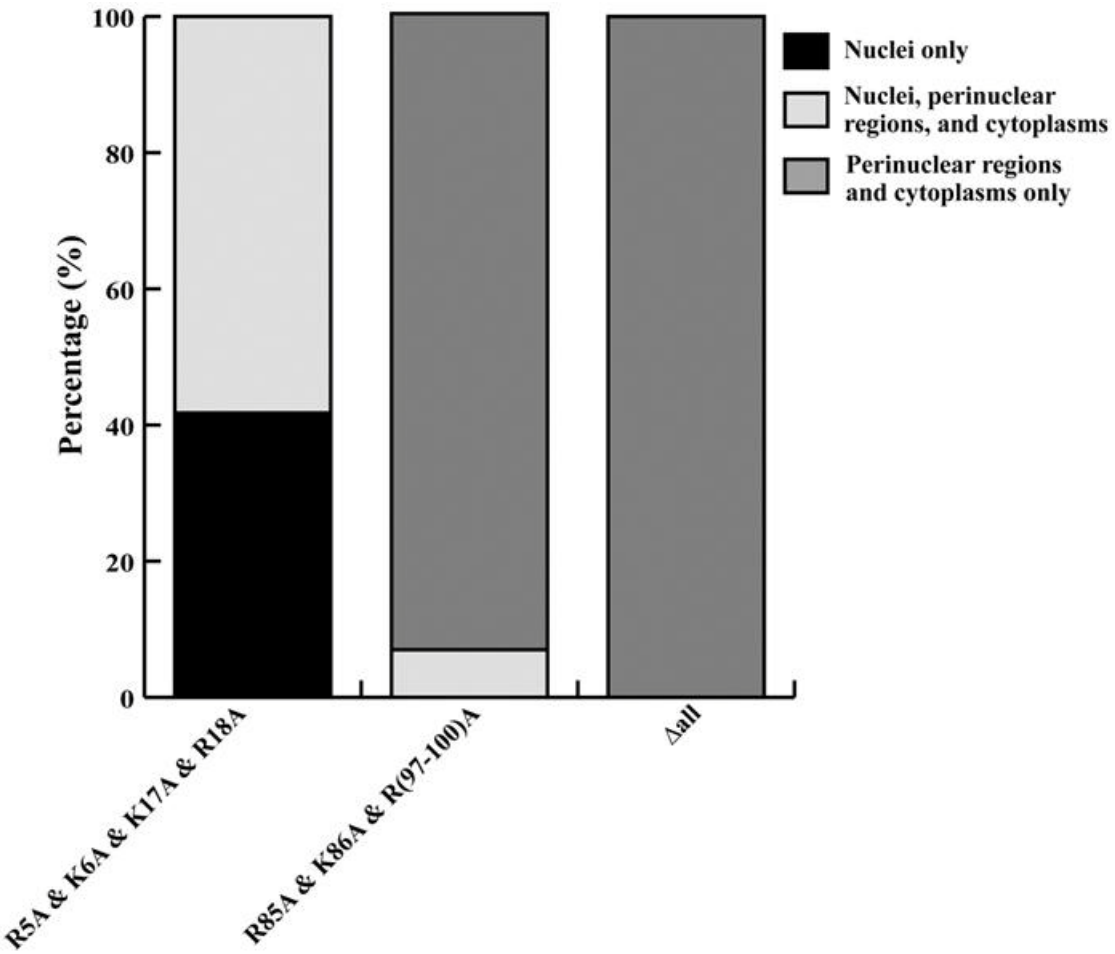

Figure 3.21: Percentage of transfected cells showing different localization patterns of mutated C proteins. Green fluorescence still can be detected in the nuclei even though both basic residue clusters are mutated in NLS1 (R5A & K6A & K17A & R18A). The effect of mutation on NLS2 [R85A & K86A & R(97-100)A] is more drastic where 93 % the transfected cells show cytoplasmic localization of C proteins. The nuclear localization of C protein is completely abolished when both the bipartite NLS motifs are mutated Δall [R5A & K6A & K17A & R18A & R85A & K86A & R(97-100)A].

In summary, Sections 3.4 and 3.5 indicated that bipartite NLS1 motif is functional. However, it contributed a minor role in translocating the DENV C proteins into the nuclei. Based on the percentages of Δall and [R85A & K86A & R(97 -100)A] in Figure 3.21, bipartite NLS1 motif might only contribute an additional 7 % towards enhancing the nuclear localization of C proteins when bipartite NLS2 motif was present and functional. As such, this could also explain why deletion of 45 amino acids from the N-terminus did not abolish the nuclear localization of C protein as

published by Wang and colleagues (2002). The results from this study further revealed that amino acid residues 97 to 100 were sufficient to abolish nuclear localization of DENV C proteins. Simultaneous mutations on all basic-residue clusters of both bipartite NLS motifs could completely abolish the C protein nuclear transportation. The data so far corroborated that there were two functional bipartite NLS motifs in DENV C proteins in which NLS2 motif, particularly residues 97-100, played the major role in nuclear translocation with NLS1 motif (residues 5 to 22) having a minor role in the process.

3.6. Effect of R(97-100)A Mutations on Dengue Virus (DENV) Replication

To examine whether mutations on residues 97-100 of DENV C protein will have any effect upon DENV virus replication, alanine substitutions were introduced on those residues in the DENV-2 infectious clone, pDVWS601 (Gualano *et al.*, 1998; Pryor *et al.*, 2001), as described in Section 2.3.9. After confirming there was no additional mutation on the mutant infectious clone, *in vitro* transcription was performed on the linearized full-length and mutant infectious clones (Section 2.3.10) to generate infectious RNA. The infectious RNA of full-length and mutant infectious clones was then transfected into BHK cells according to Section 2.3.6 to produce virus progeny. At various post-transfection time courses, supernatant of the transfected BHK cells were harvested for growth kinetic analysis and immuno-fluorescence microscopy (Section 2.4.2) was carried out to detect the expression of viral proteins in the transfected BHK cells.

Figure 3.22(A) showed that the *in vitro* transcribed RNA of full-length [(IC) (i)] and mutant [(IC97) (ii)] infectious clones was infectious because the expression of DENV envelope (E) proteins were detectable by anti-DENV 4G2 antibody (Henchal

et al., 1982) as indicated by white arrows. However, unlike the full-length infectious clone (IC), mutant infectious clone (IC97) was unable to produce viable infectious virus particles as indicated by the growth kinetic and plaque assay data in Figure 3.22(B). Similar to West Nile virus (WNV) C protein (Bhuvanakantham *et al.*, 2009), this result implicated that nuclear translocation of DENV C protein was a crucial event during the life cycle of DENV. Hence, nuclear phase of flavivirus C protein is important and warrants further investigation.

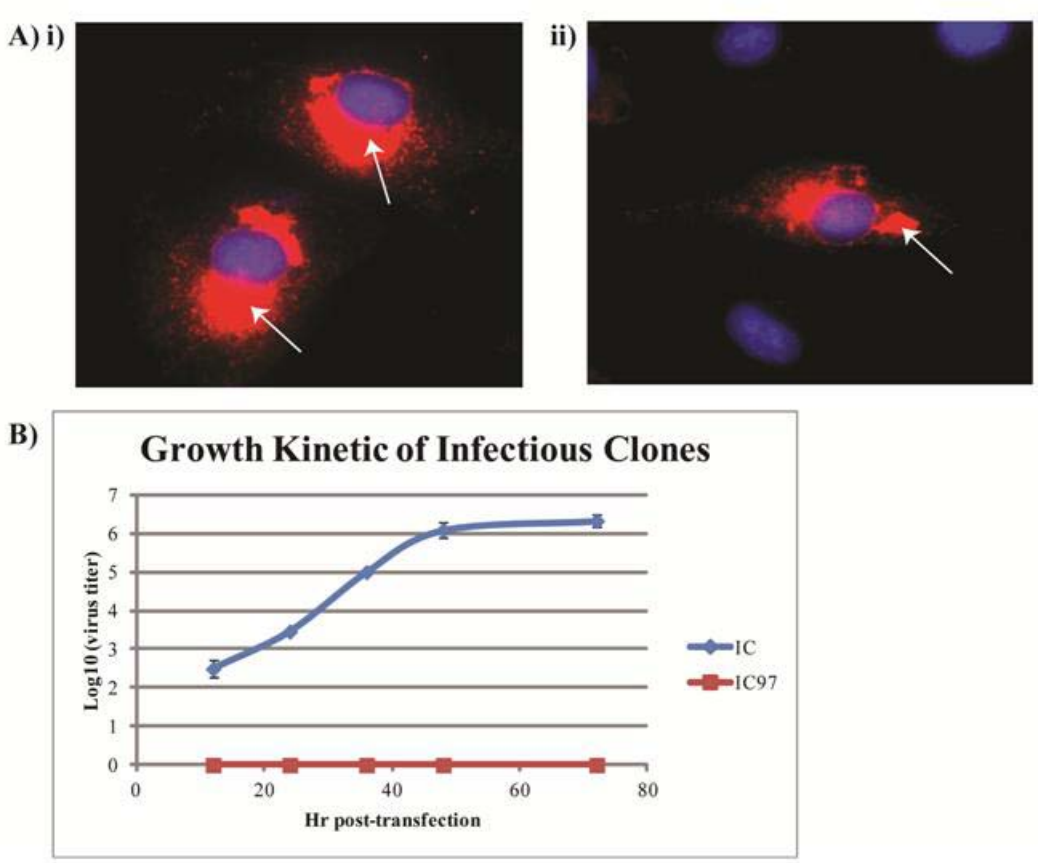

Figure 3.22: Effect of R(97-100)A mutations on DENV replication. (A) Expression of envelope protein is detected using anti-DENV 4G2 antibody, followed by anti-mouse Alexa Fluor-594 secondary antibody. Overlay images of DAPI (nuclei) and red fluorescence indicates that viral protein synthesis is taking place inside the transfected cells for both the full-length [(IC) (i)] and mutant [(IC97) (ii)] infectious clones as indicated by the white arrows. (B) Supernatant of the infectious RNA-transfected cells is harvested at various time points for growth kinetic analysis. Viable virus progeny from IC can be detected via plaque assay but IC97 mutant fails to produce detectable level of viable virus particles.

3.7. Importins-α/β Imports Dengue Virus (DENV) Capsid (C) Protein into Nucleus

3.7.1. Identifying nuclear transporting partner of Dengue virus (DENV) capsid (C) protein

After identifying the important residues responsible for the nuclear localization of DENV C protein, this project continued to unravel the host interacting partner of C protein involved in the nuclear entry process. Importin proteins are well-studied nuclear transport factors that bind to NLS-bearing proteins. Importin-α protein is known to bind to NLS motif and acts as a bridge to importin-β protein that brings the whole complex to nuclear pore complex (NPC) for translocation. However, importin-β protein is also able to transport some NLS-containing proteins directly without the aid of importin-α protein (Gorlich & Mattaj, 1996). Hence, it is intriguing to examine whether the nuclear localization of C protein is mediated by importin-α or importin-β protein.

Co-immunoprecipitation (co-IP) was carried out to pull down GFP-tagged C proteins from DENV C-transfected cell lysate using anti-GFP antibodies conjugated to magnetic beads. The C protein of WNV was also included in this study as a positive control since WNV C protein was shown to interact with importin-α protein (Bhuvanakantham *et al.*, 2009). GFP control plasmid was included as negative control. The pulled-down C proteins and any C protein-interacting proteins were resolved in SDS-PAGE and the presence of importin-α/β protein was detected by anti-importin-α and anti-importin-β antibodies (Sigma, USA). The presence of C proteins in the cell lysates and eluates was detected using anti-GFP antibody (Santa Cruz, USA).

As shown in Figure 3.23(A), immunoprecipitation was successful because GFP bands were observed after pull-down. No band was detected in mock-transfected

cells (Lanes 4 and 8) indicating that the GFP antibody was specific. Figure 3.23(B) indicated that there was a novel interaction between DENV C protein and importin-α protein. Bands were observed in Lanes 5 and 6 where DENV and WNV C proteins were co-immunoprecipitated using anti-GFP antibodies as indicated by arrows. Similar bands were not seen in Lanes 7 and 8 where GFP-control plasmid and Lipofectamine 2000 were used.

It implied that C protein and not GFP tag interacted specifically with importin-α protein. Hence, this result demonstrated that DENV C protein also interacted with importin-α protein, just as WNV C protein. However, no bands were observed from Lane 5 to Lane 8 when anti-importin-β antibody was used for detection [Figure 3.23(C)]. This indicated that there was no direct interaction between DENV C proteins or GFP tag with importin-β protein. Lanes 1 to 4 (Figure 3.23) showed the endogenous importin-β proteins in the cell lysates before pull-down. This result showed that nuclear localization of DENV C proteins was mediated by importin-α/β pathway via a direct binding to importin-α protein.

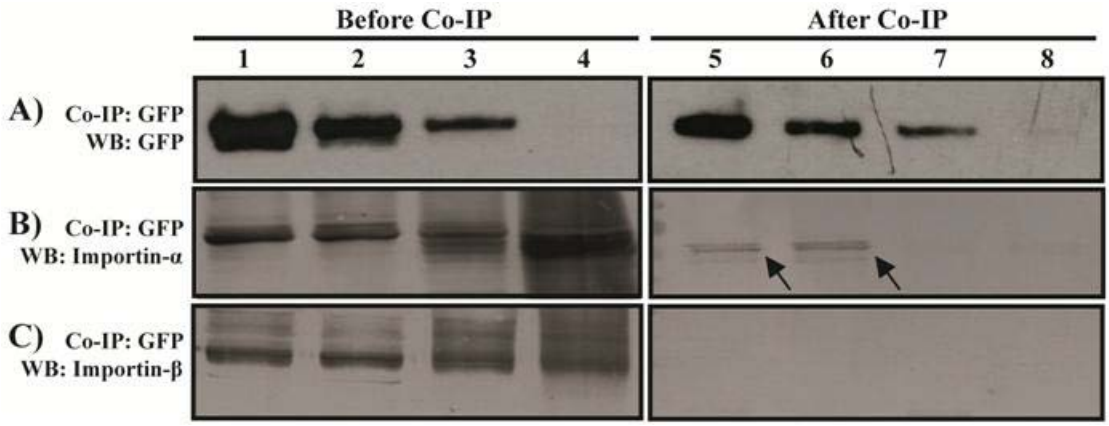

Figure 3.23: Interaction between C protein and importin-α/β proteins. (A) Anti-GFP antibody is used to detect the presence of GFP-tagged C proteins and GFP control. Pull-down is successful because GFP bands can be observed from Lanes 5 to 7. (B) Anti-importin-α antibody is used to detect for the presence of importin-α protein in Western-blot. Bands are observed in Lanes 5 and 6 as indicated by arrows but not in Lanes 7 and 8 implying that DENV and WNV C proteins interacted with importin-α protein. (C) The same samples are loaded into another gel in the same order but anti-importin-β antibody is used for Western-blot. No bands can be observed from Lanes 5 to 8. Lanes 1-4 show the endogenous importin-α/β in the cell lysates. (Lanes 1 & 5 – DENV C protein; Lanes 2 & 6 – WNV C protein; Lanes 3 & 7 – GFP control; Lanes 4 & 8 – Mock-transfected cells; co-IP – co-immunoprecipitation; WB – Western blot).

To further confirm the interaction between DENV C and importin-α proteins, reciprocal co-IP was carried out using anti-importin-α antibodies conjugated to magnetic beads. Anti-GFP antibodies were used to detect the presence of DENV C protein in the eluates. In addition to full-length DENV C protein, various NLS mutants (G42A & P43A, R85A & K86A, R(97-100)A, and R85A & K86A & R(97-100)A) were also included to study the interacting domain of DENV C protein with importin-α protein. Since R5A & K6A and K17A & R18A mutants did not impose great impact on the nuclear translocation of DENV C protein as shown in Figure 3.17(A and B), they were not included in this co-IP study. ΔNLS mutant in which the C-terminal DENV C protein from residues 85 onwards was removed, was generated and included in this experiment.

Figure 3.24(A) demonstrated that co-IP using anti-importin-α antibodies was also successful as importin-α bands were observed after pull-down. Besides, co-IP

using anti-importin-α antibodies was much better than anti-GFP antibodies (Figure 3.23) because more intense bands were observed in the eluates when anti-GFP antibodies were used for detection. Surprisingly, the binding between mutant R(97-100)A and importin-α protein was not affected at all because band was still observed in Lane 5 after co-IP. This was contradictory with the immuno-fluorescence microscopy data in Figure 3.17(E).

Densitometry analysis using ImageJ software revealed that the binding affinity between DENV C protein and importin-α protein was only affected for mutant R85A&K86A&R(97-100)A. There was approximately 50 % reduction in the band intensity as shown by Figure 3.24(B). However, the nuclear translocation of mutant R85A&K86A&R(97-100)A was completely abolished under immuno-fluorescence microscopy [Figures 3.20(B) and 3.21]. The binding between importin-α and DENV C proteins was only abrogated when NLS2 motif was removed completely from the full-length C protein (ΔNLS) [Figure 3.24(A and B)].

The result of ΔNLS mutant (Figure 3.24) tallied with WNV C protein (Bhuvanakantham *et al.*, 2009) whereby the binding between importin-α and WNV C proteins were completely abolished when the NLS motif at the C-terminus was removed. These results implied that NLS2 motif was essential for the binding of DENV C protein to importin-α protein but the binding strength did not rely merely on the basic residues clusters of NLS motif. Alanine substitution mutagenesis on the basic residues clusters did not completely abolish the binding ability of DENV C protein to importin-α protein.

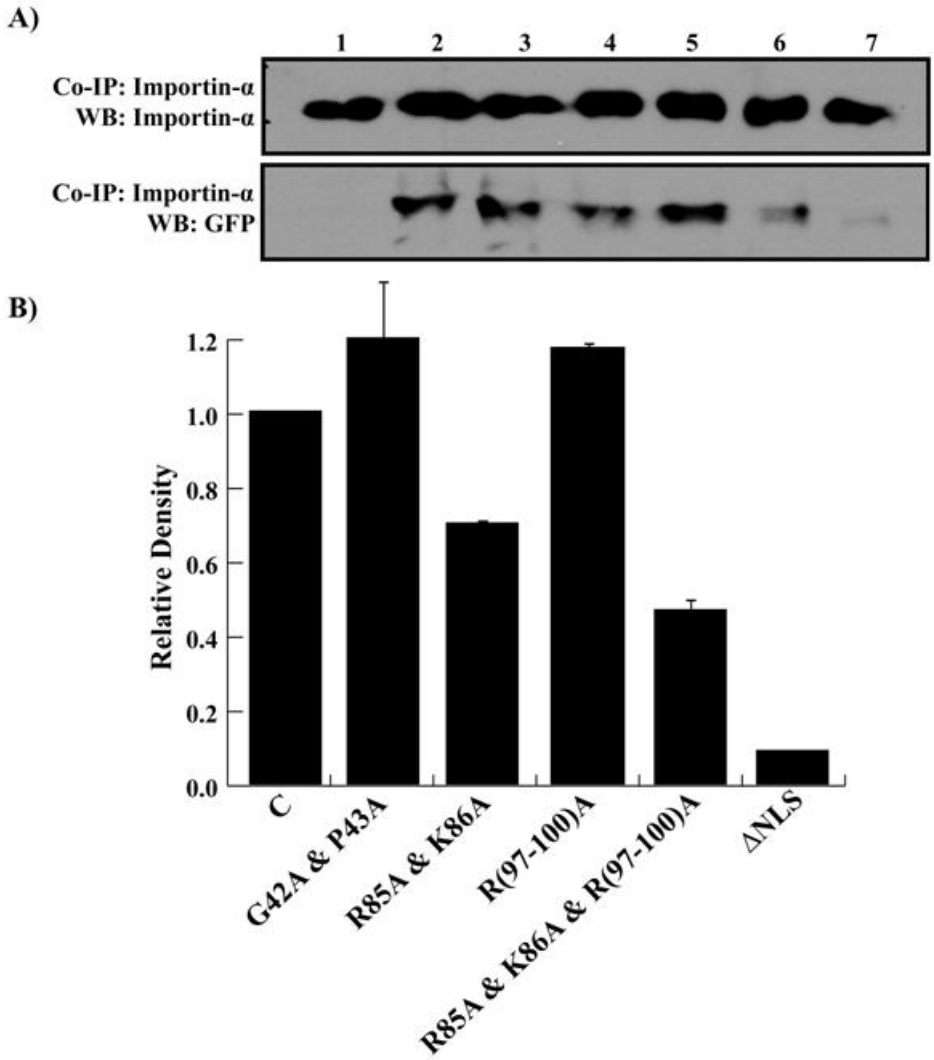

Figure 3.24: Co-immunoprecipitation study on various NLS mutants and importin-α protein. (A) Various mutated clones are pulled down with anti-importin-α antibody and detected with anti-GFP antibody. Faint bands are still observed in most of the mutants except ΔNLS where the entire C-terminus (residues 85-114) is removed from full-length C protein (Lane 1 – mock-transfected; Lane 2 – full-length C protein; Lane 3 – G42A & P43A mutant; Lane 4 – R85A & K86A mutant; Lane 5 – R(97-100)A mutant; Lane 6 – R85A & K86A & R(97-100)A; Lane 7 – ΔNLS mutant). (B) Densitometry analysis using ImageJ software. The GFP band intensities are normalized against respective importin-α band intensity for each clone. Relative density is calculated by using full-length DENV C protein as the baseline.

3.7.2. Determining binding strength of DENV C protein and importin-α

Other than densitometry analysis on Western-blot results, mammalian-2-hybrid (M2H) assay (Section 2.3.7) was also carried out to quantify the binding strength between DENV C and importin-α proteins. Importin-α gene was amplified from BHK total RNA and cloned into pFN11A (BIND) vector so that importin-α

protein would be fused to the C-terminus of GAL4 DNA-binding domain. Whereas, DENV-2 C gene was amplified from GFP-tagged C protein plasmid and ligated with pFN10A (ACT) vector so that DENV C protein would be at the C-terminus of VP16 transcriptional activation domain. If DENV C protein bound to importin-α protein, VP16 activation domain and GAL4 DNA-binding domain would be brought together resulting in transcriptional activation of a firefly luciferase reporter gene as shown in Figure 3.25. Firefly luciferase enzyme could be measured easily via luciferase assay and a luminometer. *Renilla* luciferase enzyme would also be expressed for normalization of the transfection efficiency of both vectors.

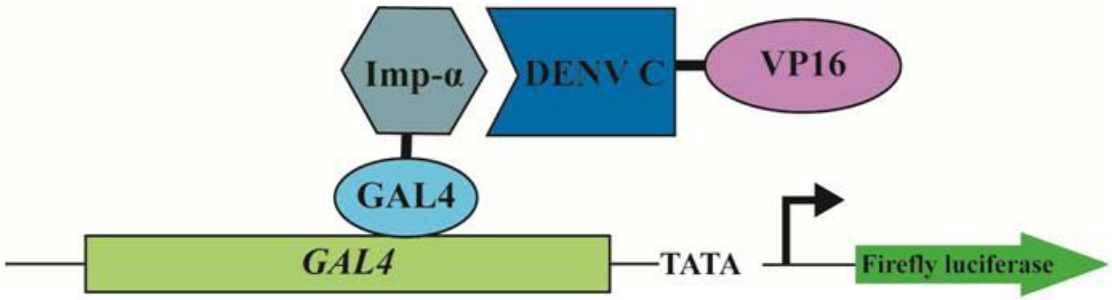

Figure 3.25: Illustration of mammalian-2-hybrid concept. Importin-α protein is fused with GAL4 DNA-binding domain while DENV C protein is fused with VP16 activation domain. When DENV C protein binds to importin-α protein, firefly luciferase reporter gene will be activated.

Figure 3.26 showed the importin-α gene (A) and full-length DENV C gene (B) were ligated with pFN11A (BIND) and pFN10A (ACT) vectors, respectively. The DNA sequences and the conceptual translation of the sequences of both genes were included in Appendix 8 (l-m).

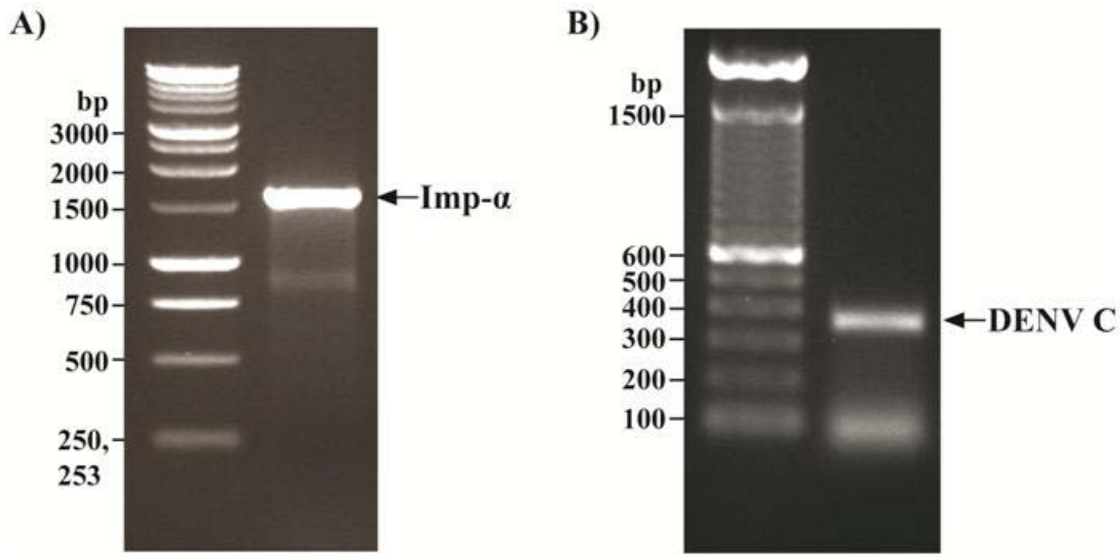

Figure 3.26: Cloning of importin-α (A) and full-length DENV C (B) genes into mammalian-2-hybrid vectors. Importin-α and DENV C genes are approximately 1587 bp and 342 bp, respectively as indicated by the arrows.

Subsequently, M2H assay was performed to measure the binding strength of full-length DENV C protein and mutated proteins with importin-α protein. Mutants R5A&K6A&K17A&R18A (DM1), R85A&K86&R(97-100)A (DM2) and Δall (DM1M2) were also generated from the mutated clones produced in Section 3.5.2. Figure 3.27(A) showed that the binding strength of DENV C protein with importin-α protein was reduced to about 50 % when NLS1 motif was mutated (DM1). The binding strength was further reduced to 20 % when NLS2 motif was mutated (DM2) and less than 20 % when both NLS1 and NLS2 motifs were mutated (DM1M2). Figure 3.27(B) showed the relative protein expression level in all the samples. The transfection efficiency among all the samples was quite equal.

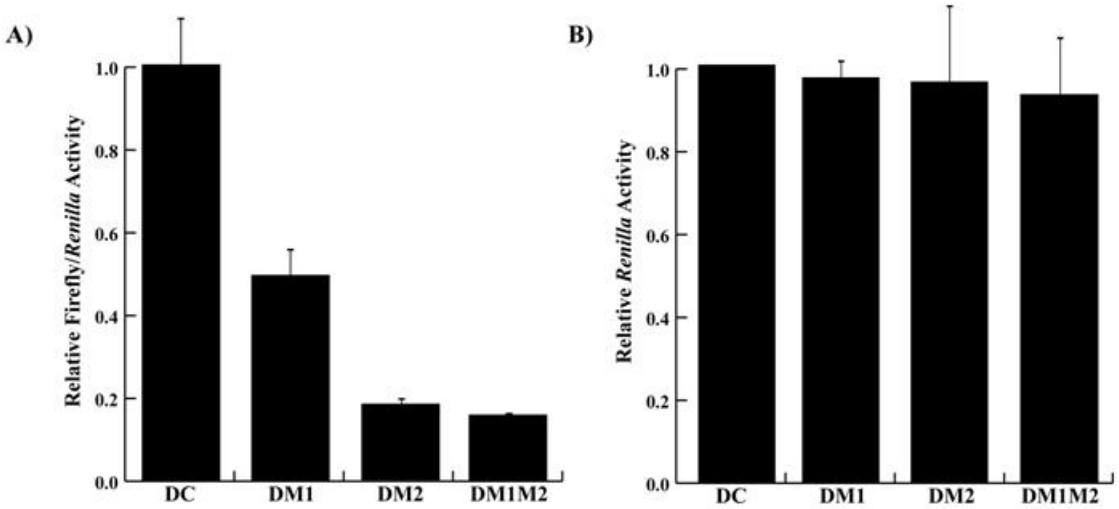

Figure 3.27: Mammalian-2-hybrid assay on the binding strength of importin-α protein with full-length DENV C and mutated proteins. (A) The relative Firefly/*Renilla* activities of full-length DENV C protein and C protein mutants [DM1 (R5A&K6A&K17A&R18A), DM2 (R85A&K86&R(97-100)A) and DM1M2(Δall)] are measured and plotted. An arbitrary value of 1 is set for the binding efficiency of full-length DENV C protein and importin-α association. The binding efficiency between C protein and importin-α is reduced up to 50% for DM1 mutant (P=0.008) and 80% for DM2 (P=0.0008) and DM1M2 (P=0.0007) mutants. (B) To normalize the transfection efficiency among all the samples, *Renilla* luciferase activities are measured. The protein expression levels among all the samples are similar..

Taken together, Section 3.7 corroborated the fact that importin-α protein was the transporting partner of DENV C protein and both NLS motifs were vital for the binding to importin-α protein. NLS2 motif was the main interacting domain of DENV C protein but either one of the basic-residues clusters was sufficient for the binding to importin-α protein.

3.8. Role of Phosphorylation in Nuclear Localization of Dengue Virus (DENV) Capsid (C) Protein

Increasing evidence showed that phosphorylation was the key regulator in controlling the binding of importin-α protein to its targeting partners for nuclear translocation (Bian *et al.*, 2007; Jans *et al.*, 2000; Lu & Ou, 2002). Recently, Bhuvanakantham and her colleagues (2010) demonstrated that nuclear localization of

WNV C protein was regulated by protein kinase C (PKC)-mediated phosphorylation. Thus, it was hypothesized that nuclear localization of DENV C protein would be regulated similarly by phosphorylation process. Bioinformatic analyses using NetPhos 2.0 and Eukaryotic Linear Motif (ELM) predicted that DENV C protein was indeed a phosphoprotein that could be phosphorylated by various kinases as shown in Table 3.2. Similarly, two different bioinformatics software were used to ensure that there was no discrepancy between software algorithms.

Table 3.2: Putative phosphorylation sites on DENV C protein. Putative phosphorylation sites are underlined and respective protein kinases acting on the putative phosphorylation sites are shown.

Enzymes	Position	Amino Acid Sequences
Protein Kinase A (PKA)	31-37	KRF<u>S</u>LGM
	98-104	RRR<u>T</u>AGM
Protein Kinase B (PKB)	20-28	RNRVS<u>T</u>VQQ
Protein Kinase C (PKC)	30-32	<u>T</u>KR
	71-73	<u>T</u>IK

As shown in Table 3.2, five putative phosphorylation sites were predicted and DENV C protein could potentially be phosphorylated by all three protein kinases (Protein Kinase A, B and C) for different purposes. It was reported that phosphorylation was also involved in regulating the binding of viral RNA to C protein (Cheong & Ng, 2011; Law *et al.*, 2003). Therefore, the five putative phosphorylation sites may not be solely responsible for nuclear localization but also for viral RNA interaction. To investigate if the putative phosphorylation site(s) was/were essential in regulating the nuclear localization of DENV C protein, site-directed mutagenesis was carried out to mutate all these five putative phosphorylation sites to alanine (Figure 3.28). The DNA sequences and the conceptual translation of the sequences of all the mutated clones were included in Appendix 8 (n-r).

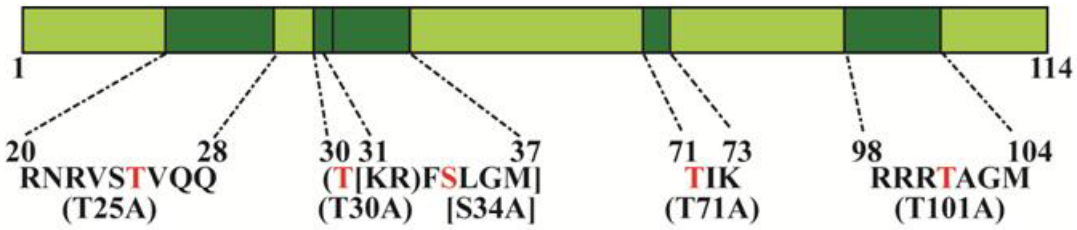

Figure 3.28: Schematic diagram of clones with mutation on putative phosphorylation site. Single site-directed mutagenesis is carried out on the five putative phosphorylation site of full-length DENV C protein.

After obtaining the phosphorylation-site mutated clones, the effect of the mutations on nuclear localization of DENV C protein was examined under fluorescence microscope. As shown in Figure 3.29, most of the putative phosphorylation sites did not affect the nuclear localization of C proteins as green fluorescent was still observed in the nuclei for mutant T25 [Figure 3.29(A)], T30 [Figure 3.29(B)], S34 [Figure 3.29(C)], and T101 [Figure 3.29(E)]. The result indicated that phosphorylation site at residue 71 (T71A) [Figure 3.29(D)] may have a functional role in regulating nuclear translocation of DENV C protein as green fluorescence was detected mostly at the perinuclear regions with residual fluorescence in the nuclei.

According to Table 3.2, residue 71 is a putative phosphorylation site by protein kinase C (PKC). Hence, the role of PKC in mediating nuclear translocation of DENV C protein was investigated. Baby Hamster Kidney (BHK) cells seeded on coverslips were transfected with GFP-tagged C protein plasmid and treated with PKC inhibitor bisindolylmaleimide (Bis) according to Section 2.4.4.

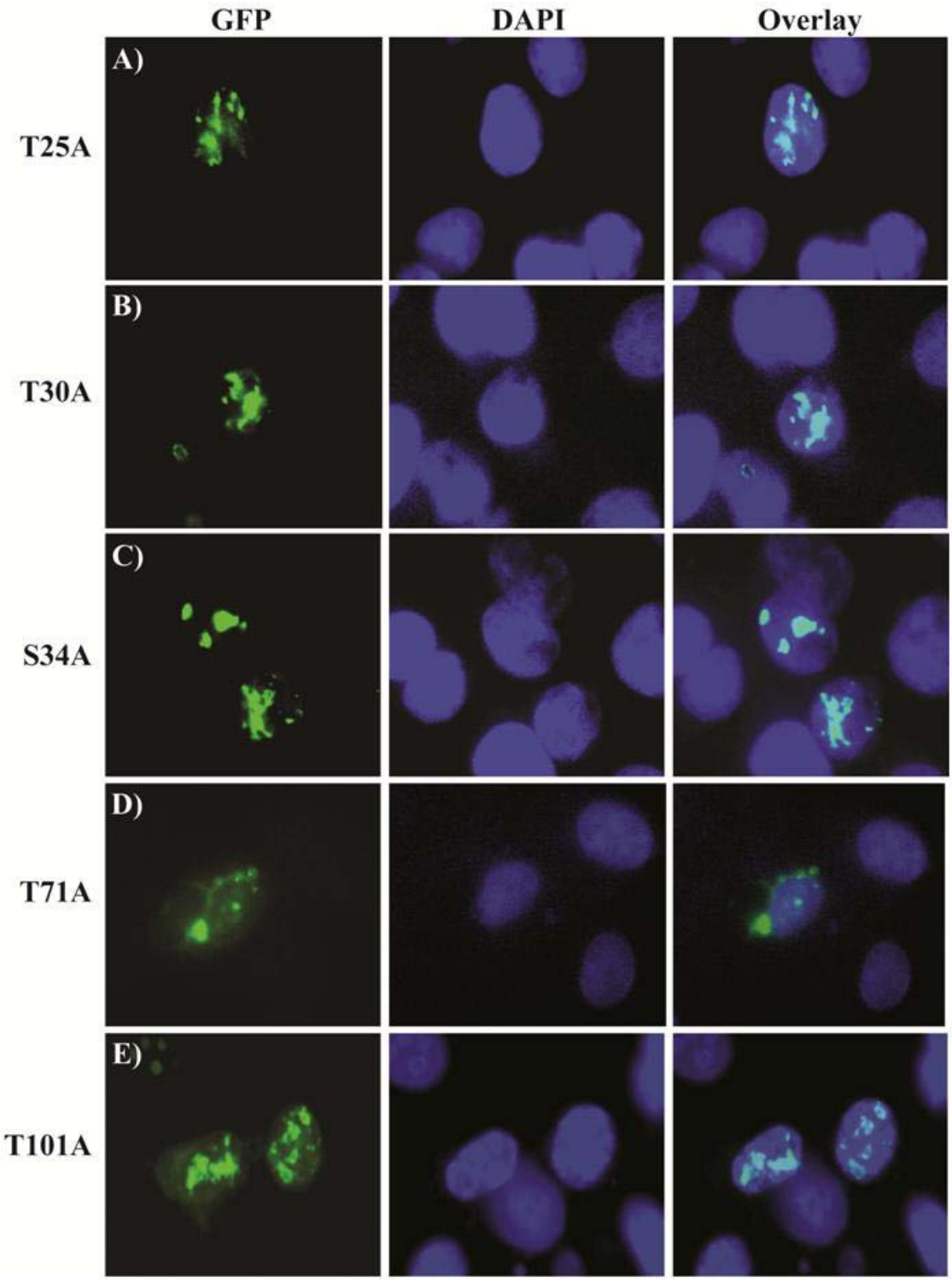

Figure 3.29: Effect of mutations on the putative phosphorylation sites of DENV C protein. Distinct green fluorescence signals are still detected in the nuclei for mutants T25A (A), T30A (B), S34A (D) and T101A (E). Only T71A (D) exhibits higher concentration of green fluorescence at the perinuclear regions with residual fluorescence in the nuclei.

As shown in Figure 3.30(A), majority of the green fluorescence was observed in the cytoplasm after treatment with PKC inhibitor. DENV C protein was unable to enter nuclei when the phosphorylation activity by PKC was inhibited. However, when protein kinase A (PKA) inhibitor, H-89 dihydrochloride, was used [Figure 3.30(B)], no effect was observed as compared to non-treatment [Figure 3.30(C)]. Bright green fluorescence was still seen in the nuclei / nucleoli of transfected cells. Hence, the effect of PKC inhibitor on nuclear localization of C protein was specific.

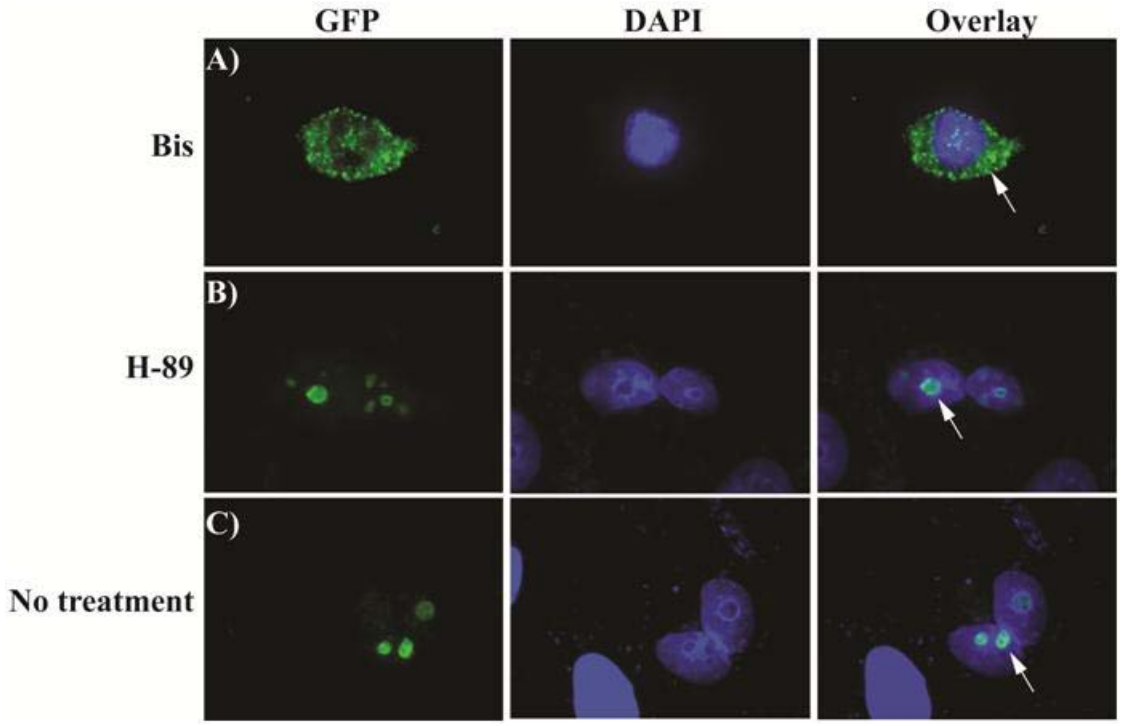

Figure 3.30: Role of protein kinase C on nuclear localization of DENV C protein. BHK cells are transfected with C-GFP plasmid and treated with (A) bisindolylmaleimide [(Bis) (PKC inhibitor)] and (B) H-89 dihydrochloride (PKA inhibitor). Majority of DENV C protein appears in the cytoplasm after treatment with Bis. However, PKA inhibitor has no effect on the nuclear localization of C protein because intense green fluorescence is still observed in the nuclei / nucleoli, which is similar to that of without treatment (C).

The result from this chapter allowed the understanding of the translocation mechanism of DENV C protein into the cell nucleus and a molecular mechanism model is proposed as shown in Figure 3.31. The first step is phosphorylation of

residue 71 of DENV C protein by protein kinase C. The phosphorylated DENV C protein proceeds to interact with importin-α protein via NLS2 motif of DENV C protein before engaging with importin-β protein allowing the DENV C-importinα-importinβ complex to translocate into the nucleus. NLS1 motif (residue 5-22) of DENV C protein enhances this nuclear translocation either by helping NLS2 motif to bind more strongly to importin-α protein or by facilitating the binding of importin-β to importin-α protein.

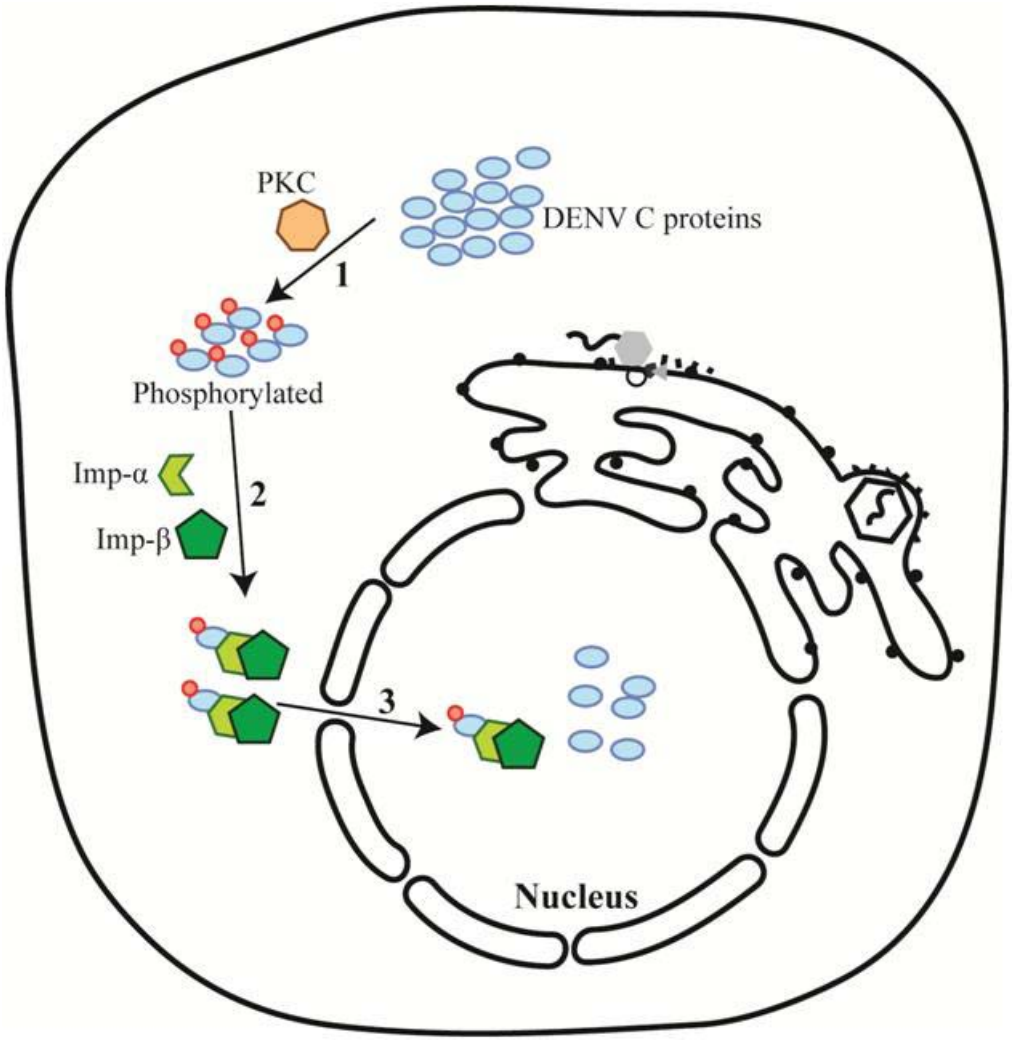

Figure 3.31: Proposed model of nuclear transportation of DENV C protein. 1. DENV-2 C protein is phosphorylated by protein kinase C at amino acid residue 71. **2.** Phosphorylated form of C protein is recognized by importin-α protein. Importin-α protein binds to phosphorylated C protein at bipartite NLS2 motif. NLS1 motif enhances the binding between C protein and importin-α protein. **3.** Importin-β protein binds to importin-α protein and brings the whole complex into the nucleus.

Nuclear translocation of C protein is an essential step during the replication of DENV. However, the roles of nuclear localization of DENV C protein are not resolved thus far. Investigating the non-structural roles of C protein in the nucleus will allow better understanding of the pathogenesis of flavivirus. The subsequent chapters will unravel this missing puzzle to understand the significance of DENV C protein nuclear phase during flavivirus replication.

4. Expression and Purification of Dengue Virus (DENV) Capsid (C) Protein

4.1. Introduction

Other than delineating the molecular mechanism of nuclear translocation of Dengue virus (DENV) capsid (C) protein, another main objective of this project was to unravel novel non-structural roles of DENV C protein in the nucleus. High-throughput screening for novel interacting partners of DENV C protein using ProtoArray® technology of human protein microarray was selected. Therefore, highly purified DENV C protein was obligatory before the screening can proceed. In this chapter, various challenges that were encountered and ways to overcome them during the expression and purification of DENV C protein to use on the ProtoArray® technology were described.

4.2. Expression and Purification of Dengue Virus (DENV) Capsid (C) Protein in Mammalian System

4.2.1. Molecular cloning of FLAG-tagged dengue virus (DENV) capsid (C) protein

In order to generate recombinant DENV C protein in a protein folding environment that is closer to the wild-type viral C protein, mammalian amino (N)-terminal FLAG stable expression kit (Sigma, USA) was chosen. DENV C protein is a small protein comprising 114 amino acids with molecular weight of approximately 12 kDa. Thus, FLAG peptide which is an octapeptide (Asp-Tyr-Lys-Asp-Asp-Asp-Asp-Lys) would be an ideal tag as its small molecular size would be highly unlikely to affect the folding of DENV C protein. pFLAG-CMV-3 vector was selected because it contained a preprotrypsin (PPT) leader sequence that would result in secretion of the

FLAG fusion protein into culture media. Hence, a stable cell line expressing FLAG fusion protein can be generated and the recombinant proteins can be easily harvested continuously from the culture media.

Figure 4.1 showed the molecular cloning of FLAG-tagged full-length DENV C protein using pFLAG-CMV-3 vector. To increase the binding strength of FLAG fusion protein during purification step, an additional FLAG peptide was included at the N-terminus of DENV C protein. A thrombin cleavage site was inserted in between DENV C protein and FLAG peptides for tags removal after purification. To insert the thrombin cleavage site and an additional FLAG peptide, overlap extension-PCR (OE-PCR) technique was employed using two overlapping forward primers (Section 2.3.3; Table 2.4). The final PCR product was cloned into pFLAG-CMV-3 vector via *HindIII* and *BamHI* restrictive enzyme recognition sites. Positive clones were sent for DNA sequencing to ensure the insert was in frame with the vector and no extra mutation. The DNA sequences and conceptual translation of the sequences were shown in Appendix 8s.

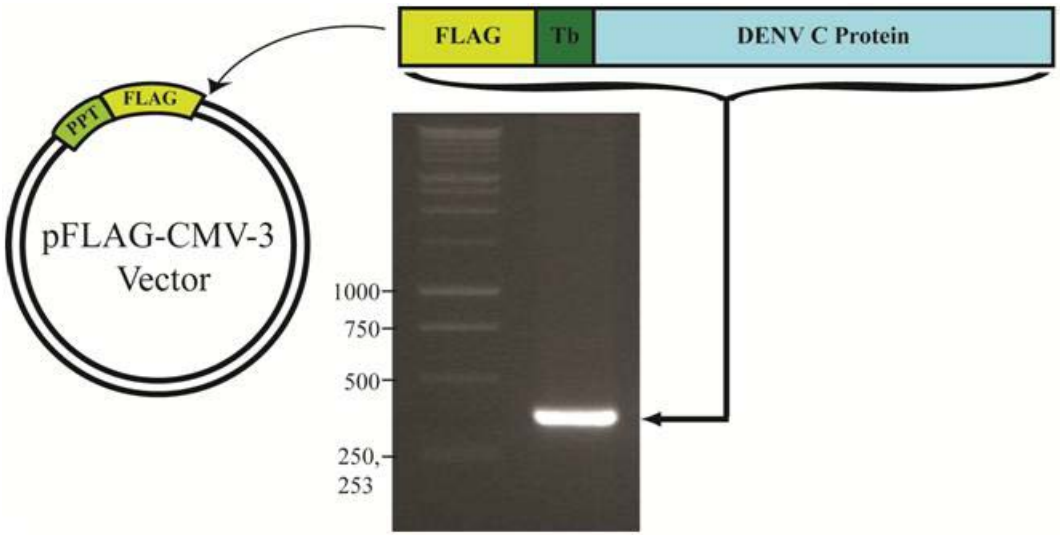

Figure 4.1: Cloning of FLAG-tagged full-length DENV C protein. An additional FLAG peptide is included at the upstream of DENV C gene before the thrombin (Tb) cleavage site. The final PCR product is ligated into pFLAG-CMV-3 vector at the downstream of preprotrypsin (PPT) leader sequence and FLAG peptide.

4.2.2. Pilot screening of FLAG-tagged full-length dengue virus (DENV) capsid (C) protein expression

After obtaining FLAG-tagged DENV C protein plasmid, pilot screening was performed to examine its expression in 293FT cells. 293FT cell line is a fast-growing variant of human embryonic kidney (HEK)-293 cell line stably-expressing the SV40 large T antigen. Comparatively, 293FT cell line showed higher transfection efficiency than normal HEK293 cells. Thus, 293FT cell line was chosen for large-scale protein expression.

293FT cells were transfected with FLAG-tagged DENV C protein plasmid in a 6-well plate and both the supernatant and cell lysates were harvested at 24 hr post-transfection. Anti-FLAG antibody was used to detect the presence of DENV C protein in the culture media and cell lysate. Unfortunately, DENV C protein was not detected in the culture media as shown in Figure 4.2. Most of the DENV C proteins still remained in the cells as band could only be observed in the cell lysate but not in the culture media (Figure 4.2).

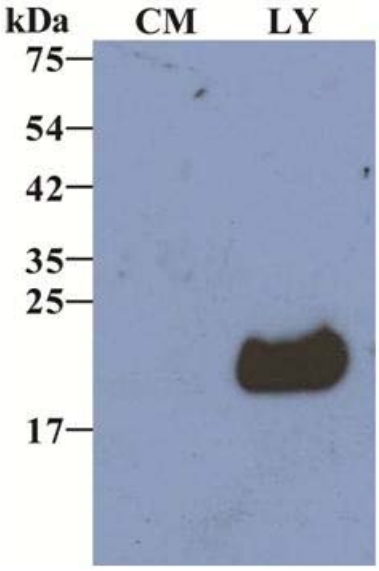

Figure 4.2: Pilot screening of FLAG-tagged DENV C protein expression in 293FT cells. The presence of DENV C protein in the culture media (CM) and cell lysates (LY) is detected using anti-FLAG antibody in Western-blot. FLAG-tagged C protein can only be detected in the cell lysates.

Possible reasons for the absence of FLAG-tagged DENV C protein in the culture media could be due to the low concentration of DENV C protein in the media or the insufficient time for protein expression. To examine these possibilities, another round of transfection was carried out in a 6-well plate and both the supernatant and cell lysates were harvested at 24 hr and 48 hr post-transfection. The 2-ml culture media was concentrated ten times to 200 µl via Vivaspin (Sartorius, Germany). Western-blot was performed to detect the presence of DENV C protein in all samples using anti-FLAG antibody.

Figure 4.3 illustrated that the level of expression of DENV C protein was higher at 24 hr post-transfection than 48 hr post-transfection as the band intensity for 24 hr post-transfection was thicker. It was noticed under upright light microscope that the number of cells at 48 hr post-transfection decreased significantly as compared to 24 hr post-transfection. This could be due to cell apoptosis triggered by C protein as previously observed in Section 3.3.4 (Figures 3.9 and 3.11). A very faint band was observed in the ten-time concentrated culture media at 24 hr post-transfection and no band was detectable in the ten-time concentrated culture media at 48 hr post-transfection. This showed that the preprotrypsin leader sequence was not functional because DENV C protein was not secreted into the culture media. This could be attributed to the two bipartite nuclear localization signal (NLS) motifs that were present on the DENV C protein as described in Section 3.4.

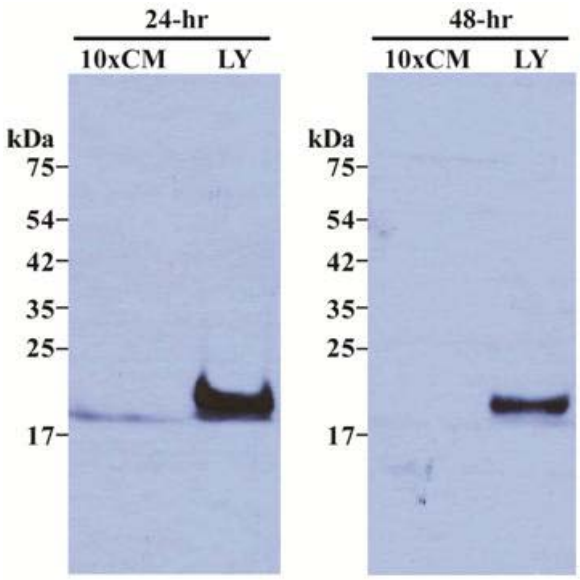

Figure 4.3: Detection of FLAG-tagged DENV C protein in the 293FT cell lysates and culture media. The presence of DENV C protein in both the concentrated culture media (10 x CM) and cell lysates (LY) harvested at 24 hr and 48 hr post-transfection are detected using anti-FLAG antibodies. Band detected in the LY at 24 hr post-transfection is much more intense than that at 48 hr post-transfection. A very faint band is detected in the 10 x CM at 24 hr post transfection and no band is observed at 48 hr post transfection.

4.2.3. Immunoprecipitation of FLAG-tagged dengue virus (DENV) capsid (C) protein in the cell lysates

Although the above attempts to express and secrete FLAG-tagged DENV C protein into the culture media were not successful, immunoprecipitation was still carried out using the cell lysates to examine the functionality of FLAG tags. One T-75 flask of 293FT cells with 80 % confluency was transfected with FLAG-tagged DENV C protein plasmid and the cell lysates were harvested at 24 hr post-transfection. Cell lysates were then incubated with anti-FLAG M2 affinity gel (Sigma, USA) overnight at 4 ^{o}C with constant rotating. Unbound proteins were collected as flow-through and the resin with bound FLAG fusion proteins was washed thrice with cold PBS (Appendix 1e) to remove any nonspecific binding proteins. FLAG fusion proteins were eluted out by competition with 3x FLAG peptides (Sigma, USA).

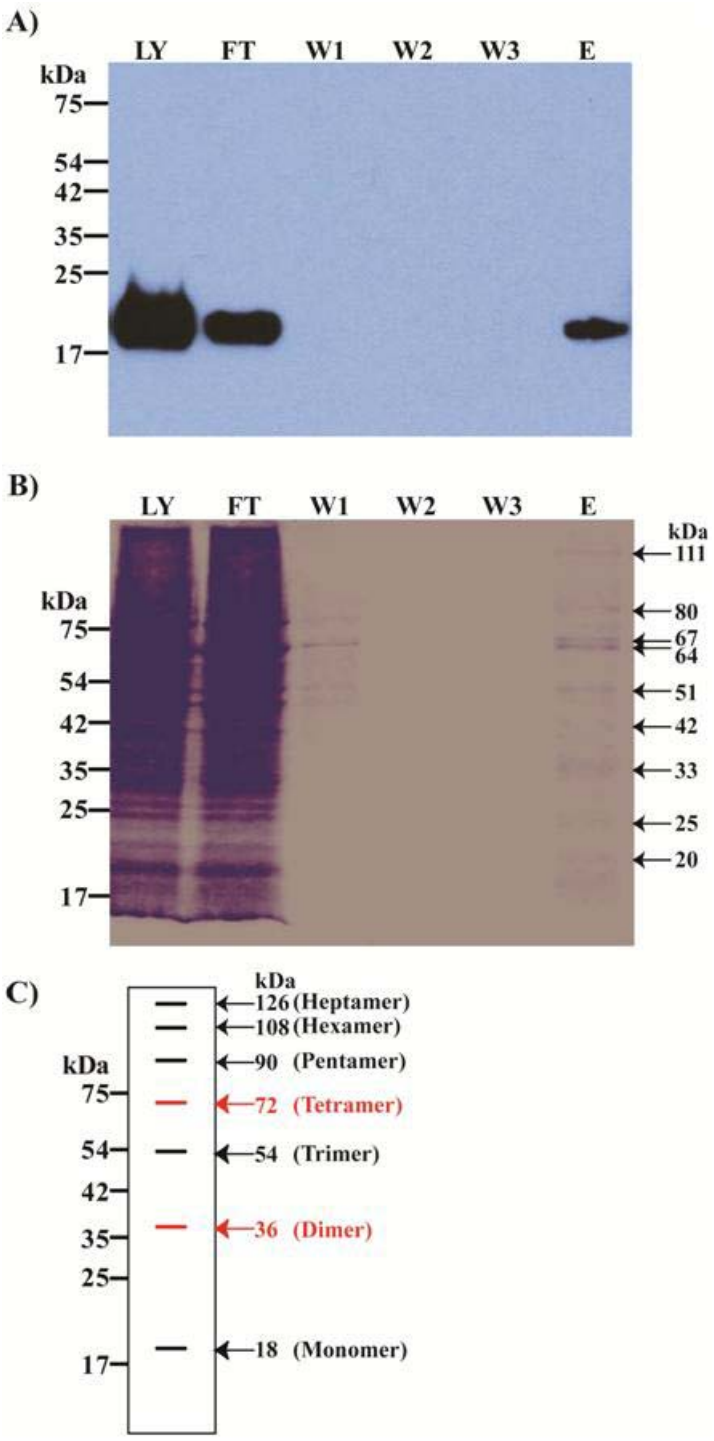

Figure 4.4: Immunoprecipitation of FLAG-tagged DENV C proteins in 293FT cell lysates. (A) The presence of DENV C proteins in the cell lysate (LY), flow-through (FT), washed samples (W) and eluate (E) are detected via Western-blot using rabbit anti-FLAG antibody. DENV C protein-corresponding bands can be detected in LY, FT and E fractions. (B) SDS-PAGE gel stained with Coomassie-blue. Multiple intense bands are observed in the LY and FT fractions. Although only one band is detected in Western-blot, multiple faint bands are seen in the E fraction. The molecular weights of the E bands are estimated based on their relative mobility. (C) Estimated band sizes of various possible oligomers of DENV C protein are drawn. Only dimer and tetramer are reported thus far as highlighted in red. The molecular weight of DENV C protein monomer is approximately 18 kDa in SDS-PAGE.

As shown in Figure 4.4 (A), there were still significant amounts of DENV C proteins in the flow-through (FT). This could be due to either the binding of FLAG-tagged DENV C protein to the resin was not strong enough or all the anti-FLAG antibodies were fully occupied and thus the FLAG fusion proteins detected in the FT were excessive proteins. No FLAG fusion proteins were detected in the Wash (W) fractions so the binding of FLAG-tagged DENV C proteins to anti-FLAG antibody was specific and with high affinity [Figure 4.4 (A)].

Despite the thick band as detected via Western-blot in Figure 4.4 (A), SDS-PAGE analysis followed by staining with Coomassie blue indicated that DENV C protein-corresponding band was not distinctively seen in lysate (LY) and FT fractions [Figure 4.4 (B)]. Instead, many intense bands were seen in those fractions. As for the eluate (E) fraction, multiple faint bands were observed. This was unanticipated because at least 4 µg of FLAG fusion proteins should be eluted out if all anti-FLAG antibodies were occupied during the binding step. One possible explanation for the multiple bands in the eluate was that they could be the different oligomers of DENV C protein. However, this postulation was not supported by the molecular sizes of the bands detected in the eluate [Figure 4.4 (B)] as compared to the estimated molecular weights of various possible oligomers [Figure 4.4 (C)]. On top of that, except monomer and dimer, all other possible oligomers [Figure 4.4 (C)] were not detected in the Western-blot [Figure 4.4 (A)]. Therefore, the multiple bands should be attributable to unspecific proteins from the cell lysate or some DENV C protein-interacting partners that were co-immunoprecipitated out during elution. To remove or decrease these non-specific bands, more stringent washing buffer was necessary.

All the results thus far indicated that mammalian N-terminal FLAG stable expression kit was not suitable for expression and purification of large-scale DENV C

protein. The FLAG-tagged DENV C protein was not secreted out into the culture media. It was also not feasible to generate 293FT cell line stably expressing DENV C protein because C protein would trigger cell apoptosis as previously described in Sections 4.2.2 and 3.3.4. Moreover, the amount of immunoprecipitated FLAG-tagged DENV C proteins from one T-75 flask of transfected 293FT cells was very low. Therefore, it was not cost-effective to use this system for large-scale production of purified DENV C protein. Nonetheless, the results showed that FLAG-tagged DENV C protein was suitable for immunoprecipitation or co-immunoprecipitation studies.

4.3. Expression and Purification of Dengue Virus (DENV) Capsid (C) Protein in Bacterial System

To overcome the quantity issue, the alternative bacterial system was used to achieve higher yield for subsequent experiments. An optimized bacterial system for expression and purification of viral proteins was developed in the laboratory (Krupakar *et al.*, 2012; Tan *et al.*, 2010).

4.3.1. Engineering of biotin acceptor peptide (BAP) into dengue virus (DENV) capsid (C) plasmid, pET28aDENVBioCap

To perform high-throughput screening for novel interacting partners using ProtoArray platform, a suitable tag must be engineered onto DENV C protein for easy detection with high sensitivity. Biotinylation has been widely used to date for purification, detection, diagnostic, protein-protein interaction studies, imaging studies, and other molecular studies (Chapman-Smith & Cronan, 1999a; de Boer *et al.*, 2003; Howarth & Ting, 2008; Postel *et al.*, 2011; Qi & Katagiri, 2011). One of the advantages of using biotinylated protein is that the detection sensitivity of the

biotinylated protein is greatly enhanced by the high affinity and specificity between biotin and streptavidin (Bayer & Wilchek, 1990).

Besides, biotin is a very small molecule (molecular weight = 244.31) so it is unlikely to affect the structure and function of DENV C protein. To ensure that the BAP will not result in any steric hindrance to the protein conformation, a secondary structure prediction was performed. As shown in Figure 4.5, the predicted secondary structures of DENV C protein with and without BAP do not differ from each other. As such, biotin was chosen to be the suitable tag for detection and a biotin acceptor signal peptide gene (Cull & Schatz, 2000) was engineered at the upstream of DENV C gene.

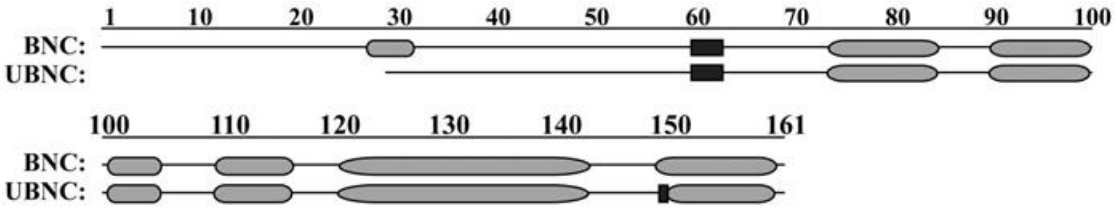

Figure 4.5: Secondary structure prediction of biotinylated DENV C protein (BNC) and unbiotinylated C protein (UBNC). The prediction shows that biotin acceptor peptide (BAP) insertion does not affect the overall secondary structure formation when BAP is added to the N-terminus of C protein. Alpha helices are represented in gray, rounded rectangles. Beta sheets are represented in black, regular rectangles.

To engineer pET28aBioCap plasmid, nucleotides from 100 to 438 in DENV-2 genome (GeneBank accession number: **M29095**) was cloned out from its cDNA, whereas the BAP sequence was amplified from a template provided by Dr. Krupakar Parthasarathy, Department of Microbiology, NUS. The template containing a BAP sequence was synthesized based on the published sequence (Cull & Schatz, 2000) followed by an enterokinase cleavage site. Both fragments were joined together through overlapping extension-PCR (OE-PCR) method as illustrated in Figure 4.6 (A). Figure 4.6 (B) showed the first and second fragments, C1 and C2, which contained

BAP sequence and DENV C gene, respectively. Since C1 fragment was approximately 90 bp only, PCR purification was carried out instead of gel purification to minimize loss of PCR product. Both fragments were then joined together using primers Biotin_F and C_R (Table 2.5 in Chapter 2) to obtain C3 fragment.

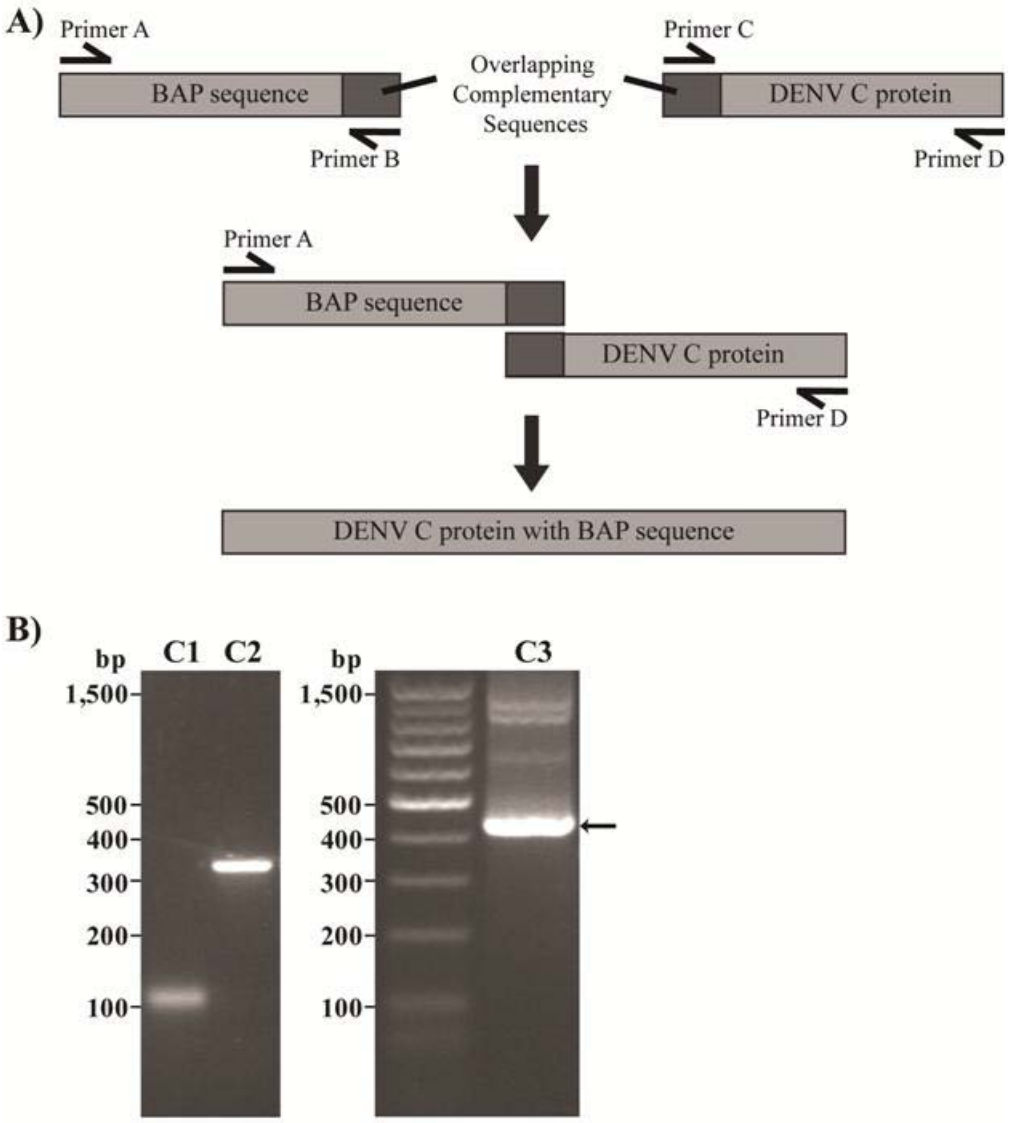

Figure 4.6: Cloning of pET28aDENVBioCap plasmid via overlapping extension PCR (OE-PCR) technique. (A) Schematic diagram showing OE-PCR technique. The 3′ overhang of biotin acceptor peptide (BAP) fragment is complementary to the 5′ overhang of DENV C gene fragment. As such, primers B and C are complementary to each other. Both fragments are joined together with primers A and D. (B) DNA gel electrophoresis of C1 fragment (BAP sequence, enterokinase cleavage site and some overlapping sequence from the 5′ overhang of C2 fragment) and C2 fragment (DENV C gene with some overlapping sequence from the 3′ overhang of C1 fragment) which are approximately 90 bp and 369 bp, respectively. Both fragments are joined together to generate C3 final product with C1 fragment at the N-terminus followed by C2 fragment. Final product is about 432 bp as indicated by arrow.

After gel purification, the final product was ligated with bacterial expression vector, pET28a, via *Nhe* I and *Xho* I cut sites. pET28a vector contained a 6 x His tag and a thrombin cleavage site at the upstream of the multiple cloning site. Hence, the recombinant full-length DENV C construct (pET28aDENVBioCap) contained 2 tags (6 x His tag and BAP) at the N-terminus and 2 different enzyme cleavage sites (thrombin cleavage site and enterokinase cleavage site) for tags removal when necessary. The 6 x His tag was used for affinity chromatography purification while BAP was the signal peptide for biotinylation. Schematic representations of the final vector construct and recombinant protein are shown in Figure 4.7 (A) and (B), respectively. Five successfully transformed bacterial colonies were picked for colony PCR screening and DNA sequencing was performed to verify the constructs. The final DNA and protein sequences are shown in Appendix 8(t). DENV C protein without BAP was also constructed for comparison purposes.

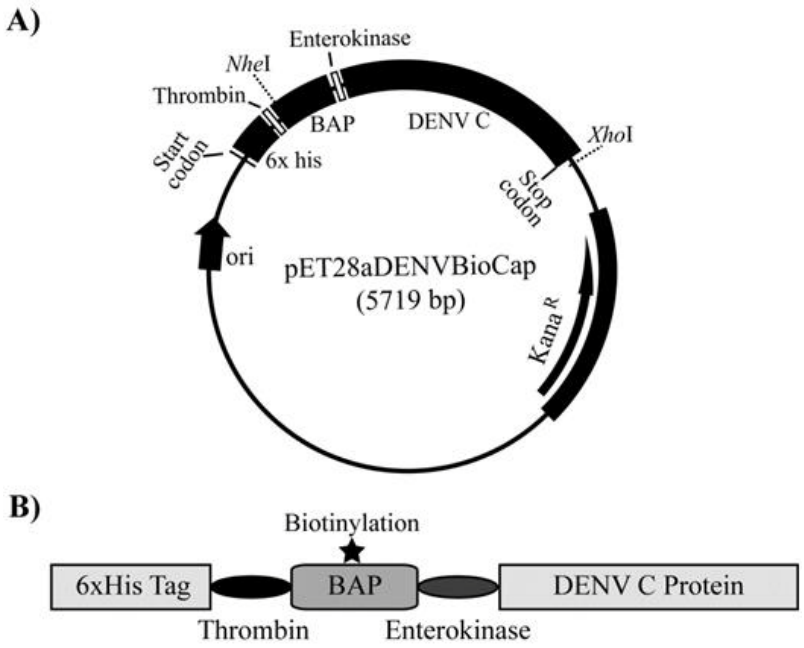

Figure 4.7: Schematic representation of pET28aDENVBioCap construct. (A) Plasmid vector map of pET28aDENVBioCap construct. (B) Final construct of recombinant protein generated. 6 x His tag is at the N-terminus followed by thrombin cleavage site and biotin acceptor peptide (BAP). Enterokinase cleavage site is included at the downstream of BAP. 6 x His tag is used for affinity purification while BAP is the signal peptide for biotinylation.

4.3.2. Pilot screening of Dengue virus (DENV) capsid (C) protein expression

To express DENV C protein, an optimal expression competent bacterial strain is requisite because 14 rare codons were detected in the full-length DENV C protein DNA sequence (Table 4.1). This raised a concern for protein expression because 12 % of the total 115 codons were rare codons. To screen for the optimal bacterial expression competent cell, pET28aDENVBioCap plasmid was transformed into BL-21 (DE3) and BL-21-CodonPlus. BL-21 (DE3) is a common bacterial strain for high expression of recombinant protein while BL-21-CodonPlus is a bacterial strain specifically engineered for expression of protein with rare codons.

Table 4.1: Rare codon analysis of full-length DENV C protein. Rare codons are highlighted in **BOLD** and underlined.

Rare Codons	Number
Arg (AGG, AGA, CGA)	12
Leu (CTA)	1
Ile (ATA)	1
Pro (CCC)	0
Full-length DENV C DNA sequence:	
atg aat aac caa **cga** aaa aag gcg **aga** aat acg cct ttc aat atg ctg aaa cgc gag **aga** aac cgc gtg tcg act gta caa cag ctg aca aag **aga** ttc tca ctt gga atg ctg cag gga **cga** gga cca tta aaa ctg ttc atg gcc ctg gtg gcg ttc ctt cgt ttc **cta** aca atc cca cca aca gca ggg **ata** ctg aag **aga** tgg gga aca att aaa aaa tca aaa gcc att aat gtt ttg **aga** ggg ttc **agg** aaa gag att gga **agg** atg ctg aac atc ttg aac **agg** **aga** cgc **aga** act gca ggc atg atc att atg ctg att cca aca gtg atg gcg taa	

The expression of DENV C protein was indeed much higher in BL-21-CodonPlus strain. As indicated in Figure 4.8 (A), an obvious band corresponding to the recombinant full-length DENV C protein was detected in the bacterial cell lysate of IPTG-induced CodonPlus strain but not in the BL-21 (DE) strain. The molecular weight of DENV C protein was approximately 18 kDa as indicated by arrow.

However, Western-blot analysis using anti-His antibody revealed that DENV C protein was expressed in both BL-21 (DE) and BL-21-CodonPlus strains because C

protein-corresponding bands were detected in the bacterial cell lysates of both strains [Figure 4.8 (B)]. Nonetheless, the observed bands were much thicker in BL-21-CodonPlus strain as compared to BL-21 (DE) strain, indicating that the expression level of DENV C protein was much higher in BL-21-CodonPlus strain. This result corroborated that DENV C protein indeed required special bacterial strain for efficient protein translation. Therefore, BL-21-CodonPlus strain was used for expression of DENV C protein subsequently.

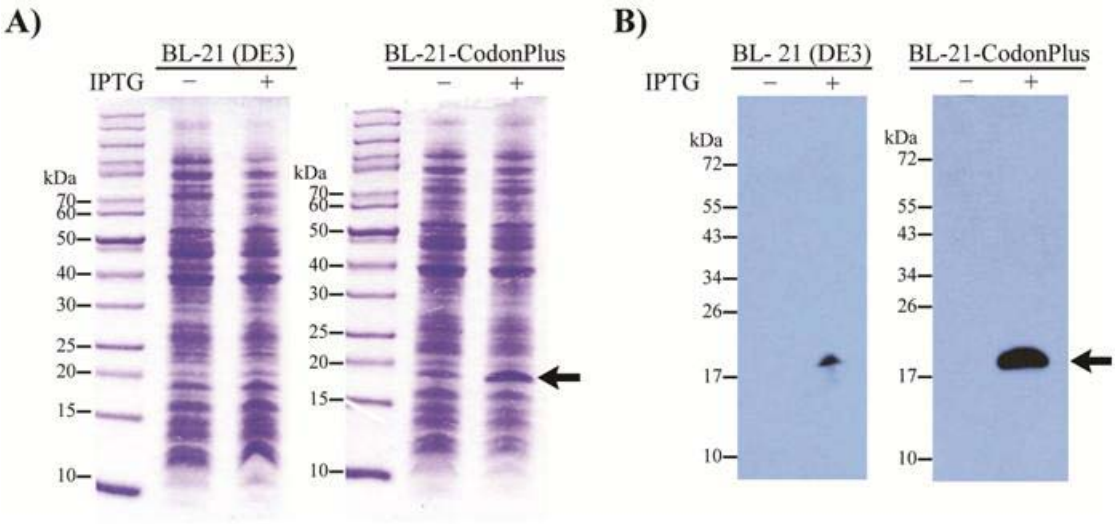

Figure 4.8: Pilot expression screening of DENV C protein. Two expression competent cell systems were tested, namely BL-21 (DE3) and BL-21-CodonPlus. The presence of C protein band in the IPTG-induced bacterial cell lysate, as indicated by arrow, is detected via SDS-PAGE stained with Coomassie blue (A) and Western blot (B) using anti-His antibody. The expression level of C protein in BL-21-CodonPlus competent cells is superior because the band intensity is much higher than that of normal BL-21 (DE3) competent cells.

After pilot expression screening using pET28aDENVBioCap plasmid, DENV C protein without biotin acceptor peptide (BAP) was also expressed in BL-21-CodonPlus competent cells for comparison purposes. Bacterial cell lysates containing DENV C proteins with and without BAP were analyzed via Western-blot using anti-His antibody. As shown in Figure 4.9, bands were observed in both DENV C proteins with and without BAP, implicating that both clones were expressing well in the BL-

21-CodonPlus strain. Recombinant DENV C protein with BAP showed higher molecular weight than that without BAP.

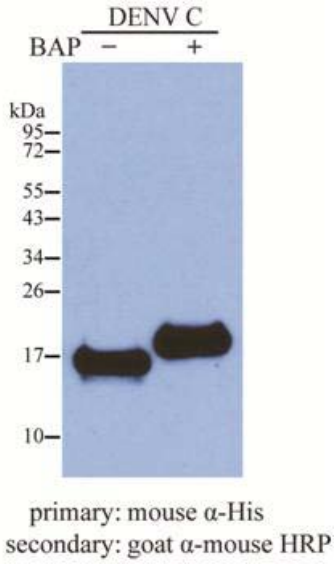

Figure 4.9: Expression of DENV C protein with and without BAP. Western-blot analysis using anti-His antibody shows that both DENV C proteins with and without BAP are expressing well in BL-21-CodonPlus competent cells. The molecular weight of DENV C protein with BAP is higher than that without BAP.

Besides detecting the proteins of interest using anti-His antibody, horse radish peroxidase-conjugated streptavidin antibody (Millipore, USA) was used to detect biotinylated proteins. Before using this streptavidin antibody for Western-blot, optimization was required.

4.3.3. Optimization of Western-blot for biotinylated protein

To optimize Western-blot protocol for horse radish peroxidase (HRP)-conjugated streptavidin antibody, commercially-available biotinylated (BN) and unbiotinylated (UBN) maltose-binding protein [(MBP) (GeneCopoeia, USA)] were purchased. Unlike anti-His antibody, usual Western-blot protocol (Section 2.5.3.2) using 5 % skim milk in TBST [Appendix 5c(iii)] as blocking buffer and antibody diluents was not suitable for streptavidin antibody. As shown in Figure 4.10 (A), BN MBP-corresponding band was not observed and the background was very high. This

problem was successfully solved when 4 % bovine serum albumin (BSA) in PBST [Appendix 5c(iv)] was used as blocking buffer and antibody diluents. BN MBP-corresponding band was not only seen clearly as indicated by arrow, the background was also very clean. Similar band was not observed in UBN lane. This optimized Western-blot protocol was used to detect biotinylated DENV C protein subsequently.

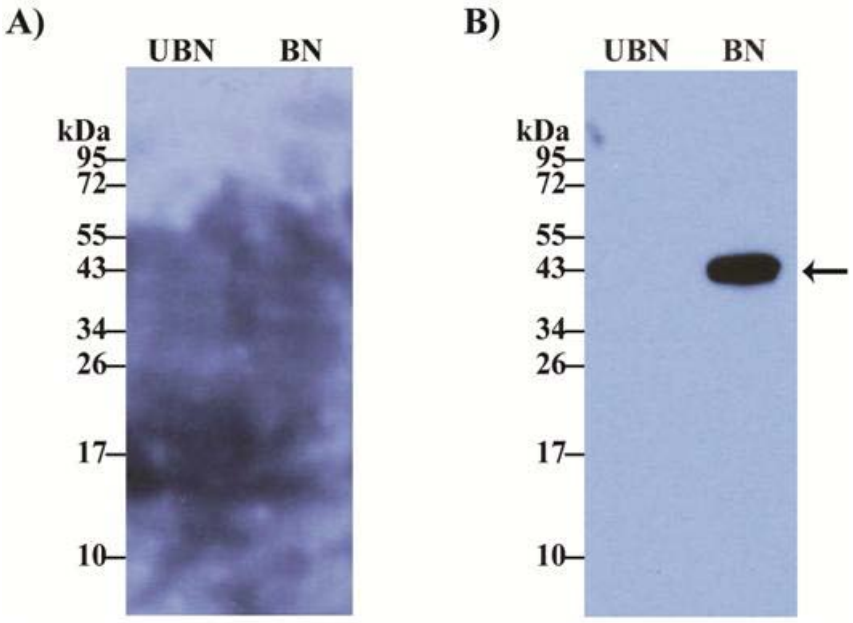

Figure 4.10: Optimization of Western-blot protocol for biotinylated proteins. (A) Western-blot using streptavidin-horse radish peroxidase (HRP) antibody and 5 % skim milk in TBST as blocking buffer and antibody diluents. Biotinylated (BN) maltose-binding protein (MBP) is not detected and the background is very high. Unbiotinylated (UBN) MBP is also included as negative control for biotinylation. (B) When 4 % bovine serum albumin (BSA) in PBST is used as blocking buffer and antibody diluents, the background becomes very clean and MBP-corresponding band is observed in BN lane and not in UBN lane.

4.3.4. Discovery of endogenous biotinylation in BL-21-CodonPlus competent cells

After optimizing the Western-blot protocol for streptavidin antibody using commercial maltose-binding protein (MBP), the biotinylation status of DENV C proteins with and without biotin acceptor peptide (BAP) was examined via the same Western-blot protocol. Before any *in vitro* biotinylation process using biotin ligase enzyme, no bands should be observed.

Surprisingly, DENV C protein with BAP was found biotinylated even before *in vitro* biotinylation process. As shown in Figure 4.11, thick band could be observed in the BAP-containing DENV C protein when streptavidin HRP antibody was used. Similar band was not detected in DENV C protein without BAP. This result suggested that DENV protein with BAP were biotinylated endogenously in BL-21-CodonPlus competent cells.

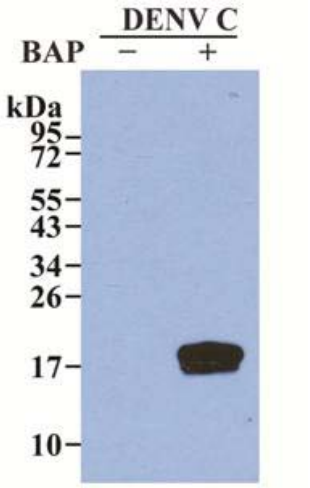

Figure 4.11: DENV C protein with biotin acceptor peptide (BAP) is biotinylated endogenously. Band is observed in the DENV C protein with BAP when horse radish peroxidase (HRP)-conjugated streptavidin antibody is used for Western blot. Similar band is not seen in the DENV C protein without BAP.

It was postulated that bacterial BL-21-CodonPlus competent cells might contain biotin holoenzyme synthetase BirA gene that encoded for biotin ligase protein in their genome. To investigate the reason behind endogenous biotinylation, BirA gene sequence was analyzed using BLAST software and the result showed that BL-21 strains indeed possessed BirA gene in their genome (Table 4.2). Besides, it was also reported that biotin molecules were present in the Luria-Bertani (LB) broth (Tolaymat & Mock, 1989). As a result, proteins engineered with BAP could be directly expressed and biotinylated in BL-21 strains cultivated in LB broth without the extra *in vitro* enzymatic biotinylation step. This discovery would be valuable for protein

engineering that requires site-specific biotinylation in bacterial system with simple steps. Proteins that required site-specific biotinylation could be produced easily by just simple overlap extension-PCR (OE-PCR) followed by expression in *Escherichia coli* BL-21 strains without the need of an additional *in vitro* biotinylation step.

Table 4.2: Competent cells identified through BLAST analysis of BirA gene.

Competent Cells	Accession Number	Features
BL-21 (DE3)	AM946981	Bifunctional biotin-[acetyl-CoA-carboxylase] ligase and transcriptional repressor
BL-21-CodonPlus	CP001665	Bifunctional BirA, biotin operon repressor/ biotin--acetyl-CoA-carboxylase ligase

4.3.5. Purification of biotinylated Dengue virus (DENV) capsid (C) protein

4.3.5.1. Extraction of Dengue virus (DENV) capsid (C) protein under denaturing condition

After confirming the expression and biotinylation status of DENV C proteins, large scale production of bacterial culture was carried out. Initial attempt was to perform all the extraction and purification steps in native form so that the protein structure could be preserved without the need of refolding. However, the extraction of DENV C protein from the bacterial cells via sonication under native condition was not effective. The solution was still very cloudy and huge amount of cell pellet was formed even after sonicating for 15 min in ice (30 sec “ON”, 30 sec “OFF”, and 45 % amplitude).

As shown in Figure 4.12, no band was observed when non-denaturing buffer (20 mM Tris, 300 mM NaCl and 10 mM Imidazole) was used. However, DENV C protein-corresponding band was observed when the cell pellet was solubilized in denaturing buffer (20 mM Tris, 300 mM NaCl, 8 M urea and 10 mM Imidazole)

without sonication. This result suggested that the recombinant full-length DENV C proteins were trapped in inclusion bodies. As such, 8 M urea was used to lyse the bacterial cell pellet and affinity chromatography purification was performed under denaturing condition.

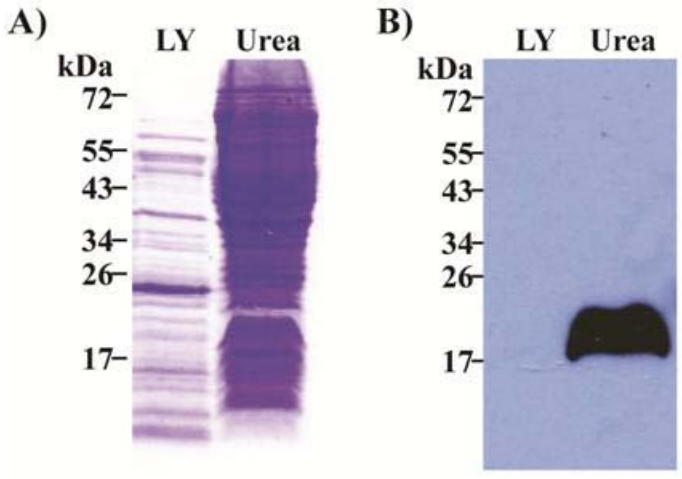

Figure 4.12: Extraction of DENV C protein under non-denaturing and denaturing conditions. Bacterial cell lysate after sonication (LY) and 8 M urea-solubilized pellet (Urea) are analyzed via Coomassie blue (A) and Western-blot using anti-His antibody (B). A thick band can only be observed in the 8M urea-solubilized pellet fraction, implying that DENV C proteins are trapped in the cell pellet.

4.3.5.2. Purification of Dengue virus (DENV) capsid (C) protein via affinity chromatography

To purify His-tagged proteins via affinity chromatography, bacterial cell lysates containing DENV C protein in 8 M urea was incubated with nickel-nitrilotriacetic acid (Ni-NTA) resin. 6 x His tag at the N-terminal recombinant full-length DENV C protein bound to the resin and unbound proteins were removed during washing with 20 mM imidazole. To ensure most of the unbound proteins were washed away, ten column volumes of wash buffer (20 mM Tris, 300 mM NaCl, 8 M urea and 20 mM Imidazole) were used. The bound proteins were eluted out with 500 mM imidazole.

Figure 4.13 (A) showed that many non-specific bands were observed in the eluates of DENV C protein, especially in the second eluate fraction. This could be due to the highly positively-charged property of DENV C protein. Nonetheless, Western-blot analysis using anti-His antibody [Figure 4.13 (B)] and streptavidin antibody [Figure 4.13 (C)] confirmed that most of the DENV C proteins were eluted out starting from fractions E2 until E10. Interestingly, a faint DENV C protein dimer-corresponding band was observed in fraction E2 when anti-His antibody was used [Figure 4.13 (B)]. Similar band was not observed when streptavidin antibody was used [Figure 4.13 (C)]. This was surprising because elution buffer contained 8 M urea whereas sample loading buffer contained sodium dodecyl sulfate (SDS) detergent and reducing reagent (β-mercaptoethanol). If the band was indeed DENV C protein dimer, the interaction between two DENV C protein monomers must be very strong. Unfortunately, the corresponding band was not obvious in Coomassie blue-stained SDS gel for mass spectrometry analysis. Besides, there were many non-specific bands in that fraction. Therefore, second round of purification was required for DENV C protein.

4.3.5.3. Aggregation issue during stepwise dialysis and concurrent refolding of partially purified Dengue virus (DENV) capsid (C) protein

Before further purification, partially purified DENV C proteins from eluates E2 to E10 were pooled together for step-wise dialysis and concurrent refolding. This would remove 8 M urea and 500 mM imidazole in the elution buffer. However, it was noticed that significant amount of full-length DENV C protein precipitated out after refolding. DENV C proteins could be detected in both the refolding solution as well as in the precipitates. This problem could be due to the hydrophobic C-terminus of

DENV C protein resulting in easy aggregation and caused major loss in amounts during refolding and dialysis.

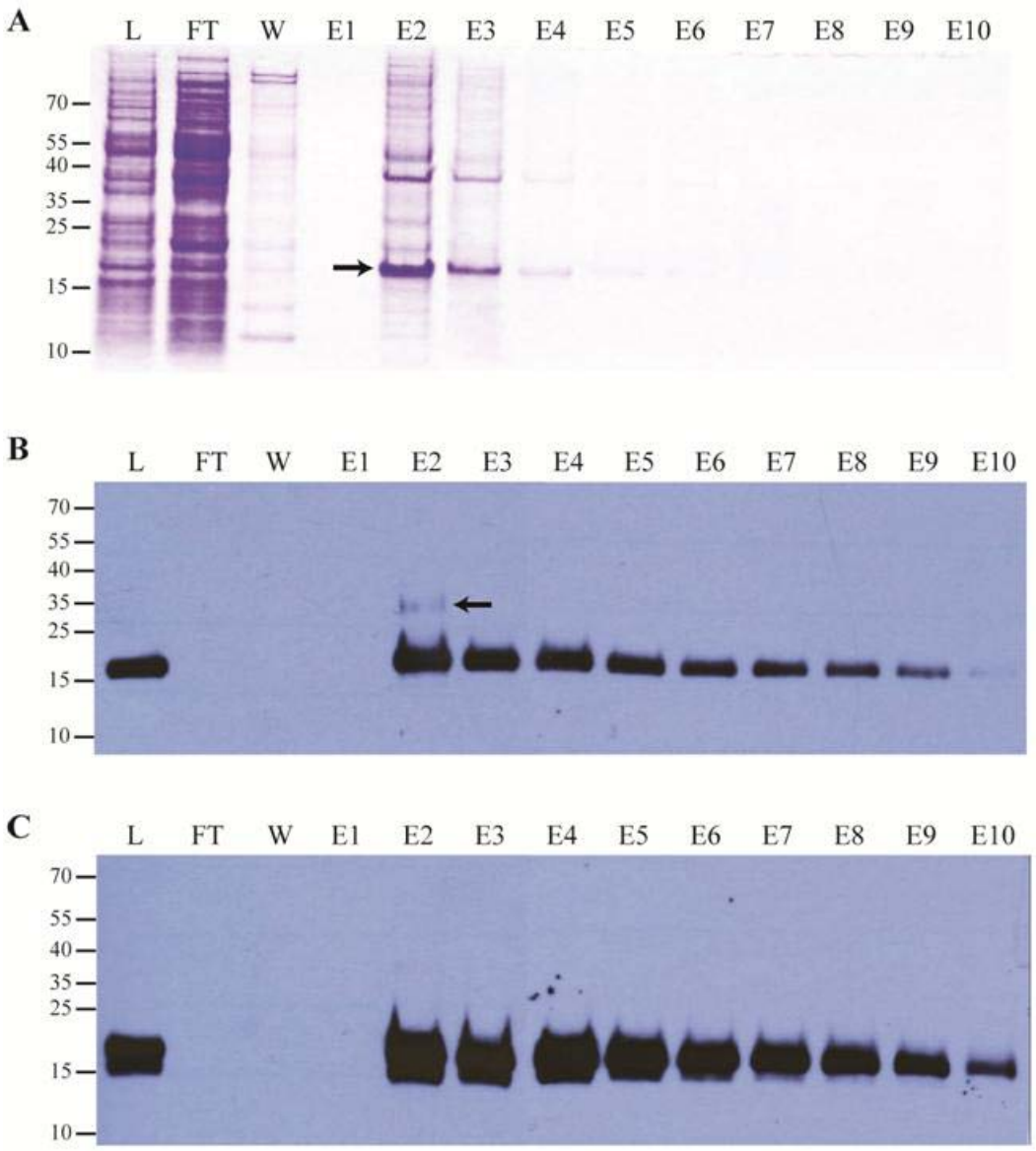

Figure 4.13: Purification of DENV C protein via affinity chromatography under denaturing condition. IPTG-induced bacteria is lysed in denaturing buffer containing 8 M urea and the lysate (L) is incubated with nickel-charged resin overnight. Next, the resin is packed in a column and the flow through (FT) is kept for SDS-PAGE. 20 mM imidazole is used to wash away the unbound proteins (W) and 500 mM imidazole is used to elute the C protein in ten fractions (E1-10). SDS-PAGE is carried out and stained with Coomassie blue (A). Fraction E2 shows the most intense band as indicated by an arrow but there are also many contaminants in the eluates. Western blot is also performed for the samples using anti-His antibody (B) and streptavidin HRP secondary antibody (C). C protein-corresponding bands can be observed from Fractions E2 until E10. The band intensity is the highest in fraction E2 and decreases until Fraction E10. A faint band corresponding to C protein dimer is observed in Fraction E2 as indicated by an arrow when anti-His antibody is used.

Initial attempt was to resolubilize the precipitates using different types of detergent. Six different reagents, namely Triton-X, Tween-20, NP-40, CHAPS {3-[(3-cholamidopropyl)dimethylammonio]-1-propanesulfonate}, digitonin and glycerol, were tested. Each of these reagents was added to the resuspension buffer (25 mM Tris and 150 mM NaCl, pH 8.0) and was used to resolubilize the precipitates of DENV C protein. After resolubilization, the mixture was spun down and both the supernatant and pellet were analyzed via SDS-PAGE and Western-blot. If the precipitate was resolubilized successfully, DENV C protein should be detected in the supernatant. However, the band corresponding to DENV C protein was not observed in all the supernatants [Figure 4.14 (A) and (B)]. They were still present in the pellets.

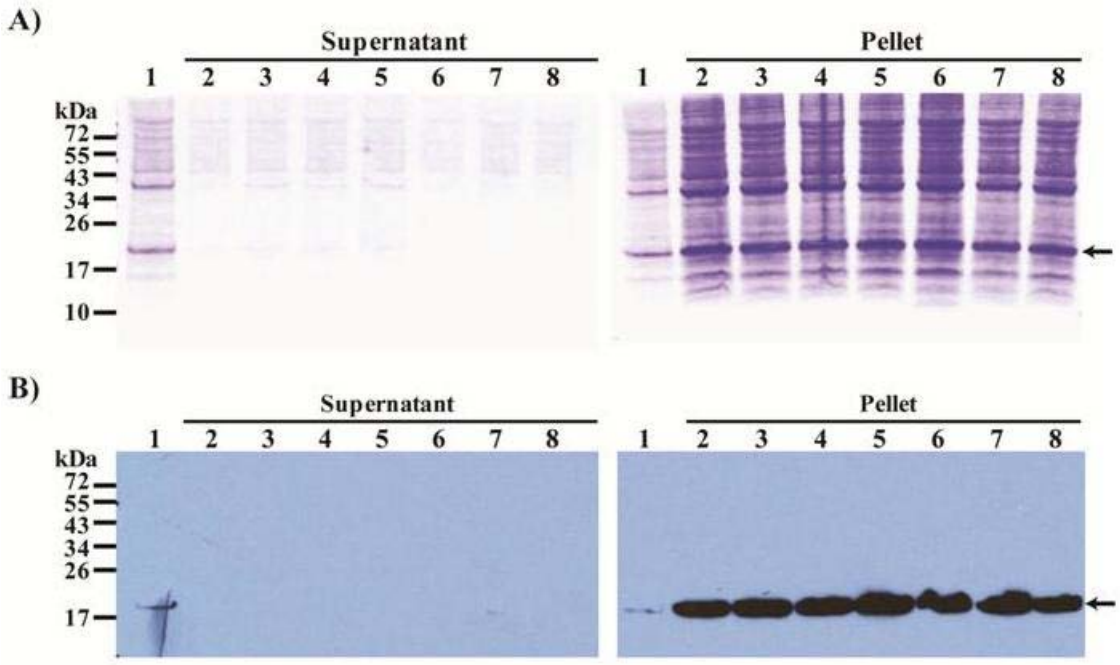

Figure 4.14: Resolubilization of DENV C protein aggregate using various detergents. Different detergents are used to resolubilize DENV C protein aggregates after dialysis and refolding. The presence of C protein is detected via Coomassie blue staining (A) and Western-blot using anti-His antibody (B). No band is observed in the supernatant fraction. DENV C proteins are still trapped in the pellet as indicated by the arrows. (Lane 1 – dialyzed sample; Lane 2 – No detergent; Lane 3 – Triton X; Lane 4 – Tween-20; Lane 5 – NP40; Lane 6 – CHAPS; Lane 7 – Digitonin; Lane 8 – Glycerol)

Another attempt was to resolubilize the aggregates of DENV C protein using different pH. The pH of resuspension buffer (25 mM Tris and 150 mM NaCl) was adjusted with 5 M hydrochloric acid to obtain pH 3 to 9 while 5 M sodium hydroxide was used to prepare pH 11 to 13.3. Figure 4.15 (A) showed that no proteins were resolubilized as no band is detected in all the supernatants from pH 3 to 10. Multiple bands were still seen in the pellets but not the supernatant. However, it was found that DENV C protein aggregate resolubilized in extreme alkaline condition. Bands were seen in the supernatant starting from pH 12 to 13 [Figure 4.15 (B) – Lanes 2 and 3]. Nonetheless, smear was observed when pH 13.3 was used to resolubilize the aggregate (Lane 4). Significant amount of DENV C proteins were rescued from the aggregate by using resuspension buffer with pH 12.

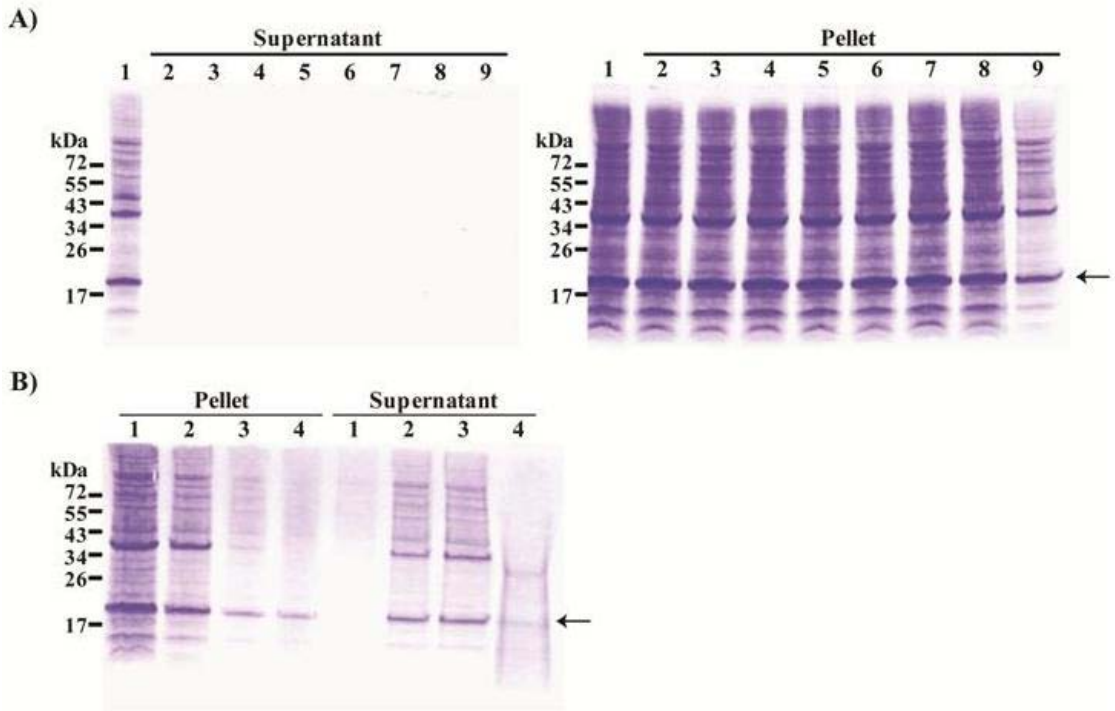

Figure 4.15: Resolubilization of DENV C protein aggregate using different pH. (A) DENV C protein aggregate is solubilized using solubilization buffer with different pH (Lane 1 – dialyzed sample; Lane 2 – pH 3; Lane 3 – pH 4; Lane 4 – pH 5; Lane 5 – pH 6; Lane 6 – pH 7; Lane 7 – pH 8; Lane 8 – pH 9; Lane 9 – pH 10). C protein is still in the pellet as no band is observed in the supernatant. (B) DENV C protein aggregate solubilizes in extreme alkaline solution as bands can only be observed in buffer with pH 12 and pH 13 (Lane 1 – pH 11; Lane 2 – pH 12; Lane 3 – pH 13; Lane 4 – pH 13.3).

Although the optimal condition of resuspension buffer to resolubilize DENV C protein aggregate was found, extreme alkaline condition was absolutely not suitable for protein storage and other downstream experiments. The quality of resolubilized DENV C protein was also questionable. Instead of resolubilizing the protein aggregates, method was developed to prevent protein aggregation during dialysis and refolding step. Recently, it was discovered in this laboratory that addition of 0.05 % Tween-20 into samples during dialysis and refolding would not only prevent protein aggregation but also enhance efficient refolding (Krupakar *et al.*, 2012).

With the addition of 0.05 % Tween-20 into denatured DENV C protein samples, protein aggregation was indeed reduced significantly. No obvious precipitation was observed and the solution was clear after stepwise dialysis and concurrent refolding. Protein aggregation problem was solved successfully. Refolded DENV C protein was then subjected to a second round of purification to obtain highly purified DENV C protein.

4.3.5.4. Second purification of full-length Dengue virus (DENV) capsid (C) protein via ion exchange chromatography

The partially purified refolded DENV C protein was further purified using ion exchange chromatography-fast protein liquid chromatography system (IEX-FPLC). Ion exchange chromatography was chosen because DENV C protein was a highly positively-charged protein. Theoretically, cation-exchanger column, Resource MonoS, should be used. However, it was found that biotinylated DENV C protein was not eluted out at a specific concentration of sodium chloride (NaCl). As shown in Figure 4.16 (A), minimal amount of proteins was eluted out slowly in an increasing gradient and reached a plateau from 700 mM of NaCl onwards.

Analysis of the samples via enzyme-linked immunosorbent assay (ELISA) using streptavidin-horse radish peroxidase (HRP) antibody also showed that biotinylated DENV C protein was eluted out slowly and reached a steady state after 700 mM of NaCl [Figure 4.16 (B)]. No distinct peak was observed in any elution fractions. This result indicated that Resource MonoS column was not suitable for separating DENV C protein from residual contaminants.

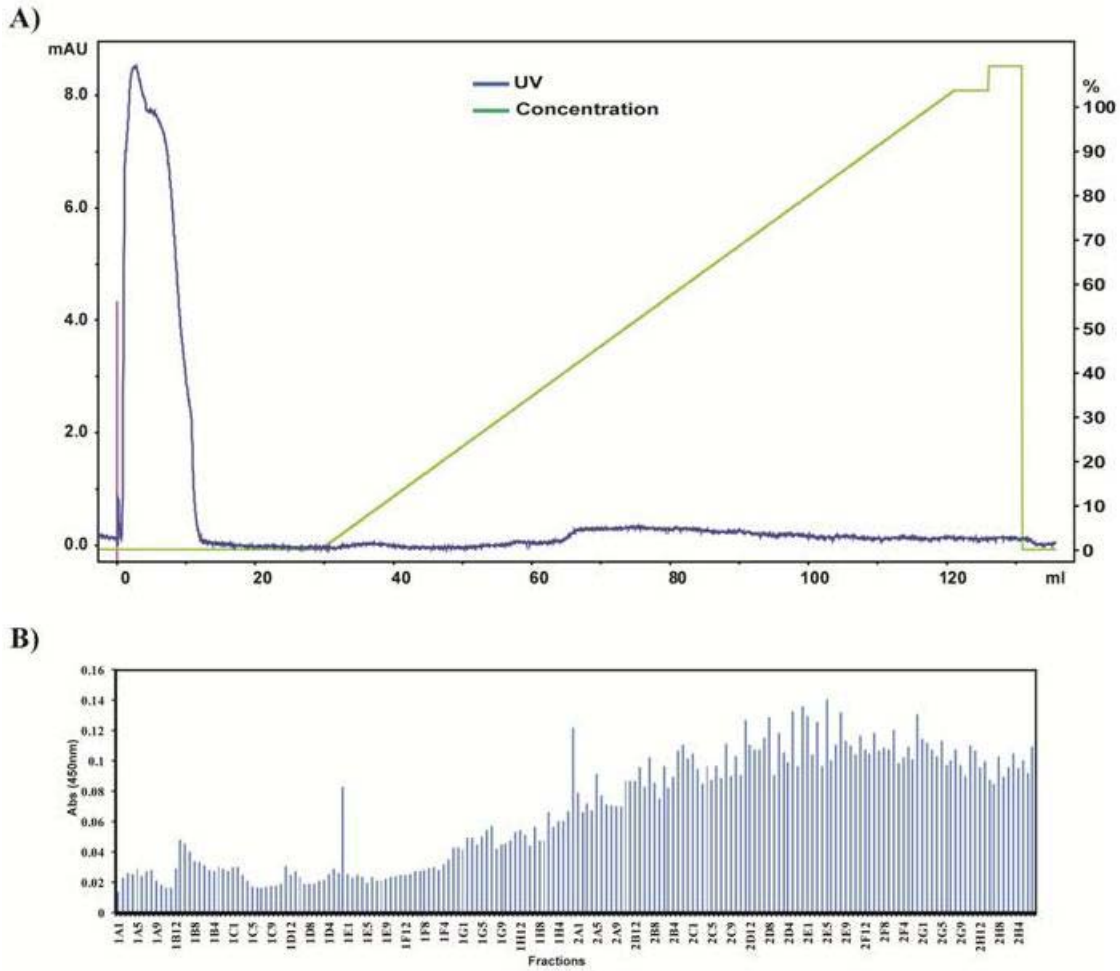

Figure 4.16: Cation exchange chromatography purification of DENV C protein using Resource MonoS column. (A) Dialysed and refolded DENV C proteins after affinity chromatography are injected into Resource MonoS ion exchange chromatography column. Bound proteins are eluted out using increasing concentration of sodium chloride until final concentration of 1 M. However, there is no obvious peak during the elution steps except a small increase of UV absorbance when the concentration of NaCl reaches 400 mM (40 %). (B) The presence of C protein is detected by ELISA using streptavidin HRP antibody. An increasing amount of biotinylated DENV C protein is detected during elution and it reaches plateau at approximately 70 % of NaCl (700 mM NaCl).

Better separation was instead obtained when anion-exchanger, Resource MonoQ, column was used. This could be due to the presence of biotin acceptor peptide (BAP) in the DENV C protein conferring its ability to bind to positively-charged beads. As indicated by Figure 4.17, biotinylated full-length DENV C protein bound perfectly to Resource MonoQ column. Although there was high UV absorbance detected in the flow through fractions, no biotinylated proteins were detected by ELISA in the flow through. The high UV absorbance was mainly contributed by the unbound proteins. In other words, most of the residual contaminants detected in Figure 4.13 were separated from biotinylated full-length DENV C protein in Resource MonoQ column.

As shown in Figure 4.17 (A), one high peak was detected when the NaCl concentration reached approximately 350 mM (35 %) during elution while there was another small peak detected at the elution concentration of 100 mM of NaCl (10 %). These peaks were confirmed to be biotinylated proteins as detected by ELISA using streptavidin HRP antibody [Figure 4.17 (B)]. In summary, the result showed that anion exchange chromatography was able to further separate most of the residual contaminants from DENV C protein after affinity chromatography.

4.3.5.5. Third purification of biotinylated full-length Dengue virus (DENV) capsid (C) protein via size-exclusion chromatography

To avoid any other contaminants that may have similar charge as biotinylated DENV C protein, eluates corresponding to the high UV absorbance peak after anion exchange chromatography were injected into size-exclusion chromatography (SEC), Superdex 75 10/300 GL column. It was previously reported that SEC could not be used to estimate the molecular weight of DENV C protein because there were many

unspecific interaction between the gel matrix and C protein (Jones *et al.*, 2003). Nevertheless, it is still a useful method to further isolate the proteins of interest from other possible residual contaminants based on the molecular weight differences.

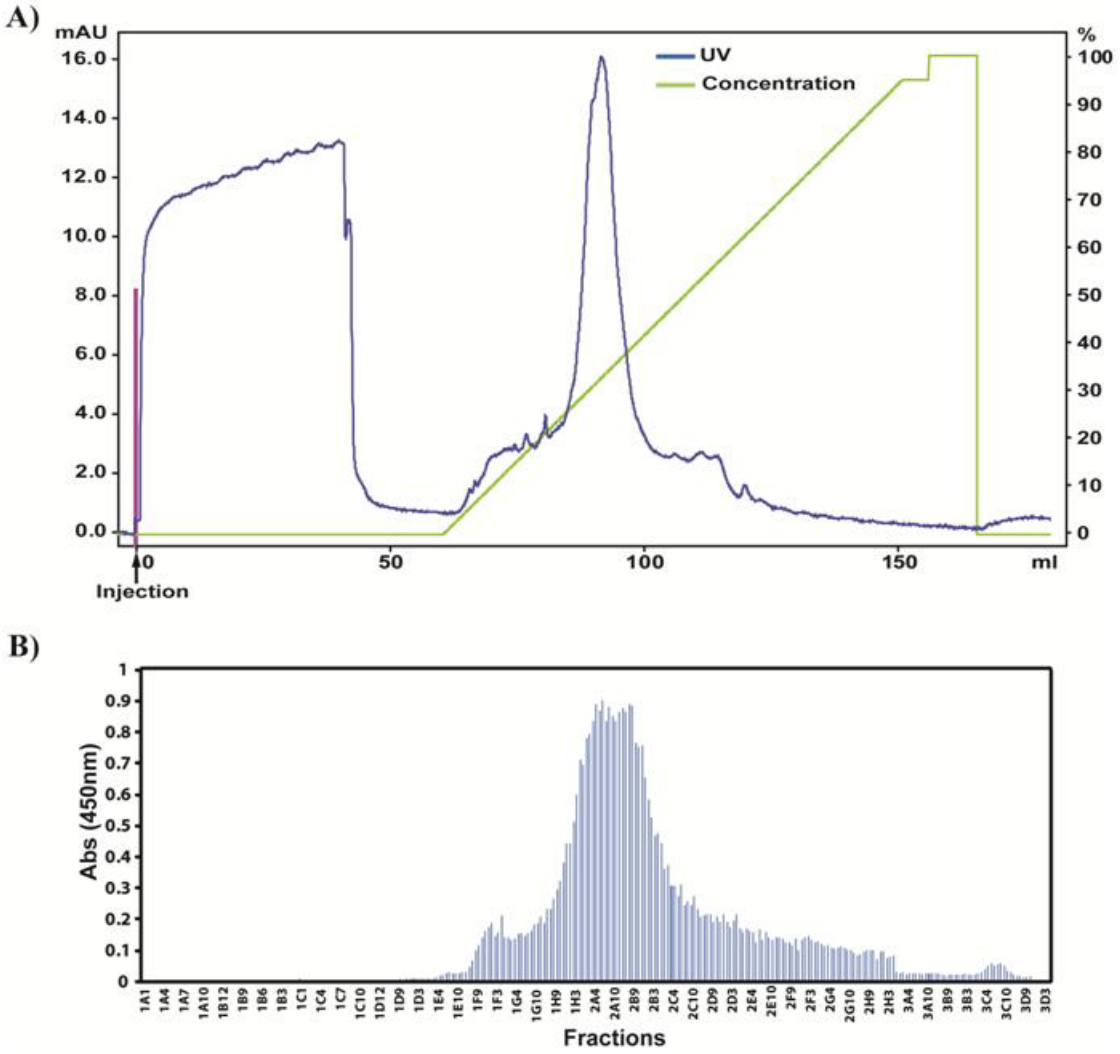

Figure 4.17: Anion exchange chromatography purification of DENV C protein using Resource MonoQ column. (A) Dialysed and refolded DENV C proteins after affinity chromatography are injected into Resource MonoQ ion exchange chromatography column. Bound proteins are eluted out using increasing concentration of sodium chloride until final NaCl concentration of 1 M. One high peak can be observed when the sodium chloride concentration reaches 350 mM. (B) The identity of the peak is confirmed to be biotinylated DENV C protein as detected by ELISA using streptavidin HRP antibody.

After size-exclusion chromatography, three peaks were observed in the chromatogram [Figure 4.18 (A)]. The highest peak (first peak) was observed at approximately 33 ml elution volume followed by two very small peaks (second and third peaks) at about 63 ml and 70 ml elution volumes, respectively. As shown in Figure 4.18 (B), only the first peak was identified to be the biotinylated DENV C protein since the fractions detected with high absorbance in ELISA using streptavidin HRP antibody coincided with the first peak in the elution profile. No absorbance was detected in ELISA for the second and third peaks observed in the chromatogram [Figure 4.18 (A)]. Besides, bands could only be seen from the sample in the first peak when detected by Western-blot using anti-His antibody and streptavidin antibody. Hence, pure biotinylated full-length DENV C protein was in the first peak. To further validate the identity of this purified protein, the eluted protein from the first peak was sent directly for matrix-assisted laser desorption/ionization-time of flight (MALDI-TOF) mass spectrometry analysis.

Mass spectrometry analysis confirmed that the purified protein obtained from the first peak of SEC was indeed DENV C protein. Table 4.3 showed all the peptide sequences identified via MALDI-TOF analysis.

Table 4.3: MALDI-TOF mass spectrometry analysis of purified DENV C protein.

Fragment	Peptide Sequence	Calculated (Da)	Measure (Da)	Error (Da)
81-89	FSLGMLQGR	1007.52	1007.49	-0.03
104-116	FLTIPPTAGILKR	1425.87	1425.8	-0.07
148-161	TAGMIIMLIPTVMA	1476.77	1476.78	0.01
70-78	VSTVQQLTK	1002.56	1002.57	-0.01
57-64	NTPFNMLK	963.48	963.49	0.01
138-144	MLNILNR	872.49	872.48	-0.01
93-102	LFMALVAFLR	1179.68	1179.69	0.01

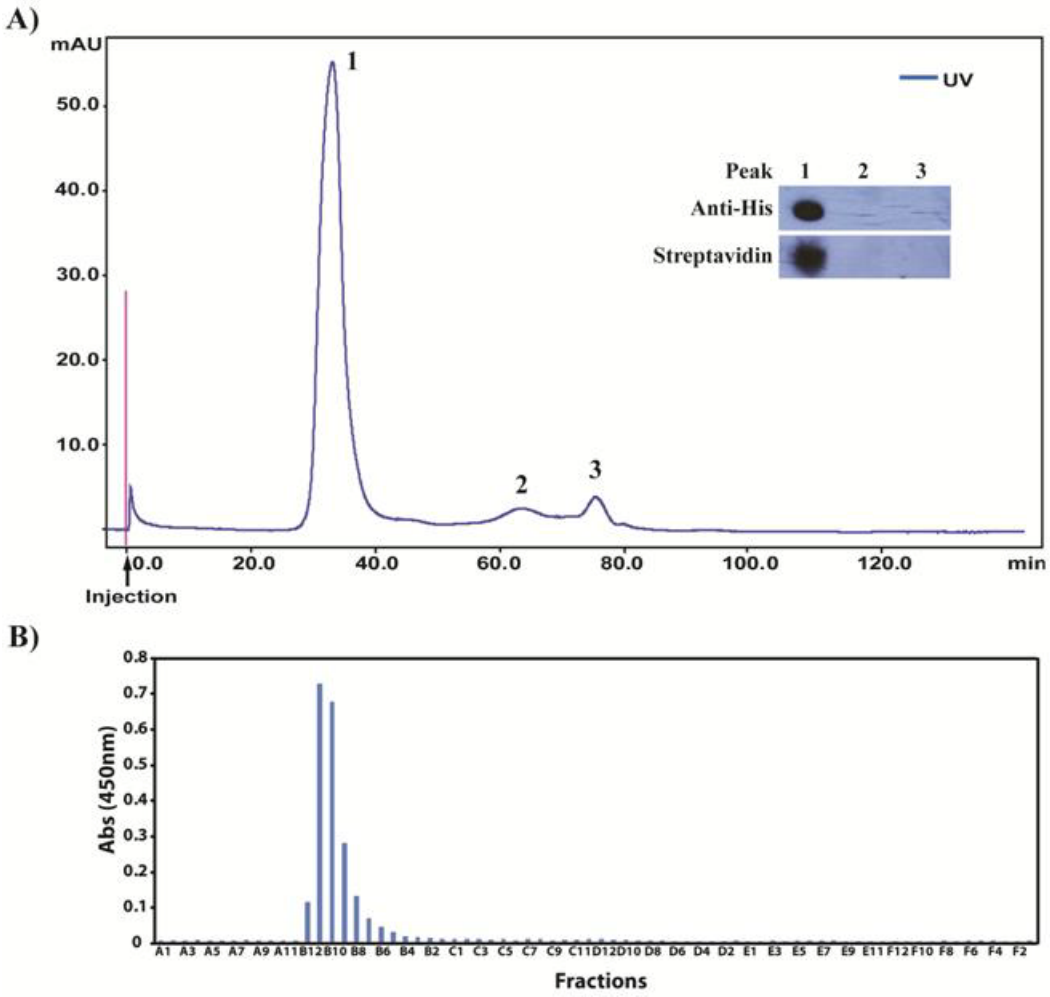

Figure 4.18: Size exclusion chromatography purification of DENV C protein using Superdex 75 column. The eluates from the anion-exchange chromatography with the highest absorbance in ELISA are combined and inserted into size exclusion chromatography for further purification. Three peaks are observed in the chromatogram (A). The high peak is identified to be DENV C protein as a band with corresponding molecular weight can be detected in Western blot when anti-His antibody and streptavidin-horse radish peroxidase antibody are used. This is further confirmed with ELISA using streptavidin HRP antibody (B).

4.4. Functional Study of Purified Biotinylated Full-Length Dengue Virus (DENV) Capsid (C) Protein

4.4.1. High *in vivo* biotinylation efficiency in BL-21-CodonPlus competent cells

After validating the identity of the highly purified biotinylated full-length DENV C protein, it was of paramount importance to examine the functionality of the purified protein and the tags. Purified full-length DENV C protein contained 2 tags at

the N-terminus, namely 6 x His tag and biotin acceptor peptide (BAP). To attach a biotin molecule onto BAP either *in vivo* or *in vitro*, bacterial biotin ligase BirA was required (Chapman-Smith & Cronan, 1999b). However, DENV C protein with BAP was found biotinylated endogenously in BL-21-CodonPlus competent cells (Section 4.3.4).

To compare the biotinylation efficiency in BL-21-CodonPlus cells, the same amount of purified biotinylated DENV C protein and commercial biotinylated maltose-binding protein (MBP) were coated on the ELISA plate and streptavidin-horse radish peroxidase (HRP) antibody was used for detection. Assuming that the coating efficiencies are the same between DENV C and MBP proteins, the absorbance detected via ELISA should be proportional to the number of coated protein molecules and inversely proportional to the power of $^{2}/_{3}$ of its molecular size. Hence, the larger the protein, the lesser the proteins can be coated on the plate.

$$Absorbance \propto \frac{Protein\ Concentration}{(Protein\ Size)^{2/3}}$$

The molecular weight of MBP is approximately 42.5 kDa while DENV C protein has an approximate mass of 15.4 kDa. Assuming that each protein molecule carries only one biotin molecule which will bind to only one streptavidin HRP complex, the absorbance of MBP should be roughly two times lower than purified DENV C proteins for the same protein concentration.

As shown in Figure 4.19 (A), the absorbance of purified biotinylated DENV C protein indeed showed approximately two times higher when compared to the commercial biotinylated MBP. The same phenomenon was also observed when the biotinylated proteins were pulled down by streptavidin-magnetic beads and detected via direct ELISA [Figure 4.19 (B)]. The absorbance of eluted biotinylated DENV C

protein was two times higher than that of eluted biotinylated MBP. No significant absorbance was detected for unbiotinylated DENV C and MBP proteins.

This result further supported that engineering an additional BAP onto a protein could result in site-specific endogenous biotinylation with high efficiency in *Escherichia coli* BL-21-CodonPlus competent cells, without the need of an extra *in vitro* enzymatic or chemical conjugation step. This strategy could produce biotinylated proteins which had equal quality as the manufactured biotinylated MBP.

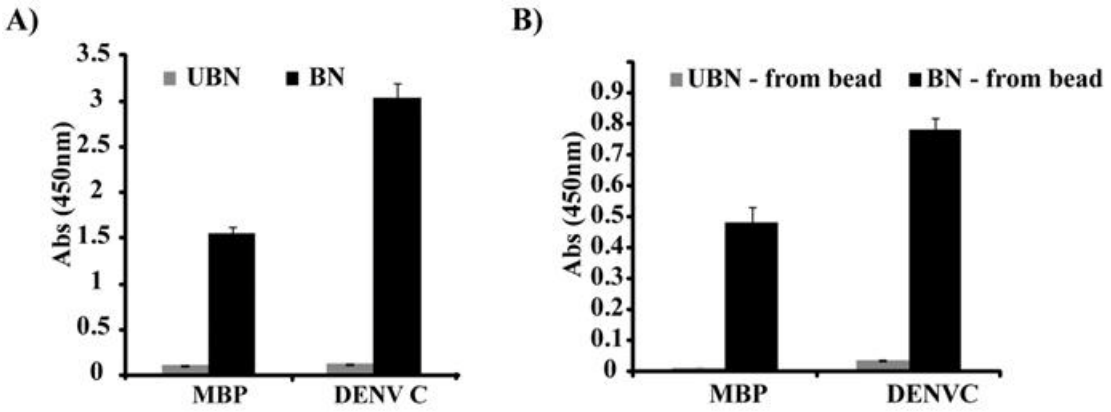

Figure 4.19: Biotinylation efficiency of purified full-length DENV C protein. (A) 30 ng of biotinylated (BN) and unbiotinylated (UBN) maltose-binding proteins (MBP) and DENV C proteins are coated on ELISA plate and streptavidin-horse radish peroxidise (HRP) antibody is used to detect the presence of biotinylated proteins. Both BN MBP and DENV C protein show high absorbance at 450 nm as compared to UBN proteins. (B) Biotin-streptavidin binding assay also shows that only BN proteins bind to streptavidin-magnetic beads and are detected in the eluates. No absorbance is detected in the eluates of UBN proteins.

4.4.2. Purified full-length Dengue virus (DENV) capsid (C) protein is functional

After determining the functionality of biotin tag in purified DENV C protein, it was essential to ensure that full-length DENV C protein was functional before it was used for any further studies. According to recent findings in this laboratory, West Nile virus (WNV) and DENV C proteins were found to interact with human Sec3 exocyst protein (Bhuvanakantham *et al.*, 2010). Thus, the functionality of purified DENV C protein was examined by revisiting the interaction between biotinylated DENV C protein and Sec3 protein using ELISA. Pure Sec3 protein (Abnova, Taiwan)

was coated overnight on ELISA plate and purified biotinylated DENV C protein was used as the probe. Bound DENV C proteins were detected with streptavidin-horse radish peroxidise antibody. As shown in Figure 4.20, statistically significant absorbance was detected in Sec3 protein-coated wells but not in bovine serum albumin (BSA)-coated wells. Thus, the purified full-length DENV C protein did interact with Sec3 protein. This corroborated that the purified biotinylated full-length DENV C protein was indeed functional and could be used for downstream studies.

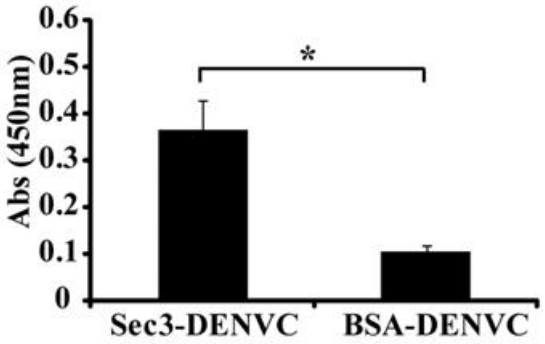

Figure 4.20: Functional assay of purified biotinylated full-length DENV C protein. The functionality of DENV C protein is examined via binding assay with Sec3 protein which is known to interact with flaviviral C protein in host cells. Pure Sec3 protein is coated onto ELISA plate and purified full-length DENV C protein is added into the well for binding. Bovine serum albumin (BSA) is used as negative control. Significant absorbance is detected using streptavidin-horseradish peroxidase antibody in the wells with Sec3 protein coated (Sec3-DENVC) but not with BSA (BSA-DENVC). *p-value<0.05

In summary, the purification of non-truncated, full-length DENV C protein was successful. To obtain highly purified DENV C protein, an optimized sequential purification protocol (affinity chromatography → anion exchange chromatography → size exclusion chromatography) was established. This sequential purification strategy could produce approximately 1 mg of purified full-length DENV C protein from 1 L of bacterial culture. With this highly purified biotinylated full-length DENV C protein, it was possible to use ProtoArray® technology-based protein microarray to discover novel interacting partners of DENV C protein (Chapter 5).

5. High-Throughput ProtoArray Screening for Novel Interacting Partners of Dengue Virus Capsid Protein

5.1. Introduction

Using the purified biotinylated full-length Dengue virus (DENV) capsid (C) protein generated in Chapter 4, high-throughput screening (HTS) was carried out to identify novel interacting partners of DENV C protein. Numerous protein-protein interaction (PPI) techniques have been developed for drug discovery and identification of novel interacting partners for hallmark proteins in a pathway or disease. For HTS of novel interacting partners, yeast two-hybrid, bacteria two-hybrid, pull-down assay, tandem affinity purification, and phage display are commonly used (Lievens *et al.*, 2010; Petschnigg *et al.*, 2011; Williamson & Sutcliffe, 2010; Wright *et al.*, 2010). To date, chip-based technologies are expanding and more sophisticated screening technologies have been developed (Heeres & Hergenrother, 2011; Katz *et al.*, 2011; Tomizaki *et al.*, 2010; Torres *et al.*, 2010). In this Chapter, protein microarray from Life Technologies, namely ProtoArray® Human Protein Microarray PPI Complete Kit, was employed for HTS study of novel DENV C protein-interacting partners.

5.2. Description of ProtoArray® Technology-Based Protein Microarray

ProtoArray® Human Protein Microarray PPI Complete Kit contains more than 9000 purified functional human proteins printed on a glass slide. The purified human proteins encompass various cellular kinases, enzymes, nuclear proteins, signalling proteins and other important cellular proteins as stated in Table 5.1. All these proteins are cloned based on open reading frame (ORF) selected from Invitrogen's Ultimate human ORF clone collection. They are expressed as N-terminal glutathione S

transferase (GST) or 6x His-tag fusion proteins via baculovirus-based expression system and purified under non-denaturing conditions to preserve their native protein structures.

Table 5.1: Content and classifications of human proteins coated on ProtoArray glass slide. Some of the proteins belong to more than one class.

Class	Number of protein on Array
Protein kinases (unique)	**268**
Protein kinases (including domains, splice variants, and mutants)	**776**
Transcription factors	**328**
Membrane proteins	**2635**
Nuclear proteins	**2252**
Signal transduction	**1526**
Secreted proteins	**192**
Cell communication	**1687**
Metabolism	**3862**
Cell death	**505**
Protease / peptidase activity	**219**

There are two tags on the purified full-length Dengue virus (DENV) capsid (C) protein, namely 6x His tag and biotin tag (Chapter 4). Since most of the human proteins printed on the array are tagged with 6x His tag or GST tag, anti-His and anti-GST antibodies cannot be used as the detection reagent. As such, biotin tag was opted for the detection target in this screening. The strong binding affinity and specificity between biotin and streptavidin also helped in high detection sensitivity. Therefore, streptavidin-Alexa Fluor® 647 antibody was chosen as the detection reagent as it yielded very good signal to noise ratio.

All the purified functional human proteins were printed in duplicate on a nitrocellulose-coated 1 inch x 3 inch glass slide in a temperature- and humidity-controlled environment to ensure quality consistency. As shown in Figure 5.1, a protein microarray comprises 48 subarrays containing 484 spots (22 x 22 formats) in which each spot has a median diameter of approximately 110 μm. Alexa Fluor® 647

antibodies are coated in each subarray as reference spots for proper alignment with microarray protein identity data file during data acquisition. Decreasing concentration of BioEase™ (biotin) positive control proteins are also printed in each subarray to ensure the streptavidin-Alexa Fluor® 647 antibody used is functional and the probing is properly performed.

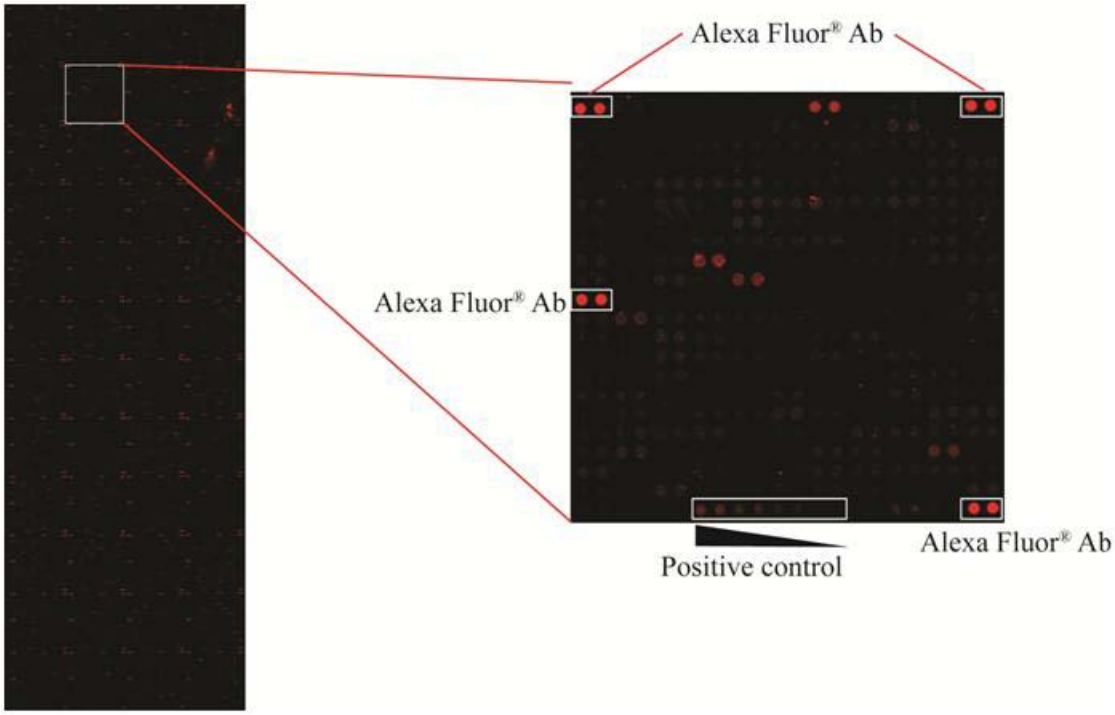

Figure 5.1: Image of scanned ProtoArray glass slide. There are 48 subarrays in total and one of the subarrays is enlarged. Each subarray contains 484 spots (22 rows x 22 columns). Four pairs of antibody spots labelled with Alexa Fluor 647 in each subarray are used as the reference spots for orientation and alignment analysis. Decreasing concentration of biotins is included as positive controls for streptavidin-Alexa Fluor® 647 antibody probing.

Figure 5.2 showed the workflow of ProtoArray screening. About 10 µg of purified biotinylated full-length Dengue virus (DENV) capsid (C) protein (50 µg/ml) was used as probe for binding with the human proteins. Bound DENV C proteins were detected using streptavidin-Alexa Fluor® 647 antibody. The entire experiment was carried out at 4 ^{o}C to ensure protein integrity. After scanning the microarray glass slide via a fluorescence microarray scanner – Axon GenePix 4000B scanner, data acquisition was carried out using GenePix® Pro software and the specific ".GAL" file

that defined the array grid. Data analysis was done using ProtoArray® Prospector software to analyze the pixel intensity information and to identify statistically significant interactors.

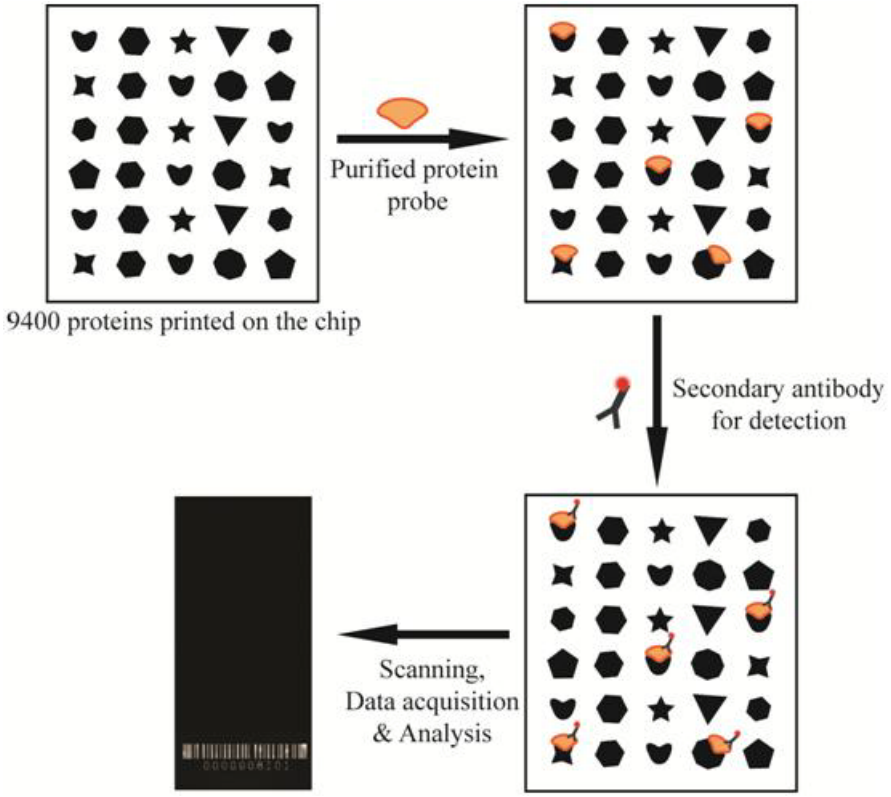

Figure 5.2: Workflow of ProtoArray screening. Purified biotinylated DENV C protein is used to probe the protein microarray and the bound protein complexes are detected with streptavidin-Alexa Fluor® 647 antibody. The fluorescence signal intensity of each spot is measured via Axon GenePix 4000B scanner and data acquisition is carried out using GenePix® Pro software. Statistically significant interactors are identified via ProtoArray® Prospector software.

This high-throughput screening (HTS) method allowed identification of direct protein-protein interaction in a robust and cost-effective manner. More than 9000 human proteins can be screened within one day without any additional cloning steps or cultivation of micro-organism. This technology has been employed to identify potential biomarkers and to map protein-protein interactome for better understanding or discovery of novel pathways in diseases (Fenner *et al.*, 2010; Le Roux *et al.*, 2010; Virok *et al.*, 2011). This is the first time this technology was employed for virus-host interaction study.

5.3. Screening of Novel Interacting Partners for Dengue Virus (DENV) Capsid (C) Protein via ProtoArray® Technology-Based Protein Microarray

After data acquisition, data analysis was carried out using ProtoArray® Prospector software to identify statistically significant interacting partners. As shown in Figure 5.3, there were a total of 578 potential DENV C protein-binding partners detected to have z-score value of one or greater. Z-score indicates how far and in what direction the sample's value deviates from the distribution's mean in units of standard deviations. The larger the z-score, the more statistically significant the identified interacting partner. Protein interactors with z-score value greater than 3 ($Z>3$; $P<0.002$) and with coefficient of variation (CV) for the two fluorescence signals less than 0.5, were deemed to be statistically significant. After filtering some of the protein interactors without known functions and with biotin-binding property, 31 significant potential DENV C protein-interacting partners were identified as shown in Table 5.2.

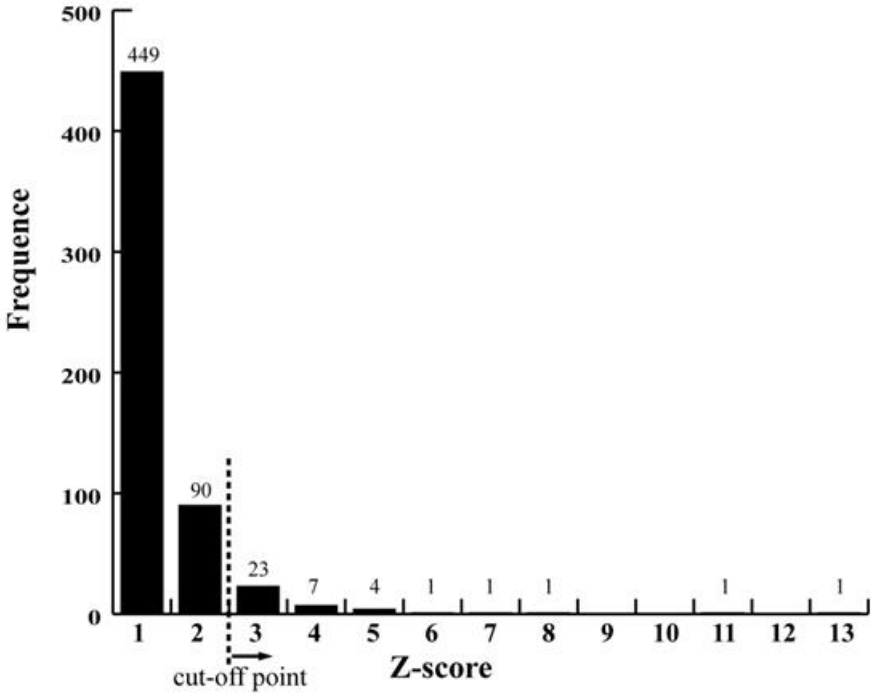

Figure 5.3: Number of identified protein interactors with z-score value of one or greater. Z-score cut-off value of 3 is taken to be statistically significant interactors for DENV C protein.

Table 5.2: Significant interacting partners of DENV C protein identified using z-score cut-off value of 3. Interactors with coefficient of variation (CV) value larger than 0.5 for the fluorescence signals from the duplicate are excluded.

No.	Identity	Symbol	Database ID	Array ID	Signal Intensity	CV	Z-score	Function
1.	Cortactin	CTTN	NM_138565.1	B39R03C15	3076.5	0.03517	13.41837	Regulate and organize actin cytoskeleton
2.	SLAIN motif family, member 2	SLAIN2	BC031691.2	B09R09C13	2569.5	0.04981	11.08491	Control microtubule growth and organization
3.	Immunoglobulin (CD79A) binding protein 1	IGBP1	NM_001551.1	B09R16C19	1938	0.02043	8.17845	Binds to surface IgM receptor and may involve in the activation signal transduction pathway
4.	Choline kinase alpha	CHKA	NM_001277.1	B46R09C15	1738	0.03743	7.25795	Catalyzes the phosphorylation of ethanolamine and plays a role in phosphatidylcholine biosynthesis.
5.	DIM1 dimethyladenosine transferase 1 homolog (S. cerevisiae)	DIMT1	NM_014473.2	B08R18C19	1666.5	0.26943	6.92887	Dimethylates 18S rRNA in the 40S particle
6.	Ubiquitin-conjugating enzyme E2S	UBE2S	BC004236.2	B38R06C13	1353.5	0.00366	5.4883	Catalyzes 'Lys-11'-linked polyubiquitination on the anaphase promoting complex/ cyclosome (APC/C) substrates
7.	AF4/FMR2 family, member 4	AFF4	BC025700.1	B06R09C07	1251	0.06896	5.01654	Regulates transcriptional activity
8.	WAS / WASL interacting protein family, member 1	WIPF1	BC002914.1	B48R20C19	1159	0.02562	4.59312	Control the organization of actin cytoskeleton
9.	Aurora kinase A	AURKA	BC006423.1	B06R10C09	1158	0.04519	4.58851	Cell cycle-regulated kinase regulates microtubules formation and stabilizes spindle poles during mitosis
10.	RAD51 associated	RAD51AP1	BC016330.1	B33R03C01	1143	0.00990	4.51948	Involved in common DNA damage

No.	Identity	Symbol	Database ID	Array ID	Signal Intensity	CV	Z-score	Function
	protein 1							response pathway
11.	Additional sex combs like 1 (Drosophila)	ASXL1	BC064984.1	B28R18C13	1072	0.04485	4.1927	Regulates transcriptional activity
12.	CDKN2A interacting protein	CDKN2AIP / CARF	BC022270.1	B12R15C09	1031.5	0.13642	4.0063	Activates p53/TP53 via CDKN2A-dependent and CDKN2A-independent pathways
13.	Calcium channel, voltage-dependent, beta 1 subunit	CACNB1	NM_000723.3	B16R04C21	1017.5	0.12162	3.94187	Increases peak calcium current, modulates G protein inhibition, and shifts the voltage- dependent activation and inactivation.
14.	Spermidine / spermine N1-acetyltransferase family member 2	SAT2	NM_133491.2	B44R08C07	1008.5	0.00351	3.90044	Catalyzes the acetylation of polyamines
15.	Eukaryotic translation initiation factor 1A, X-linked	EIF1AX	NM_001412.2	B38R18C19	997	0.15461	3.84751	Enchances ribosome dissociation into subunits and stabilizes the binding of Met-tRNA(I) to 40S ribosomal subunits
16.	Signal recognition particle 19kDa	SRP19	BC010947.1/ NM_003135.1	B47R17C17/ B02R18C03	971.5/ 818	0.34573 / 0.16770	3.73015/ 3.02367	Mediates the assembly of signal recognition particle
17.	Calcium / calmodulin-dependent protein kinase II alpha	CAMK2A	NM_171825.2	B13R15C19	969	0.11238	3.71865	Involved in hippocampal long-term potentiation by switching calmodulin-dependent activity to calmodulin independent
18.	Piccolo (presynaptic cytomatrix protein)	PCLO	BC001304.1	B21R10C01	929	0.02740	3.53455	Involved in the organization of synaptic active zone and synaptic vesicle trafficking
19.	Nuclear speckle splicing regulatory	NSRP1	NM_032141.1	B12R07C13	927.5	0.16544	3.52764	Mediates pre-mRNA alternative splicing regulation

No.	Identity	Symbol	Database ID	Array ID	Signal Intensity	CV	Z-score	Function
	protein 1							
20.	NIMA (never in mitosis gene a)-related kinase 7	NEK7	NM_133494.1	B12R18C09	918.5	0.19169	3.48622	Controls initiation of mitosis
21.	Checkpoint suppressor 1 / Forkhead box N3	CHES1 / FOXN3	NM_005197.2	B40R19C13	918	0.27730	3.48392	Transcriptional repressor involved in DNA damage-inducible cell cycle arrests at G1 and G2 phases
22.	Rtf1, Paf1/RNA polymerase II complex component, homolog (S. cerevisiae)	RTF1	NM_015138.2	B44R16C19	882.5	0.02484	3.32053	Regulates transcriptional activity
23.	Microtubule-associated protein 2	MAP2	NM_031845.1	B40R07C17	875	0.03879	3.28601	Function unclear. Thought to be involved in microtubule assembly and stabilizing the microtubules against depolymerization
24.	Potassium channel tetramerisation domain containing 18	KCTD18	NM_152387.2	B06R19C19	856	0.02313	3.19857	Molecular determinants for subfamily-specific assembly of alpha-subunits into functional tetrameric voltage-gated potassium channels
25.	Cyclin B3	CCNB3	NM_033671.1	B17R08C03	853.5	0.05385	3.18706	Involved in cell cycle control
26.	Eukaryotic translation initiation factor 1A, Y-linked	EIF1AY	BC005248.1	B29R12C05	852.5	0.12691	3.18246	Enchances ribosome dissociation into subunits and stabilizes the binding of Met-tRNA(I) to 40S ribosomal subunits
27.	Vaccinia related kinase 1	VRK1	NM_003384.1	B43R08C03	845	0.17406	3.14794	Serine / Threonine kinase that is involved in regulating cell proliferation and prevent the interaction between p53 / TP53 and MDM2

No.	Identity	Symbol	Database ID	Array ID	Signal Intensity	CV	Z-score	Function
28.	Protein kinase C, iota	PRKCI	NM_002740.1	B17R10C07	841	0.00504	3.12953	Calcium-independent and phospholipid-dependent serine/ threonine kinase involved various cellular processes
29.	WD repeat domain 5	WDR5	NM_017588.1	B29R10C09	840.5	0.01598	3.12723	Involved in histone modification and acetylation of histone H3
30.	p53-regulated DDA3 (DDA3) / proline/serine-rich coiled-coil 1	PSRC1	NM_032636.2	B40R12C17	822	0.02925	3.04208	Regulates mitotic spindle and involved in p53 / TP53-regulated growth suppression
31.	Elongation factor 1 homolog (ELF1, S. cerevisiae)	ELOF1	NM_032377.2	B38R06C11	816.5	0.00260	3.01677	Maintains proper chromatin structure in actively transcribed regions

5.3.1. Functional classification of the interacting partners

The list of identified interacting partners in Table 5.2 can be grouped into five main categories as shown in Figure 5.4. Four proteins are involved in signaling activities such as B cell activation (IGBP1), synaptic signaling (CAMK2A and PCLO) and signaling pathway activation (PRKCI). Another category is metabolic processing like phosphatidylcholine biosynthesis (CHKA) and acetylation of polyamines (SAT2). Six protein interactors are categorized into intracellular trafficking. Most of them are with high z-score values. Cortactin (CTTN), for example, is the top in the list with z-score value of 13.41837. Other proteins that are involved in intracellular trafficking are SLAIN2, WIPF1, CACNB1, MAP2 and KCTD18 proteins.

Two main categories of the novel interacting partners are cell cycle control and regulation of transcriptional and translational activities. In cell cycle control, further classification can be made into cell cycle arrest (CHES1 and CCNB3), DNA repair (RAD51AP1), mitotic spindle organization (AURKA, NEK7 and PSRCI), p53 pathway (CDKN2AIP and VRK1) and polyubiquitination (UBE2S). Some of the protein interactors are involved in apoptotic pathway which is also a regulatory pathway for cell cycle arrest. For instance, AURKA and VRK1 are essential serine / threonine kinases involved in stabilizing p53 protein while CDKN2AIP is one of the activators of p53 pathway.

Ten protein interactors are pertaining to the regulation of host transcriptional and translational activities. AFF4, ASXL1, RTF1, ELOF1 and WDR5 proteins are involved in transcriptional activity regulation while EIF1AX and EIF1AY proteins are translation initiators. Other transcriptional and translational activities include messenger RNA (NSRP1) and ribosomal RNA (DIMT1) processing and targeting proteins to membrane for translation (SRP19).

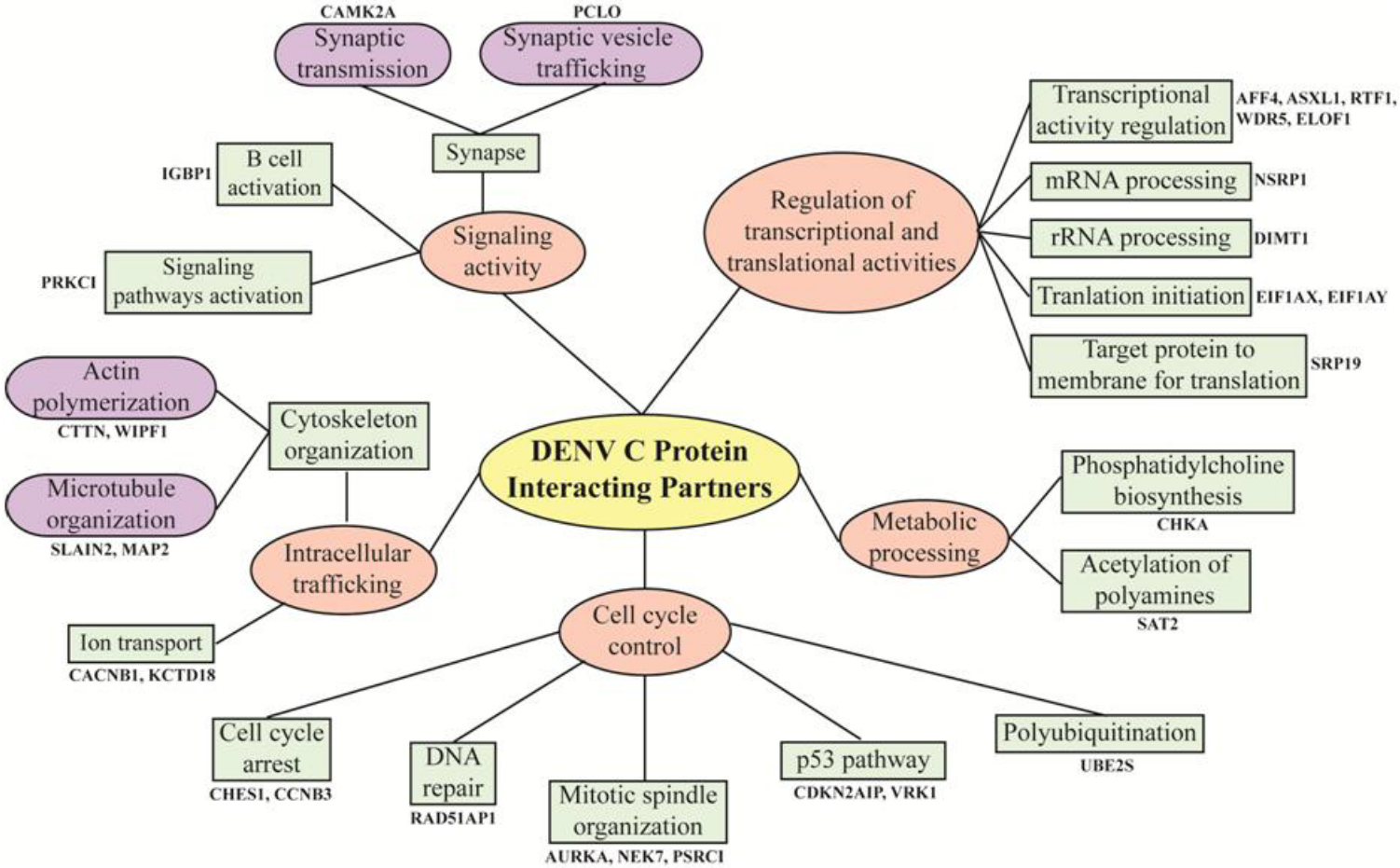

Figure 5.4: Functional classification of the interacting partners of DENV C protein. The function of each interacting protein is analysed and classified. Cell cycle and regulation of transcription and translation are the two major categories of DENV C protein-interacting partners.

5.3.2. Compartmentalization of the interacting partners

To unravel the non-structural roles of DENV C protein in the nucleus, novel protein interactors compartmentalized in the nucleus were identified. Hence, the localization of each protein interactor was studied and illustrated in Figure 5.5 (A). The list of the identified interacting partners of DENV C protein was quite well-dispersed throughout the cell nucleus and cytoplasm. Approximately 55 % of the identified proteins localized in the nucleus while the other half was distributed in the cytoplasm [Figure 5.5 (B)]. This was exciting because a comprehensive list of DENV C protein-nuclear interactors involved in the virus replication was identified from this ProtoArray® high-throughput screening.

Among all the nuclear proteins, five of them (SRP19, DIMT1, AFF4, RFT1, and CDKN2AIP) were from the nucleolus compartment. These five proteins deserve further investigation because DENV C protein was found localized predominantly in the nucleoli as previously shown in Figures 3.2-3.4 (Chapter 3).

The cytoplasmic interacting proteins with DENV C proteins are PCLO, NEK7, VRK1, CTTN, MAP2, and SLAIN2 proteins which are related to cytoskeleton. Five proteins (CACNB1, KCTD18, CAMK2A, PCLO and PRKCI) are localized in the plasma membrane while four proteins (WIPF1, PCLO, CAMK2A, and PRKCI) are in the transport vesicles.

Some of the proteins are localized in several compartments in the cells. For instance, PRKCI (protein kinase C-iota type) is a calcium-independent and phospholipid-dependent protein kinase found in the cytoplasm, plasma membrane, endosome and nucleus. PRKCI protein carries various important physiological roles such as cell differentiation and polarity, cell survival, and regulation of microtubule dynamics in the early secretory pathway (Suzuki *et al.*, 2003). From Figure 5.5, it

showed that DENV C protein has many opportunities to interact with large arrays of proteins in both nucleus and cytoplasm.

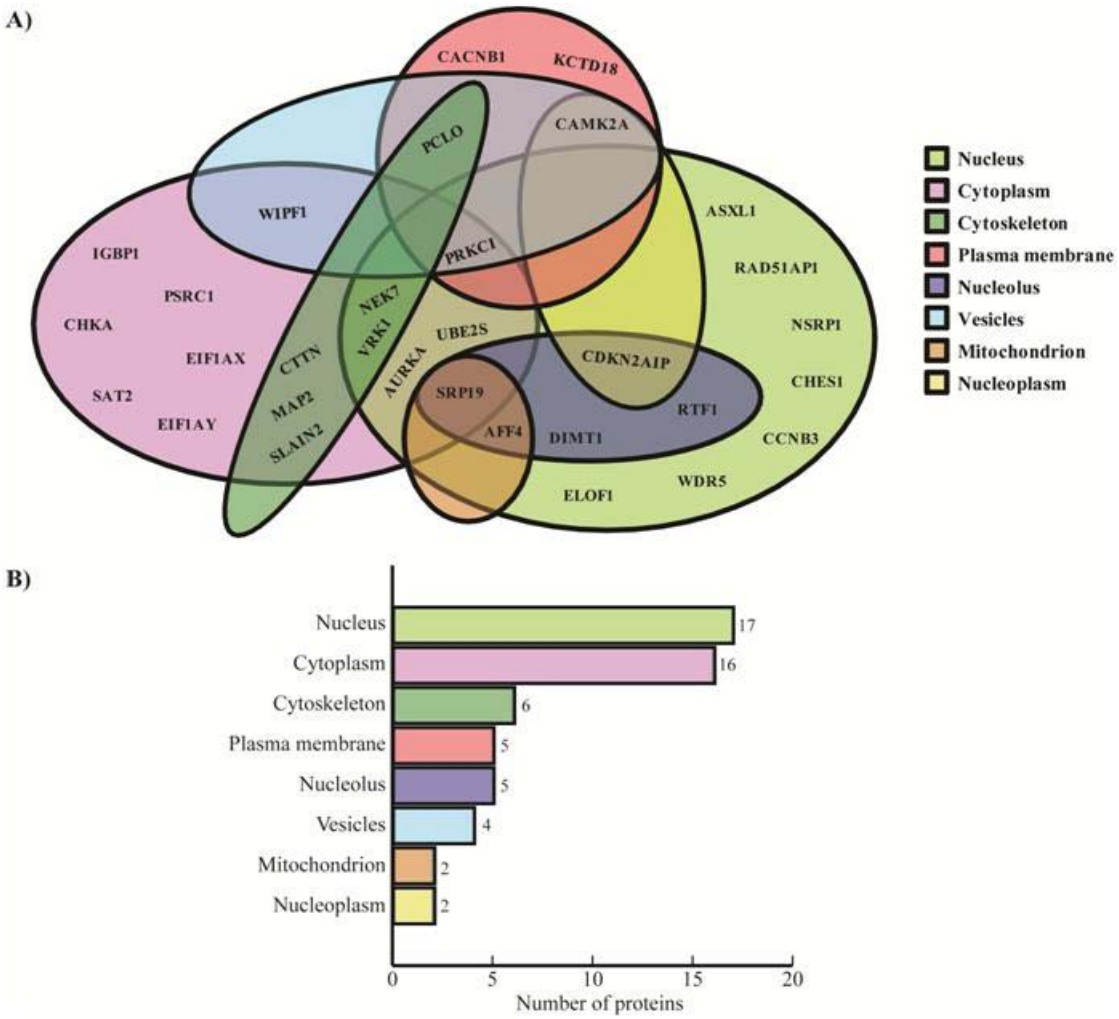

Figure 5.5: Localization of DENV C protein-interacting partners identified via ProtoArray® platform. (A) The cellular localization of each individual protein is shown. Some of them localize in more than one cellular compartment. Majority of the DENV C protein-interacting partners localize in the nucleus followed by cytoplasm. (B) The total proteins in each cellular compartment are also calculated and charted.

5.4. Non-Structural Role of Dengue Virus (DENV) Capsid (C) Protein in the Nucleus

To delineate the significance of nuclear localization of DENV C protein during virus replication, a list of identified interacting partners that localize in the nucleolus compartment were chosen for further investigation. Five nucleolar proteins (SRP19, DIMT1, AFF4, RFT1, and CDKN2AIP) mainly involved in the regulation of

transcriptional and translational activities and cell cycle control categories (Figure 5.4) were examined.

5.4.1. Role of Dengue virus (DENV) capsid (C) protein in cell cycle arrest

5.4.1.1. Validation of the binding between Dengue virus (DENV) capsid (C) protein and identified interacting partners

Before investigating the roles of DENV C protein in cell cycle arrest, the binding between the identified interacting partners and DENV C protein was first verified via enzyme-linked immunosorbent assay (ELISA). Among the five nucleolar proteins, only cyclin-dependent kinase inhibitor 2A interacting protein (CDKN2AIP or CARF) is involved in cell cycle control and p53 pathway. The other four proteins (SRP19, DIMT1, AFF4, and RFT1) were examined later in Section 5.4.2.

To expand the investigation of the role of DENV C protein in cell cycle control, more nuclear interactors that are also related to cell cycle control and p53 pathway (CHES1 and VRK1 proteins) were included. The role of DENV C protein in p53 pathway was examined because of the involvement of C protein in activating p53 pathway as previously reported in WNV by Bhuvanakantham and colleagues (2010). Cyclin B3 (CCNB3) protein was also chosen for further validation since eukaryotic linear motif (ELM) analysis revealed that there are putative cyclin binding motifs on DENV C proteins as shown in Table 5.3. From the putative cyclin binding motifs on DENV C protein, it was noticed that DENV-1 was similar to DENV-3 whereas DENV-2 was similar to DENV-4. Such phenomenon was also observed in the DENV sequence analyses done by Khan and colleagues (2008).

Table 5.3: Putative cyclin binding sites of Dengue virus capsid proteins identified via eukaryotic linear motif (ELM) analysis

Serotype	Accession Number	Positions	Amino Acid Sequence
DENV-1	NP_722457.2	35-38	KGLL
		55-59	RFLAI
DENV-2	NP_739581	55-59	RFLTI
		90-94	RMLNI
DENV-3	YP_001531165	35-38	KGLL
		55-59	RFLAI
DENV-4	ADA00410	54-58	RVLSI
		78-81	KILI
		89-93	RMLNI

Commercially-available pure proteins were purchased and coated on ELISA plate. Purified biotinylated full-length DENV C protein that was produced from Chapter 4 was used as probe for binding and streptavidin-horseradish peroxidise (HRP) antibody was used to detect the presence of bound DENV C proteins. As shown in Figure 5.6 (A), all four proteins showed significant higher absorbance as compared to bovine albumin serum (BSA), implicating that these four identified interacting partners indeed bound to full-length DENV C protein in an ELISA-based platform. Human Sec3 and Sec6 proteins were used as positive and negative controls, respectively, for binding with DENV C protein in this experiment [Figure 5.6 (B)]. This result corroborated that DENV C protein was involved in cell cycle arrest and p53 pathway.

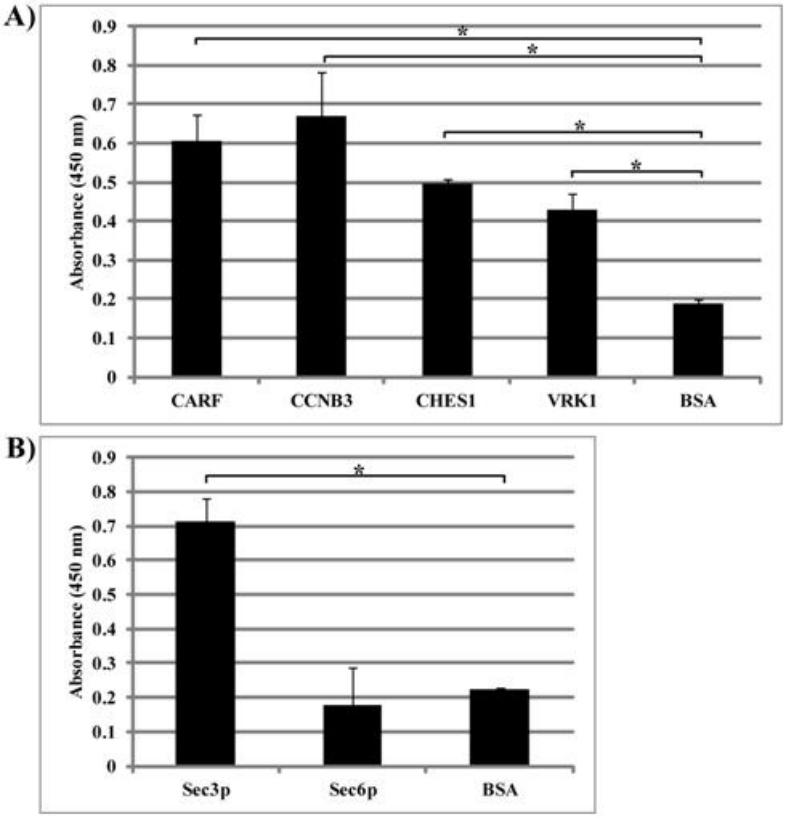

Figure 5.6: Verification of the binding between identified interacting partners and DENV C protein via ELISA. (A) Commercially-available proteins of the identified protein interactors of DENV C protein are coated on MaxiSorp 96-well plate in triplicates. Purified biotinylated DENV C proteins are added into the wells for binding and bound proteins are detected via streptavidin-horseradish peroxidase (HRP) secondary antibody. The absorbance is measured at 450 nm. All four protein interactors show high absorbance as compared to bovine albumin serum (BSA). (B) Sec3p and Sec6p proteins are used as positive and negative controls, respectively, for binding with DENV C protein. *p-value < 0.05

5.4.1.2. Dengue virus (DENV) capsid (C) protein arrested cell cycle at S-phase

Since the validated protein interactors were related to cell cycle arrest, investigation was carried out to examine the role of DENV C protein in cell cycle arrest. Green fluorescent protein (GFP)-tagged DENV C protein was transfected into human embryonic kidney (HEK)-293 cells (Section 2.3.6) and the cells were harvested for fluorescent-activated cell sorting (FACS) analysis (Section 2.7.1) at 12 hr, 24 hr, 36 hr, and 48 hr post-transfection. GFP control was included as negative

control. First gating was applied to the transfected cells expressing GFP. Cell cycle profile of the green fluorescing cells was subsequently analyzed.

Figure 5.7 showed the cell cycle profiles of DENV C protein-transfected cells and GFP control-transfected cells at 12 hr, 24 hr, 36 hr, and 48 hr post transfection. The percentage of cells in each cell cycle phase was counted and plotted in Figure 5.8. As shown in Figure 5.8, the percentage of cell population in S-phase was significantly higher in DENV C protein-transfected cells as compared to GFP control-transfected cells at 24 hr ($P=0.0142$) and 48 hr ($P=0.0063$) post-transfection. On the other hand, the percentage of DENV C protein-transfected cells at G1-phase was lower than control cells. It was also observed that the percentage of DENV C protein-transfected HEK293 cells in G2- / M-phase was lower than mock-transfected cells at 36 hr post-transfection ($P=0.0227$). Hence, this result implicated that DENV C protein promoted cell cycle progression from G1- to S-phase.

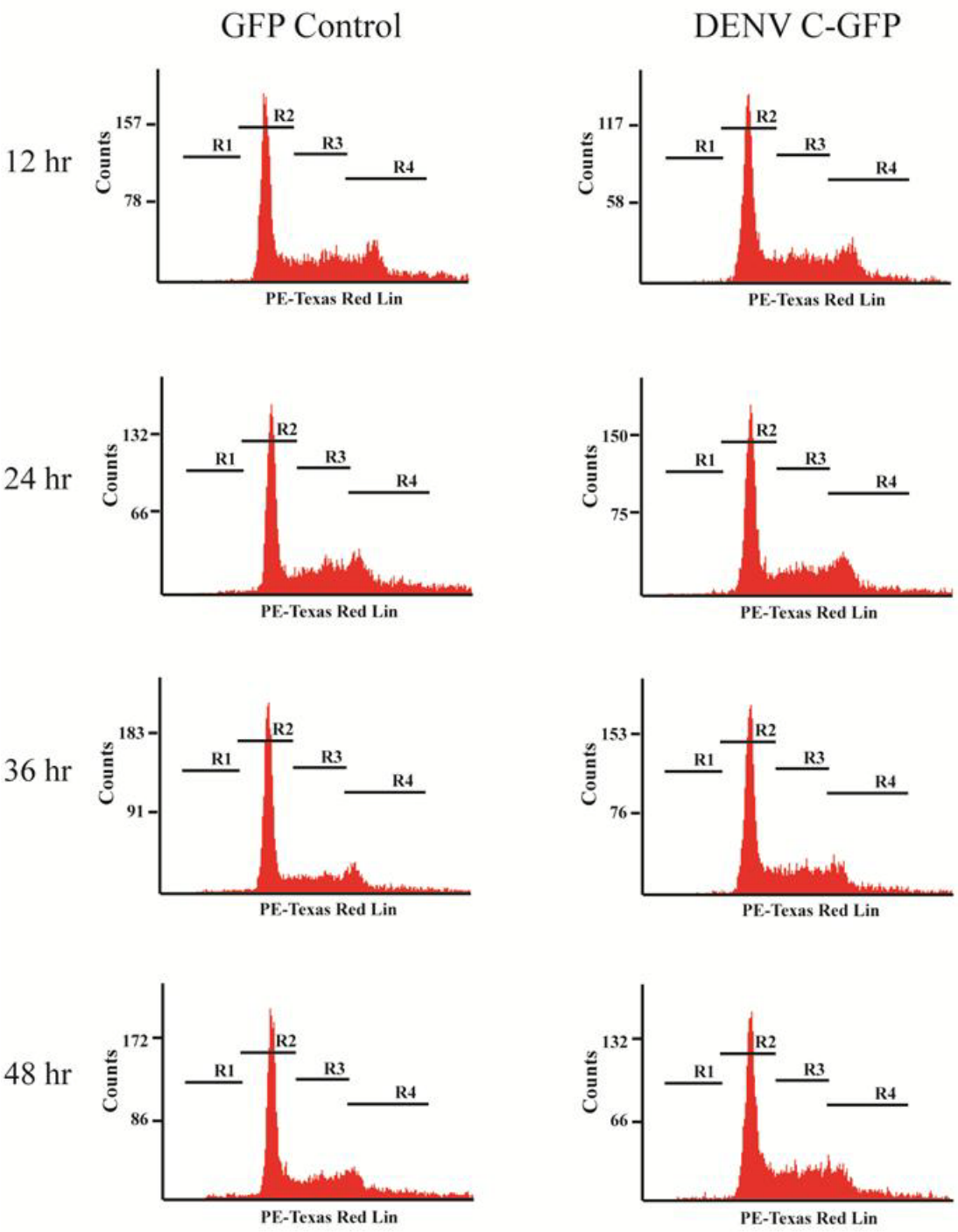

Figure 5.7: Cell cycle profile of DENV C protein-transfected and GFP control-transfected HEK293 cells. Propidium iodide is used to stain the nuclei and cell cycle phases are analyzed via fluorescent-activated cell sorting (FACS). R1 – Apoptotic cells; R2 – G1-phase; R3 – S-phase; R4 – G2- / M-phase.

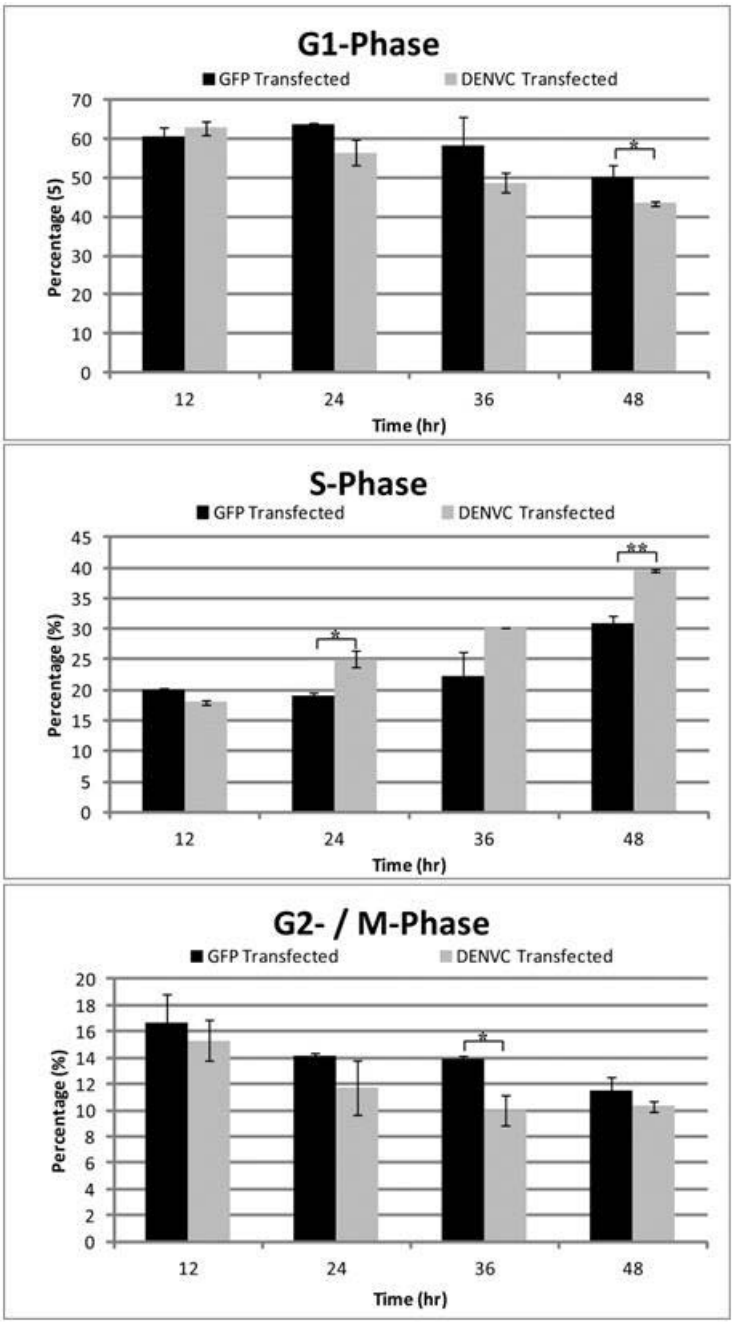

Figure 5.8: Cell cycle arrest induced by DENV C protein on HEK293 cells. HEK293 cells are transfected with GFP-tagged DENV C protein and GFP control plasmids. Cell cycle profiles of the GFP expressing cells are analyzed via FACS. The values here are the averages of two independent experiments. S-phase cell cycle arrest is observed in DENV C protein-transfected cells at 24 hr and 48 hr post-transfection. *p-value < 0.05; **p-value < 0.01

5.4.1.3. Cell cycle arrest during wild type flavivirus infection

To investigate whether DENV C protein-induced cell cycle arrest is real in wild-type DENV infection, FACS (Section 2.7.1) was carried out to analyze the cell

cycle profile of DENV-infected cells. HEK293 cells were infected with DENV-2 at multiplicity of infection (M.O.I.) of one. All the cells were infected synchronously at 4 ^{o}C before they were incubated at 37 ^{o}C. This synchronization step is essential to ensure all cells were infected at the same time. Infected cells were fixed at every 12 hr interval with cold ethanol. All the fixed cells were stained with propidium iodide and cell cycle analyses were carried out using flow cytometer.

Figure 5.9 demonstrated that similar S-phase cell cycle arrest was observed in DENV-infected HEK293 cells and this cell cycle arrest occurred as early as 12 hr post-infection (p.i.). As compared to mock-infected cells at S-phase, significant higher amount of DENV-infected was observed at 12 hr (P=0.022), 36 hr (P=0.0187) and 48 hr (P=0.008) p.i. Concurrently, the percentage of infected HEK293 cells in G1-phase was significantly lower than mock-infected cells (P=0.008). In addition, G2- / M-phase arrest was also observed in the DENV-infected cells. Percentage of DENV-infected cells in G2- / M-phase was higher than mock-infected cells at 24 hr p.i. (P=0.004) and 48 hr p.i. (P=0.002). This cell cycle arrest time points correlated well with the exponential and peak of the virus growth curve as shown in Figure 5.10. Thus, cell cycle arrest by DENV C protein was confirmed in wild-type virus infection and this was tallied with the virus titers during replication.

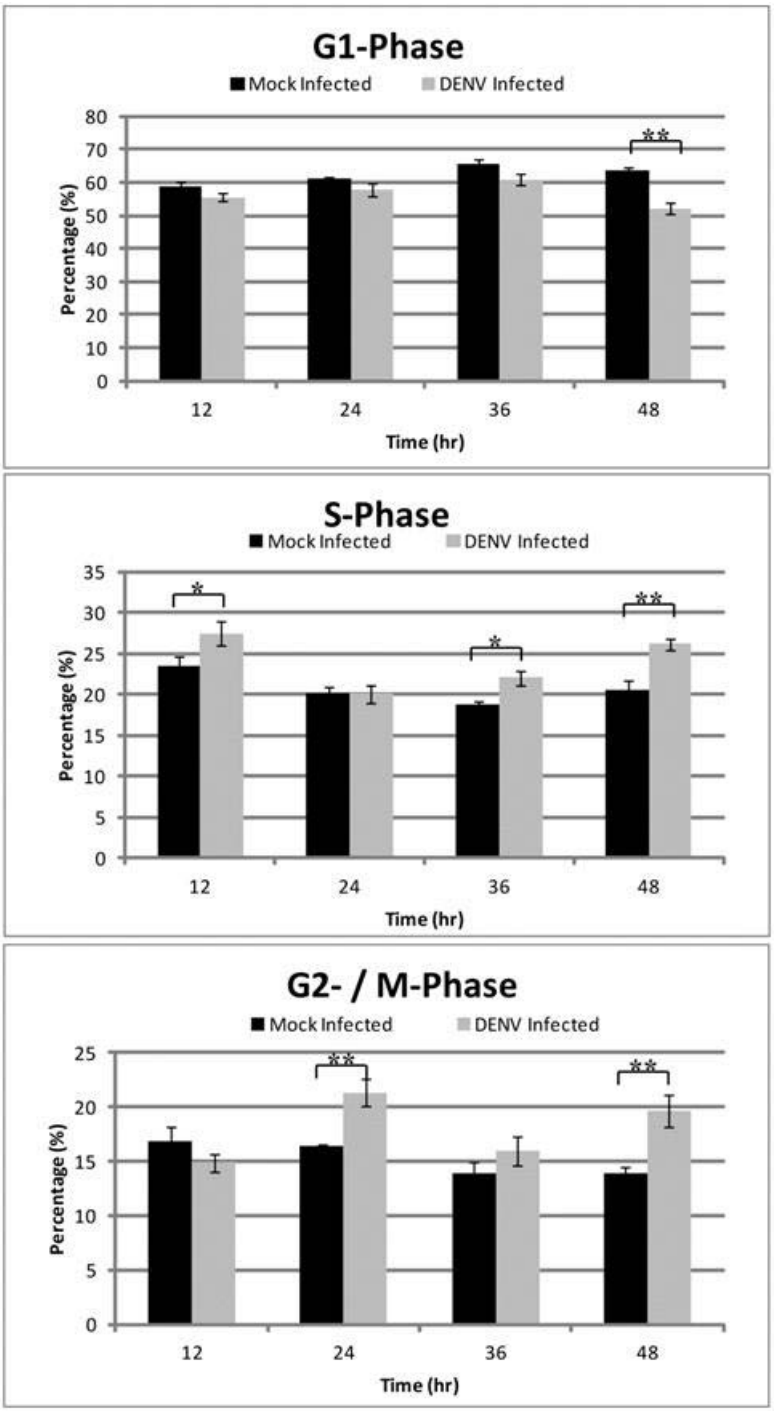

Figure 5.9: Cell cycle arrest induced by DENV on HEK293 cells. The percentage of cells in each cell cycle phase is counted and averaged from three independent experiments. Significant higher population of DENV-infected cells is arrested in S-phase and G2- / M-phase at 48 hr post infection (p.i.) as compared to mock-infected cells. *p-value < 0.05; **p-value < 0.01

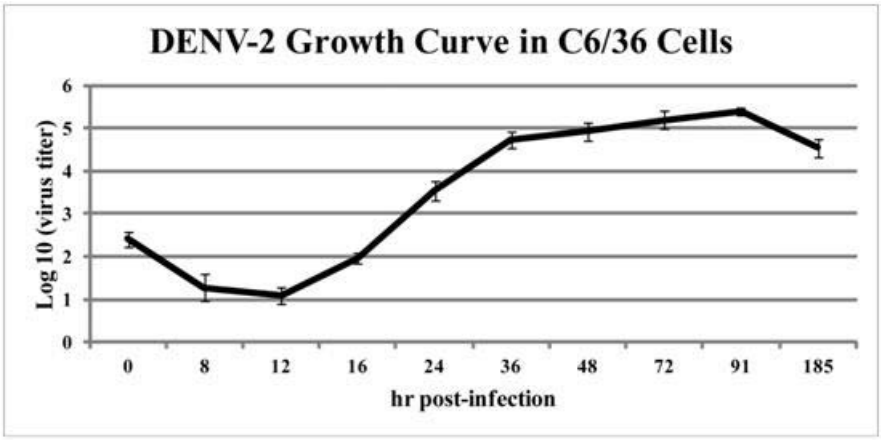

Figure 5.10: Growth curve of DENV-2 in C6/36 cells. Mosquito C6/36 cells are infected with DENV-2 and the supernatant is harvested at various time courses for virus titer quantitation via plaque assay. Virus titer drops initially and starts increasing exponentially from 12 hr p.i. onwards until 48 hr p.i. The virus titer drops again from 91 hr p.i. onwards.

West Nile virus (WNV) C protein was also reported to localize in host cell nucleus during infection (Bhuvanakantham *et al.*, 2009). To examine whether WNV C protein has similar role in controlling cell cycle or this cell cycle arrest is only specific to DENV, similar experiment was carried out using West Nile virus (WNV). The only difference in the protocol was that cell cycle analyses were performed at every 2 hr interval instead of 12 hr because WNV reaches virus peak production faster than DENV. One complete life cycle for DENV is about 48 hr whereas WNV needs approximately 24 hr. Since the replication cycle of WNV was fast, emphasis of this study was on the first 12 hr.

As shown in Figure 5.11, WNV also arrested HEK293 cells at S-phase during infection. The percentage of WNV infected-cell populations at S-phase was indeed significantly higher (P=0.0001) than mock-infected cells at 24 hr p.i. Unlike DENV-infected HEK293 cells, WNV-infected cell population at G2- / M-phase was lower than mock-infected cells. Therefore, both flaviviruses, DENV and WNV, arrested HEK293 cells at S-phase during replication but only DENV further promoted cell cycle progression from S- to G2- / M-phase in HEK293 cells.

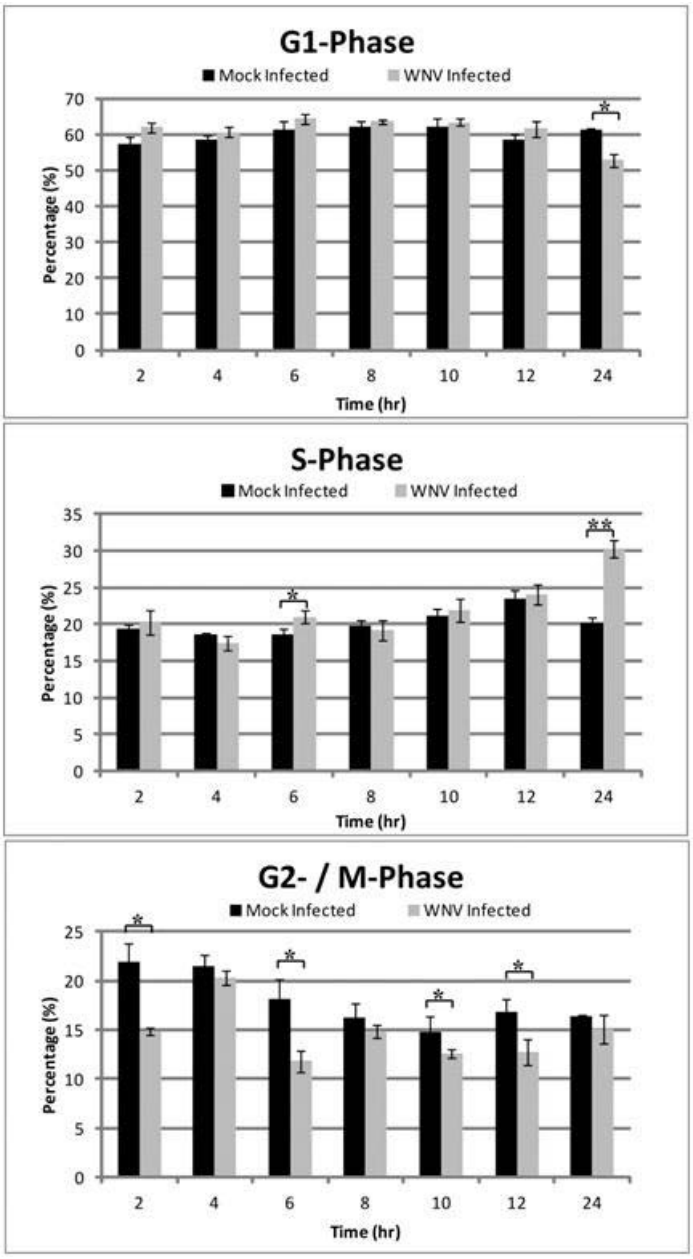

Figure 5.11: S-phase cell cycle arrest induced by WNV on HEK293 cells. The percentage of cell populations in each cell cycle phase is plotted after analysis via FACS. At 24 hr p.i., significant higher population of WNV-infected cells is at S-phase as compared to mock-infected cells. However, infected cell population in G2- / M-phase is lower than mock-infected cells. *p-value < 0.05; **p-value < 0.01

5.4.1.4. Flavivirus-induced cell cycle arrest is cell-type specific

To further investigate if this flavivirus-induced cell cycle arrest is cell line and virus specific, cell cycle profile of DENV- and WNV-infected Baby Hamster Kidney (BHK) cells and C6/36 mosquito cells were also examined. Figure 5.12 showed that DENV also arrested BHK cells at S-phase during replication. The percentage of

infected cells at S-phase was significantly higher than mock-infected cells at 12 hr (P=0.0162), 24 hr (P=0.0343), 36 hr (P=0.0138), and 48 hr (P=0.007) p.i. Concurrently, the percentage of infected cells at G1-phase was lower than mock-infected cells at 36 hr (P=0.00673) and 48 hr (P=0.00168) p.i. Hence, this result implicated DENV also promoted BHK cell cycle progression from G1- to S-phase. Nevertheless, unlike HEK293 cells, G2- / M-phase arrest was not observed in DENV-infected BHK cells. The percentage of DENV-infected BHK cells in G2- / M-phase was, on the other hand, lower than mock-infected cells. This indicated that DENV arrested BHK cells at S-phase and thus resulted in decreased G2- / M-phase cells population.

As for WNV-infected BHK cells, S-phase cell cycle arrest was also observed during infection. Figure 5.13 showed that the population of infected cells at S-phase was significantly higher than mock-infected cells from 8 hr p.i. onwards. At the same time, the percentage of infected cells at G1-phase was significantly lower than mock-infected. Therefore, WNV also promoted cell cycle progression from G1- to S-phase in BHK cells. The effect of S-phase cell cycle arrest by WNV on BHK cells was much more obvious and earlier than that of WNV on HEK293 cells (Figure 5.11). In addition, G2- / M-phase cell cycle arrest was also observed in WNV-infected BHK cells at 24 hr p.i. This G2- / M-phase cell cycle arrest was similar to DENV infection on HEK293 cells (Figure 5.9). This confirmed that both DENV and WNV induced similar cell cycle arrest at S- and G2- / M-phases so that the cells were still at the replicating stage for better virus replication.

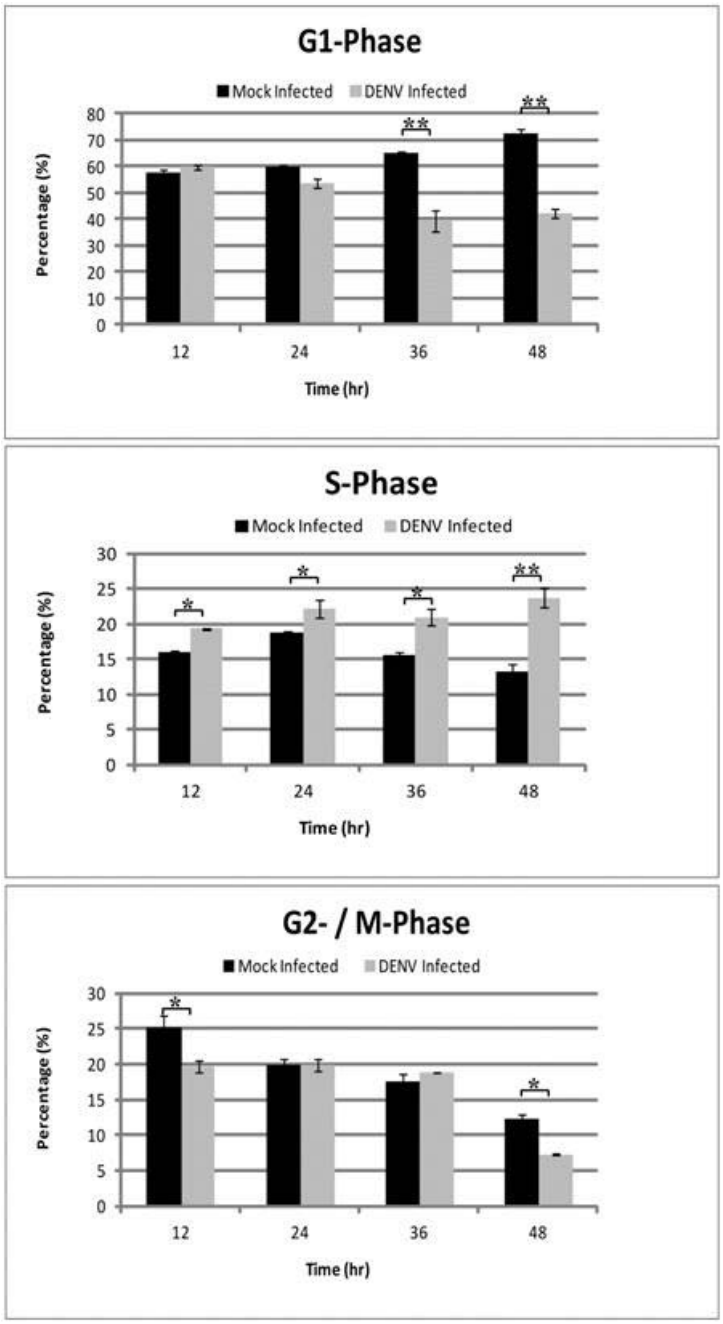

Figure 5.12: Cell cycle arrest induced by DENV on BHK cells. The percentage of DENV-infected BHK cells at S-phase is also significantly higher than mock-infected cells. On the other hand, the percentage of DENV-infected BHK cells at G1-phase is significantly lower than mock-infected cells. *p-value < 0.05; **p-value < 0.01

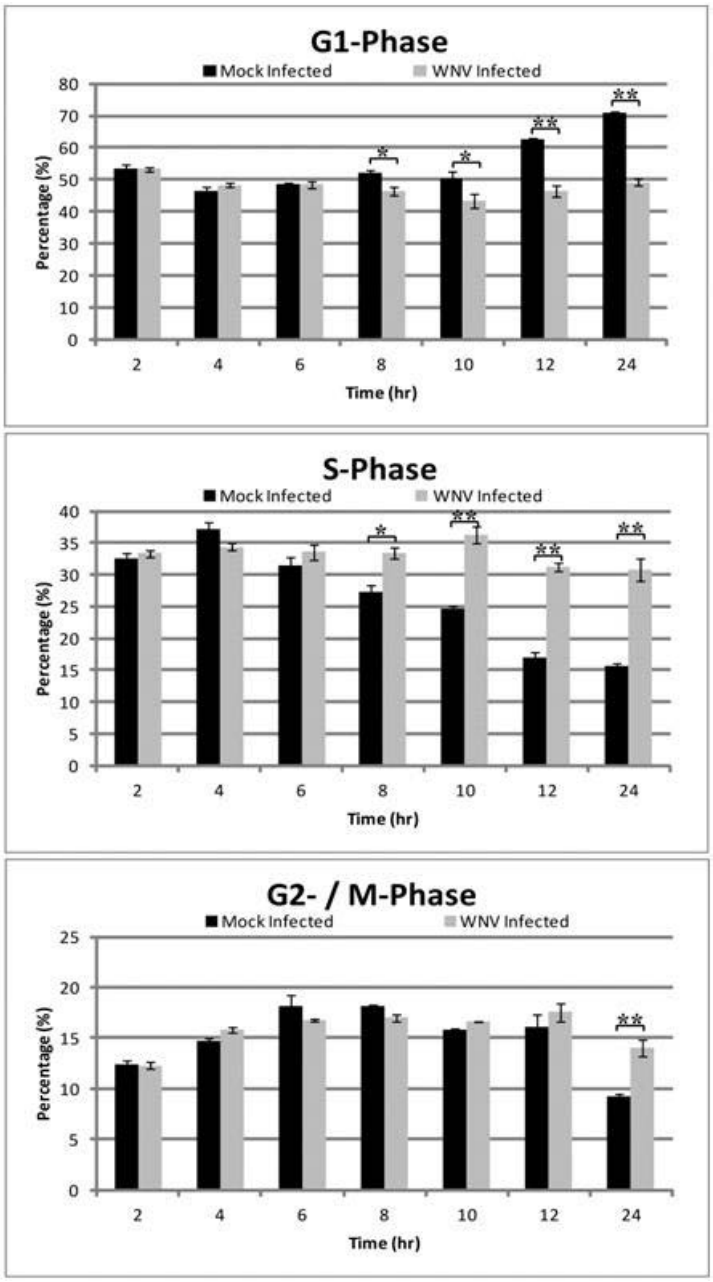

Figure 5.13: Cell cycle arrest induced by WNV on BHK cells. The percentage of WNV-infected BHK cells at S-phase is significantly higher than mock-infected cells from 8 hr p.i. onwards while the percentage of infected cells at G1-phase is significantly lower than mock-infected cells for the same time points. G2- / M-phase cell cycle arrest is also observed at 24 hr p.i.

However, unlike mammalian cells, cell cycle arrest induced by flavivirus on C6/36 mosquito cells was different. Cell cycle arrest was also observed for DENV infection as shown in Figure 5.14 but DENV arrested C6/36 at G2- / M-phase instead of S-phase. As compared to mock-infected cells, higher percentage of DENV-infected

C6/36 cells remained in G2- / M-phase, especially at 48 hr p.i. (P=0.048). On the other hand, the percentage of infected cells at G1-phase was lower than mock-infected cells (P=0.047) whereas no significant difference was observed between DENV-infected and mock-infected cells in S-phase. This demonstrated that DENV arrested mammalian cells at S-phase but arrested mosquito cells at G2- / M-phase.

To examine if G2- / M-phase arrest also occurred in WNV-infected C6/36 cells, similar experiment was performed. In contrast, no significant differences were observed between WNV-infected and mock-infected C6/36 cells. The percentages of cells at each cell cycle phase were similar for both WNV-infected and mock-infected cells as shown in Figure 5.15. This implied that WNV arrested BHK cells at S-phase but WNV did not affect the cell cycle of insect cell line, C6/36.

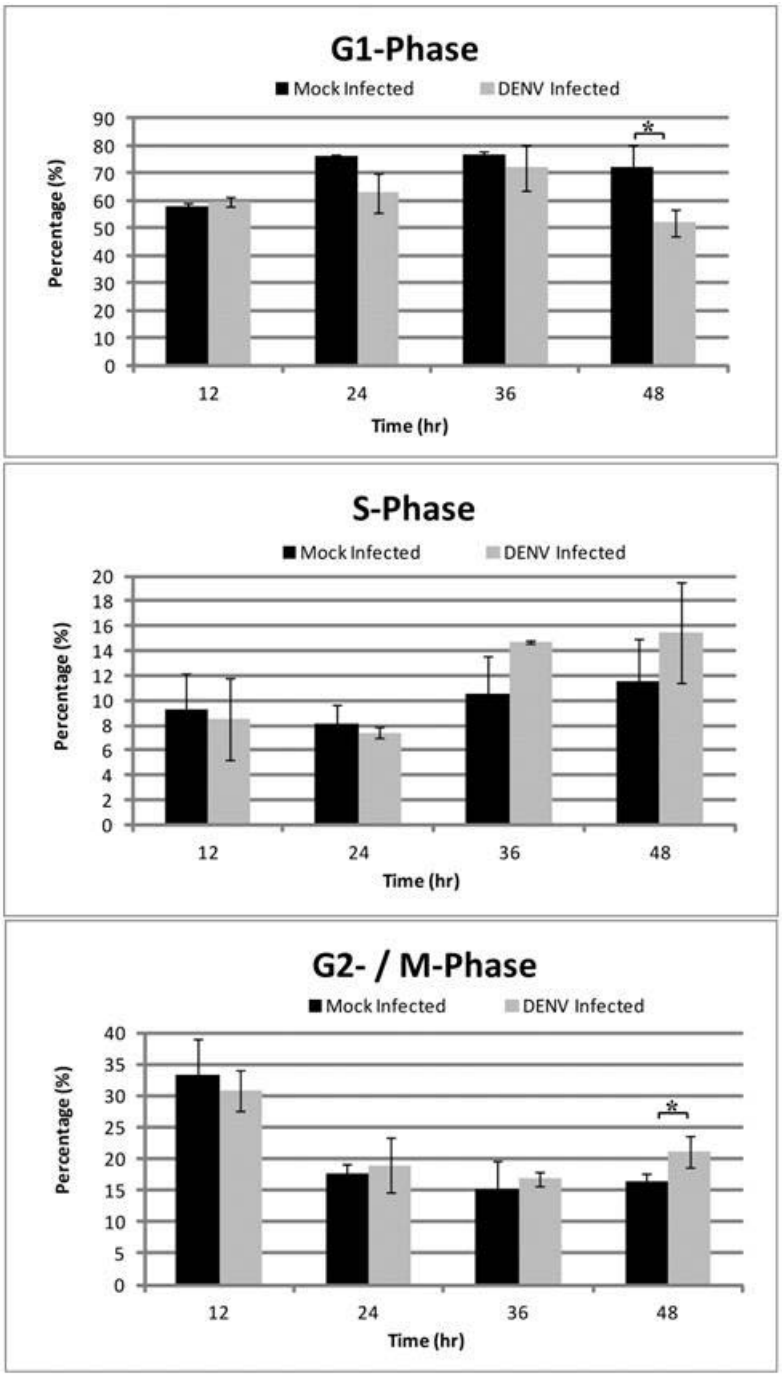

Figure 5.14: Cell cycle arrest induced by DENV on C6/36 cells. The population of C6/36 cells in S-phase between DENV-infected and mock-infected does not differ significantly. However, the percentage of DENV-infected cells at G1-phase is significantly lower than mock-infected cells at 48 hr p.i. On the other hand, higher number of DENV-infected cells are arrested at G2- / M-phase as compared to mock-infected cells 48 hr p.i. * p-value < 0.05.

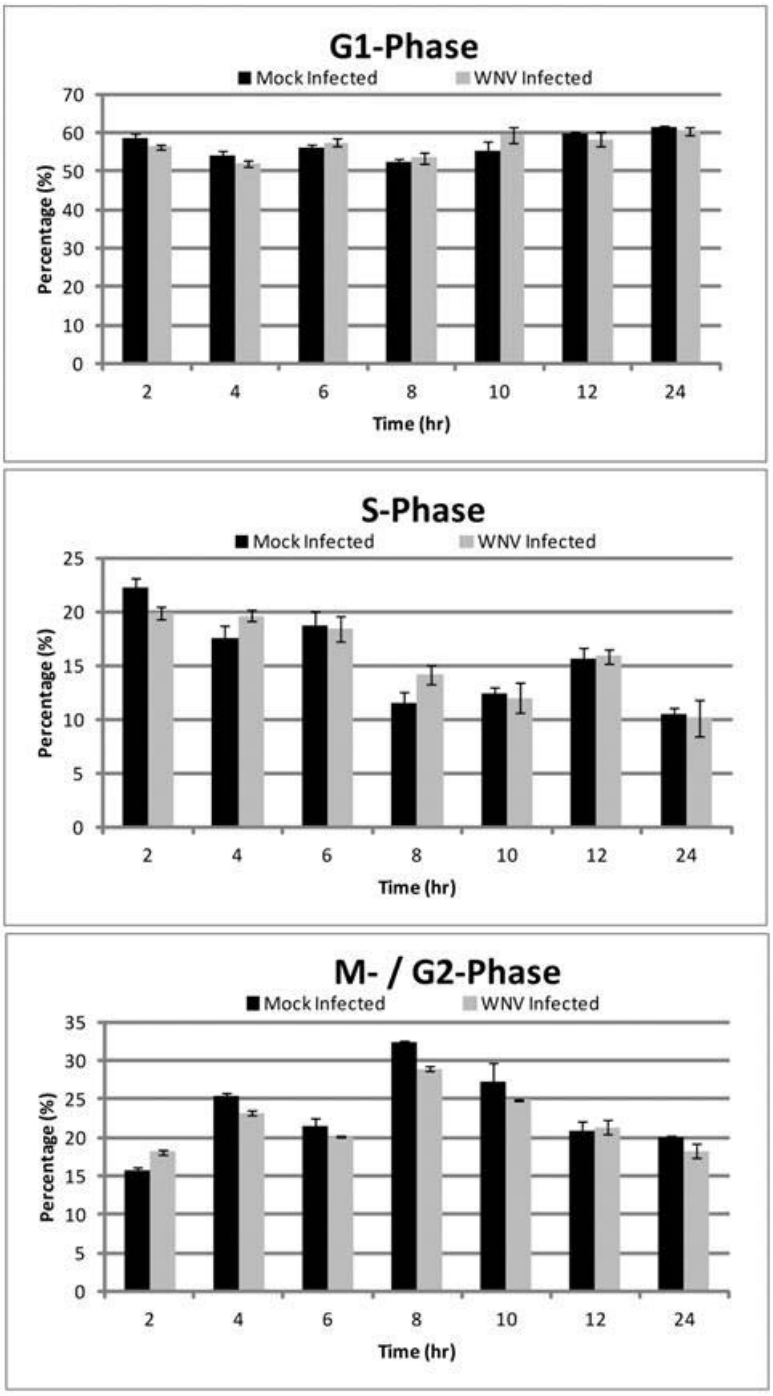

Figure 5.15: Cell cycle arrest induced by WNV on C6/36 cells. No significant difference is observed in any cell cycle phase between WNV-infected and mock-infected cells.

The wild-type virus infection results supported that flaviviruses indeed induced cell cycle arrest during replication. Both DENV and WNV induced S-phase arrest in HEK293 and BHK cells but DENV arrested C6/36 cells at G2- / M-phase whereas WNV did not affect the cell cycle of C6/36 cells.

5.4.1.5. Effect of cell cycle arrest upon Dengue virus (DENV) infection

Since flavivirus induced cell cycle arrest at S-phase during infection, it was hypothesized that S phase was more favourable for flavivirus replication. To examine the effect of each cell cycle phase on DENV infection, HEK293 cells were arrested at each cell cycle phase using various drugs (Section 2.7.2) and infection was performed on the cell cycle synchronized cells. The effect of the cell cycle arrest on DENV replication was examined by quantitating the virus titer in the supernatant via plaque assay (Section 2.2.2) at 48 hr post-infection. HEK293 cells were chosen for further downstream experiments because both BHK and HEK293 cells were arrested similarly by DENV and WNV at S-phase during infection.

Figure 5.16 (A) showed the cell cycle profiles of all the treated cells at 48 hr post-infection. As compared to no treatment control (i), serum starvation was able to arrest the cells at G1-phase (ii). 40 mM thymidine (Thy) was used to arrest cell cycle at S-phase (iii) whereas 100 ng/ml nocodazole (Noco) was able to arrest cell cycle at G2- / M-phase (iv). DENV production was significantly reduced by up to 2 log when the host cell cycle was arrested at G1-phase [Figure 5.16 (B)]. There was no significant difference in virus titer when the cells were arrested at S-phase and G2- / M-phase. To rule out the possibility of cytotoxicity that in turn led to virus titer reduction, cytotoxicity assay was carried out. As shown in Figure 5.16 (C), the treatments did not show any significant cytotoxicity effect as compared to no treatment control. Hence, this result demonstrated that G1-phase was not favourable for DENV replication. Figures 5.7 to 5.15 implicated that DENV promoted host cell cycle progression to S-phase during infection to favour its replication.

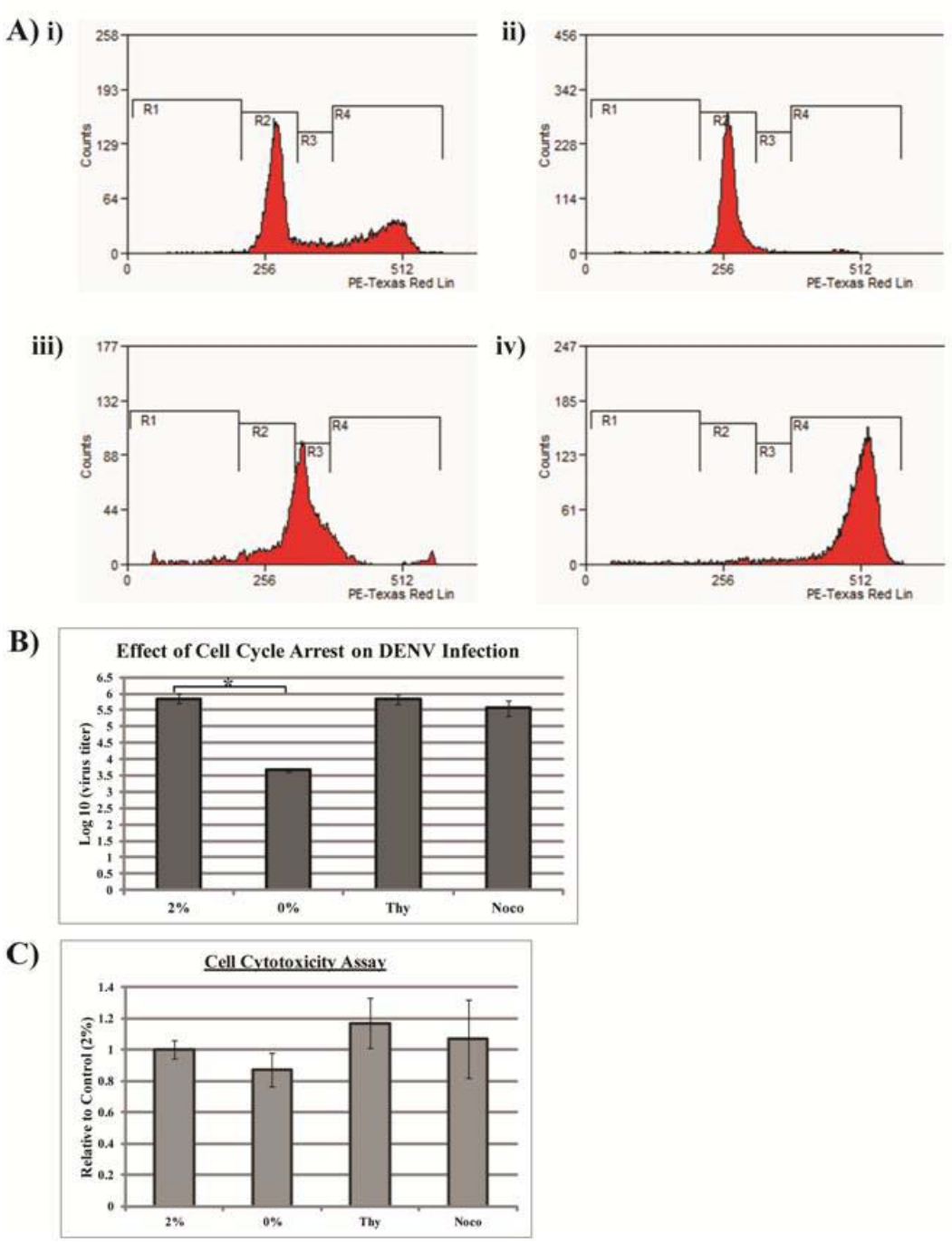

Figure 5.16: Effect of cell cycle arrest on DENV infection. (A) HEK293 cells are synchronized in different cell cycle phases using various treatments. (i) Growth media supplemented with 2 % fetal calf serum (FCS) is used as no treatment control. (ii) Serum starvation (0%) is used to arrest cells at G1-phase. 40 mM thymidine (Thy) is used for S-phase arrest while (iv) 100 ng/ml nocodazole (Noco) is used for G2- / M-phase arrest. (B) Virus titer in the supernatant is quantitated via plaque assay at 48 hr post-infection. As compared to no treatment control (2%), no significant difference in virus titer is observed after treatment with Thy and Noco. However, DENV production is significantly reduced in cells arrested at G1-phase. (C) Cell cytotoxicity assay is carried out to examine the toxicity of the treatments. No significant cytotoxicity effect is observed in all the treatments as compared to no treatment control. (R1 – dead cells; R2 – G1-phase; R3 – S-phase; R4 – G2- / M-phase) *p-value < 0.05

5.4.1.6. Effect of DENV infection on cell cycle-related genes

Since the ProtoArray® (Figure 5.6) and FACS analyses (Figure 5.7-5.15) results implicated that flaviviruses arrested host cell cycle during infection to aid their replication, further investigation was carried out to examine the changes in cell cycle-related genes expression level during infection. In order to have a comprehensive list of cell cycle-related genes, Human Cell Cycle PCR array from SABiosciences was employed (Section 2.7.3). A total of 84 key genes pertaining to cell cycle regulation can be screened simultaneously in one single 96-well plate. Important genes that regulate transitions between each cell cycle phase, checkpoints and arrest are included in the PCR array. HEK293 cells were infected with DENV at M.O.I. of 1 and the total RNA was harvested at 48 hr post-infection (p.i.) for PCR array analysis. A more stringent fold change cut-off value (> 3) was considered significant difference to prevent false positive.

3D PCR array profile (A) and scatter plot (B) in Figure 5.17 revealed that there were three significantly up-regulated genes in the DENV-infected cells as compared to mock-infected cells at 48 hr post-infection. The identity and functions of the up-regulated genes was illustrated in Table 5.4.

Table 5.4: Cell cycle-related genes that are up-regulated during DENV infection

Symbols	Gene Name	Fold Change	Functions
GADD45A	Growth arrest and DNA-damage-inducible, alpha	5.89	Main regulator of p38/JNK pathway, mediating G2- / M-checkpoint in response to environmental stress via p53-dependent and -independent mechanisms
HERC5	Hect domain and RLD 5	4.92	Ubiquitin E3 ligase that mediates ISGylation of protein targets
CDKN2B	Cyclin-dependent kinase inhibitor 2B (p15, inhibits CDK4)	3.68	A CDK inhibitor that prevents cell cycle G1-phase progression by interrupting the binding of cyclin D to CDK4 or CDK6

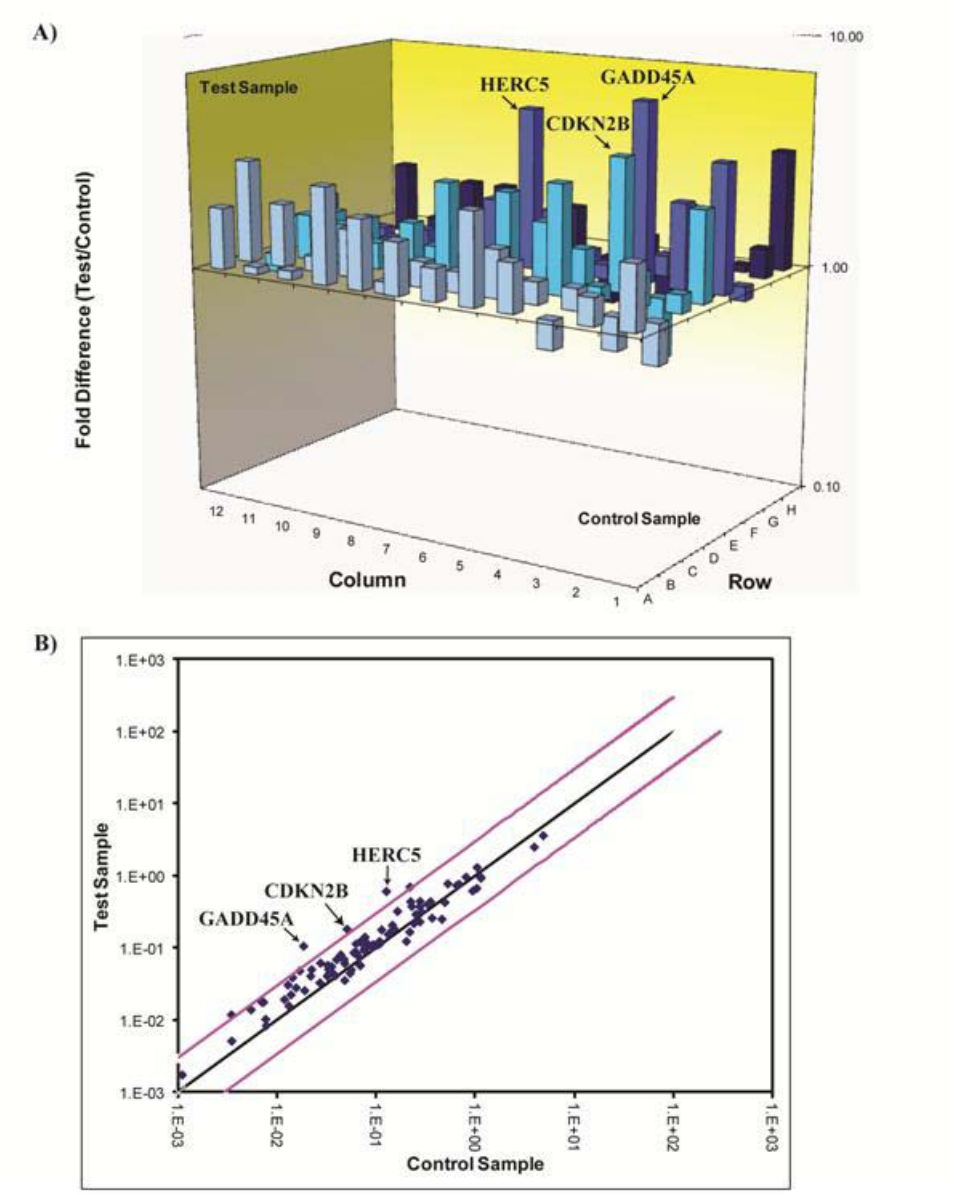

Figure 5.17: PCR array analysis of DENV-infected cells. HEK293 cells are infected with DENV at M.O.I. of 1 and total RNA is extracted from the infected cells for PCR array analysis at 48 hr post-infection. 3D profile (A) and scatter plot (B) show that three genes are significantly up-regulated in DENV-infected cells at 48 hr post-infection. The purple lines in scatter plot indicate the significant fold-change in the gene expression level threshold which is more than 3.

ProtoArray® identified four cell cycle-related interacting partners (CCNB3, CDKN2AIP, CHES1 and VRK1) of DENV C protein while PCR array discovered three more genes (GADD45A, HERC5 and CDKN2B) that were up-regulated during DENV infection. Hence, to examine the gene expression levels of all these seven genes in DENV-infected cells at 48 hr post-infection, real-time PCR (Section 2.3.8)

was carried out. As shown in Figure 5.18 (A), there was only a slight increase in CHES1 gene level as compared to mock-infected cells. Nevertheless, significant increase was observed in all other genes at 48 hr post-infection. To examine whether these genes up-regulation was specific to DENV laboratory strain only, DENV-2 clinical isolate from Singapore (05K4137) with low passage number (Passage 3) was used to infect HEK293 cells. At 48 hr post-infection, it was observed that all seven genes were significantly up-regulated [Figure 5.18 (B)]. In summary, DENV promoted cell cycle progression during infection to favour its replication and seven cell cycle-related genes (GADD45A, HERC5, CDKN2B, CCNB3, CDKN2AIP, CHES1, and VRK1) were up-regulated. Among these seven genes, CCNB3, CHES1, CDKN2AIP and VRK1 were found to have direct interaction with DENV C protein.

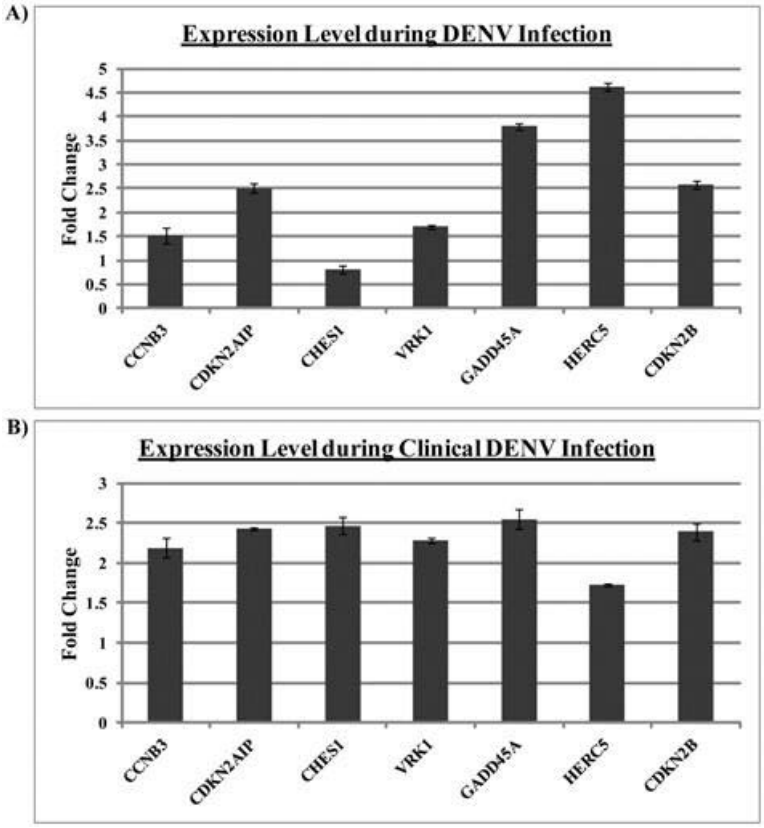

Figure 5.18: Gene expression level of identified interacting partners of DENV C protein during DENV infection. HEK293 cells are infected with DENV and total RNA is harvested for real-time PCR analysis at 48 hr post-infection. Both DENV-2 laboratory strain (A) and clinical isolate (B) up-regulate all seven genes during infection. The up-regulation is also observed in clinical isolate-infected cells.

5.4.2. Role of Dengue virus (DENV) capsid (C) protein in regulating host transcriptional and translational activity

5.4.2.1. Validation of the binding between Dengue virus (DENV) capsid (C) protein and identified interacting partners

Other than cell cycle control, regulating host transcriptional and translational activities was another main category of the identified interacting partners of DENV C protein. Among the five nucleolar proteins, four (SPR19, DIMT1, AFF4 and RFT1) of them (Figures 5.4 and 5.5) are pertaining to regulation of transcriptional and translational activities. These proteins may be useful for DENV viral proteins biogenesis. Before examining the role of the four nucleolar proteins, the binding between these proteins (SRP19, DIMT1, AFF4 and RFT1) and DENV C protein were first validated via enzyme-linked immunosorbent assay (ELISA).

Commercially-available pure proteins were purchased from Abnova (USA) and coated on ELISA plate (Section 2.5.3.7). Bovine serum albumin (BSA) was also coated on the ELISA plate as negative control. Purified full-length biotinylated DENV C protein (Chapter 4) was then added into the well as probe for binding. Bound DENV C protein was detected by streptavidin-horseradish peroxidase (HRP) antibody. As shown in Figure 5.19, all four identified interacting partners bound to DENV C protein. Significant higher absorbance was observed in all four nucleolar proteins as compared to BSA. Hence, DENV C protein interacted with AFFT, DIMT1, RFT1, and SRP19 proteins in an ELISA-based platform.

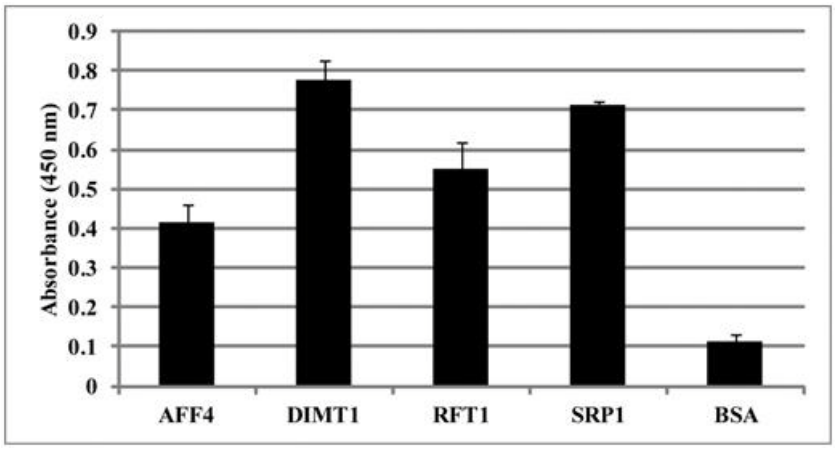

Figure 5.19: Validation of the binding between DENV C protein and interacting partners identified via ProtoArray® platform. Pure AFF4, DIMT1, RFT1, and SRP19 proteins are coated on MaxiSorp 96-well plate and purified biotinylated DENV C protein is used as probe. Bound C protein is detected by streptavidin-horseradish peroxidase secondary antibody. As compared to negative control, bovine serum albumin (BSA), significant higher absorbance is detected for all four interacting partners.

Among these four nucleolar proteins, DIMT1 and SRP19 were chosen for further investigation because purified proteins and working antibodies are commercially available. DIMT1 is an 18S ribosomal RNA (rRNA) dimethylase that specifically dimethylates adenosines of 18S rRNA in the 40S ribosomal particle. SRP19 is a ribonucleoprotein that facilitates targeting specific protein to endoplasmic reticulum during protein translation.

To further confirm the interaction between DENV C protein and DIMT1 / SRP19 proteins, a reciprocal ELISA binding assay was carried out by coating DENV C protein on the ELISA plate and glutathione S-transferase (GST)-tagged DIMT1 and SRP19 proteins were used as probes. The bound complexes were then detected by HRP-conjugated anti-GST antibodies. As demonstrated by Figure 5.20, the reciprocal ELISA binding assay result also supported that DIMT1 and SRP19 proteins indeed interacted with DENV C protein. Besides, Figure 5.21 also showed that biotinylated full-length DENV C protein interacted with both SRP19 and DIMT1 proteins coated on ELISA plates in an increasing dose-dependent manner.

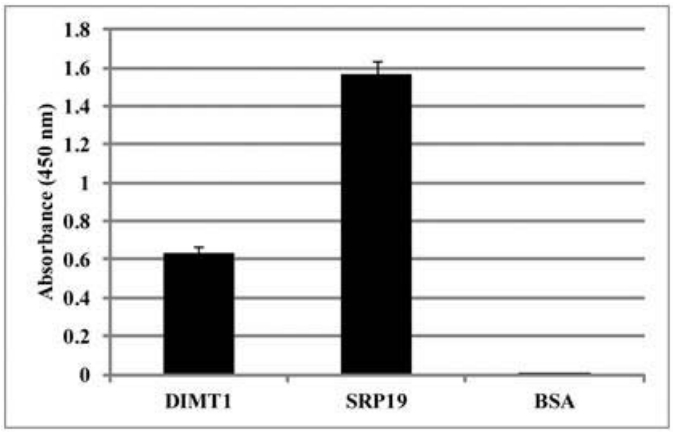

Figure 5.20: Reciprocal binding assay to confirm the interaction between DENV C protein and SRP19 / DIMT1 proteins. Purified DENV C protein (100 ng) is coated on the MaxiSorp well in triplicates. Same amount of SRP19 and DIMT1 proteins are added into the wells and bound proteins are detected by horseradish peroxidase (HRP)-conjugated anti-glutathione S transferase (GST) antibody. Higher absorbance is also detected for SRP19 and DIMT1 protein as compared to the negative control, bovine serum albumin (BSA).

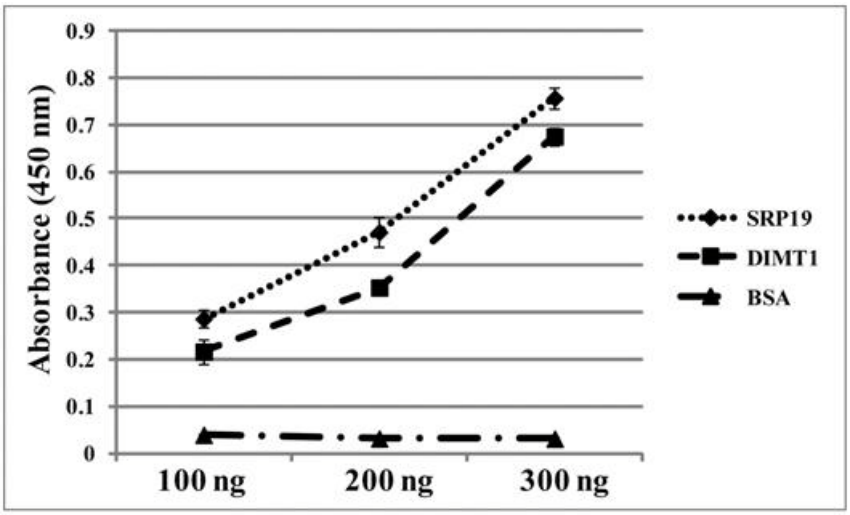

Figure 5.21: Protein binding assay with increasing amount of SRP19 / DIMT1 proteins. Increasing amount of SRP19 and DIMT1 proteins (100 ng, 200 ng, and 300 ng) are coated on MaxiSorp well in triplicates. Same amount of purified biotinylated DENV C proteins (100 ng) are added into each well for binding. Streptavidin-horseradish peroxidase (HRP) is used to detect bound DENV C protein. Unlike bovine serum albumin (BSA), DENV C protein interacts with SRP19 and DIMT1 proteins in an increasing dose-dependent manner.

The bindings between DENV C protein and DIMT1 / SRP19 proteins were not only observed *in vitro*, but also *in vivo*. Immuno-fluorescence assay result in Figure 5.22 (A and B) illustrated that DENV C protein co-localized with DIMT1 and

SRP19 proteins in BHK cell nucleus, especially in the nucleolus. Co-localization analysis using JACoP plugin (Bolte & Cordelieres, 2006) in ImageJ software (Section 2.4.5) demonstrated that the Pearson's coefficients for the positive correlation between DENV C protein and SRP19 or DIMT1 proteins were 0.864 and 0.930, respectively [Figure 5.22 B(i and ii)]. The closer the coefficient value to 1, the higher the correlation between DENV C protein and the interacting partners. The results corroborated that SRP19 and DIMT1 proteins were novel interacting partners of DENV C protein.

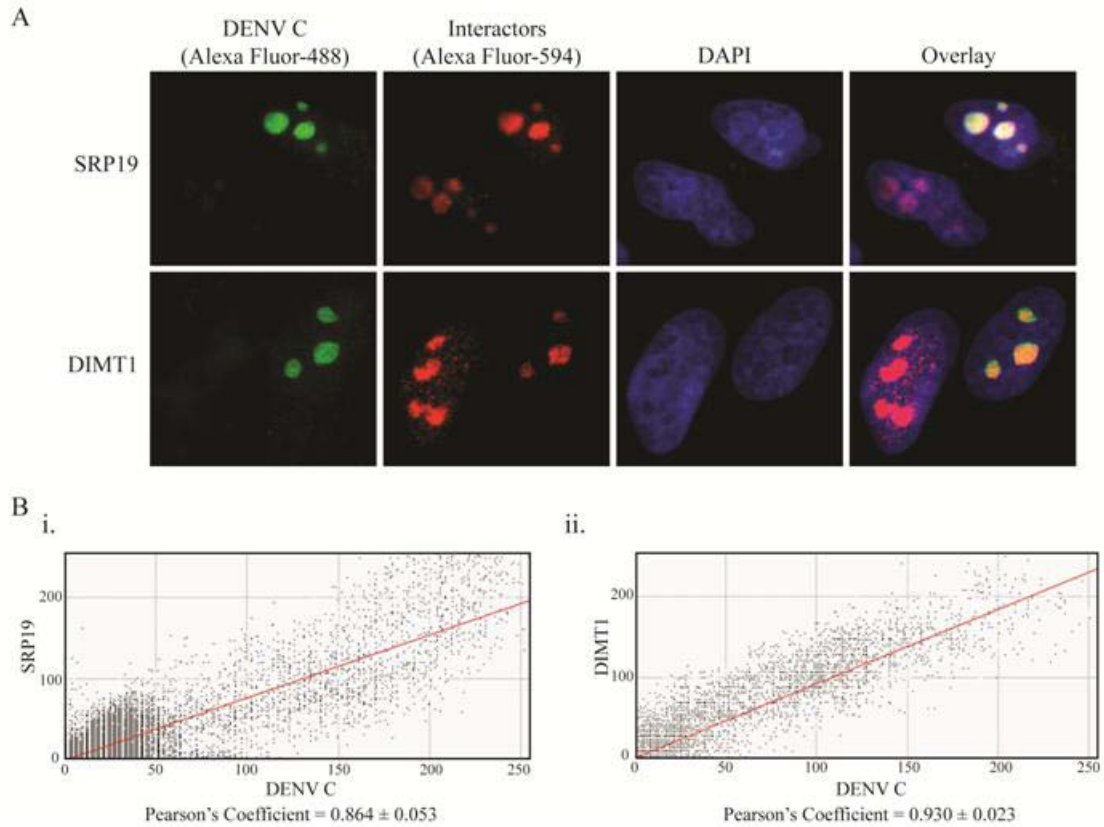

Figure 5.22: Co-localization between DENV C protein and SRP19 / DIMT1 proteins in the nucleolus. (A) FLAG-tagged full-length DENV C plasmid is transfected into BHK cells seeded on coverslips. The transfected cells are fixed and stained with anti-FLAG and anti-SRP19 / DIMT1 antibodies. Alexa Fluor-488 secondary antibody is used to detect anti-FLAG antibody while Alexa Fluor-594 secondary antibody is used for anti-SRP19 / DIMT1 antibodies. 4',6'-diamino-2-phenylindole (DAPI) is used to stain the nucleus. The overlay images show that DENV C protein co-localizes with SRP19 and DIMT1 in the nucleus. (B) Co-localization analysis is performed using JACoP plugin in ImageJ software. The cytofluorograms of SRP19 (i) and DIMT1 (ii) show that there is a positive correlation between SRP19 / DIMT1 proteins and DENV C protein with Pearson's coefficient of 0.864 and 0.930, respectively.

5.4.2.2. Effect of signal recognition particle 19 (SRP19) and dimethyladenosine transferase 1 homolog (DIMT1) gene over-expression and knock-down upon Dengue virus (DENV) replication

To delineate the role of SRP19 and DIMT1 proteins during DENV replication, over-expression and knock-down experiments were carried out. DIMT1 is involved in ribosomal biogenesis whereas SRP19 is related to protein biogenesis. The hypothesis was that DENV C protein controlled these host protein in the nucleolus through direct interaction to aid virus replication.

To over-express SRP19 and DIMT1 genes, commercially available clones were purchased from OriGene, USA. After confirming the DNA sequence and identity of the clones via DNA sequencing, the plasmids were transfected into HEK293 cells according to Section 2.3.6. To examine the effect of the genes over-expression upon DENV infection, the transfected cells were infected with DENV at M.O.I of 1 after 24 hr post-transfection (Section 2.8). Empty vector clone expressing myc-FLAG tag only was used as a negative control. After 24 hr post-infection, the infected cell lysates were collected for RNA extraction and protein analyses.

Western-blot (Section 2.5.3.2) and real time-PCR (Section 2.3.8) were carried out to ensure that SRP19 and DIMT1 proteins were over-expressed. Since both clones contained a myc-FLAG tag at the C-terminus, the presence of over-expressed SRP19 and DIMT1 proteins were detected by anti-FLAG antibody. The molecular weight of SRP19 and DIMT1 proteins are approximately 20 kDa and 36 kDa, respectively. Figure 5.23 (A) demonstrated that both proteins were expressed well in the transfected HEK293 cells as thick bands were observed in both the infected (INF) and mock-infected (UI) Lanes. Real-time PCR result in Figure 5.23 (B) also showed that SRP19 (i) and DIMT1 genes (ii) were significantly higher in the respective clone

transfected cells as compared to tag control. Interestingly, it was also noticed that SRP19 and DIMT1 gene levels in the infected cells (INF) was significantly higher as compared to mock-infected cells (UI). This implied that SRP19 and DIMT1 genes were up-regulated during DENV infection.

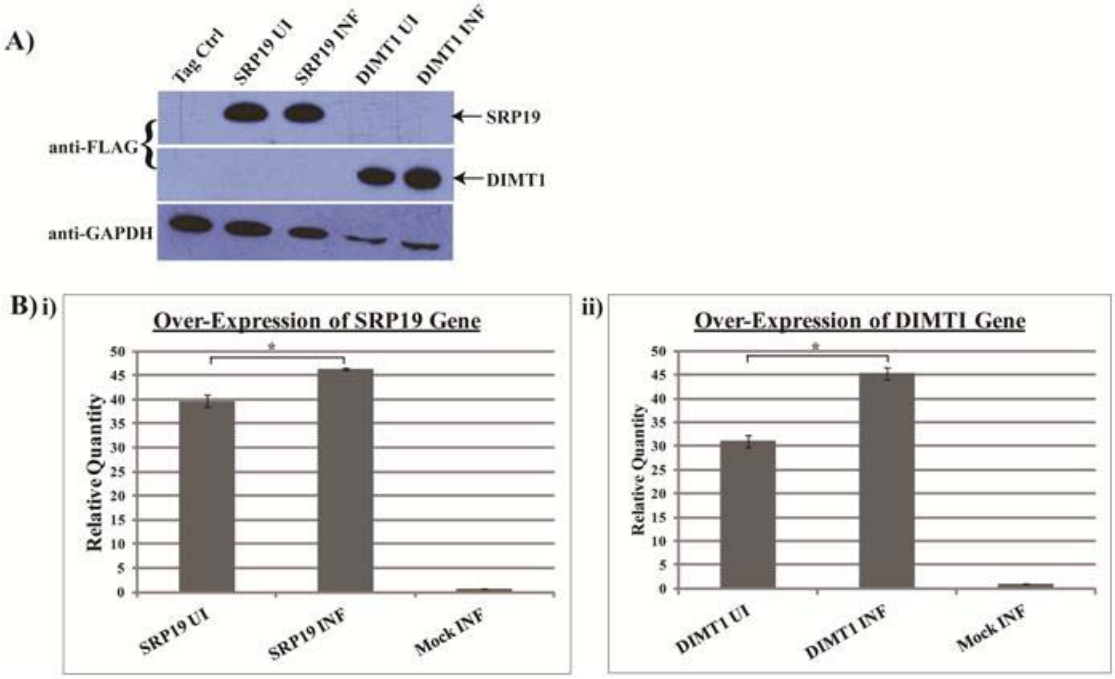

Figure 5.23: Over-expression of SRP19 and DIMT1 proteins in HEK293 cells. (A) HEK293 cells are transfected with SPR19 and DIMT1 plasmids and the over-expressed proteins are detected via Western-blot using anti-FLAG antibody. Glyceraldehyde 3-phosphate dehydrogenase (GAPDH) antibody is used as loading control antibody. SRP19- and DIMT1-corresponding bands are observed in both the infected (INF) and mock-infected (UI) cells. Tag control (Tag Ctrl) is used as negative control to examine the effect of genes over-expression on DENV infection. (B) Real-time PCR result showing the over-expression of SRP19 (i) and DIMT1 (ii) genes in the transfected cells. The genes level in the infected cells (INF) is significantly higher than the mock-infected cells (UI). *p-value < 0.05

To examine the effect of the SRP19 and DIMT1 proteins over-expression upon DENV infection, virus titer in the supernatant of the infected cells were quantitated via plaque assay (Section 2.2.2). As shown in Figure 5.24 (A), the virus titers in DIMT1 protein over-expressed cells was not significantly different from that in myc-FLAG tag over-expressed cells. In other words, over-expression of DIMT1

protein did not have any effect on DENV replication. Nevertheless, there was a statistically significant reduction in virus titer (P=0.0131) when SRP19 protein was over-expressed in HEK293 cells [Figure 5.24 (A)]. There was approximately 60 % virus titer reduction as compared to tag control cells [Figure 5.24 (B)].

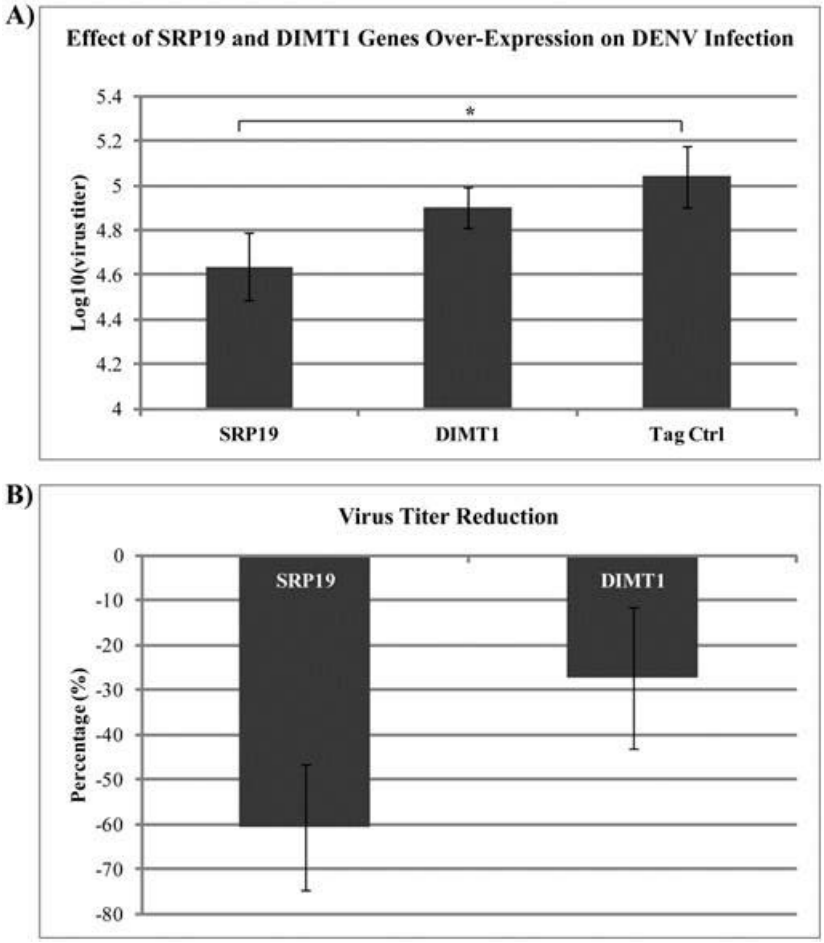

Figure 5.24: Effect of SRP19 and DIMT1 proteins over-expression on DENV infection. (A) The supernatant of the infected cells is harvested for plaque assay. There is no significant difference in virus titer between DIMT1 protein and tag control over-expressed cells. However, virus titer in SRP19 protein over-expressed cells is significantly lower than that in tag control over-expressed cells. *p-value<0.05 (B) Percentage of virus titer reduction in SRP19 and DIMT1 protein over-expressed cells as compared to tag control over-expressed cells. This data is contributed by two independent experiments.

As for knock-down experiment, human shRNA constructs of SRP19 and DIMT1 genes were purchased from OriGene, USA. To ensure multiple splice variants were targeted during knock-down, four unique shRNA constructs for each gene were

combined in one single transfection in HEK293 cells (Section 2.9). Scrambled shRNA was included as a negative control. Besides, the shRNA constructs contained green fluorescent protein (GFP) so transfection efficiency could be monitored. Figure 5.25 (A) illustrated the transfection efficiency of the shRNA constructs into HEK293 cells at 24 hr post-transfection. Intense green fluorescence was clearly observed in majority of the cell population.

The transfected cells were then infected with DENV at M.O.I of 1. After 24 hr post-infection, the infected cells were collected for real-time PCR (Section 2.3.8) and Western-blot (Section 2.5.3.2) analyses. As shown in Figure 5.25 (B), both the SRP19 (i) and DIMT1 (ii) genes were successfully knock-downed by approximately 80 %, even after 48 hr post-transfection. Reduction in band intensity was observed for both SRP19 and DIMT1 proteins in Western-blot [Figure 5.25 C(i)]. Densitometry analysis showed that both SRP19 and DIMT1 protein expression levels were reduced to approximately 50 % and 40 %, respectively [Figure 5.25 C(ii)].

The effect of SRP19 and DIMT1 genes knock-down upon DENV infection was examined by quantitating the virus titer in the supernatant of infected cells via plaque assay (Section 2.2.2). Figure 5.26 showed that there was no significant virus titer reduction in both the SRP19 and DIMT1 genes knock-downed cells. Hence, SRP19 and DIMT1 genes knock-down did not affect DENV production.

In brief, over-expression and knock-down of DIMT1 genes did not affect DENV production (Figures 5.24 and 5.26). Nevertheless, the underlying reason for the binding of DENV C protein to DIMT1 protein still warrants further investigation. On the other hand, over-expression of SRP19 protein resulted in significant virus titer reduction although knock-down of SRP19 gene did not have any effect on DENV production.

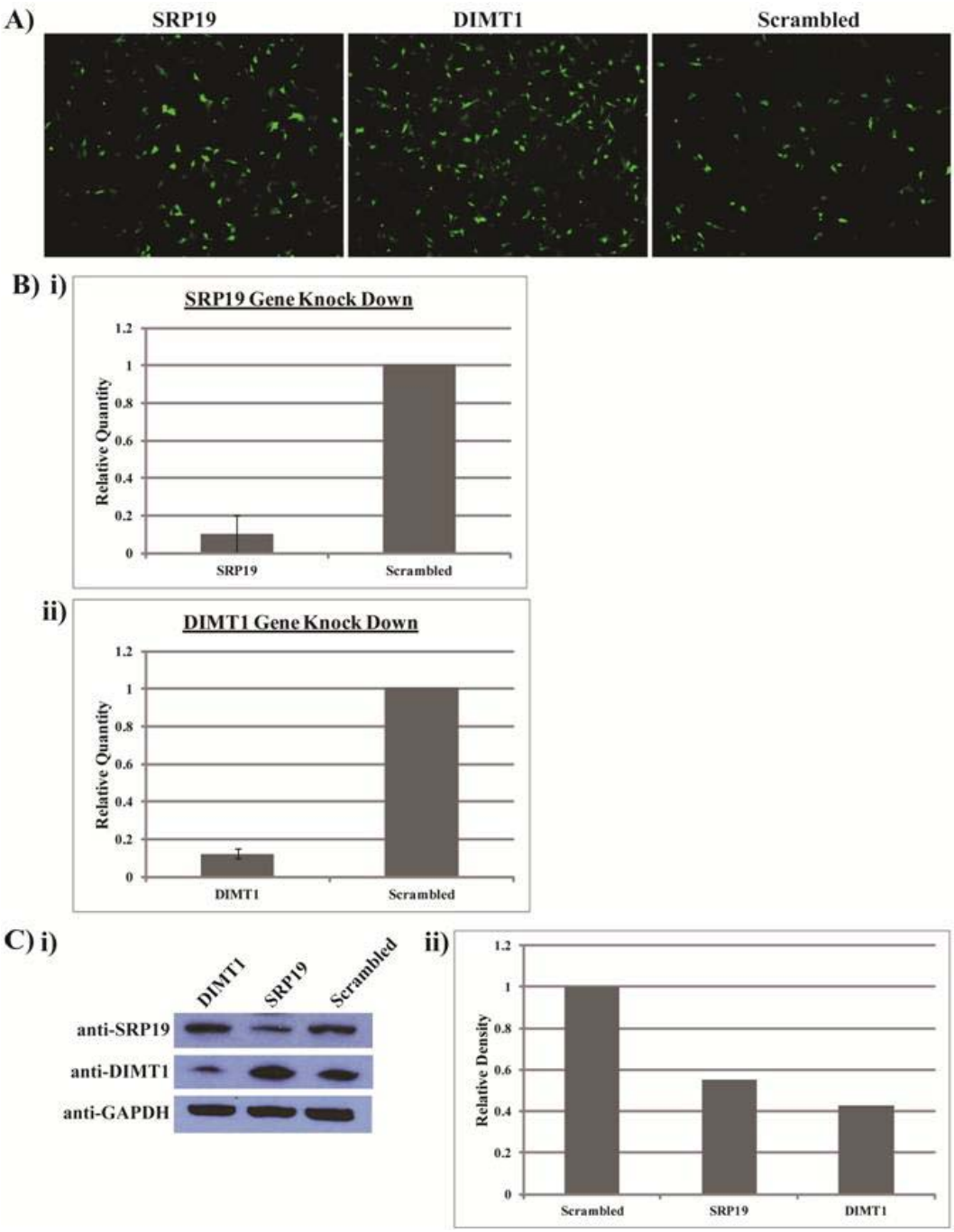

Figure 5.25: Knock-down of SRP19 and DIMT1 genes. (A) Human shRNA constructs targeting SRP19 and DIMT1 genes are transfected into HEK293 cells. Transfection efficiency is monitored by green fluorescent protein (GFP) expression. Immuno-fluorescence images (10 x magnifications) show the expression of GFP in the transfected cells. (B) At 24 hr post-transfection, the cells are infected with DENV. Total RNA was extracted from the infected cells at 24 hr post-infection and real-time PCR is performed to detect SRP19 (i) and DIMT1 (ii) genes level. Both of the genes level is significantly reduced as compared to scrambled shRNA-transfected cells. (C) The protein expression level of SRP19 and DIMT1 proteins is detected via Western-blot (i) and densitometry analysis is carried out using ImageJ software (ii). After normalization with GAPDH loading control, SRP19 and DIMT1 protein expression levels are reduced to approximately 50 % and 40 %, respectively, as compared to scrambled.

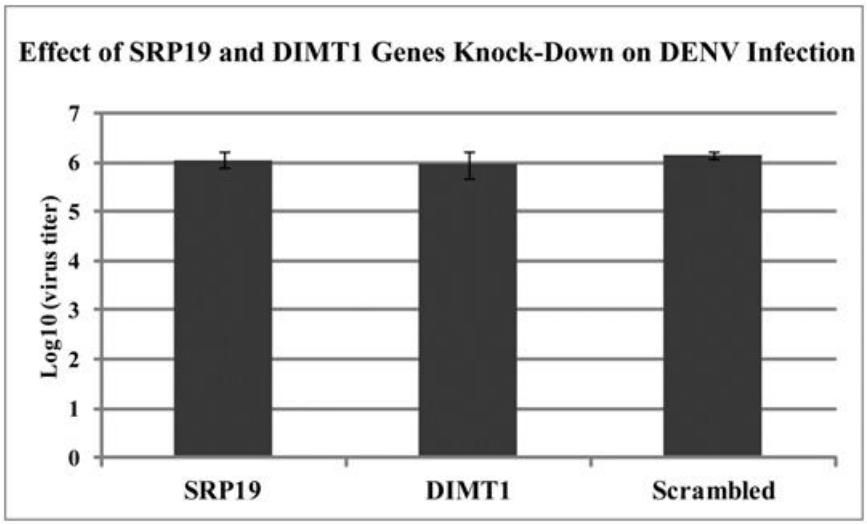

Figure 5.26: Effect of SRP19 and DIMT1 genes knock-down upon DENV infection. Supernatant of SRP19 and DIMT1 genes knock-downed HEK293 cells is harvested for plaque assay analysis. No significant difference in virus titer is observed in all the SRP19-, DIMT1- and scrambled-transfected cells.

5.4.2.3. Role of signal recognition particle 19 (SRP19) during Dengue virus (DENV) infection

The main function of signal recognition particle 19 (SRP19) is to facilitate the binding of SRP RNA, also known as 7SL RNA, to other SRP components such as SRP54, SRP68 and SRP72 proteins to form SRP ribonucleoprotein complex (Wild *et al.*, 2010). This SRP ribonucleoprotein complex is a ubiquitous initiator of protein translocator that facilitates targeting nascent polypeptide to the rough endoplasmic reticulum (ER) so that translating protein could be inserted into the membrane (Grudnik *et al.*, 2009; Lutcke, 1995; Rapiejko & Gilmore, 1992). This is an important process for DENV replication too because the replication site of flavivirus is at the ER regions where the viral genome is translated into a single polyprotein. However, it was also reported that ribonucleoprotein complex bound to translating protein can retard the protein elongation before targeting them to the ER (Lutcke, 1995; Walter *et al.*, 1981). Therefore, there are two possible outcomes for the interaction between SRP19 protein and DENV C protein: (1) DENV C protein binds to SRP19 protein and

brings the whole ribonucleoprotein complex to the virus replication site to facilitate viral protein translation. (2) Ribonucleoprotein complex binds to translating DENV polyprotein and retards the protein elongation. Figures 5.24 and 5.26 indicated that over-expression of SRP19 protein resulted in lower virus yield and on the other hand, knock-down of SRP19 gene did not affect DENV production. Hence, this implied that the presence of SRP19 protein was in fact inhibiting DENV replication.

To investigate the level of SRP19 protein expression level during DENV replication, HEK293 cells were infected with DENV at M.O.I. of 1 and the infected cells were harvested for real-time PCR (Section 2.3.8) and Western-blot (Section 2.5.3.2) analyses at 24 hr, 48 hr, and 72 hr post-infection. As shown in Figure 5.27 (A), the gene expression level was up-regulated from 24 hr post-infection to 72 hr post-infection as compared to mock-infected cells. This result confirmed the observation in Figure 5.23 B(i) that DENV infection resulted in up-regulation of SRP19 genes. It was interesting to note that SRP19 protein level was, on the other hand, down-regulated during DENV infection [Figure 5.27 B(i and ii)]. The SRP19 protein level increased slightly at 24 hr post-infection and then decreased significantly at 72 hr post-infection by up to 80 %. This result indicated that host cells attempted to up-regulate the expression of SRP19 gene but DENV reduced the SRP19 protein level. This revealed that over-expression of SRP19 led to reduction of virus titer in Figure 5.24.

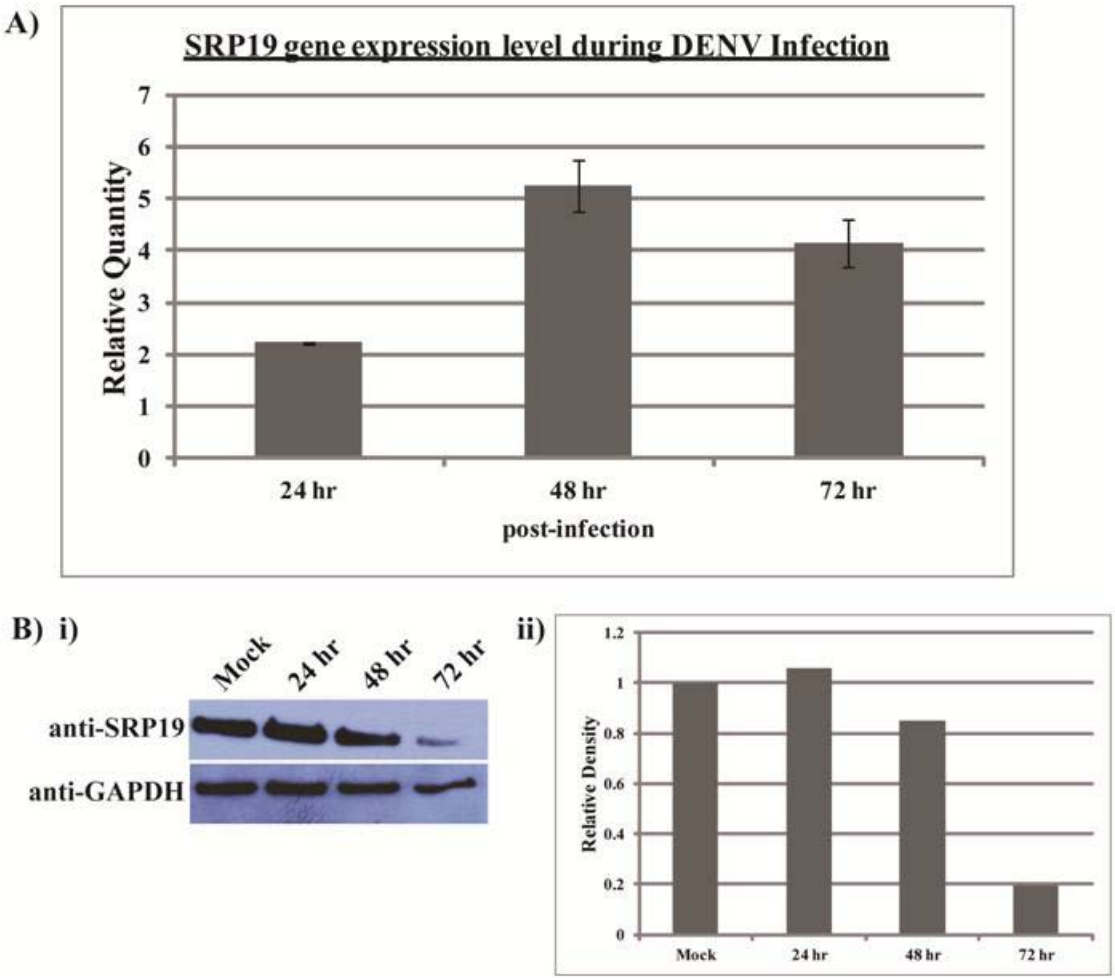

Figure 5.27: Expression of SRP19 protein during DENV infection. (A) HEK293 cells are infected with DENV at M.O.I. of 1 and at various post-infection time points, total RNA was extracted from the infected cells for real-time PCR analysis. SRP19 gene is generally up-regulated during DENV infection. The gene level increases from 24 hr to 48 hr post-infection and then decreases at 72 hr post-infection. (B) The protein expression level of SRP19 protein is detected via Western-blot (i) and the band intensity is analyzed via densitometry using ImageJ software (ii). After normalization with GAPDH loading control, SRP19 protein expression level increases slightly at 24 hr post-infection and then decreases from 48 hr to 72 hr post-infection.

The results so far implicated that SRP19 protein inhibited DENV replication. To examine whether SRP19 protein affects the viral RNA replication, real-time PCR (Section 2.3.8) was carried out to detect the level of intracellular DENV RNA in the infected cells that were over-expressing SRP19 proteins. Figure 5.28 demonstrated that intracellular DENV RNA was reduced significantly in SRP19 protein over-expressed HEK293 cells. On the other hand, no significant difference in viral RNA

level was detected in SRP19 gene and scrambled knock-downed cells. Hence, excessive SRP19 protein reduced DENV RNA replication which in turn resulted in lower virus titer.

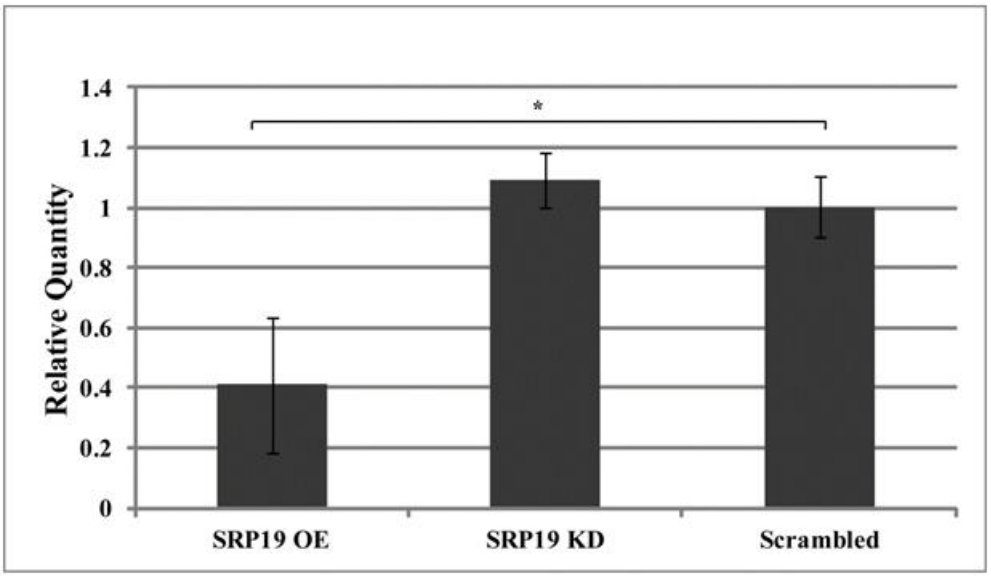

Figure 5.28: DENV RNA level in the SRP19 gene over-expressed and knock-downed HEK293 cells. HEK293 cells over-expressing SRP19 protein are infected with DENV and at 24 hr post-infection, viral RNA was extracted from the infected cells for real-time PCR analysis. SRP19 gene and scrambled knock-downed HEK293 cells are included as negative controls. Intracellular DENV RNA is reduced to approximately 60 % in SRP19 over-expressed cells whereas no difference is observed for both SRP19 gene and scrambled knock-downed cells. *p-value < 0.05

Since SRP19 protein inhibited DENV replication, it is possible that DENV attempts to counter this effect through the action of DENV C protein in the nucleolus. Newly synthesized DENV C protein translocated into nucleolus to reduce SRP19 protein level, thereby nullifying the effect of SRP19 protein creating a conducive environment for virus replication. To investigate this hypothesis, HEK293 cells were transfected with DENV C plasmid (Section 2.3.6) and Western-blot (Section 2.5.3.2) was carried out to detect the level of SRP19 protein at 24 hr post-transfection.

As shown in Figure 5.29 A(i), the SRP19 protein band intensity was much lower in DENV C-transfected cells as compared to mock-transfected cells.

Densitometry analysis revealed that the SRP19 protein level was reduced to approximately 60 % [Figure 5.29 A(ii)]. To measure the level of SRP19 protein in the whole cells lysates, transfected cell lysates were coated onto 96-well plate and anti-SRP19 antibody was used to detect the presence of SRP19 protein. The absorbance was then normalized with housekeeping protein, glyceraldehydes 3-phosphate dehydrogenase (GAPDH). Figure 5.29 (B) showed that SRP19 protein was indeed reduced significantly in the DENV C-transfected cells as compared to mock-transfected cells. Co-immuno precipitation (Co-IP) was also carried out to examine if the degradation of SRP19 protein was due to the direct interaction with DENV C protein. Figure 5.29 (C) demonstrated that DENV C protein was pulled down together with SRP19 protein, implicating that DENV C protein degraded SRP19 protein via direct interaction.

In summary, excessive SRP19 protein resulted in decreased DENV viral RNA and thus caused lower virus production. Hence, one of the non-structural roles of DENV C protein in the nucleolus was to counter the effect of SRP19 protein by degrading the protein through direct interaction.

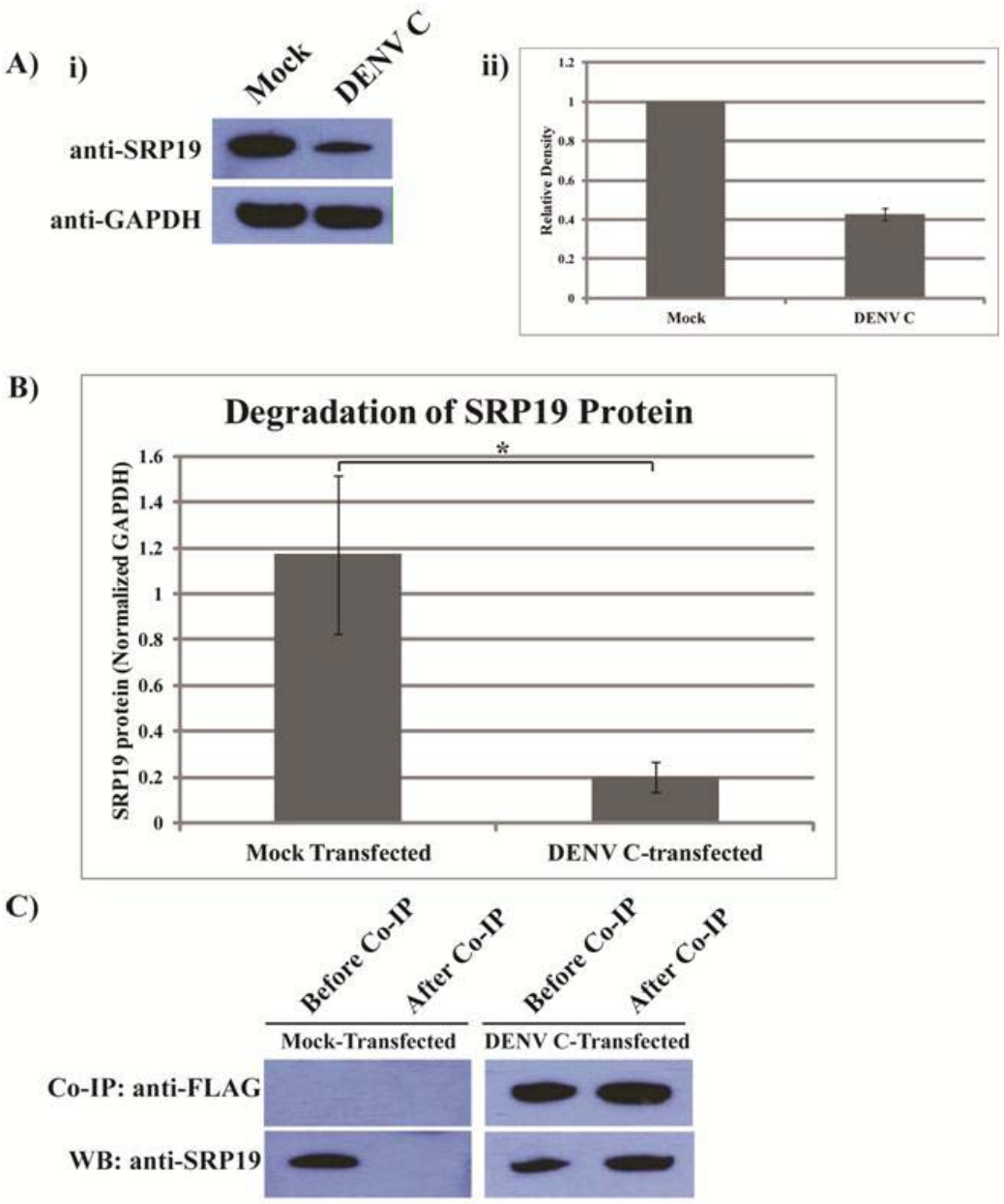

Figure 5.29: Degradation of SRP19 protein by DENV C protein. (A) HEK293 cells are transfected with DENV C protein and the level of SRP19 protein at 24 hr post-transfection is detected via Western-blot (i). As compared to mock-transfected cells, significant reduction in SRP19 protein band intensity is observed for DENV C-transfected cells. Densitometry analysis (ii) is performed using ImageJ software and normalized with GAPDH loading control. As compared to mock-transfected cells, SRP19 protein level is reduced to approximately 60 %. (B) ELISA is also carried out to quantitate the level of SRP19 protein in the whole cell lysates. SRP19 protein is reduced significantly in the DENV C-transfected cells (P=0.004). (C) Co-immuno precipitation (Co-IP) is carried out to pull-down FLAG-tagged DENV C protein and the presence of SRP19 protein is detected using anti-SRP19 antibody via Western-blot (WB). A band corresponding to SRP19 protein can be observed in the DENV C protein-transfected cells after Co-IP, indicating that there is a direct interaction between DENV C and SRP19 proteins. *p-value < 0.05

6. Discussions

The single, positive-stranded RNA genome of flavivirus encodes for three structural proteins and seven non-structural proteins. It is not surprising that flavivirus employs a sophisticated method to overcome its limited genomic information constraint by having multifunctional viral proteins. With those multifunctional viral proteins, flavivirus can hijack the host cellular components and manipulate host intracellular or even extracellular environment to establish its infection within its host. Dengue virus (DENV) capsid (C) protein is a viral structural protein that performs multifunctional roles during virus replication and pathogenesis. Understanding the non-structural roles of DENV structural C protein will help to uncover the missing puzzle of the underlying molecular mechanism of DENV replication. Only by stitching all these missing pieces together, novel antiviral strategies can be rationally designed.

The main function of DENV structural C protein is to bind to progeny DENV RNA genome, homo-oligomerize, and assemble into spherical cage-like nucleocapsid. Even though DENV C protein is the first viral protein synthesized, its structural role is only required during virus assembly which is at the late phase of virus life cycle. Therefore, it is not surprising that DENV C proteins will have other functions to perform before the assembly stage.

One such non-structural function was the translocation of DENV C proteins into the nuclei. Lad and colleagues (1993) demonstrated that replication of DENV and West Nile virus (WNV) was negatively affected in the enucleated cells (cells without nuclei). Bhuvanakantham and co-workers (2009) further illustrated that abolishment of nuclear localization signal (NLS) of WNV C protein halted viable virus production.

This confirmed the importance of the presence of flavivirus C protein in the nucleus. Nonetheless, the exact mechanism of nuclear translocation of DENV C protein and its roles in the nucleus have yet to be clearly unravelled. The findings from this project have delineated the molecular mechanism of nuclear translocation of DENV C protein and uncovered some of the potential non-structural roles of C protein in the nucleus.

The results confirmed that DENV C proteins indeed localized in the nuclei / nucleoli of transfected cells, independent of other viral proteins (Figures 3.2-3.4). However, it was discovered that not all the DENV C proteins were required to translocate into the nucleus (Figures 3.5-3.7). It is possible that only sub-molar quantity of DENV C protein is sufficient to carry out its non-structural roles in the nucleus.

Two bipartite NLS motifs (residues 5-22 and 85-100) in DENV C protein were proven to be functional (Figure 3.14). It is not surprising that DENV C protein needs more than one functional NLS motif to ensure efficient nuclear import of DENV C proteins. Suzuki and co-workers (2005) showed that Hepatitis C virus (HCV) C protein contained a non-classical NLS motif which comprised three basic-residue clusters of which at least two out of three were required for efficient nuclear translocation. The nucleoprotein (NP) of Influenza A virus, a negative-stranded RNA virus, also contained two functional NLS motifs for the nuclear import of NP proteins (Wu *et al.*, 2007).

In this study, amino acid residues from 97 to 100 of bipartite NLS2 motif was found to be the most crucial residues for nuclear localization of DENV C protein while bipartite NLS1 motif (residues 5-22) enhanced the nuclear translocation ability (Figures 3.17-3.21). One of the advantages of this study as compared to Wang and

colleagues (2002) is that site-directed mutagenesis was performed instead of truncation of the protein. This is because site-directed mutagenesis can minimize the negative impact on the protein folding and also pinpoint the exact amino acid residues that are crucial for nuclear translocation of DENV C proteins.

In addition, this finding also resolved the discrepancy of the published results by Mori and colleagues (2005). It was proven that mutation on residues 42 and 43 did not completely abolish the nuclear localization of DENV C protein (Figures 3.17 and 3.18) as claimed by Mori and colleagues (2005). Ward and Davidson (2007) also supported that the nuclear localization of DENV C protein was not completely abrogated when the residues 42 and 43 were mutated to alanine in an infectious clone. However, mutations on these residues did affect virus yield. The actual reason why these residues are important for virus production has yet to be answered. One reason could be that residues 42 and 43 are in the linker region connecting two α-helices (α1 and α2) as shown in Figure 6.1. Hence, mutations on these two residues may affect the structure of C protein which in turn disrupt virus assembly event.

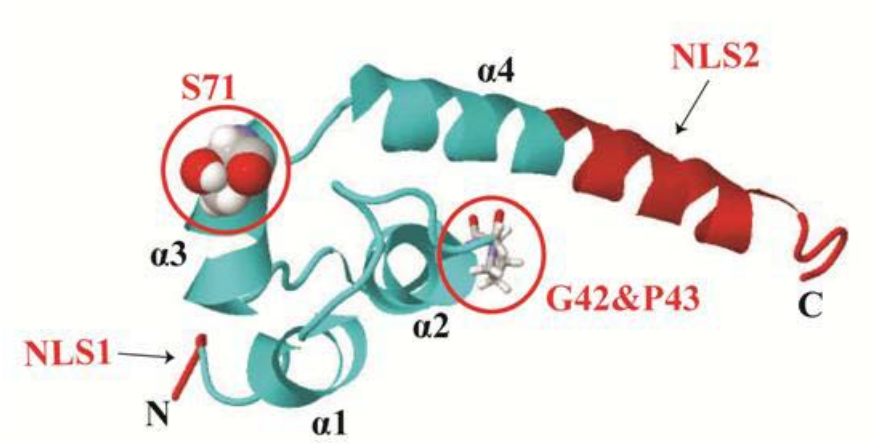

Figure 6.1: Positions of NLS1, NLS2 motifs, residues S71 and G42&P43 in DENV C protein. Protein image is reproduced by Rasmol (http://rasmol.org/) using 1R6R.pdb file from Research Collaboratory for Structural Bioinformatics (RCSB) Protein Data Bank website (http://www.rcsb.org/). It only shows residues from 21 to 100. Both NLS1 and NLS2 motifs are highlighted in red. Residue 71 is shown in space-filled form while residues 42 and 43 are shown in ball-and-stick representation. This diagram is modified from Ma and colleagues' publication **(2004).**

Similar to WNV C protein (Bhuvanakantham *et al.*, 2009), this project demonstrated that there was a direct binding between DENV C protein and importin-α protein but not with importin-β protein (Figure 3.23). Importin-α protein has two separate NLS binding sites, namely major and minor sites (Fontes *et al.*, 2000). Co-immunoprecipitation (co-IP) and mammalian-2-hybrid (M2H) assay indicated that the whole NLS2 motif of DENV C protein was the main binding site for the interaction with importin-α protein while NLS1 motif was important to enhance this binding (Figures 3.24 and 3.27). Requirement of two NLS motifs for efficient binding to importin-α protein was also reported in other viruses such as simian immunodeficiency virus (SIV). Translocation of Vpx protein of SIV into nucleus involved interaction between importin-α protein and two NLSs (amino acid residues 20-40 at N-terminus and residues 65-75 at C-terminus) in Vpx protein (Singhal *et al.*, 2006).

It is known that phosphorylation is involved in regulating the binding between importin-α protein and NLS-bearing proteins (Fontes *et al.*, 2003). Further investigation in this study showed that protein kinase C (PKC) was important for the translocation of DENV C protein into nucleus (Figure 3.30). It was also demonstrated that residue 71 of DENV C protein, which was shown in space-filled form in Figure 6.1, located in the middle of NLS1 and NLS2 motifs, was the phosphorylation site for nuclear translocation of DENV C protein (Figure 3.29). This finding is similar to WNV C protein as reported by Bhuvanakantham and colleagues (2010) and other viruses such as Hepatitis B virus (HBV). Kann and colleagues (1999) showed that only phosphorylated core particles of HBV can bind to importin-α and importin-β proteins for nucleus import. As such, phosphorylation is a common regulator for nuclear transportation of viral proteins.

A model for the molecular mechanism of nuclear translocation of DENV C protein is summarized in Figure 6.2. First, newly synthesized DENV C protein is phosphorylated by PKC at residue 71. The phosphorylated C protein is then recognized by importin-α protein that binds to C protein at bipartite NLS2 motif (residues 85-100). Bipartite NLS1 motif (residues 5-22) enhances the binding between DENV C protein and importin-α protein. Following that, importin-β protein binds to the importin-α protein and brings the whole complex into the nucleus.

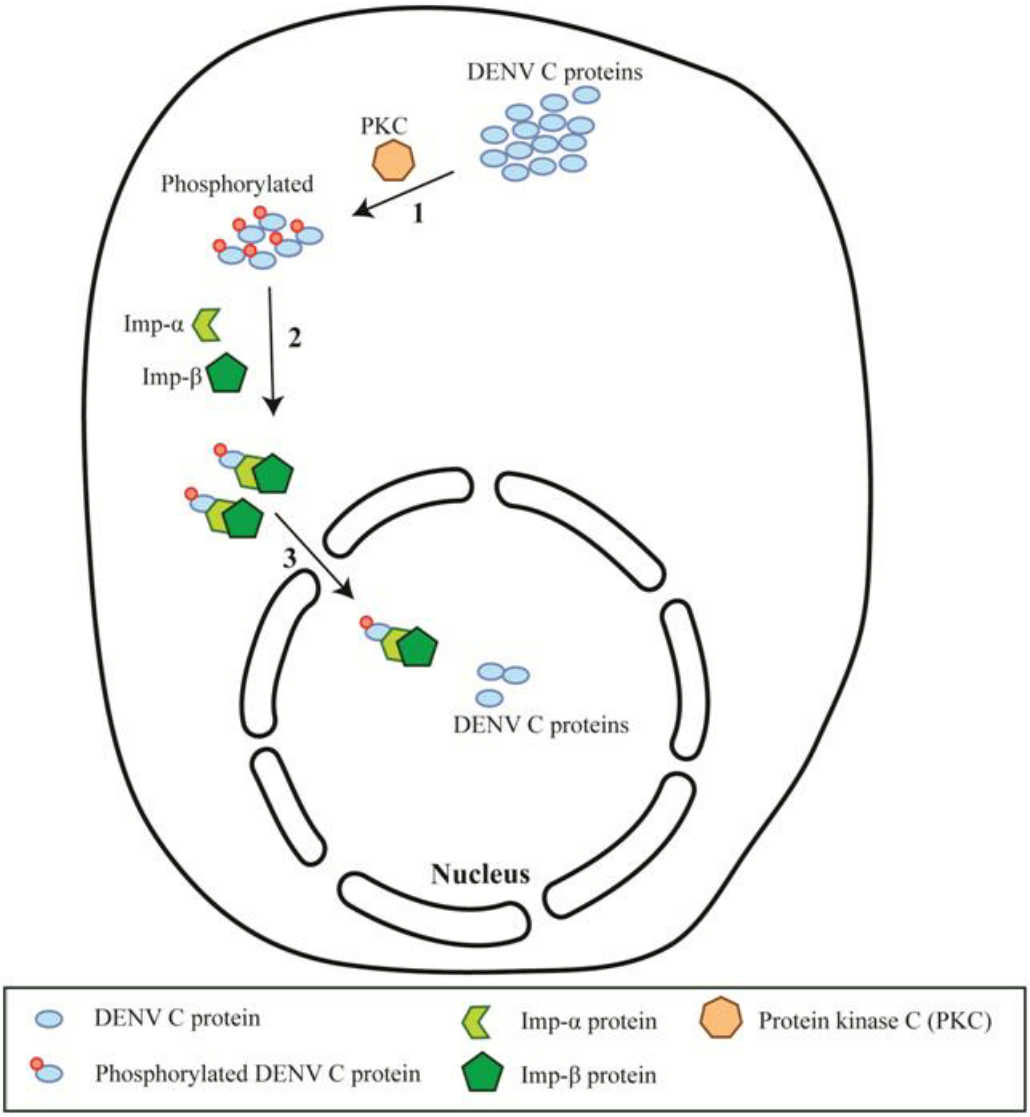

Figure 6.2: Model of transportation mechanism of DENV C protein into nucleus. 1. DENV C protein is phosphorylated by protein kinase C at amino acid residue 71. **2.** Phosphorylated form of C protein is recognized by importin-α protein which is recognized by importin-β protein. Importin-α protein binds directly to phosphorylated C protein at NLS2 motif and NLS1 motif enhances the binding. Importin-β protein binds to importin-α protein. **3.** Importin-β brings the whole complex into the nucleus.

Alanine substitution mutagenesis of DENV infectious clone at residues 97-100 of DENV C protein demonstrated that no viable virus was produced when nuclear localization ability of DENV C protein was abolished (Figure 3.22). Hence, this substantiated the fact that nuclear phase of C protein during DENV replication was a crucial event. Thus, this project continued to decipher more roles of DENV C protein in the nucleus and several important non-structural roles of DENV C protein were uncovered.

High-throughput protein microarray screening using ProtoArray® platform identified 31 novel interacting partners of DENV C protein, among which 17 of them localized in the nucleus (Table 5.2 and Figure 5.5). The high-throughput screening method employed in this study allowed identification of direct protein-protein interaction in a robust and cost-effective manner. All 9400 proteins can be screened within one day without any additional cloning steps or cultivation of micro-organism. This robust technology is employed to map protein-protein interactome for better understanding or discovery of novel pathways in diseases (Fenner *et al.*, 2010; Virok *et al.*, 2011).

Nevertheless, it is noted that not all the known protein are available in the ProtoArray® platform. Some proteins contain several isoforms but not all of them are available in this platform. This is understandable because some proteins are not easily expressed and purified. Although there are five isoforms of importin-α proteins available in the ProtoArray® platform, importin-α protein that was identified to be the transporting partner of DENV C protein (Figure 3.23) was not picked up by this ProtoArray® platform. One of the possible reasons is that phosphorylation is required for the binding between DENV C protein and importin-α proteins. Therefore, non-phosphorylated recombinant DENV C protein was not able to bind to importin-α

proteins in the ProtoArray® platform. Although this ProtoArray® technology is not able to reflect the controlled event of protein-protein interaction inside the cell, direct interaction between DENV C protein and human proteins can be identified easily in this platform. Screening of more than 9000 human proteins in one protein microarray is considered one of the highest end technologies available to date. It is a very useful technology for the first screening to identify potential interacting partners that have direct binding with DENV C protein.

Although the obtained potential interactors are novel, most of the interactors do cluster into important pathways or processes that involved flavivirus C protein (Figure 5.4). For instance, protein interactors such as CTTN, WIPF1, SLAIN2, and MAP2 proteins are pertaining to cytoskeleton organization (Figure 5.4). DENV C protein may help in the virus budding during maturation by promoting actin polymerization and regulating microtubule organization via interaction with these potential interactors. CTTN and WIPF1 are important regulators controlling the organization of actin cytoskeleton whereas SLAIN2 and MAP2 are involved in microtubule organization. It was reported that maturation of flavivirus was associated with rough endoplasmic reticulum (ER), vesicles and convoluted smooth membranes, followed by virus egression from vacuolar lumen through exocytosis (Hase *et al.*, 1987; Ng, 1987). Chu and co-workers also demonstrated that WNV C protein and E protein bound to actin filament and microtubule during virus maturation (Chu & Ng, 2002; Chu *et al.*, 2003). Thus, ProtoArray® was able to uncover protein interactors that may be involved during the maturation and egression of flavivirus.

Besides, CACNB1 and KCTD18 which are involved in regulating calcium and potassium ions transport were also identified as potential DENV C protein-binding partners. It was reported that mature DENV C protein interacted with lipid droplets

(LD) in the cytoplasm to provide a scaffold for genome encapsidation during assembly and this C protein-LD interaction was potassium ion dependent (Carvalho *et al.*, 2012; Samsa *et al.*, 2009). Hence, DENV C protein might manipulate intracellular potassium ions via direct interaction with KCTD18 channels. Other putative interacting partners of DENV C protein were associated with metabolic processes (CHKA and SAT2), B cell activation (IGBP1), activation of synapse (CAMK2A and PCLO) and signaling pathway activation (PRKCI). Among all these putative interacting partners, SAT gene was reported to be up-regulated during WNV infection in A172 brain cells (Koh & Ng, 2005). Thus, flavivirus C protein could be attributed to this gene up-regulation.

DENV C protein localized predominantly in the nucleoli of infected cells. Therefore, it is deemed that DENV C protein might be associated with ribosomal biogenesis in the nucleolus to promote viral protein synthesis. Nucleolus is involved in a number of cellular mechanism including ribosomal rRNA synthesis, ribosomal biogenesis, gene silencing, senescence and cell cycle regulation (Olson *et al.*, 2002). DENV C protein of other positive-stranded RNA virus such as Semliki Forest virus (SFV) was shown to be associated with 60S ribosomal subunit to promote assembly and uncoating of nucleocapsid during infection (Singh & Helenius, 1992; Ulmanen *et al.*, 1976).

Nucleopcapsid of porcine reproductive and respiratory syndrome virus (PRRSV) was demonstrated to interact with small nucleolar RNA (snoRNA)-associated protein fibrillarin that is involved in pre-ribosomal RNA processing in the nucleolus (Yoo *et al.*, 2003). HCV was also shown to enhance ribosomal RNA transcription through the action of NS5A protein to activate upstream binding factor (UBF) in the nucleolus (Raychaudhuri *et al.*, 2009).

The findings from this project revealed that over-expression and knock-down of DIMT1 gene, which is involved in ribosomal RNA synthesis, did not affect DENV production. Interestingly, over-expression of SRP19 protein was shown to reduce DENV replication (Figure 5.24). SRP19 protein (144 amino acids) is one of the main components of SRP ribonucleoprotein complex that recognizes and targets specific proteins to the endoplasmic reticulum (ER) (Walter *et al.*, 1981). Ribonucleoprotein complex contains a 300-nucleotide length 7SL RNA and one or more SRP proteins, namely SRP-9, -14, -19, -54, -68, and -72 (Grudnik *et al.*, 2009). SRP19 binds to the signal peptide of newly synthesized proteins and targets the synthesizing proteins together with ribosomes to the translocon (protein translocation channel in the ER membrane) via the interaction with SRP receptor (Lutcke, 1995; Maity *et al.*, 2006; Walter *et al.*, 1981). Such binding between SRP19 and synthesizing protein complex leads to protein elongation arrest (Walter & Blobel, 1983). Once the whole complex is translocated into ER lumen, SRP19 will be released from the receptor and ribosomes via guanosine triphosphate (GTP) hydrolysis and protein synthesis will resume (Grudnik *et al.*, 2009; Rapiejko & Gilmore, 1992).

During DENV infection, it was demonstrated that SRP19 gene expression was up-regulated but the protein level was reduced (Figure 5.27). Hence, it implied that host cell attempted to up-regulate SRP19 gene to form more ribonucleoprotein complexes. However, excessive SRP19 protein reduced DENV RNA replication resulting in lower virus titer (Figure 5.28). To encounter this effect, DENV degraded SRP19 protein level via DENV C protein direct interaction in the nucleolus. The interplay between DENV C protein and SRP19 protein is portrayed in Figure 6.3.

Another main category of the identified interacting partners of DENV C protein is involved in cell cycle control (Figure 5.4). Cell cycle is a series of events tightly

regulated for the survival of cells, including detection of DNA damage, DNA repair, cellular response to stress, invasion of pathogens and uncontrolled cell division. Investigation revealed that both DENV and WNV infections arrested HEK293 and BHK cells in S-phase (Figures 5.7-5.11). This cell cycle arrest was shown to be attributed to DENV C protein (Figure 5.15). Besides, it was also shown that G1-phase was not favourable for DENV replication because arresting host cell at G1-phase affected DENV replication significantly (Figure 5.14). The S-phase arrest phenomenon was also reported in other viruses such as infectious bronchitis virus (IBV) in H1299 and Vero cells (Li *et al.*, 2007). S-phase is the point where DNA replication occurs during cell cycle. Hence, the results implied that flaviviruses may alter host cell cycle to promote favourable micro-environment for virus replication.

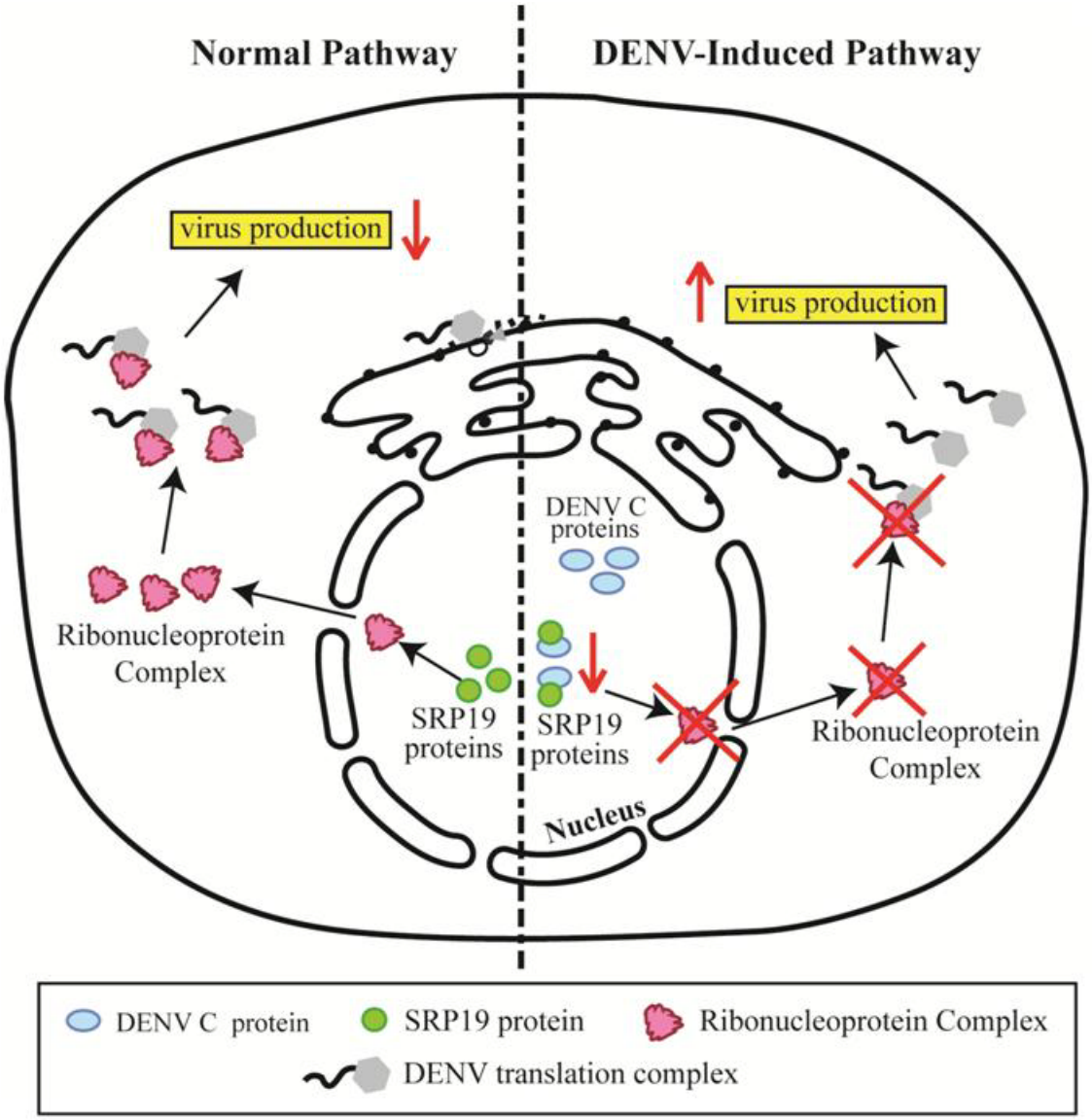

Figure 6.3: Model depicting the role of SRP19 and DENV C proteins during DENV replication. In normal circumstance, SRP19 protein facilitates the formation of ribonucleoprotein complex which will translocate into cytoplasm to direct translating protein to the rough endoplasmic reticulum. However, high level of SRP19 protein causes decrease in viral RNA replication, resulting in reduced virus production. To counteract the effect of ribonucleoprotein complex formation, DENV C protein in the nucleolus binds to and degrades SRP19 protein (DENV-induced pathway), resulting in reduced ribonucleoprotein complex formation. DENV protein synthesis and RNA replication are not interrupted and thus increases virus production.

Scholle and co-workers (2004) demonstrated that viral RNA synthesis was enhanced in the S-phase of HCV-infected Huh-7 cells. Other than enhancing viral RNA production, membrane biosynthesis was also shown to be increased during S-

phase in mammalian cells (Jackowski, 1996). As cellular membranes are essential for the replication of flaviviruses by providing surfaces for viral translation, RNA replication and viral assembly (Gillespie *et al.*, 2010; Lindenbach *et al.*, 2007; Nakano *et al.*, 2009), DENV and WNV may arrest mammalian cells at S-phase to increase the accumulation of membrane phospholipids which subsequently enhance the viral replication and assembly.

Other than S-phase arrest, it was also noticed that significant amount of DENV-infected HEK293 cells (Figure 5.8) and WNV-infected BHK cells (Figure 5.11) were arrested at G2- / M-phase as compared to mock-infected cells. In fact, G2- / M-phase arrest was also found in other related viruses. For instance, Honda and colleagues (2000) showed that G2- / M-phase arrest promoted HCV viral protein translation through internal ribosome entry sites (IRESs)-dependent manner. By doing so, cell growth would be delayed to allow sufficient time for virus production.

Flavivirus-induced cell cycle arrest appeared to be cell line specific. DENV-infected C6/36 cells were arrested at G2- / M-phase instead of S-phase (Figure 5.12). However, infection with wild-type WNV showed no significant cell cycle arrest in C6/36 cells (Figure 5.9). The different effect of DENV infection on mammalian and mosquito cells could be due to the accessibility of different cell cycle components in the cells. Sinarachatanant and Olson (1973) reported that replication of DENV was different in C6/36 cells compared to rhesus monkey kidney cells. Additionally, differences in viral protein processing were also observed in DENV-2-infected Vero and C6/36 cells (Smith & Wright, 1985). The results also showed that cell cycle arrest does not only vary among different cell lines, but also among different viruses within the same family. This could be due to the evolutionary adaptation of DENV and WNV in different cell lines. Hence, different mechanisms are adopted by the viruses

to establish their infections in different hosts. This may explain the different extent of infectivities of DENV and WNV in different cell lines and possibly different target organs in human infections.

Different viral proteins were reported attributable to the cell cycle arrest for different positive-stranded RNA viruses. HCV, for instance, was shown to promote cell growth through the action of NS5A protein to suppress the transcription of cdk inhibitor, $p21^{WAF1}$gene (Ghosh *et al.*, 1999). Nucleocapsid of Coronavirus was demonstrated to inhibit S phase progression in mammalian cells by binding to the cyclin-cyclin dependent kinase (cdk) complex (Surjit *et al.*, 2006). The findings from this project demonstrated that DENV C protein promoted cell cycle progression to S- and G2- / M-phases through direct interactions with CCNB3, CHES1 and GADD45A proteins as illustrated in Figure 6.4.

DENV C protein bound to cyclin B3 (CCNB3) that was associated with cdk2 kinase resulted in S phase progression. CCNB3 or cyclin B3 is a regulatory subunit of cyclin-dependent kinase 2 (CDK2) protein which is essential for cell cycle progression from G1 to S phase (Nguyen *et al.*, 2002). The gene level of CCNB3 was also found to be up-regulated during DENV infection (Figure 5.17). However, PCR array data showed that host cells attempted to counter this cell cycle progression by up-regulating CDKN2B which is a CDK inhibitor that prevents cell cycle G1 progression by interrupting the binding of cyclin D to CDK4 or CDK6.

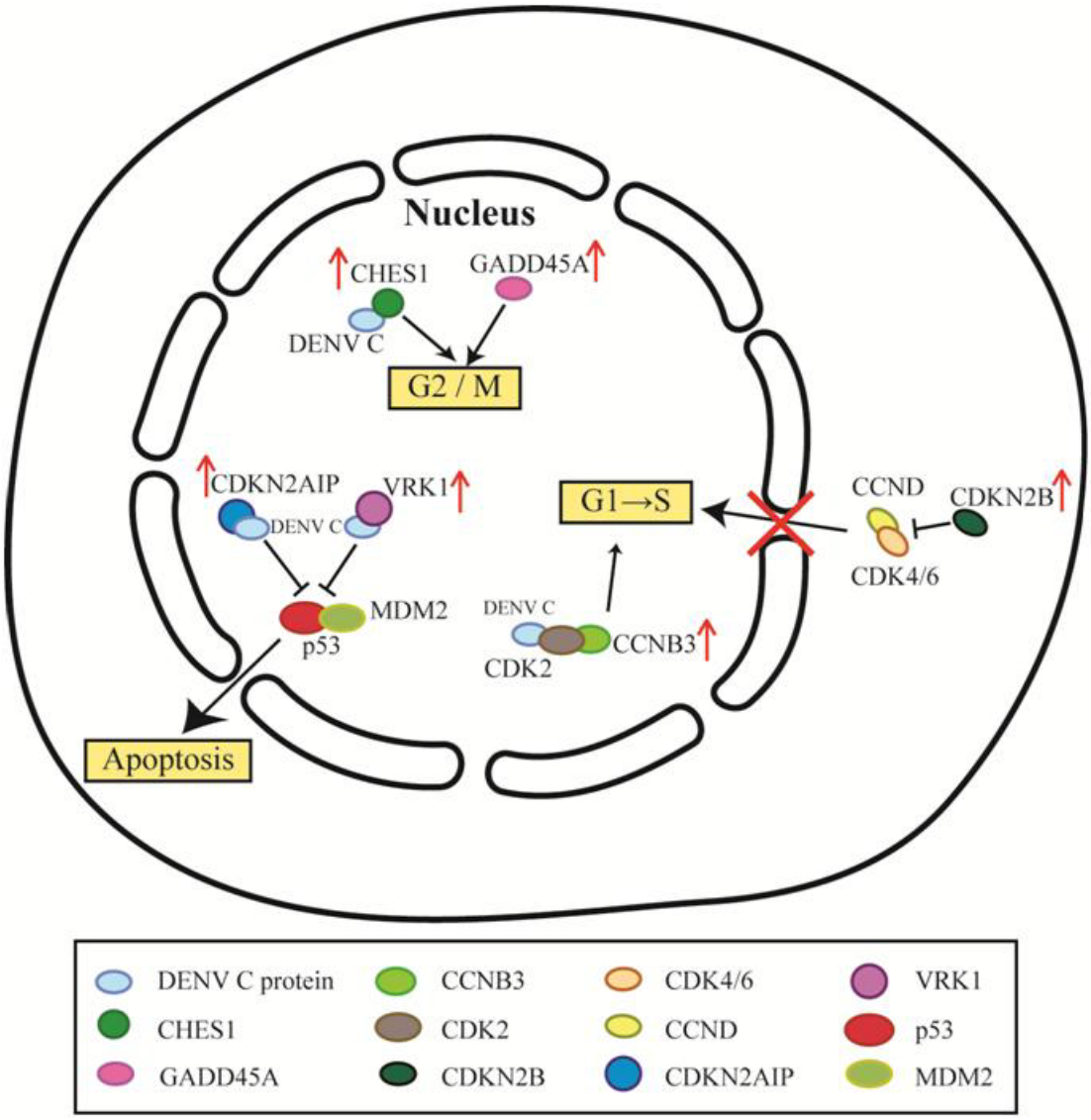

Figure 6.4: The role of DENV C protein in cell cycle control and apoptosis. Although host up-regulates CDKN2B to prevent S-phase entry, DENV C protein in the nucleus interacts with CCNB3 to promote cell cycle progression from G1-phase to S-phase. S-phase is more favourable for DENV replication. CHES1 and GADD45A are also up-regulated to arrest cell cycle at G2- / M-phase. Besides, DENV C protein binds to CDKN2AIP and VRK1 proteins, resulting in p53-dependent apoptosis.

DENV did not target on CCNB3 protein only to achieve S-phase progression, it also up-regulated CHES1 and GADD45A to arrest cell cycle at G2- / M-phase as observed in Figures 5.8 and 5.11. GADD45A gene is a main regulator of p38/JNK pathway, mediating G2- / M-phase checkpoint in response to environmental stress via p53-dependent and -independent mechanisms (Rosemary Siafakas & Richardson,

2009) while CHES1 or FOXN3 is involved in cell cycle checkpoint at G1- and G2-phase in response to DNA damage (Busygina *et al.*, 2006).

Despite all the evidence showing the interaction of virus with host cell cycle, it is worth noting that cell cycle arrest could also be induced in response to cellular stress. Under cellular stress, p53 will be activated and induce cell cycle arrest or apoptosis (Harper & Brooks, 2006; Hiscox, 2007; Suzuki *et al.*, 2012). It is possible that the cell cycle arrest is the downstream effect of virus infection rather than the direct effect of virus-host interaction.

However, it is still controversial as to whether DENV C protein induces apoptosis or prevents apoptosis for its own benefits. DENV C protein was reported to induce apoptosis (Limjindaporn *et al.*, 2007; Netsawang *et al.*, 2010) and WNV C protein was shown to induce apoptosis by sequestrating HDM2 to stabilize p53 (Bhuvanakantham *et al.*, 2010; Yang *et al.*, 2008). On the other hand, there was also report indicating that DENV C protein subverted apoptotic event to favour virus production by manipulating cyclophilin-binding ligand (CAML) level via direct interaction (Li *et al.*, 2012). Thus, the advantage of activating p53 by flavivirus C protein still remains disputable.

Some of the identified DENV C protein interactors were related to p53 pathway and apoptosis. CDK2AIP and VRK1, for instance, are known to activate p53 by perturbing the interaction between p53 and MDM2. Hence, DENV C protein may induce apoptosis by stabilizing p53 through direct interaction with CDK2AIP and VRK1 proteins which in turn sequestrated MDM2 protein resulting in p53-mediated apoptosis as reported by Bhuvanakantham and colleagues (2010). Both CDK2AIP and VRK1 genes were found also to be up-regulated during DENV infection (Figure

5.17). The role of DENV C protein in causing p53-mediated apoptosis through direct interaction with CDK2AIP and VRK1 proteins was also illustrated in Figure 6.4.

In this study, ubiquitin-conjugating enzyme (UBE2S) was also shown to be the potential interacting partner of DENV C protein (Figure 5.4). Ubiquitin-proteasome pathway was reported to be crucial biological process for DENV infection (Kanlaya *et al.*, 2010). It was demonstrated that ubiquitin-activating enzyme E1 (UBE1) was up-regulated in the infected HUVEC cells and inhibition of this enzyme affected viral protein synthesis. The significant of ubiquitin-proteasome pathway for flavivirus genome amplification was also supported by Fernandez-Garcia and co-workers (2011). However, Nag and Finley (2012) illustrated that enhancing the proteasome activity by inhibiting proteasome-associated deubiquitinating enzyme USP14, reduced DENV propagation. As such, the association between ubiquitin-proteasome pathway and flavivirus replication is still unclear and warrants further investigation.

Taken altogether, this study unravelled the transportation mechanism of DENV C protein into nucleus and delineated the non-structural roles of DENV C protein in the nucleus. A summary on the mechanism of DENV C protein nuclear translocation and its non-structural functions is provided in Figure 6.5.

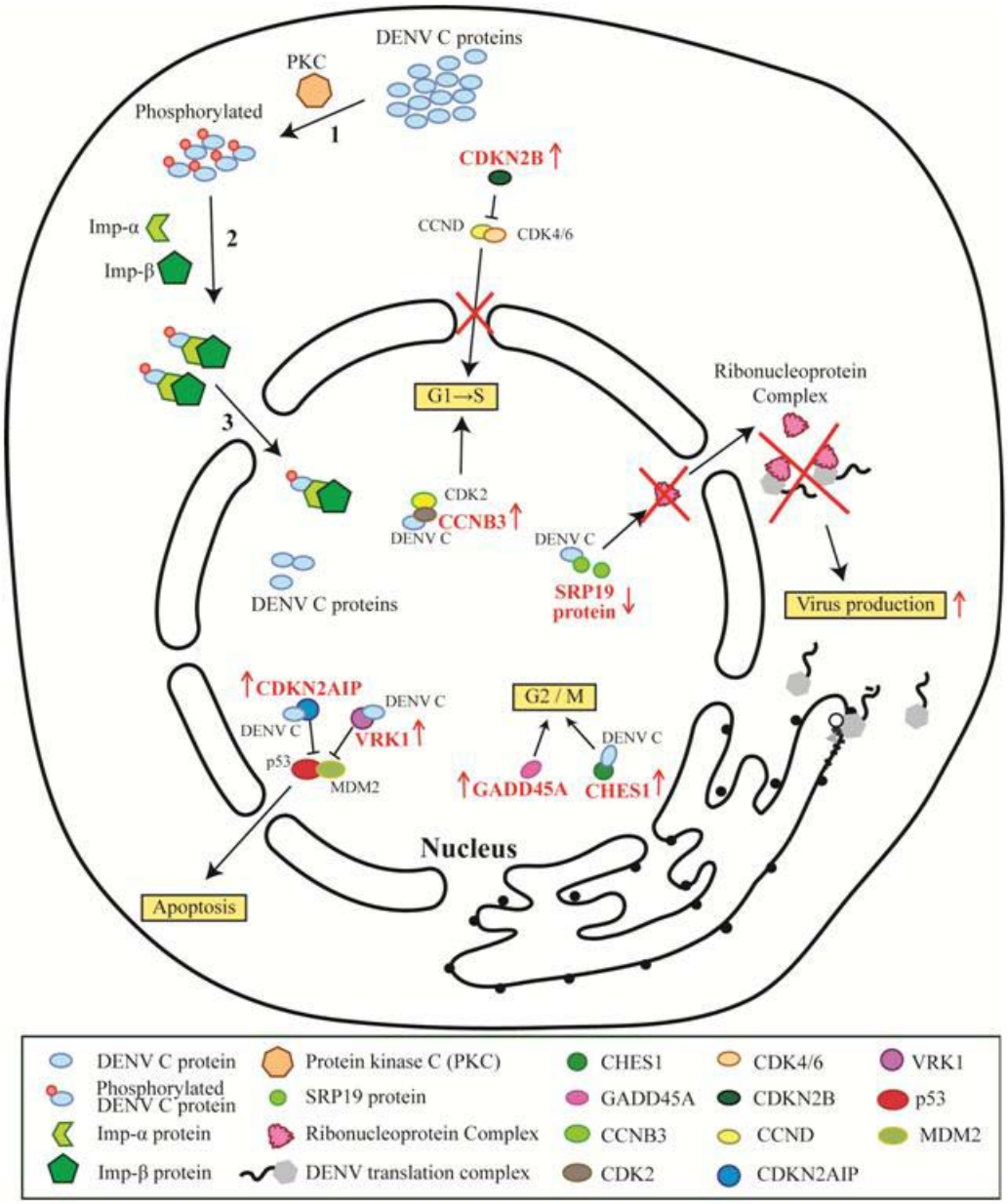

Figure 6.5: Model depicting the nuclear translocation mechanism of DENV C protein and its non-structural roles in the nucleus. 1. DENV C protein is phosphorylated by protein kinase C (PKC) at residue 71. **2.** Importin-α protein can recognize phosphorylated DENV C protein and bind to the C protein at NLS2 motif. NLS1 motif of DENV C protein enhances the binding with importin-α protein. **3.** Importin-β protein binds to importin-α protein and brings the whole complex into the nucleus. In the nucleus, DENV C protein carries out several non-structural functions. It binds to SRP19 protein and causes diminishing level of SRP19 proteins. As a result, SRP19 cannot facilitate the formation of ribonucleoprotein complex that causes decrease in virus production. DENV C protein also plays an important role to arrest host cell cycle at S- and G2- / M-phases to favour virus replication. Host cell attempts to prevent S-phase entry by up-regulating CDK inhibitor, CDKN2B protein. However, DENV C protein counters this effect through direct interaction with CCNB3 to promote cell cycle progression from G1- to S-phase. In addition, DENV C protein also binds to CHES1 and GADD45A protein to promote further cell cycle progression from S- phase to G2- / M-phase. DENV C protein also induces p53-dependent apoptosis via direct interaction with CDKN2AIP and VRK1 proteins.

Other than discovering the non-structural roles of DENV C protein in the nucleus, an optimized protocol to engineer, express and purify the biotinylated, full-length DENV C protein was developed in this study. Biotinylation is a popular process in protein engineering to ease detection and purification (Chapman-Smith & Cronan, 1999; Cull & Schatz, 2000). Biotinylated hemagglutinin, for instance, was generated to develop a subtype-specific serological assay to diagnose influenza A virus in patients' sera (Postel *et al.*, 2011). One of the advantages of using biotinylated protein is that the detection sensitivity of the biotinylated protein is greatly enhanced by the high affinity and specificity between biotin and streptavidin (Bayer & Wilchek, 1990a). This advantage is exploited for techniques such as co-immunoprecipitation or library screening of interaction proteome (He *et al.*, 2009; Markham *et al.*, 2007; Moreland *et al.*, 2010). Not only that, site-specific biotinylation was also developed as a means for molecular labeling and imaging (Howarth & Ting, 2008; Sueda *et al.*, 2011). Thus, biotinylated DENV C protein generated in this study is useful for various cellular, molecular and imaging experiments because of the high detection limit while the function of the protein is still well preserved.

There are various approaches to biotinylate a protein, either chemically or enzymatically (Cull & Schatz, 2000). Various commercial kits are available in the market for chemical biotinylation by conjugating biotin molecules on proteins or antibodies that contain primary amines. However, chemical biotinylation may lead to non-specific and non-homogenous incorporation of biotin which might result in possible loss of activity of the protein (Bayer & Wilchek, 1990b). Moreover, another step of removing the excess biotin reagent will increase the chance of losing more proteins.

To produce biotinylated DENV C protein, this study opted for site-specific biotinylation by engineering a biotin acceptor signal peptide (BAP) in the upstream of DENV C proteins (Figures 4.6 and 4.7). To attach a biotin molecule onto BAP either *in vivo* or *in vitro*, bacterial biotin ligase BirA is required (Chapman-Smith & Cronan, 1999; Cull & Schatz, 2000; Tan *et al.*, 2004; Yang *et al.*, 2004). Instead of the need to perform this biotinylation step *in vitro*, it was discovered that biotinylation of the BAP-containing proteins occurred endogenously in *Escherichia coli* BL-21 strains with high efficiency (Figure 4.11). As such, other proteins that require site-specific biotinylation may be produced easily by just simple OE-PCR and expression in *Escherichia coli* BL-21 strains without the need of an additional *in vitro* biotinylation step. A provisional patent (Singapore patent application number: 201208602-1) was filed for this discovery and optimized protocol.

The expression and purification of non-truncated, full-length DENV C protein was indeed challenging. The presence of rare codons in the C protein sequence necessitates unique expression competent strain for its optimal protein expression (Figure 4.8). Due to the hydrophobic C-terminus, aggregation easily occurred and most of the expressed proteins were trapped in the inclusion bodies (Figure 4.12). As such, 8 M urea was used to denature the proteins and to perform affinity chromatography under denaturing condition. The aggregation problem during dialysis and refolding was also solved successfully by using non-ionic detergent (Section 4.3.5.3). This is indeed critical in making this protein purification a success.

Unlike domain III (DIII) protein (Tan *et al.*, 2010), one single purification step was simply not adequate to produce pure DENV C protein. To obtain highly purified DENV C protein, two more purification steps were included in the protocol, namely ion-exchange chromatography [(IEX) (Figures 4.16 and 4.17)] and size-exclusion

chromatography [(SEC) (Figure 4.18)]. This sequential purification strategy can produce approximately 1 mg of purified full-length DENV C protein from 1 L of bacterial culture. Hence, this optimized sequential purification strategy may be useful for other proteins that have the similar properties.

Purified full-length DENV C protein is useful for various molecular studies to further understand the underlying mechanism of C protein in pathogenesis. For instance, it can be used to study the interaction of NS2B-NS3 serine proteinase and C protein. In order to produce mature C protein for encapsidation and assembly, full-length C protein has to be cleaved by NS2B-NS3 protein complex. Thus, it is crucial to identify the binding sites of NS2B-NS3 complex to full-length C protein, which is still unknown. It will in turn lead to the development of novel anti-viral drugs targeting the assembly of virus particles. Besides, it is also interesting to examine whether the cleaved C-terminus plays any unidentified role in the pathogenesis. The crystal structure of DENV NS2B-NS3 protein complex has been resolved (Erbel *et al.*, 2006). However, the crystal structure of full-length DENV C protein is still not yet available, although the NMR structure of partial DENV C protein was obtained (Ma *et al.*, 2004).

Ma and co-workers (2004) proposed a model for the interaction between C protein and its viral genome using the partial DENV C protein. However, to date, this model is not validated and the exact mechanism of encapsidation is still unclear. Investigation of how DENV C protein interacts with its RNA and oligomerizes into nucleocapsid during maturation is vital for better understanding of the pathogenesis. Recent publications also demonstrated that N-terminus of DENV C protein was antigenic in mice study and the first 18 amino acid residues were involved in the virus assembly during maturation (Puttikhunt *et al.*, 2009; Samsa *et al.*, 2012). As a result,

this purified non-truncated DENV C protein is absolutely desirable for delineating the whole process of encapsidation and virus assembly.

Conclusion

Unravelling the mechanism of nuclear translocation of DENV C protein and its non-structural roles in the nucleus is important to better understand how flaviviruses establish infections in different hosts. This project has elucidated the molecular transportation mechanism and identified novel functions of DENV C proteins. Better understanding of the replication of DENV will help in the development of novel antiviral drug. For instance, drugs inhibiting the nuclear import of DENV / WNV C protein, which were shown to be essential for viral replication, can be used as an anti-viral therapy strategy. Arylene bis-(methyl ketone) compounds such as CNI-H0292 and CNI-H1194 which inhibit the nuclear import of pre-integration complex (PIC) in human macrophages and monocytes, has been used to block HIV-1 replication specifically (Dubrovsky *et al.*, 1995). These drugs are also considered to be included as one of the components in multi-drug cocktail for anti-HIV therapy (Glushakova *et al.*, 2000). Therefore, this type of drugs can also be tested for their efficacy in inhibiting flavivirus replication.

Cell cycle arrest-related drugs could also be used as anti-viral drugs. For example, chemotherapeutic agents which can arrest cell cycle at specific cell cycle phase have been used to suppress virus replication (Foli *et al.*, 2007). Hydroxyurea and mycophenolic acid were shown by Foli and colleagues (2007) to be useful to inhibit HIV-1 replication by arresting the proliferative CD4 cells at G1 phase.

Therefore, the observed findings on cell cycle arrest in this study could also contribute to the development of novel antiviral strategies for flaviviruses.

Future Direction

This project has successfully identified several non-structural roles of DENV C protein in the nucleus. Two of the most exciting potential roles of DENV C protein in the nucleus are pertaining to cell cycle control and regulation of transcriptional and translational activities. It was found that DENV tried to drive host cell cycle from G1-phase to S- and G2- / M-phases during infection because virus production was significantly reduced when host cells were arrested at G1-phase. Further investigation demonstrated that DENV C protein interacted with cyclin B3 (CCNB3), GADD45A, and CHES1 proteins to promote cell cycle progression from G1- to S-phase and from S- to G2- / M-phase. To uncover the underlying molecular mechanism behind this cell cycle manipulation, the whole profile of cyclins and cyclin-dependent kinases (cdks) expression during wild-type virus infection and over-expression of DENV C protein should be determined via quantitative real-time reverse transcription polymerase chain reaction and Western blotting. This will reveal the entire cascade of affected genes and proteins in the cell cycle signalling pathway. Hence, a more comprehensive understanding of the interplay between flavivirus C protein and cell cycle control can be obtained.

The importance of C protein-cell cycle-related protein interactions during virus replication can also be examined by performing gene silencing and over-expression studies. When host genes or proteins that are found to be inhibiting flavivirus replication are knock-downed, virus production should increase or vice

versa. These experiments should also be repeated using infectious clones carrying mutations on the bipartite NLS or phosphorylation sites that are important for nuclear translocation as negative controls to substantiate the effect of C protein in the nucleus. Truncation mapping analyses can then be performed to delineate the actual binding sites of C proteins and the interacting partners.

Another exciting non-structural role of DENV C protein in the nucleus is to manipulate host transcriptional and translational activities. Over-expression of SRP19 protein was found to reduce DENV viral RNA and virus titer. However, over-expression of DENV C protein degraded SRP19 protien via direct interaction. Hence, it is hypothesized that DENV C protein attempts to counteract the anti-viral effect of SRP19 protein by degrading it. To examine whether DENV C protein causes degradation of SRP19 protein through proteasome pathway, MG132 which is a proteasome inhibitor can be employed. Cells are treated with MG132 first for 1 hr before infection with DENV or transfection with recombinant DENV C proteins. MG132 drug should be present throughout the infection or transfection period. At 24-hr post infection or transfection, the level of SRP19 protein is quantitated via ELISA platform. To further investigating which proteasome pathway is involved in the degradation of SRP19 protein, the proteolytic activities of 20S proteasome can be examined using Proteasome-Glo cell-based assay kits for chymotrypsin-like, trypsin-like and caspase-like activities (Promega, USA).

SRP19 protein is only part of the ribonucleoprotein complex to target specific secreted protein to the ER for protein translation. Hence, the effect of ribonucleoprotein complex upon DENV replication should also be examined. Co-immuno precipitation can be carried out to pull down viral replication complex using anti-viral RNA or anti-NS1 antibodies after cross-linking. If the ribonucleoprotein

complex indeed interacts with viral replication complex, ribonucleoprotein complex should be detected in the pull-down elute using anti-H/ACA ribonucleoprotein complex antibody. The effect of over-expression of DENV C protein upon ribonucleoprotein complex level can then be examined. If SRP19 protein level is reduced by DENV C protein during infection, the level of ribonucleoprotein complex in the cytoplasm should also be decreased. If this hypothesis holds true, DENV C protein with mutations on the essential bipartite NLS motif should not affect the levels of SRP 19 proteins and ribonucleoprotein complex.

Investigating these novel non-structural roles of flavivirus C protein in the nucleus will provide better understanding of the underlying molecular mechanism of flavivirus infection. This knowledge is essential for more refinement of anti-viral drug designs and development.

References

Acosta, E. G., Castilla, V. & Damonte, E. B. (2008). Functional entry of dengue virus into *Aedes albopictus* mosquito cells is dependent on clathrin-mediated endocytosis. *J Gen Virol* **89**, 474-484.

Ada, G. L. & Anderson, S. G. (1959). Yield of infective ribonucleic acid from impure Murray Valley encephalitis virus after different treatments. *Nature* **183**, 799-800.

Alcon, S., Talarmin, A., Debruyne, M., Falconar, A., Deubel, V. & Flamand, M. (2002). Enzyme-linked immunosorbent assay specific to Dengue virus type 1 nonstructural protein NS1 reveals circulation of the antigen in the blood during the acute phase of disease in patients experiencing primary or secondary infections. *J Clin Microbiol* **40**, 376-381.

Amberg, S. M. & Rice, C. M. (1999). Mutagenesis of the NS2B-NS3-mediated cleavage site in the flavivirus capsid protein demonstrates a requirement for coordinated processing. *J Virol* **73**, 8083-8094.

Avirutnan, P., Fuchs, A., Hauhart, R. E., Somnuke, P., Youn, S., Diamond, M. S. & Atkinson, J. P. (2010). Antagonism of the complement component C4 by flavivirus nonstructural protein NS1. *J Exp Med* **207**, 793-806.

Bayer, E. A. & Wilchek, M. (1990a). Avidin- and streptavidin-containing probes. *Methods Enzymol* **184**, 174-187.

Bayer, E. A. & Wilchek, M. (1990b). Protein biotinylation. *Methods Enzymol* **184**, 138-160.

Benarroch, D., Selisko, B., Locatelli, G. A., Maga, G., Romette, J. L. & Canard, B. (2004). The RNA helicase, nucleotide 5'-triphosphatase, and RNA 5'-triphosphatase activities of Dengue virus protein NS3 are Mg2+-dependent and require a functional Walker B motif in the helicase catalytic core. *Virology* **328**, 208-218.

Bhatt, S., Gething, P. W., Brady, O. J., Messina, J. P., Farlow, A. W., Moyes, C. L., Drake, J. M., Brownstein, J. S., Hoen, A. G., Sankoh, O., Myers, M. F., George, D. B., Jaenisch, T., Wint, G. R., Simmons, C. P., Scott, T. W., Farrar, J. J. & Hay, S. I. (2013). The global distribution and burden of dengue. *Nature* **496**, 504-507.

Bhuvanakantham, R. & Ng, M. L. (2005). Analysis of self-association of West Nile virus capsid protein and the crucial role played by Trp 69 in homodimerization. *Biochem Biophys Res Commun* **329**, 246-255.

Bhuvanakantham, R., Cheong, Y. K. & Ng, M. L. (2010). West Nile virus capsid protein interaction with importin and HDM2 protein is regulated by protein kinase C-mediated phosphorylation. *Microbes Infect* **12**, 615-625.

Bhuvanakantham, R., Chong, M. K. & Ng, M. L. (2009). Specific interaction of capsid protein and importin-alpha/beta influences West Nile virus production. *Biochem Biophys Res Commun* **389**, 63-69.

Bhuvanakantham, R., Li, J., Tan, T. T. T. & Ng, M. L. (2010). Human Sec3 protein is a novel transcriptional and translational repressor of flavivirus. *Cell Microbiol* **12**, 453-472.

Bian, X. L., Rosas-Acosta, G., Wu, Y. C. & Wilson, V. G. (2007). Nuclear import of bovine papillomavirus type 1 E1 protein is mediated by multiple alpha importins and is negatively regulated by phosphorylation near a nuclear localization signal. *J Virol* **81**, 2899-2908.

Bolte, S. & Cordelieres, F. P. (2006). A guided tour into subcellular colocalization analysis in light microscopy. *J Microsc-Oxford* **224**, 213-232.

Bressanelli, S., Stiasny, K., Allison, S. L., Stura, E. A., Duquerroy, S., Lescar, J., Heinz, F. X. & Rey, F. A. (2004). Structure of a flavivirus envelope glycoprotein in its low-pH-induced membrane fusion conformation. *EMBO J* **23**, 728-738.

Brooks, A. J., Johansson, M., John, A. V., Xu, Y., Jans, D. A. & Vasudevan, S. G. (2002). The interdomain region of dengue NS5 protein that binds to the viral helicase NS3 contains independently functional importin beta 1 and importin alpha/beta-recognized nuclear localization signals. *J Biol Chem* **277**, 36399-36407.

Bulich, R. & Aaskov, J. G. (1992). Nuclear localization of dengue 2 virus core protein detected with monoclonal antibodies. *J Gen Virol* **73** (Pt 11), 2999-3003.

Busygina, V., Kottemann, M. C., Scott, K. L., Plon, S. E. & Bale, A. E. (2006). Multiple endocrine neoplasia type 1 interacts with forkhead transcription factor CHES1 in DNA damage response. *Cancer Res* **66**, 8397-8403.

Cabrera-Hernandez, A., Thepparit, C., Suksanpaisan, L. & Smith, D. R. (2007). Dengue virus entry into liver (HepG2) cells is independent of hsp90 and hsp70. *J Med Virol* **79**, 386-392.

Calisher, C. H. & Gould, E. A. (2003). Taxonomy of the virus family *Flaviviridae*. *Adv Virus Res* **59**, 1-19.

Carvalho, F. A., Carneiro, F. A., Martins, I. C., Assuncao-Miranda, I., Faustino, A. F., Pereira, R. M., Bozza, P. T., Castanho, M. A., Mohana-Borges, R. & other authors (2012). Dengue virus capsid protein binding to hepatic lipid droplets (LD) is potassium ion dependent and is mediated by LD surface proteins. *J Virol* **86**, 2096-2108.

Chambers, T. J., Hahn, C. S., Galler, R. & Rice, C. M. (1990). Flavivirus genome organization, expression, and replication. *Annu Rev Microbiol* **44**, 649-688.

Chang, G. J. (1997). Molecular biology of dengue viruses In Dengue and Dengue Hemorrhagic Fever, pp. 175-191 Edited by D. J. Gubler & G. Kuno: New York: CAB International.

Chang, Y. S., Liao, C. L., Tsao, C. H., Chen, M. C., Liu, C. I., Chen, L. K. & Lin, Y. L. (1999). Membrane permeabilization by small hydrophobic nonstructural proteins of Japanese encephalitis virus. *J Virol* **73**, 6257-6264.

Chapman-Smith, A. & Cronan, J. E., Jr. (1999). *In vivo* enzymatic protein biotinylation. *Biomol Eng* **16**, 119-125.

Chapman-Smith, A. & Cronan, J. E., Jr. (1999a). The enzymatic biotinylation of proteins: a post-translational modification of exceptional specificity. *Trends Biochem Sci* **24**, 359-363.

Chapman-Smith, A. & Cronan, J. E., Jr. (1999b). Molecular biology of biotin attachment to proteins. *J Nutr* **129**, 477S-484S.

Chen, Y. C., Wang, S. Y. & King, C. C. (1999). Bacterial lipopolysaccharide inhibits dengue virus infection of primary human monocytes/macrophages by blockade of virus entry via a CD14-dependent mechanism. *J Virol* **73**, 2650-2657.

Chen, Y., Maguire, T., Hileman, R. E., Fromm, J. R., Esko, J. D., Linhardt, R. J. & Marks, R. M. (1997). Dengue virus infectivity depends on envelope protein binding to target cell heparan sulfate. *Nat Med* **3**, 866-871.

Cheong, Y. K. & Ng, M. L. (2011). Dephosphorylation of West Nile virus capsid protein enhances the processes of nucleocapsid assembly. *Microbes Infect* **13**, 76-84.

Chu, J. J. & Ng, M. L. (2002). Trafficking mechanism of West Nile (Sarafend) virus structural proteins. *J Med Virol* **67**, 127-136.

Chu, J. J. & Ng, M. L. (2004a). Infectious entry of West Nile virus occurs through a clathrin-mediated endocytic pathway. *J Virol* **78**, 10543-10555.

Chu, J. J. & Ng, M. L. (2004b). Interaction of West Nile virus with alpha v beta 3 integrin mediates virus entry into cells. *J Biol Chem* **279**, 54533-54541.

Chu, J. J. H., Choo, B. G. H., Lee, J. W. M. & Ng, M. L. (2003). Actin filaments participate in West Nile (Sarafend) virus maturation process. *J Med Virol* **71**, 463-472.

Cologna, R., Spagnolo, J. F. & Hogue, B. G. (2000). Identification of nucleocapsid binding sites within coronavirus-defective genomes. *Virology* **277**, 235-249.

Couvelard, A., Marianneau, P., Bedel, C., Drouet, M. T., Vachon, F., Henin, D. & Deubel, V. (1999). Report of a fatal case of dengue infection with hepatitis:

demonstration of dengue antigens in hepatocytes and liver apoptosis. *Hum Pathol* **30**, 1106-1110.

Cull, M. G. & Schatz, P. J. (2000). Biotinylation of proteins *in vivo* and *in vitro* using small peptide tags. *Methods Enzymol* **326**, 430-440.

de Boer, E., Rodriguez, P., Bonte, E., Krijgsveld, J., Katsantoni, E., Heck, A., Grosveld, F. & Strouboulis, J. (2003). Efficient biotinylation and single-step purification of tagged transcription factors in mammalian cells and transgenic mice. *Proc Natl Acad Sci U S A* **100**, 7480-7485.

Dingwall, C. & Laskey, R. A. (1991). Nuclear targeting sequences--a consensus? *Trends Biochem Sci* **16**, 478-481.

Dokland, T., Walsh, M., Mackenzie, J. M., Khromykh, A. A., Ee, K. H. & Wang, S. (2004). West Nile virus core protein; tetramer structure and ribbon formation. *Structure* **12**, 1157-1163.

Dubrovsky, L., Ulrich, P., Nuovo, G. J., Manogue, K. R., Cerami, A. & Bukrinsky, M. (1995). Nuclear localization signal of HIV-1 as a novel target for therapeutic intervention. *Mol Med* **1**, 217-230.

Erbel, P., Schiering, N., D'Arcy, A., Renatus, M., Kroemer, M., Lim, S. P., Yin, Z., Keller, T. H., Vasudevan, S. G. & other authors (2006). Structural basis for the activation of flaviviral NS3 proteases from dengue and West Nile virus. *Nat Struct Mol Biol* **13**, 372-373.

Falcon, V., Acosta-Rivero, N., Chinea, G., de la Rosa, M. C., Menendez, I., Duenas-Carrera, S., Gra, B., Rodriguez, A., Tsutsumi, V., Shibayama, M., Luna-Munoz, J., Miranda-Sanchez, M. M., Morales-Grillo, J. & Kouri, J. (2003). Nuclear localization of nucleocapsid-like particles and HCV core protein in hepatocytes of a chronically HCV-infected patient. *Biochem Biophys Res Commun* **310**, 54-58.

Falgout, B., Pethel, M., Zhang, Y. M. & Lai, C. J. (1991). Both nonstructural proteins NS2B and NS3 are required for the proteolytic processing of dengue virus nonstructural proteins. *J Virol* **65**, 2467-2475.

Fenner, B. J., Scannell, M. & Prehn, J. H. M. (2010). Expanding the substantial iInteractome of NEMO using protein microarrays. *PLoS One* **5**(1):e8799

Fernandez-Garcia, M. D., Meertens, L., Bonazzi, M., Cossart, P., Arenzana-Seisdedos, F. & Amara, A. (2011). Appraising the roles of CBLL1 and the ubiquitin/proteasome system for flavivirus entry and replication. *J Virol* **85**, 2980-2989.

Foli, A., Maiocchi, M. A., Lisziewicz, J. & Lori, F. (2007). A checkpoint in the cell cycle progression as a therapeutic target to inhibit HIV replication. *J Infect Dis* **196**, 1409-1415.

Fontes, M. R., Teh, T. & Kobe, B. (2000). Structural basis of recognition of monopartite and bipartite nuclear localization sequences by mammalian importin-alpha. *J Mol Biol* **297**, 1183-1194.

Fontes, M. R., Teh, T., Toth, G., John, A., Pavo, I., Jans, D. A. & Kobe, B. (2003). Role of flanking sequences and phosphorylation in the recognition of the simian-virus-40 large T-antigen nuclear localization sequences by importin-alpha. *Biochem J* **375**, 339-349.

Friedrich, B., Quensel, C., Sommer, T., Hartmann, E. & Kohler, M. (2006). Nuclear localization signal and protein context both mediate importin alpha specificity of nuclear import substrates. *Mol Cell Biol* **26**, 8697-8709.

Geigenmuller-Gnirke, U., Nitschko, H. & Schlesinger, S. (1993). Deletion analysis of the capsid protein of Sindbis virus: identification of the RNA binding region. *J Virol* **67**, 1620-1626.

Ghosh, A. K., Steele, R., Meyer, K., Ray, R. & Ray, R. B. (1999). Hepatitis C virus NS5A protein modulates cell cycle regulatory genes and promotes cell growth. *J Gen Virol* **80**, 1179-1183.

Gillespie, L. K., Hoenen, A., Morgan, G. & Mackenzie, J. M. (2010). The endoplasmic reticulum provides the membrane platform for biogenesis of the flavivirus replication complex. *J Virol* **84**, 10438-10447.

Glushakova, S., Dubrovsky, L., Grivel, J., Haffar, O. & Bukrinsky, M. (2000). Small molecule inhibitor of HIV-1 nuclear import suppresses HIV-1 replication in human lymphoid tissue ex vivo: a potential addition to current anti-HIV drug repertoire. *Antiviral Res* **47**, 89-95.

Gorlich, D. & Mattaj, I. W. (1996). Nucleocytoplasmic transport. *Science* **271**, 1513-1518.

Grudnik, P., Bange, G. & Sinning, I. (2009). Protein targeting by the signal recognition particle. *Biol Chem* **390**, 775-782.

Gualano, R. C., Pryor, M. J., Cauchi, M. R., Wright, P. J. & Davidson, A. D. (1998). Identification of a major determinant of mouse neurovirulence of dengue virus type 2 using stably cloned genomic-length cDNA. *J Gen Virol* **79** (Pt 3), 437-446.

Gubler, D. J. (1997). Dengue and dengue hemorrhagic fever: Its history and resurgence as a global public health problem In Dengue and Dengue Hemorrhagic Fever, pp. 1-22 Edited by D. J. Gubler & G. Kuno: New York: CAB International.

Gubler, D. J. (1998). Dengue and dengue hemorrhagic fever. *Clin Microbiol Rev* **11**, 480-496.

Gubler, D. J. (2011). Dengue, urbanization and globalization: The unholy trinity of the 21(st) century. *Trop Med Health* **39**, 3-11.

Gustin, K. E. & Sarnow, P. (2006). Positive-strand RNA viruses and the nucleus. In Viruses and the Nucleus, pp. 161-184. Edited by J. Hiscox: Wiley.

Harper, J. V. & Brooks, G. (2006). The eukaryotic cell cycle. In Viruses and the Nucleus, pp. 25-68. Edited by J. Hiscox: Wiley.

Hase, T., Summers, P. L., Eckels, K. H. & Baze, W. B. (1987). An electron and immunoelectron microscopic study of dengue-2 virus-iInfection of cultured mosquito cells - Maturation events. *Arch Virol* **92**, 273-291.

He, Y. F., Bao, H. M., Xiao, X. F., Zuo, S., Du, R. Y., Tang, S. W., Yang, P. Y. & Chen, X. (2009). Biotin tagging coupled with amino acid-coded mass tagging for efficient and precise screening of interaction proteome in mammalian cells. *Proteomics* **9**, 5414-5424.

Heeres, J. T. & Hergenrother, P. J. (2011). High-throughput screening for modulators of protein-protein interactions: use of photonic crystal biosensors and complementary technologies. *Chem Soc Rev* **40**, 4398-4410.

Heinz, F. X. & Allison, S. L. (2000). Structures and mechanisms in flavivirus fusion. *Adv Virus Res* **55**, 231-269.

Henchal, E. A. & Putnak, J. R. (1990). The dengue viruses. *Clin Microbiol Rev* **3**, 376-396.

Henchal, E. A., Gentry, M. K., McCown, J. M. & Brandt, W. E. (1982). Dengue virus-specific and flavivirus group determinants identified with monoclonal antibodies by indirect immunofluorescence. *Am J Trop Med Hyg* **31**, 830-836.

Hershkovitz, O., Rosental, B., Rosenberg, L. A., Navarro-Sanchez, M. E., Jivov, S., Zilka, A., Gershoni-Yahalom, O., Brient-Litzler, E., Bedouelle, H., Ho, J. W., Campbell, K. S., Rager-Zisman, B., Despres, P. & Porgador, A. (2009). NKp44 receptor mediates interaction of the envelope glycoproteins from the West Nile and dengue viruses with NK cells. *J Immunol* **183**, 2610-2621.

Higgins, D. G., Bleasby, A. J. & Fuchs, R. (1992). CLUSTAL V: improved software for multiple sequence alignment. *Computer applications in the biosciences : CABIOS* **8**, 189-191.

Higgins, D. G. & Sharp, P. M. (1989). Fast and sensitive multiple sequence alignments on a microcomputer. *Computer applications in the biosciences : CABIOS* **5**, 151-153.

Hilgard, P. & Stockert, R. (2000). Heparan sulfate proteoglycans initiate dengue virus infection of hepatocytes. *Hepatology* **32**, 1069-1077.

Hiscox, J. A. (2003). The interaction of animal cytoplasmic RNA viruses with the nucleus to facilitate replication. *Virus Res* **95**, 13-22.

Hiscox, J. A. (2007). RNA viruses: hijacking the dynamic nucleolus. *Nat Rev Microbiol* **5**, 119-127.

Holtzclaw, B. J. (2002). Dengue fever In Emerging Infectious Diseases: Trends and Issues, pp. 103-112 Edited by F. R. Lashley & J. D. Durham: New York: Springer.

Honda, M., Kaneko, S., Matsushita, E., Kobayashi, K., Abell, G. A. & Lemon, S. M. (2000). Cell cycle regulation of hepatitis C virus internal ribosomal entry site-directed translation. *Gastroenterology* **118**, 152-162.

Howarth, M. & Ting, A. Y. (2008). Imaging proteins in live mammalian cells with biotin ligase and monovalent streptavidin. *Nat Protoc* **3**, 534-545.

Ivanyi-Nagy, R., Lavergne, J. P., Gabus, C., Ficheux, D. & Darlix, J. L. (2008). RNA chaperoning and intrinsic disorder in the core proteins of *Flaviviridae*. *Nucleic Acids Res* **36**, 712-725.

Jackowski, S. (1996). Cell cycle regulation of membrane phospholipid metabolism. *J Biol Chem* **271**, 20219-20222.

Jans, D. A., Xiao, C. Y. & Lam, M. H. (2000). Nuclear targeting signal recognition: a key control point in nuclear transport? *BioEssays* **22**, 532-544.

Jindadamrongwech, S., Thepparit, C. & Smith, D. R. (2004). Identification of GRP 78 (BiP) as a liver cell expressed receptor element for dengue virus serotype 2. *Arch Virol* **149**, 915-927.

Jones, C. T., Ma, L. X., Burgner, J. W., Groesch, T. D., Post, C. B. & Kuhn, R. J. (2003). Flavivirus capsid is a dimeric alpha-helical protein. *J Virol* **77**, 7143-7149.

Jones, M., Davidson, A., Hibbert, L., Gruenwald, P., Schlaak, J., Ball, S., Foster, G. R. & Jacobs, M. (2005). Dengue virus inhibits alpha interferon signaling by reducing STAT2 expression. *J Virol* **79**, 5414-5420.

Kangwanpong, D., Bhamarapravati, N. & Lucia, H. L. (1995). Diagnosing dengue virus infection in archived autopsy tissues by means of the *in situ* PCR method: a case report. *Clin Diagn Virol* **3**, 165-172.

Kanlaya, R., Pattanakitsakul, S. N., Sinchaikul, S., Chen, S. T. & Thongboonkerd, V. (2010). The ubiquitin-proteasome pathway is important for dengue virus infection in primary human endothelial cells. *J Proteome Res* **9**, 4960-4971.

Kann, M., Sodeik, B., Vlachou, A., Gerlich, W. H. & Helenius, A. (1999). Phosphorylation-dependent binding of hepatitis B virus core particles to the nuclear pore complex. *J Cell Biol* **145**, 45-55.

Kapoor, M., Zhang, L. W., Ramachandra, M., Kusukawa, J., Ebner, K. E. & Padmanabhan, R. (1995). Association between NS3 and NS5 proteins of dengue virus type-2 in the putative RNA replicase is linked to differential phosphorylation of NS5. *J Biol Chem* **270**, 19100-19106.

Katz, C., Levy-Beladev, L., Rotem-Bamberger, S., Rito, T., Rudiger, S. G. D. & Friedler, A. (2011). Studying protein-protein interactions using peptide arrays. *Chem Soc Rev* **40**, 2131-2145.

Khan, A. M., Miotto, O., Nascimento, E. J., Srinivasan, K. N., Heiny, A. T., Zhang, G. L., Marques, E. T., Tan, T. W., Brusic, V., Salmon, J. & August, J. T. (2008). Conservation and variability of dengue virus proteins: implications for vaccine design. *PLoS Negl Trop Dis* **2**, e272.

Khromykh, A. A. & Westaway, E. G. (1996). RNA binding properties of core protein of the flavivirus Kunjin. *Arch Virol* **141**, 685-699.

Khromykh, A. A., Kenney, M. T. & Westaway, E. G. (1998). Trans-complementation of flavivirus RNA polymerase gene NS5 by using Kunjin virus replicon-expressing BHK cells. *J Virol* **72**, 7270-7279.

Koh, W. L. & Ng, M. L. (2005). Molecular mechanisms of West Nile virus pathogenesis in brain cell. *Emerg Infect Dis* **11**, 629-632.

Kou, Z., Quinn, M., Chen, H., Rodrigo, W. W., Rose, R. C., Schlesinger, J. J. & Jin, X. (2008). Monocytes, but not T or B cells, are the principal target cells for dengue virus (DV) infection among human peripheral blood mononuclear cells. *J Med Virol* **80**, 134-146.

Kramer, L. D. & Ebel, G. D. (2003). Dynamics of flavivirus infection in mosquitoes. In Advances in Virus Research, pp. 187-216 Edited by T. J. Chambers & T. P. Monath: Elsevier Academic Press.

Krishnan, M. N., Sukumaran, B., Pal, U., Agaisse, H., Murray, J. L., Hodge, T. W. & Fikrig, E. (2007). Rab 5 is required for the cellular entry of dengue and West Nile viruses. *J Virol* **81**, 4881-4885.

Krupakar, P., Ngo, A. M. L. & Ng, M. L. (2012). Optimized purification protocol for proteins isolated from inclusion bodies. In Protein Purification, pp. 147-170. Edited by Miguel Benitez & V. Aguirre. New York: Nova Science.

Kuhn, R. J., Zhang, W., Rossmann, M. G., Pletnev, S. V., Corver, J., Lenches, E., Jones, C. T., Mukhopadhyay, S., Chipman, P. R., Strauss, E. G., Baker, T. S. & Strauss, J. H. (2002). Structure of dengue virus: Implications for flavivirus organization, maturation, and fusion. *Cell* **108**, 717-725.

Lad, V. J., Gupta, A. K., Ghosh, S. N. & Banerjee, K. (1993). Immunofluorescence studies on the replication of some arboviruses in nucleated and enucleated cells. *Acta Virol* **37**, 79-83.

Law, L. M., Everitt, J. C., Beatch, M. D., Holmes, C. F. & Hobman, T. C. (2003). Phosphorylation of rubella virus capsid regulates its RNA binding activity and virus replication. *J Virol* **77**, 1764-1771.

Le Roux, S., Devys, A., Girard, C., Harb, J. & Hourmant, M. (2010). Biomarkers for the diagnosis of the stable kidney transplant and chronic transplant injury using the ProtoArray(R) technology. *Transplant Proc* **42**, 3475-3481.

Lee, E. & Lobigs, M. (2000). Substitutions at the putative receptor-binding site of an encephalitic flavivirus alter virulence and host cell tropism and reveal a role for glycosaminoglycans in entry. *J Virol* **74**, 8867-8875.

Li, F. Q., Tam, J. P. & Liu, D. X. (2007). Cell cycle arrest and apoptosis induced by the coronavirus infectious bronchitis virus in the absence of p53. *Virology* **365**, 435-445.

Li, H., Clum, S., You, S., Ebner, K. E. & Padmanabhan, R. (1999). The serine protease and RNA-stimulated nucleoside triphosphatase and RNA helicase functional domains of dengue virus type 2 NS3 converge within a region of 20 amino acids. *J Virol* **73**, 3108-3116.

Li, J., Huang, R., Liao, W., Chen, Z. & Zhang, S. (2012). Dengue virus utilizes calcium modulating cyclophilin-binding ligand to subvert apoptosis. *Biochem Biophys Res Commun* **418**, 622-627.

Lievens, S., Eyckerman, S., Lemmens, I. & Tavernier, J. (2010). Large-scale protein interactome mapping: strategies and opportunities. *Expert Rev Proteomic* **7**, 679-690.

Limjindaporn, T., Netsawang, J., Noisakran, S., Thiemmeca, S., Wongwiwat, W., Sudsaward, S., Avirutnan, P., Puttikhunt, C., Kasinrerk, W., Sriburi, R., Sittisombut, N., Yenchitsomanus, P. T. & Maiasit, P. (2007). Sensitization to Fas-mediated apoptosis by dengue virus capsid protein. *Biochem Biophys Res Commun* **362**, 334-339.

Lindenbach, B. D., Thiel, H. J. & Rice, C. M. (2007). *Flaviviridae*: The viruses and their replication. In Fields Virology, 5 edn, pp. 1101-1152. Edited by D. M. Knipe & P. M. Howley: Philadelphia: Lippincott-Raven Publishers.

Liu, W. J., Chen, H. B. & Khromykh, A. A. (2003). Molecular and functional analyses of Kunjin virus infectious cDNA clones demonstrate the essential roles for NS2A in virus assembly and for a nonconservative residue in NS3 in RNA replication. *J Virol* **77**, 7804-7813.

Lu, W. & Ou, J. H. (2002). Phosphorylation of hepatitis C virus core protein by protein kinase A and protein kinase C. *Virology* **300**, 20-30.

Lutcke, H. (1995). Signal recognition particle (SRP), a ubiquitous initiator of protein translocation. *Eur J Biochem* **228**, 531-550.

Ma, L., Jones, C. T., Groesch, T. D., Kuhn, R. J. & Post, C. B. (2004). Solution structure of dengue virus capsid protein reveals another fold. *Proc Natl Acad Sci U S A* **101**, 3414-3419.

Mackenzie, J. M. & Westaway, E. G. (2001). Assembly and maturation of the flavivirus Kunjin virus appear to occur in the rough endoplasmic reticulum and along the secretory pathway, respectively. *J Virol* **75**, 10787-10799.

Mackenzie, J. M., Jones, M. K. & Young, P. R. (1996). Immunolocalization of the dengue virus nonstructural glycoprotein NS1 suggests a role in viral RNA replication. *Virology* **220**, 232-240.

Mackenzie, J. M., Khromykh, A. A., Jones, M. K. & Westaway, E. G. (1998). Subcellular localization and some biochemical properties of the flavivirus Kunjin nonstructural proteins NS2A and NS4A. *Virology* **245**, 203-215.

Maity, T. S., Leonard, C. W., Rose, M. A., Fried, H. M. & Weeks, K. M. (2006). Compartmentalization directs assembly of the signal recognition particle. *Biochemistry* **45**, 14955-14964.

Majno, G. & Joris, I. (1995). Apoptosis, oncosis, and necrosis. An overview of cell death. *Am J Pathol* **146**, 3-15.

Markham, K., Bai, Y. & Schmitt-Ulms, G. (2007). Co-immunoprecipitations revisited: an update on experimental concepts and their implementation for sensitive interactome investigations of endogenous proteins. *Anal Bioanal Chem* **389**, 461-473.

Markoff, L. (1989). *In vitro* processing of dengue virus structural proteins: cleavage of the pre-membrane protein. *J Virol* **63**, 3345-3352.

Mazzon, M., Jones, M., Davidson, A., Chain, B. & Jacobs, M. (2009). Dengue virus NS5 inhibits interferon-alpha signaling by blocking signal transducer and activator of transcription 2 phosphorylation. *J Infect Dis* **200**, 1261-1270.

Miller, S., Kastner, S., Krijnse-Locker, J., Buhler, S. & Bartenschlager, R. (2007). The non-structural protein 4A of dengue virus is an integral membrane protein inducing membrane alterations in a 2K-regulated manner. *J Biol Chem* **282**, 8873-8882.

Modis, Y., Ogata, S., Clements, D. & Harrison, S. C. (2004). Structure of the dengue virus envelope protein after membrane fusion. *Nature* **427**, 313-319.

Moreland, N. J., Tay, M. Y., Lim, E., Paradkar, P. N., Doan, D. N., Yau, Y. H., Geifman Shochat, S. & Vasudevan, S. G. (2010). High affinity human

antibody fragments to dengue virus non-structural protein 3. *PLoS Negl Trop Dis* **4**, e881.

Mori, Y., Okabayashi, T., Yamashita, T., Zhao, Z., Wakita, T., Yasui, K., Hasebe, F., Tadano, M., Konishi, E., Moriishi, K. & Matsuura, Y. (2005). Nuclear localization of Japanese encephalitis virus core protein enhances viral replication. *J Virol* **79**, 3448-3458.

Mukhopadhyay, S., Kuhn, R. J. & Rossmann, M. G. (2005). A structural perspective of the Flavivirus life cycle. *Nat Rev Microbiol* **3**, 13-22.

Muramatsu, S., Ishido, S., Fujita, T., Itoh, M. & Hotta, H. (1997). Nuclear localization of the NS3 protein of hepatitis C virus and factors affecting the localization. *J Virol* **71**, 4954-4961.

Nag, D. K. & Finley, D. (2012). A small-molecule inhibitor of deubiquitinating enzyme USP14 inhibits Dengue virus replication. *Virus Res* **165**, 103-106.

Nakano, T., Inoue, I., Shinozaki, R., Matsui, M., Akatsuka, T., Takahashi, S., Tanaka, K., Akita, M., Seo, M. & other authors (2009). A possible role of lysophospholipids produced by calcium-independent phospholipase A(2) in membrane-raft budding and fission. *Biochim Biophys Acta* **1788**, 2222-2228.

Navarro-Sanchez, E., Altmeyer, R., Amara, A., Schwartz, O., Fieschi, F., Virelizier, J. L., Arenzana-Seisdedos, F. & Despres, P. (2003). Dendritic-cell-specific ICAM3-grabbing non-integrin is essential for the productive infection of human dendritic cells by mosquito-cell-derived dengue viruses. *EMBO Rep* **4**, 723-728.

Netsawang, J., Noisakran, S., Puttikhunt, C., Kasinrerk, W., Wongwiwat, W., Malasit, P., Yenchitsomanus, P. T. & Limjindaporn, T. (2010). Nuclear localization of dengue virus capsid protein is required for DAXX interaction and apoptosis. *Virus Res* **147**, 275-283.

Ng, M. L. (1987). Ultrastructural studies of Kunjin virus-infected *Aedes albopictus* cells. *J Gen Virol* **68**, 577-582.

Ng, M. L., Howe, J., Sreenivasan, V. & Mulders, J. J. (1994). Flavivirus West Nile (Sarafend) egress at the plasma membrane. *Arch Virol* **137**, 303-313.

Ng, M. L., Tan, S. H. & Chu, J. J. (2001). Transport and budding at two distinct sites of visible nucleocapsids of West Nile (Sarafend) virus. *J Med Virol* **65**, 758-764.

Nguyen, T. B., Manova, K., Capodieci, P., Lindon, C., Bottega, S., Wang, X. Y., Refik-Rogers, J., Pines, J., Wolgemuth, D. J. & other authors (2002). Characterization and expression of mammalian cyclin B3, a prepachytene meiotic cyclin. *J Biol Chem* **277**, 41960-41969.

Noisakran, S., Dechtawewat, T., Rinkaewkan, P., Puttikhunt, C., Kanjanahaluethai, A., Kasinrerk, W., Sittisombut, N. & Malasit, P. (2007). Characterization of dengue virus NS1-stably expressed in 293T cell lines. *J Virol Methods* **142**, 67-80.

Oh, W., Yang, M. R., Lee, E. W., Park, K. M., Pyo, S., Yang, J. S., Lee, H. W. & Song, J. (2006). Jab1 mediates cytoplasmic localization and degradation of West Nile virus capsid protein. *J Biol Chem* **281**, 30166-30174.

Olson, M. O., Hingorani, K. & Szebeni, A. (2002). Conventional and nonconventional roles of the nucleolus. *Int Rev Cytol 219*, 199-266.

Patkar, C. G., Jones, C. T., Chang, Y. H., Warrier, R. & Kuhn, R. J. (2007). Functional requirements of the yellow fever virus capsid protein. *J Virol* **81**, 6471-6481.

Peranen, J., Rikkonen, M., Liljestrom, P. & Kaariainen, L. (1990). Nuclear localization of Semliki Forest virus-specific nonstructural protein nsP2. *J Virol* **64**, 1888-1896.

Perera, R. & Kuhn, R. J. (2008). Structural proteomics of dengue virus. *Curr Opin Microbiol* **11**, 369-377.

Petschnigg, J., Snider, J. & Stagljar, I. (2011). Interactive proteomics research technologies: recent applications and advances. *Curr Opin Biotech* **22**, 50-58.

Postel, A., Letzel, T., Muller, F., Ehricht, R., Pourquier, P., Dauber, M., Grund, C., Beer, M. & Harder, T. C. (2011). *In vivo* biotinylated recombinant influenza A virus hemagglutinin for use in subtype-specific serodiagnostic assays. *Anal Biochem* **411**, 22-31.

Postel, A., Letzel, T., Muller, F., Ehricht, R., Pourquier, P., Dauber, M., Grund, C., Beer, M. & Harder, T. C. (2011). *In vivo* biotinylated recombinant influenza A virus hemagglutinin for use in subtype-specific serodiagnostic assays. *Anal Biochem* **411**, 22-31.

Pryor, M. J., Carr, J. M., Hocking, H., Davidson, A. D., Li, P. & Wright, P. J. (2001). Replication of dengue virus type 2 in human monocyte-derived macrophages: comparisons of isolates and recombinant viruses with substitutions at amino acid 390 in the envelope glycoprotein. *Am J Trop Med Hyg* **65**, 427-434.

Pryor, M. J., Rawlinson, S. M., Butcher, R. E., Barton, C. L., Waterhouse, T. A., Vasudevan, S. G., Bardin, P. G., Wright, P. J., Jans, D. A. & Davidson, A. D. (2007). Nuclear localization of dengue virus nonstructural protein 5 through its importin alpha/beta-recognized nuclear localization sequences is integral to viral infection. *Traffic* **8**, 795-807.

Puttikhunt, C., Ong-ajchaowlerd, P., Prommool, T., Sangiambut, S., Netsawang, J., Limjindaporn, T., Malasit, P. & Kasinrerk, W. (2009). Production and

characterization of anti-dengue capsid antibodies suggesting the N terminus region covering the first 20 amino acids of dengue virus capsid protein is predominantly immunogenic in mice. *Arch Virol* **154**, 1211-1221.

Qi, Y. & Katagiri, F. (2011). Purification of resistance protein complexes using a biotinylated affinity (HPB) tag. *Methods Mol Biol* **712**, 21-30.

Rapiejko, P. J. & Gilmore, R. (1992). Protein translocation across the ER requires a functional GTP binding site in the alpha subunit of the signal recognition particle receptor. *J Cell Biol* **117**, 493-503.

Ray, D., Shah, A., Tilgner, M., Guo, Y., Zhao, Y., Dong, H., Deas, T. S., Zhou, Y., Li, H. & Shi, P. Y. (2006). West Nile virus 5'-cap structure is formed by sequential guanine N-7 and ribose 2'-O methylations by nonstructural protein 5. *J Virol* **80**, 8362-8370.

Raychaudhuri, S., Fontanes, V., Barat, B. & Dasgupta, A. (2009). Activation of ribosomal RNA transcription by hepatitis C virus involves upstream binding factor phosphorylation via induction of cyclin D1. *Cancer Res* **69**, 2057-2064.

Reguly, T. & Wrana, J. L. (2003). In or out? The dynamics of Smad nucleocytoplasmic shuttling. *Trends Cell Biol* **13**, 216-220.

Rodriguez-Madoz, J. R., Belicha-Villanueva, A., Bernal-Rubio, D., Ashour, J., Ayllon, J. & Fernandez-Sesma, A. (2010). Inhibition of the type I interferon response in human dendritic cells by dengue virus infection requires a catalytically active NS2B3 complex. *J Virol* **84**, 9760-9774.

Roehrig, J. T. (1997). Immunochemistry of dengue viruses In Dengue and Dengue Hemorrhagic Fever, pp. 175-191 Edited by D. J. Gubler & G. Kuno: New York: CAB International.

Rosemary Siafakas, A. & Richardson, D. R. (2009). Growth arrest and DNA damage-45 alpha (GADD45alpha). *Int J Biochem Cell Biol* **41**, 986-989.

Samsa, M. M., Mondotte, J. A., Caramelo, J. J. & Gamarnik, A. V. (2012). Uncoupling cis-Acting RNA elements from coding sequences revealed a requirement of the N-terminal region of dengue virus capsid protein in virus particle formation. *J Virol* **86**, 1046-1058.

Samsa, M. M., Mondotte, J. A., Iglesias, N. G., Assuncao-Miranda, I., Barbosa-Lima, G., Da Poian, A. T., Bozza, P. T. & Gamarnik, A. V. (2009). Dengue Virus Capsid Protein Usurps Lipid Droplets for Viral Particle Formation. *PLoS Pathog.* **5**.

Sangiambut, S., Keelapang, P., Aaskov, J., Puttikhunt, C., Kasinrerk, W., Malasit, P. & Sittisombut, N. (2008). Multiple regions in dengue virus capsid protein contribute to nuclear localization during virus infection. *J Gen Virol* **89**, 1254-1264.

Scholle, F., Li, K., Bodola, F., Ikeda, M., Luxon, B. A. & Lemon, S. M. (2004). Virus-host cell interactions during hepatitis C virus RNA replication: Impact of polyprotein expression on the cellular transcriptome and cell cycle association with viral RNA synthesis. *J Virol* **78**, 1513-1524.

Severson, W. E., Xu, X. & Jonsson, C. B. (2001). Cis-acting signals in encapsidation of Hantaan virus S-segment viral genomic RNA by its N protein. *J Virol* **75**, 2646-2652.

Simmons, C. P., Farrar, J. J., Nguyen v, V. & Wills, B. (2012). Dengue. *N Engl J Med* **366**, 1423-1432.

Sinarachatanant, P. & Olson, L. C. (1973). Replication of dengue virus type 2 in Aedes albopictus cell culture. *J Virol* **12**, 275-283.

Singh, I. & Helenius, A. (1992). Role of Ribosomes in Semliki Forest Virus Nucleocapsid Uncoating. *J Virol* **66**, 7049-7058.

Singhal, P. K., Kumar, P. R., Rao, M. R., Kyasani, M. & Mahalingam, S. (2006). Simian immunodeficiency virus Vpx is imported into the nucleus via importin alpha-dependent and -independent pathways. *J Virol* **80**, 526-536.

Smith, G. W. & Wright, P. J. (1985). Synthesis of proteins and glycoproteins in dengue type 2 virus-infected vero and *Aedes albopictus* cells. *J Gen Virol* **66** (Pt 3), 559-571.

Stadler, K., Allison, S. L., Schalich, J. & Heinz, F. X. (1997). Proteolytic activation of tick-borne encephalitis virus by furin. *J Virol* **71**, 8475-8481.

Stapleton, J. T., Foung, S., Muerhoff, A. S., Bukh, J. & Simmonds, P. (2011). The GB viruses: a review and proposed classification of GBV-A, GBV-C (HGV), and GBV-D in genus Pegivirus within the family *Flaviviridae*. *J Gen Virol* **92**, 233-246.

Sueda, S., Yoneda, S. & Hayashi, H. (2011). Site-specific labeling of proteins by using biotin protein ligase conjugated with fluorophores. *Chembiochem* **12**, 1367-1375.

Suksanpaisan, L., Cabrera-Hernandez, A. & Smith, D. R. (2007). Infection of human primary hepatocytes with dengue virus serotype 2. *J Med Virol* **79**, 300-307.

Surjit, M., Liu, B. P., Chow, V. T. K. & Lal, S. K. (2006). The nucleocapsid protein of severe acute respiratory syndrome-coronavirus inhibits the activity of cyclin-cyclin-dependent kinase complex and blocks S phase progression in mammalian cells. *J Biol Chem* **281**, 10669-10681.

Suzuki, A., Akimoto, K. & Ohno, S. (2003). Protein kinase C lambda/iota (PKClambda/iota): a PKC isotype essential for the development of multicellular organisms. *J Biochem* **133**, 9-16.

Suzuki, A., Kogo, R., Kawahara, K., Sasaki, M., Nishio, M., Maehama, T., Sasaki, T., Mimori, K. & Mori, M. (2012). A new PICTure of nucleolar stress. *Cancer Sci* **103**, 632-637.

Suzuki, R., Sakamoto, S., Tsutsumi, T., Rikimaru, A., Tanaka, K., Shimoike, T., Moriishi, K., Iwasaki, T., Mizumoto, K., Matsuura, Y., Miyamura, T. & Suzuki, T. (2005). Molecular determinants for subcellular localization of hepatitis C virus core protein. *J Virol* **79**, 1271-1281.

Suzuki, R., Sakamoto, S., Tsutsumi, T., Rikimaru, A., Tanaka, K., Shimoike, T., Moriishi, K., Iwasaki, T., Mizumoto, K. & other authors (2005). Molecular determinants for subcellular localization of hepatitis C virus core protein. *J Virol* **79**, 1271-1281.

Tadano, M., Makino, Y., Fukunaga, T., Okuno, Y. & Fukai, K. (1989). Detection of dengue 4 virus core protein in the nucleus. I. A monoclonal antibody to dengue 4 virus reacts with the antigen in the nucleus and cytoplasm. *J Gen Virol* **70** (Pt 6), 1409-1415.

Tan, L. C., Chua, A. J., Goh, L. S., Pua, S. M., Cheong, Y. K. & Ng, M. L. (2010). Rapid purification of recombinant dengue and West Nile virus envelope Domain III proteins by metal affinity membrane chromatography. *Protein Expr Purif* **74**, 129-137.

Tan, L. P., Lue, R. Y., Chen, G. Y. & Yao, S. Q. (2004). Improving the intein-mediated, site-specific protein biotinylation strategies both *in vitro* and *in vivo*. *Bioorg Med Chem Lett* **14**, 6067-6070.

Tassaneetrithep, B., Burgess, T. H., Granelli-Piperno, A., Trumpfheller, C., Finke, J., Sun, W., Eller, M. A., Pattanapanyasat, K., Sarasombath, S., Birx, D. L., Steinman, R. M., Schlesinger, S. & Marovich, M. A. (2003). DC-SIGN (CD209) mediates dengue virus infection of human dendritic cells. *J Exp Med* **197**, 823-829.

Tolaymat, N. & Mock, D. M. (1989). Biotin analysis of commercial vitamin and other nutritional supplements. *J Nutr* **119**, 1357-1360.

Tomizaki, K., Usui, K. & Mihara, H. (2010). Protein-protein interactions and selection: array-based techniques for screening disease-associated biomarkers in predictive/early diagnosis. *FEBS J* **277**, 1996-2005.

Torres, F. E., Recht, M. I., Coyle, J. E., Bruce, R. H. & Williams, G. (2010). Higher throughput calorimetry: opportunities, approaches and challenges. *Curr Opin Struc Biol* **20**, 598-605.

Uchil, P. D. & Satchidanandam, V. (2003). Architecture of the flaviviral replication complex. Protease, nuclease, and detergents reveal encasement within double-layered membrane compartments. *J Biol Chem* **278**, 24388-24398.

Ulmanen, I., Soderlund, H. & Kaariainen, L. (1976). Semliki Forest virus capsid protein associates with 60s ribosomal-subunit in infected-cells. *J Virol* **20**, 203-210.

Umareddy, I., Chao, A., Sampath, A., Gu, F. & Vasudevan, S. G. (2006). Dengue virus NS4B interacts with NS3 and dissociates it from single-stranded RNA. *J Gen Virol* **87**, 2605-2614.

Virok, D. P., Simon, D., Bozso, Z., Rajko, R., Datki, Z., Balint, E., Szegedi, V., Janaky, T., Penke, B. & Fulop, L. (2011). Protein array-based interactome analysis of amyloid-beta indicates an inhibition of protein translation. *J Proteome Res* **10**, 1538-1547.

Walter, P. & Blobel, G. (1983). Subcellular distribution of signal recognition particle and 7SL-RNA determined with polypeptide-specific antibodies and complementary DNA probe. *J Cell Biol* **97**, 1693-1699.

Walter, P., Ibrahimi, I. & Blobel, G. (1981). Translocation of proteins across the endoplasmic reticulum. I. Signal recognition protein (SRP) binds to in-vitro-assembled polysomes synthesizing secretory protein. *J Cell Biol* **91**, 545-550.

Wang, S. H., Syu, W. J., Huang, K. J., Lei, H. Y., Yao, C. W., King, C. C. & Hu, S. T. (2002). Intracellular localization and determination of a nuclear localization signal of the core protein of dengue virus. *J Gen Virol* **83**, 3093-3102.

Ward, R. & Davidson, A. D. (2007). Structure function analysis of the dengue virus type 2 capsid protein. In Third Asian Regional Dengue Research Network Meeting. Taipei, Taiwan.

Weis, K. (1998). Importins and exportins: how to get in and out of the nucleus. *Trends Biochem Sci* **23**, 185-189.

Welsch, S., Miller, S., Romero-Brey, I., Merz, A., Bleck, C. K., Walther, P., Fuller, S. D., Antony, C., Krijnse-Locker, J. & Bartenschlager, R. (2009). Composition and three-dimensional architecture of the dengue virus replication and assembly sites. *Cell Host Microbe* **5**, 365-375.

Wengler, G. & Wengler, G. (1993). The NS 3 nonstructural protein of flaviviruses contains an RNA triphosphatase activity. *Virology* **197**, 265-273.

Westaway, E. G. (1987). Flavivirus replication strategy. *Adv Virus Res* **33**, 45-90.

Westaway, E. G., Khromykh, A. A., Kenney, M. T., Mackenzie, J. M. & Jones, M. K. (1997a). Proteins C and NS4B of the flavivirus Kunjin translocate independently into the nucleus. *Virology* **234**, 31-41.

Westaway, E. G., Mackenzie, J. M., Kenney, M. T., Jones, M. K. & Khromykh, A. A. (1997b). Ultrastructure of Kunjin virus-infected cells: colocalization of

NS1 and NS3 with double-stranded RNA, and of NS2B with NS3, in virus-induced membrane structures. *J Virol* **71**, 6650-6661.

Whittaker, G. R. & Helenius, A. (1998). Nuclear import and export of viruses and virus genomes. *Virology* **246**, 1-23.

WHO (1997). Dengue Hemorrhagic Fever: Diagnosis, Treatment, Prevention and Control: World Health Organization.

WHO (2009). Dengue Guidelines for Diagnosis, Treatment, Prevention and Control: World Health Organization.

WHO (2012). Global strategy for dengue prevention and control 2012-2020, p. 5: World Health Organization.

Wild, K., Bange, G., Bozkurt, G., Segnitz, B., Hendricks, A. & Sinning, I. (2010). Structural insights into the assembly of the human and archaeal signal recognition particles. *Acta Crystallogr D Biol Crystallogr* **66**, 295-303.

Williamson, M. P. & Sutcliffe, M. J. (2010). Protein-protein interactions. *Biochem Soc Trans* **38**, 875-878.

Wright, G. J., Martin, S., Bushell, K. M. & Sollner, C. (2010). High-throughput identification of transient extracellular protein interactions. *Biochem Soc Trans* **38**, 919-922.

Wu, W. W., Sun, Y. H. & Pante, N. (2007). Nuclear import of influenza A viral ribonucleoprotein complexes is mediated by two nuclear localization sequences on viral nucleoprotein. *Virol J* **4**, 49.

Yang, J., Jaramillo, A., Shi, R., Kwok, W. W. & Mohanakumar, T. (2004). *In vivo* biotinylation of the major histocompatibility complex (MHC) class II/peptide complex by coexpression of BirA enzyme for the generation of MHC class II/tetramers. *Hum Immunol* **65**, 692-699.

Yang, M. R., Lee, S. R., Oh, W., Lee, E. W., Yeh, J. Y., Nah, J. J., Joo, Y. S., Shin, J., Lee, H. W., Pyo, S. & Song, J. (2008). West Nile virus capsid protein induces p53-mediated apoptosis via the sequestration of HDM2 to the nucleolus. *Cell Microbiol* **10**, 165-176.

Yasui, K., Wakita, T., Tsukiyama-Kohara, K., Funahashi, S. I., Ichikawa, M., Kajita, T., Moradpour, D., Wands, J. R. & Kohara, M. (1998). The native form and maturation process of hepatitis C virus core protein. *J Virol* **72**, 6048-6055.

Yoo, D., Wootton, S. K., Li, G., Song, C. & Rowland, R. R. (2003). Colocalization and interaction of the porcine arterivirus nucleocapsid protein with the small nucleolar RNA-associated protein fibrillarin. *J Virol* **77**, 12173-12183.

Zhang, W., Chipman, P. R., Corver, J., Johnson, P. R., Zhang, Y., Mukhopadhyay, S., Baker, T. S., Strauss, J. H., Rossmann, M. G. & Kuhn, R. J. (2003). Visualization of membrane protein domains by cryo-electron microscopy of dengue virus. *Nat Struct Biol* **10**, 907-912.

Zlotnick, A. (2003). Are weak protein-protein interactions the general rule in capsid assembly? *Virology* **315**, 269-274.

APPENDIX 1: MEDIA FOR TISSUE CULTURE

a) RPMI-1640 Growth Medium

Items	Amount	Source
RPMI-1640 powder	16.4 g	Sigma, USA
$NaHCO_3$	2.0 g	Merck, Germany
Foetal Calf Serum (FCS)	100 ml	Biological Industries, Israel

One bottle of powdered RPMI-1640 with HEPES and $NaHCO_3$ were dissolved in 900 ml of autoclaved Reverse Osmosis (RO) water and the pH was adjusted to 7.2 with 5 M NaOH. Sterilization was carried out by filtration with 0.2 micron filter and then 100 ml FCS was added into the medium. It was stored at 4 ^{o}C.

b) L-15 Growth Medium

Items	Amount	Source
L-15 powder	13.8 g	Sigma, USA
Foetal Calf Serum (FCS)	100 ml	Biological Industries, Israel

One bottle of L-15 powder was dissolved in 900 ml of autoclaved RO water and the pH was adjusted to 7.2 with 5 M NaOH. Sterilization was carried out by filtration through a 0.2 micron filter. One hundred ml FCS which had been inactivated at 56 ^{o}C for half an hour was added to the medium. It was stored at 4 ^{o}C.

c) Dulbecco's Modified Eagle's Medium (DMEM) Growth Medium

Items	Amount	Source
DMEM powder	13.8 g	Sigma, USA
$NaHCO_3$	3.7 g	Merck, Germany
Foetal Calf Serum (FCS)	100 ml	Biological Industries, Israel

One bottle DMEM powder and $NaHCO_3$ were dissolved in 900 ml of autoclaved RO water and the pH was adjusted to 7.2 with 5 M NaOH. Sterilization was carried out by filtration through a 0.2 micron filter. One hundred ml FCS which had been inactivated at 56 ^oC for half an hour was added to the medium. It was stored at 4 ^oC.

d) Dulbecco's Modified Eagle's Medium (DMEM)-293FT Growth Medium

Items	Amount	Source
DMEM powder	13.8 g	Sigma, USA
$NaHCO_3$	3.7 g	Merck, Germany
200 mM L-Glutamine (100x)	10 ml	Invitrogen, USA
10 mM MEM Non-Essential Amino Acids (100x)	10 ml	Invitrogen, USA
100 mM MEM Sodium Pyruvate (100x)	10 ml	Invitrogen, USA
Geneticin® (500 mg/ml)	1 ml	Invitrogen, USA
Foetal Calf Serum (FCS)	100 ml	Biological Industries, Israel

One bottle of DMEM powder and $NaHCO_3$ were dissolved in 900 ml of autoclaved RO water and the pH was adjusted to 7.2 with 5 M NaOH. Sterilization was carried out by filtration through a 0.2 micron filter. One hundred ml FCS which had been inactivated at 56 ^oC for half an hour was added to the medium, followed by L-glutamine, NEAA, sodium pyruvate and Geneticin®. The medium was stored at 4 ^oC and it was stable for 6 months.

e) 1 x Phosphate-Buffered Saline (PBS), pH 7.4

Items	Amount	Source
NaCl	8.0 g	Merck, Germany
KCl	0.2 g	Merck, Germany
KH_2PO_4	0.2 g	Merck, Germany
Na_2HPO_4	11.5 g	Merck, Germany

All the above items were dissolved in 900 ml RO water and the pH was adjusted to 7.4 with 5 M NaOH before topping up to 1 L. It was autoclaved and stored at 4 ^{o}C.

f) Trypsin

Ten ml of sterile porcine pancreas-derived trypsin 10x solution (Sigma-Aldrich, USA) was diluted with 90 ml of sterile 1x PBS (Appendix 1e). The trypsin solution was stored at 4 ^{o}C and warmed up to 37 ^{o}C before use.

APPENDIX 2: MEDIA FOR VIRUS INFECTION AND PLAQUE ASSAY

a) Virus Diluent

Items	Amount	Source
Hank's Balanced Salt	9.8 g	Sigma, USA
Bovine Albumin Fraction V	0.2 g	Invitrogen, USA

One bottle of Hank's balanced salt powder and bovine albumin fraction V were dissolved in 900 ml autoclaved RO water and the pH was adjusted to 7.2 with 5 M NaOH. Final solution was topped up to 1 L and sterilization was carried out by filtration with 0.2 micron filter.

b) Overlay Medium

Items	Amount	Source
RPMI-1640 powder	16.4 g	Sigma, USA
$NaHCO_3$	2.0 g	Merck, Germany
Foetal Calf Serum (FCS)	100 ml	Biological Industries, Israel
Carboxymethylcellulose (CMC)	4 g	Calbiochem, USA

One bottle of powdered RPMI-1640 with HEPES and $NaHCO_3$ were dissolved in 480 ml autoclaved RO water and the pH was adjusted to 7.2 with 5 M NaOH. Sterilization was carried out by filtration with 0.2 micron filter and then 20 ml FCS was added into the medium to obtain double-strength (2X) maintenance medium. Four gram of CMC was dissolved in 200 ml of RO water and autoclaved. Then, 200 ml of the 2X maintenance medium was mixed thoroughly with the autoclaved CMC to obtain 400 ml of overlay medium.

c) Crystal Violet Staining Solution

Items	Amount	Source
Crystal Violet	1.85 g	Sigma, USA
37 % formaldehyde	270 ml	Merck, Germany
1 x PBS	120 ml	Appendix 1e

All the above items were mixed to make a final working crystal violet staining solution for plaque assay. Formaldehyde is volatile and hazardous so preparation must be done inside a fume hood.

APPENDIX 3: MATERIALS FOR MOLECULAR TECHNIQUES

a) 2 % Agarose Gel

Items	Amount	Source
Agarose	2.0 g	Bio-Rad, USA
1 x Tris / Acetate / EDTA (TAE)	Top up to 100 ml	
GelRed™ Nucleic Acid Gel Stain (10,000X)	10 µl	Biotium, USA

Agarose powder was boiled with 1 x TAE buffer (diluted from 10 x TAE buffer in Appendix 3b) in microwave until all powder was dissolved and the solution became clear. The solution was then cooled down with running water and gel red was added into the solution. After mixing well, all the solution was poured into a casting tray with combs. After the polymerization was complete, the gel was put into an electrophoresis tank with 1 x TAE buffer and the comb was removed.

b) 10 x Tris / Acetate / EDTA (TAE) Buffer, pH 8.5

Items	Amount	Source
Tris Base	48.4 g	Promega, USA
Glacial Acetic Acid	11.4 ml	BDH Laboratory Supplies, UK
$Na_2EDTA.2H_2O$	7.44 g	BDH Laboratory Supplies, UK

All the above items were mixed together and topped up to 1 L with RO water. The pH was then adjusted to 8.5 with 5 M NaOH and stored at room temperature.

c) Luria-Bertani (LB) Agar

Items	Amount	Source
Tryptone	10 g	Oxoid, UK
NaCl	10 g	Merck, Germany
Yeast Extract	5 g	Oxoid, UK
Agarose	18 g	1st Base, Singapore

All the above items were weighed and dissolved in 1 L RO water. The mixture was autoclaved at 121 ^{o}C and 15 lb presure for 15 min. After autoclaving, the bottle was cooled down to 55 ^{o}C in a water bath before appropriate antibiotic (ampicillin or kanamycin) was added. The mixture was pour into Petri dishes (Sterilin, UK) and allowed to solify at room temperature in a Biosafety Cabinet. The plates were stored at 4 ^{o}C.

d) Luria-Bertani (LB) Broth

Items	Amount	Source
Tryptone	10 g	Oxoid, UK
NaCl	10 g	Merck, Germany
Yeast Extract	5 g	Difco, USA

The above items were weighed and dissolved in 1 L RO water and autoclaved at 121 ^{o}C and 15 lb presure for 15 min. When the bottle was cooled down to 55 ^{o}C, appropriate antibiotic (ampicillin or kanamycin) was added. Storage was at 4 ^{o}C.

e) 8 % Non-Denaturing Polyacrylamide Gel

Items	Amount	Source
Acrylamide / Bisacrylamide (19:1)	3.2 ml	Bio-Rad, USA
10 x Tris/Borate/EDTA (TBE)	1.2 ml	Appendix 3f
10 % Ammonium Persulfate (APS)	200 µl	USB, USA
N,N,N'N'-tetramethylethylenediamine (TEMED)	10 µl	Invitrogen, USA

Acrylamide / bisacrylamide (19:1) and 10 x TBE buffer were mixed together and topped up to the final volume of 12 ml with RO water. After the gel casting apparatus was assembled, TEMED and 10 % APS were added into the solution and mixed thoroughly. The mixture was then pipetted into the spaces between the gel plates immediately and a comb was inserted onto the plates. After polymerization was complete, the comb was removed and the gel could be used or stored at 4 ^{o}C.

f) 10 x Tris / Borate / EDTA (TBE) Buffer, pH 8.0

Items	Amount	Source
Tris Base	108 g	Promega, USA
Boric Acid	55 g	Merck, Germany
EDTA (0.5 M)	40 ml	BDH Laboratory Supplies, UK

All the above items were mixed together and topped up to 1 L with RO water. The pH was adjusted to 8.0 with 5 M NaOH and stored at room temperature.

g) Diethylpyprocarbonate (DEPC)-Treated Water for Real-Time Polymerase Chain Reaction (PCR)

Items	Amount	Source
Diethylpyprocarbonate (DEPC)	1 ml	Sigma, USA

Diethylpyprocarbonate (DEPC) was dissolved in 1 L of RO water overnight with constant stirring. After DEPC dissolved completely in the water, it was autoclaved to break down the DEPC. DEPC-treated water should be aliquoted into eppendorf tubes inside a dedicated clean PCR hood.

APPENDIX 4: MATERIALS FOR PROTEIN EXPRESSION AND PURIFICATION

a) Resuspension Buffer

Items	Amount	Source
Tris Base	2.42 g	Promega, USA
NaCl	17.53 g	Merck, Germany

The above items were dissolved in 900 ml RO water and pH was adjusted to 8 using HCl. The final volume was topped up to 1 L to obtain resuspension buffer (20 mM Tris and 300 mM NaCl).

b) Resuspension Buffer with Triton-X

Items	Amount	Source
Tris Base	2.42 g	Promega, USA
NaCl	17.53 g	Merck, Germany
Triton-X	10 ml	

Tris and NaCl were dissolved in 900 ml RO water and pH was adjusted to 8 using HCl before adding Triton-X. The final volume was topped up to 1 L to obtain resuspension buffer (20 mM Tris and 300 mM NaCl) with 1 % Triton-X.

c) Lysis Buffer

Items	Amount	Source
Tris Base	2.42 g	Promega, USA
NaCl	17.53 g	Merck, Germany
Urea	480.48 g	Vivantis, Malaysia
Imidazole	0.68 g	Sigma, USA

The above items were dissolved in 900 ml RO water and pH was adjusted to 8 using HCl. The final volume was topped up to 1 L to obtain lysis buffer (8M Urea, 20 mM Tris, 300 mM NaCl and 10 mM imidazole). One tablet of EDTA-free protease inhibitor (Roche, Switzerland) was added into 100 ml of lysis buffer.

d) Wash Buffer

Items	Amount	Source
Tris Base	2.42 g	Promega, USA
NaCl	17.53 g	Merck, Germany
Urea	480.48 g	Vivantis, Malaysia
Imidazole	1.36 g	Sigma, USA

The above items were dissolved in 900 ml RO water and pH was adjusted to 8 using HCl. The final volume was topped up to 1 L to obtain wash buffer (8M Urea, 20 mM Tris, 300 mM NaCl and 20 mM imidazole).

e) Elution Buffer

Items	Amount	Source
Tris Base	2.42 g	Promega, USA
NaCl	17.53 g	Merck, Germany
Urea	480.48 g	Vivantis, Malaysia
Imidazole	34 g	Sigma, USA

The above items were dissolved in 900 ml RO water and pH was adjusted to 8 using HCl. The final volume was topped up to 1 L to obtain elution buffer (8M Urea, 20 mM Tris, 300 mM NaCl and 500 mM imidazole).

f) Refolding Buffer

Items	Amount	Source
Tris Base	3.03 g	Promega, USA

Tris was dissolved in 900 ml RO water and pH was adjusted to 8 using HCl. The final volume was topped up to 1 L to obtain 25 mM Tris refolding buffer.

g) Starting Buffer for Mono Q Ion-Exchange Chromatography

Items	Amount	Source
Tris Base	2.42 g	Promega, USA

Tris was dissolved in 900 ml RO water and pH was adjusted to 8.0 using HCl. The final volume was topped up to 1 L to obtain 20 mM Tris-HCl buffer.

h) Elution Buffer for Mono Q Ion-Exchange Chromatography

Items	Amount	Source
Tris Base	3.03 g	Promega, USA
NaCl	58.44 g	Merck, Germany

Tris and NaCl were dissolved in 900 ml RO water and pH was adjusted to 8.0 using HCl. The final volume was topped up to 1 L to obtain elution buffer (20 mM Tris and 1 M NaCl).

i) Starting Buffer for Mono S Ion-Exchange Chromatography

Items	Amount	Source
2-[N-morpholino]ethanesulphonic acid (MES)	3.9 g	Sigma, USA

The above item was dissolved in 900 ml RO water and pH was adjusted to 6.0 using NaOH. The final volume was topped up to 1 L to obtain 20 mM MES buffer.

j) Elution Buffer for Mono S Ion-Exchange Chromatography

Items	Amount	Source
MES	3.9 g	Sigma, USA
NaCl	58.44 g	Merck, Germany

The above items were dissolved in 900 ml RO water and pH was adjusted to 6.0 using NaOH. The final volume was topped up to 1 L to obtain elution buffer (20 mM MES and 1 M NaCl).

APPENDIX 5: MATERIALS FOR PROTEIN ANALYSIS

a) Glycine Gel

i) 12 % Separating Glycine Gel

Items	Amount	Source
40 % Acrylamide / Bisacrylamide	3 ml	Merck, Germany
1.5 M Tris buffer, pH 8.8	3.5 ml	Appendix 5a(iii)
Sodium Dodecyl Sulphate (SDS)	100 µl	Merck, Germany
RO Water	3.5 ml	
10 % Ammonium Persulfate (APS)	100 µl	USB, USA
N,N,N'N'-tetramethylethylenediamine (TEMED)	4 µl	Invitrogen, USA

Gel casting apparatus was assembled first. 40 % acrylamide / bisacrylamide, Tris buffer, SDS and RO water were mixed together before adding APS and TEMED. Final solution was mixed thoroughly and pipetted carefully into the spaces between the gel plates. A layer of isopropanol (Fisher Chemical, USA) was added carefully on top of the mixture to avoid oxygen getting in and inhibit polymerization. It was left to polymerize.

ii) 5 % Stacking Glycine Gel

Items	Amount	Source
40 % Acrylamide / Bisacrylamide	500 µl	Merck, Germany
1.5 M Tris buffer, pH 6.8	670 µl	Appendix 5a(iv)
Sodium Dodecyl Sulphate (SDS)	40 µl	Merck, Germany
RO Water	2.8 ml	
10 % Ammonium Persulfate (APS)	40 µl	USB, USA
N,N,N'N'-tetramethylethylenediamine (TEMED)	4 µl	Invitrogen, USA

Similarly, acrylamide / bisacrylamide, Tris buffer, SDS and RO water were mixed first before adding APS and TEMED. After mixing thoroughly, the layer of isopropanol was discarded from the polymerized gel and the mixture was pipetted carefully onto the gel to avoid bubbles. Lastly, comb was inserted and it was made sure that there was no bubble around the bottom of the wells.

iii) 1.5 M Tris Buffer, pH 8.8

Items	Amount	Source
Tris Base	182 g	Promega, USA

Tris base was dissolved in 900 ml RO water and the pH was adjusted to 8.8 using hydrochloric acid (HCl). After that, it was topped up to 1L and stored at 4^{o}C.

iv) 1.5 M Tris Buffer, pH 6.8

Items	Amount	Source
Tris Base	182 g	Promega, USA

Tris base was dissolved in 900 ml RO water and the pH was adjusted to 6.8 using hydrochloric acid (HCl) before topping up to 1 L. It was stored at 4^{o}C.

v) Glycine Running Buffer

Items	Amount	Source
Tris Base	6.07 g	Promega, USA
Glycine	28.73 g	Merck, Germany
Sodium Dodecyl Sulphate (SDS)	2.0 g	Merck, Germany

Tris base and glycine were dissolved in 900 ml RO water and the pH was adjusted to 8.8 before adding SDS. The final volume was topped up to 1 L. For upper tank running buffer, buffer to RO water ratio of 1:1 was prepared while ratio of 1:4.3 was prepared for lower tank running buffer.

b) Tricine Gel

i) 12 % Separating Tricine Gel

Items	Amount	Source
40 % Acrylamide / Bisacrylamide	3 ml	Merck, Germany
Tricine Gel Buffer	3.3 ml	Appendix 5b(iii)
Glycerol (87 % w/v)	1.3 g	Merck, Germany
RO Water	3.65 ml	
10 % Ammonium Persulfate (APS)	100 µl	USB, USA
N,N,N'N'-tetramethylethylenediamine (TEMED)	5 µl	Invitrogen, USA

Gel casting apparatus was assembled first. 40 % acrylamide / bisacrylamide, tricine gel buffer, glycerol and RO water were mixed before adding APS and TEMED. Final solution was mixed thoroughly and pipetted carefully into the spaces between the gel plates. A layer of isopropanol (Fisher Chemical, USA) was added carefully on top of the mixture to avoid oxygen getting in and inhibit polymerization. It was left to polymerize.

ii) 5 % Stacking Tricine Gel

Items	Amount	Source
40 % Acrylamide / Bisacrylamide	625 µl	Merck, Germany
Tricine Gel Buffer	1.24 ml	Appendix 5d
RO Water	3.08 ml	
10 % Ammonium Persulfate (APS)	50 µl	USB, USA
N,N,N'N'-tetramethylethylenediamine (TEMED)	5 µl	Invitrogen, USA

Acrylamide / bisacrylamide, tricine gel buffer, and RO water were mixed first before adding APS and TEMED. After mixing thoroughly, the layer of isopropanol was discarded from the gel and the mixture was pipetted carefully onto the gel to avoid bubbles. Lastly, comb was inserted and ensures that there was no bubble around the wells.

iii) Tricine Gel Buffer

Items	Amount	Source
Tris Base	181.7 g	Promega, USA
Sodium Dodecyl Sulphate (SDS)	1.5 g	Merck, Germany

Tris base was dissolved in 400 ml of RO water and the pH was adjusted to 8.5 using hydrochloric acid (HCl). After that, SDS was added and it was topped up to 500 ml.

iv) Tricine Gel Upper Tank Running Buffer

Items	Amount	Source
Tris Base	12.1 g	Promega, USA
Tricine	17.9 g	Sigma, USA
Sodium Dodecyl Sulphate (SDS)	1.0 g	Merck, Germany

Tris base and tricine were dissolved in 900 ml of RO water and the pH was adjusted to 8.5 with hydrochloric acid (HCl) before adding SDS. The final volume was topped up to 1 L.

v) Tricine Gel Lower Tank Running Buffer

Items	Amount	Source
Tris Base	24.2 g	Promega, USA

Tris base were dissolved in 900 ml of RO water and the pH was adjusted to 8.5 using hydrochloric acid (HCl). The final volume was topped up to 1 L.

c) Materials for Western Blot

i) 5 % Skim Milk Blocking Buffer

Items	Amount	Source
Skimed Milk Powder	5 g	Anlene, Australia
1 x TBST	100 ml	Appendix 5c(iii)

Skimed milk powder was dissolved thoroughly in TBST. This mixture was used for blocking and diluents for antibodies.

ii) 4 % Bovine Serum Albumin Blocking Buffer

Items	Amount	Source
Bovine Serum Albumin	4 g	Sigma, USA
1 x PBST	100 ml	Appendix 5c(iv)

Bovine serum albumin was weighed and dissolved thoroughly in PBST. This mixture was used for blocking and diluents for antibodies.

iii) 1 x Tris Buffered Saline / Tween-20 (TBST)

Items	Amount	Source
Tris Base	12.2 g	Promega, USA
NaCl	8 g	Merck, Germany
RO Water	900 ml	
Tween-20	1 ml	Sigma, USA

Tris base and NaCl were dissolved in 900 ml of RO water and the pH was adjusted to 7.7 using hydrochloric acid (HCl) before adding Tween-20. The final volume was topped up to 1 L.

iv) Phosphate Buffered Saline / Tween-20 (PBST)

Items	Amount	Source
1 x PBS	1 L	Appendix 1e
Tween-20	1 ml	Sigma, USA

One ml of Tween-20 was added into 1 L of PBS.

d) Coomassie Staining and Destaining

i) Coomassie Blue Staining Solution

Items	Amount	Source
Methanol	450 ml	Schedelco, Singapore
Glacial Acetic Acid	100 ml	Merck, Germany
RO Water	450 ml	
Coomassie Brilliant Blue R-20	1 g	Sigma, USA

Methanol, glacial acetic acid and RO water were mixed first and then Coomassie Brilliant Blue R-20 was weighed and poured into the mixture. Preparation was done in a fume hood because of the pungent vapour from acetic acid.

ii) Destaining Solution I

Items	Amount	Source
Methanol	400 ml	Schedelco, Singapore
Glacial Acetic Acid	100 ml	Merck, Germany
RO Water	500 ml	

The above solutions were mixed in a fume hood because of the pungent vapour from acetic acid.

iii) Destaining Solution II

Items	Amount	Source
Methanol	50 ml	Schedelco, Singapore
Glacial Acetic Acid	70 ml	Merck, Germany
RO Water	880 ml	

The above solutions were mixed in a fume hood because of the pungent vapour from acetic acid.

e) Silver Staining

i) Fixative Enhancer Solution

Items	Amount	Source
Methanol	200 ml	Schedelco, Singapore
Glacial Acetic Acid	40 ml	Merck, Germany
Fixative Enhancer Concentrate	40 ml	Bio-Rad, USA
RO Water	120 ml	

The above solutions were mixed in a fume hood because of the pungent vapour from acetic acid.

ii) Development Accelerator Solution

Items	Amount	Source
RO Water	35 ml	
Silver Complex Solution	5 ml	Bio-Rad, USA
Reduction Moderator Solution	5 ml	Bio-Rad, USA
Image Development Reagent	5 ml	Bio-Rad, USA

Reverse osmosis (RO) water was placed into a beaker first followed by Silver Complex Solution, Reduction Moderator Solution, and Image Development Reagent in order. Teflon-coated stirring bar was used to ensure proper mixing of the solutions. This mixture was prepared within 5 min of use for silver staining.

APPENDIX 6: MATERIALS FOR FLUORESCENCE-ACTIVATED CELL SORTING (FACS) ANALYSIS

a) Propidium Iodide Staining Solution

Items	Amount	Source
Propidium Iodide	200 µg	Sigma, USA
Triton-X	10 µl	Sigma, USA
RNase A	2 mg	Applichem GmbH, Germany

Propidium iodide was dissolved in 10 ml of 1 x PBS (Appendix 1e) and the bottle was covered with aluminium foil to protect it from light. Triton-X was then added into the mixture. RNase A was only added when it was needed. The solution was kept at 4 ^{o}C.

APPENDIX 7: SOFTWARE USED FOR THIS PROJECT

Bioinformatics software used in this project

Function	Name	URL
Sequence alignment and comparison	BLAST	**http://www.ncbi.nlm.nih.gov/blast/bl2seq/wblast2.cgi** (blastn; blastp)
Multiple sequence alignment	ClustalW	**http://www.ebi.ac.uk/clustalw/**
Protein sequence analysis	-PROSITE	**http://ca.expasy.org/prosite/**
	-MyHits	**http://hits.isb-sib.ch/cgi-bin/index**
	-ELM	**http://elm.eu.org/**
	-NetPhos 2.0 Server	**http://www.cbs.dtu.dk/services/NetPhos/**
Nucleic acid sequence translation	EMBOSS Transeq	**http://www.ebi.ac.uk/emboss/transeq/**
Protein structure homology modeling	SWISS-MODEL	**http://swissmodel.expasy.org//SWISS-MODEL.html**
Cell cycle analysis	WinMDI 2.8	**http://facs.scripps.edu/software.html**
Co-localization and densitometry analysis	ImageJ	**http://rsbweb.nih.gov/ij/**

APPENDIX 8: DNA SEQUENCES AND CONCEPTUAL TRANLSATION OF DNA INSERTIONS

a) pcDNA3.1/CT-GFP-TOPO vector with full length capsid gene

```
atggatgaccaacggaaaaaggcgagaaatacgcctttcaatatgctgaaacgcgagaga
 M  D  D  Q  R  K  K  A  R  N  T  P  F  N  M  L  K  R  E  R
aaccgcgtgtcgactgtacaacagctgacaaagagattctcacttggaatgctgcaggga
 N  R  V  S  T  V  Q  Q  L  T  K  R  F  S  L  G  M  L  Q  G
cgaggaccattaaaactgttcatggccctggtggcgttccttcgtttcctaacaatccca
 R  G  P  L  K  L  F  M  A  L  V  A  F  L  R  F  L  T  I  P
ccaacagcagggatactgaagagatggggaacaattaaaaaatcaaaagccattaatgtt
 P  T  A  G  I  L  K  R  W  G  T  I  K  K  S  K  A  I  N  V
ttgagagggttcaggaaagagattggaaggatgctggacatcttgaacaggagacgcaga
 L  R  G  F  R  K  E  I  G  R  M  L  D  I  L  N  R  R  R  R
actgcaggcatgatcattatgctgattccaacagtgatggcg
 T  A  G  M  I  I  M  L  I  P  T  V  M  A
```

b) pcDNA3.1/CT-TOPO vector with NLS1 fragment

```
atggggcggaaaaaggcgagaaacacgcctttcaatatgctgaaacgcgagagaaaccgc
 M  G  R  K  K  A  R  N  T  P  F  N  M  L  K  R  E  R  N  R
```

c) pcDNA3.1/CT-TOPO vector with NLS2 fragment

```
atggggaggaaagagattggaaggatgctgaacatcttgaacaggagacgcagaact
 M  G  R  K  E  I  G  R  M  L  N  I  L  N  R  R  R  R  T
```

d) R5A & K6A

```
atggatgaccaagcggcgaaggcgagaaacacgcctttcaatatgctgaaacncgagaga
 M  D  D  Q  A  A  K  A  R  N  T  P  F  N  M  L  K  X  E  R
aaccgcgtgtcgactgtacaacagctgacaaagagattctcacttggaatgctgcaggga
 N  R  V  S  T  V  Q  Q  L  T  K  R  F  S  L  G  M  L  Q  G
cgaggaccattaaaactgttcatggccctggtggcgttccttcgtttcctaacaatccca
 R  G  P  L  K  L  F  M  A  L  V  A  F  L  R  F  L  T  I  P
ccaacagcagggatactgaagagatggggaacaattaaaaaatcaaaagccattaatgtt
 P  T  A  G  I  L  K  R  W  G  T  I  K  K  S  K  A  I  N  V
ttgagagggttcaggaaagagattggaaggatgctggacatcttgaacaggagacgcaga
 L  R  G  F  R  K  E  I  G  R  M  L  D  I  L  N  R  R  R  R
actgcaggcatgatcattatgctgattccaacagtgatggcg
 T  A  G  M  I  I  M  L  I  P  T  V  M  A
```

e) K17A & R18A

```
atggatgaccaacggaaaaaggcgagaaatacgcctttcaatatgctggcggcggagaga
 M  D  D  Q  R  K  K  A  R  N  T  P  F  N  M  L  A  A  E  R
aaccgcgtgtcgactgtacaacagctgacaaagagattctcacttggaatgctgcaggga
 N  R  V  S  T  V  Q  Q  L  T  K  R  F  S  L  G  M  L  Q  G
cgaggaccattaaaactgttcatggccctggtggcgttccttcgtttcctaacaatccca
 R  G  P  L  K  L  F  M  A  L  V  A  F  L  R  F  L  T  I  P
ccaacagcagggatactgaagagatggggaacaattaaaaaatcaaaagccattaatgtt
 P  T  A  G  I  L  K  R  W  G  T  I  K  K  S  K  A  I  N  V
ttgagagggttcaggaaagagattggaaggatgctggacatcttgaacaggagacgcaga
 L  R  G  F  R  K  E  I  G  R  M  L  D  I  L  N  R  R  R  R
actgcaggcatgatcattatgctgattccaacagtgatggcg
 T  A  G  M  I  I  M  L  I  P  T  V  M  A
```

f) G42A & P43A

```
atggatgaccaacggaaaaaggcgagaaatacgcctttcaatatgctgaaacgcgagaga
 M  D  D  Q  R  K  K  A  R  N  T  P  F  N  M  L  K  R  E  R
aaccgcgtgtcgactgtacaacagctgacaaagagattctcacttggaatgctgcaggga
 N  R  V  S  T  V  Q  Q  L  T  K  R  F  S  L  G  M  L  Q  G
cgagcagcattaaaactgttcatggccctggtggcgttccttcgtttcctaacaatccca
 R  A  A  L  K  L  F  M  A  L  V  A  F  L  R  F  L  T  I  P
ccaacagcagggatactgaagagatggggaacaattaaaaaatcaaaagccattaatgtt
 P  T  A  G  I  L  K  R  W  G  T  I  K  K  S  K  A  I  N  V
ttgagagggttcaggaaagagattggaaggatgctggacatcttgaacaggagacgcaga
 L  R  G  F  R  K  E  I  G  R  M  L  D  I  L  N  R  R  R  R
actgcaggcatgatcattatgctgattccaacagtgatggcg
 T  A  G  M  I  I  M  L  I  P  T  V  M  A
```

g) R85A & K86A

```
atggatgaccaacggaaaaaggcgagaaatacgcctttcaatatgctgaaacgcgagaga
 M  D  D  Q  R  K  K  A  R  N  T  P  F  N  M  L  K  R  E  R
aaccgcgtgtcgactgtacaacagctgacaaagagattctcacttggaatgctgcaggga
 N  R  V  S  T  V  Q  Q  L  T  K  R  F  S  L  G  M  L  Q  G
cgaggaccattaaaactgttcatggccctggtggcgttccttcgtttcctaacaatccca
 R  G  P  L  K  L  F  M  A  L  V  A  F  L  R  F  L  T  I  P
ccaacagcagggatactgaagagatggggaacaattaaaaaatcaaaagccattaatgtt
 P  T  A  G  I  L  K  R  W  G  T  I  K  K  S  K  A  I  N  V
ttgagagggttcgcggcggagattggaaggatgctggacatcttgaacaggagacgcaga
 L  R  G  F  A  A  E  I  G  R  M  L  D  I  L  N  R  R  R  R
actgcaggcatgatcattatgctgattccaacagtgatggcg
 T  A  G  M  I  I  M  L  I  P  T  V  M  A
```

h) R(97-100)A

```
atggatgaccaacggaaaaaggcgagaaatacgcctttcaatatgctgaaacgcgagaga
 M  D  D  Q  R  K  K  A  R  N  T  P  F  N  M  L  K  R  E  R
aaccgcgtgtcgactgtacaacagctgacaaagagattctcacttggaatgctgcaggga
 N  R  V  S  T  V  Q  Q  L  T  K  R  F  S  L  G  M  L  Q  G
cgaggaccattaaaactgttcatggccctggtggcgttccttcgtttcctaacaatccca
 R  G  P  L  K  L  F  M  A  L  V  A  F  L  R  F  L  T  I  P
ccaacagcagggatactgaagagatggggaacaattaaaaaatcaaaagccattaatgtt
 P  T  A  G  I  L  K  R  W  G  T  I  K  K  S  K  A  I  N  V
ttgagagggttcaggaaagagattggaaggatgctgaacatcttgaacgcggcagccgct
 L  R  G  F  R  K  E  I  G  R  M  L  N  I  L  N  A  A  A  A
actgcaggcatgatcattatgctgattccaacagtgatggcg
 T  A  G  M  I  I  M  L  I  P  T  V  M  A
```

i) R5A & K6A & K17A & R18A

```
atggatgaccaagcggcgaaggcgagaaacacgcctttcaatatgctggcggcgagag
a
 M  D  D  Q  A  A  K  A  R  N  T  P  F  N  M  L  A  A  E  R
aaccgcgtgtcgactgtacaacagctgacaaagagattctcacttggaatgctgcaggg
a
 N  R  V  S  T  V  Q  Q  L  T  K  R  F  S  L  G  M  L  Q  G
cgaggaccattaaaactgttcatggccctggtggcgttccttcgtttcctaacaatccc
a
 R  G  P  L  K  L  F  M  A  L  V  A  F  L  R  F  L  T  I  P
ccaacagcagggatactgaagagatggggaacaattaaaaaatcaaaagccattaatgt
t
 P  T  A  G  I  L  K  R  W  G  T  I  K  K  S  K  A  I  N  V
ttgagagggttcaggaaagagattggaaggatgctggacatcttgaacaggagacgcag
a
 L  R  G  F  R  K  E  I  G  R  M  L  D  I  L  N  R  R  R  R
actgcaggcatgatcattatgctgattccaacagtgatggcgg
 T  A  G  M  I  I  M  L  I  P  T  V  M  A
```

j) R85A & K86A & R(97-100)A

```
atggatgaccaacggaaaaaggcgagaaatacgcctttcaatatgctgaaacgcgagaga
 M  D  D  Q  R  K  K  A  R  N  T  P  F  N  M  L  K  R  E  R
aaccgcgtgtcgactgtacaacagctgacaaagagattctcacttggaatgctgcaggga
 N  R  V  S  T  V  Q  Q  L  T  K  R  F  S  L  G  M  L  Q  G
cgaggaccattaaaactgttcatggccctggtggcgttccttcgtttcctaacaatccca
 R  G  P  L  K  L  F  M  A  L  V  A  F  L  R  F  L  T  I  P
ccaacagcagggatactgaagagatggggaacaattaaaaaatcaaaagccattaatgtt
 P  T  A  G  I  L  K  R  W  G  T  I  K  K  S  K  A  I  N  V
ttgagagggttcgcggcggagattggaaggatgctgaacatcttgaacgcggcagccgct
 L  R  G  F  A  A  E  I  G  R  M  L  N  I  L  N  A  A  A  A
actgcaggcatgatcattatgctgattccaacagtgatggcg
 T  A  G  M  I  I  M  L  I  P  T  V  M  A
```

k) Δall (R5A & K6A & K17A & R18A & R85A & K86A & R(97-100)A

```
atggatgaccaagcggcgaaggcgagaaacacgcctttcaatatgctggcggcggagag
a
 M  D  D  Q  A  A  K  A  R  N  T  P  F  N  M  L  A  A  E  R
aaccgcgtgtcgactgtacaacagctgacaaagagattctcacttggaatgctgcagga
 N  R  V  S  T  V  Q  Q  L  T  K  R  F  S  L  G  M  L  Q  G
cgaggaccattaaaactgttcatggccctggtggcgttccttcgtttcctaacaatccca
 R  G  P  L  K  L  F  M  A  L  V  A  F  L  R  F  L  T  I  P
ccaacagcagggatactgaagagatggggaacaattaaaaaatcaaaagccattaatgtt
 P  T  A  G  I  L  K  R  W  G  T  I  K  K  S  K  A  I  N  V
ttgagagggttcgcggcggagattggaaggatgctgaacatcttgaacgcggcagccgct
 L  R  G  F  A  A  E  I  G  R  M  L  N  I  L  N  A  A  A  A
actgcaggcatgatcattatgctgattccaacagtgatggcg
 T  A  G  M  I  I  M  L  I  P  T  V  M  A
```

l) DENVC-AD

```
atgaataaccaacgaaaaaaggcgagaaatacgcctttcaatatgctgaaacgcgagag
a
 M  N  N  Q  R  K  K  A  R  N  T  P  F  N  M  L  K  R  E  R
aaccgcgtgtcgactgtacaacagctgacaaagagattctcacttggaatgctgcaggg
a
 N  R  V  S  T  V  Q  Q  L  T  K  R  F  S  L  G  M  L  Q  G
cgaggaccattaaaactgttcatggccctggtggcgttccttcgtttcctaacaatccc
a
 R  G  P  L  K  L  F  M  A  L  V  A  F  L  R  F  L  T  I  P
ccaacagcagggatactgaagagatggggaacaattaaaaaatcaaaagccattaatgt
t
 P  T  A  G  I  L  K  R  W  G  T  I  K  K  S  K  A  I  N  V
ttgagagggttcaggaaagagattggaaggatgctgaacatcttgaacaggagacgcag
a
 L  R  G  F  R  K  E  I  G  R  M  L  N  I  L  N  R  R  R  R
actgcaggcatgatcattatgctgattccaacagtgatggcg
 T  A  G  M  I  I  M  L  I  P  T  V  M  A
```

m) Impα-DBD

```
atgtccaccaacgagaatgctaatacaccagctgcccgtcttcacagattcaagaacaa
g
 M  S  T  N  E  N  A  N  T  P  A  A  R  L  H  R  F  K  N  K
ggaaaagacagtacagaaatgaggcgtcgcagaatagaggtcaatgtggagctgaggaa
a
 G  K  D  S  T  E  M  R  R  R  R  I  E  V  N  V  E  L  R  K
gctaagaaggatgaccagatgctgaagaggagaaatgtaagctcatttcctgatgatgc
t
 A  K  K  D  D  Q  M  L  K  R  R  N  V  S  S  F  P  D  D  A
acttctccgctgcaggaaaaccgcaacaaccagggcactgtaaattggtctgttgatga
c
 T  S  P  L  Q  E  N  R  N  N  Q  G  T  V  N  W  S  V  D  D
attgtcaaaggcataaatagcagcaatgtggaaaatcagctccaagctactcaagctgc
c
 I  V  K  G  I  N  S  S  N  V  E  N  Q  L  Q  A  T  Q  A  A
aggaaactactttccagagaaaaacagccccccatagacaacataatccgggctggttt
g
 R  K  L  L  S  R  E  K  Q  P  P  I  D  N  I  I  R  A  G  L
attccgaaatttgtgtccttcttgggcagaactgattgtagtcccattcagtttgaatc
t
 I  P  K  F  V  S  F  L  G  R  T  D  C  S  P  I  Q  F  E  S
gcttgggcactcactaacattgcttctgggacatcagaacaaaccaaggctgtggtaga
t
 A  W  A  L  T  N  I  A  S  G  T  S  E  Q  T  K  A  V  V  D
ggaggtgccatcccagcattcatttctctgttggcatctccccatgctcacatcagtga
a
 G  G  A  I  P  A  F  I  S  L  L  A  S  P  H  A  H  I  S  E
caagctgtctgggctctaggaaacattgcaggtgatggctcagtgttccgagacttggt
t
 Q  A  V  W  A  L  G  N  I  A  G  D  G  S  V  F  R  D  L  V
attaagtacggtgcagttgacccactgttggctctccttgcagttcctgatatgtcatc
t
 I  K  Y  G  A  V  D  P  L  L  A  L  L  A  V  P  D  M  S  S
ttagcatgtggctacttacgtaatcttacctggacactttctaatctttgccgcaacaa
g
 L  A  C  G  Y  L  R  N  L  T  W  T  L  S  N  L  C  R  N  K
aatcctgcacccccgatagatgctgttgagcagattcttcctaccttagttcggctcct
g
 N  P  A  P  P  I  D  A  V  E  Q  I  L  P  T  L  V  R  L  L
catcatgatgatccagaagtattagcagatacctgctgggctatttcctaccttactga
t
 H  H  D  D  P  E  V  L  A  D  T  C  W  A  I  S  Y  L  T  D
ggtccaaatgaacgaattggcatggtggtgaaaacaggagttgtgccccaacttgtgaa
g
 G  P  N  E  R  I  G  M  V  V  K  T  G  V  V  P  Q  L  V  K
cttctaggagcttctgaattgccaattgtgactcctgccctaagagccatagggaatat
t
 L  L  G  A  S  E  L  P  I  V  T  P  A  L  R  A  I  G  N  I
```

gtcactggtacagatgaacagactcaggttgtgattgatgcaggagcactcgccgtctt
t
 V T G T D E Q T Q V V I D A G A L A V F
cccagcctgctcaccaaccccaaaactaacattcagaaggaagctacgtggacaatgtc
a
 P S L L T N P K T N I Q K E A T W T M S
aacatcacagccggccgccaggaccagatacagcaagttgtgaatcatggattagtccc
a
 N I T A G R Q D Q I Q Q V V N H G L V P
ttccttgtcagtgttctctctaaggcagattttaagacacaaaaggaagctgtgtgggc
c
 F L V S V L S K A D F K T Q K E A V W A
gtgaccaactataccagtggtggaacagttgaacagattgtgtaccttgttcactgtgg
c
 V T N Y T S G G T V E Q I V Y L V H C G
ataatagaaccgttgatgaacctcttaactgcaaaagataccaagattattctggttat
c
 I I E P L M N L L T A K D T K I I L V I
ctggatgccatttcaaatatctttcaggctgctgagaaactaggtgaaactgagaaact
t
 L D A I S N I F Q A A E K L G E T E K L
agtataatgattgaagaatgtggaggcttagacaaaattgaagctctacaaaaccatga
a
 S I M I E E C G G L D K I E A L Q N H E
aatgagtctgtgtataaggcttcgttaagcttaattgagaagtatttctctgtagagga
a
 N E S V Y K A S L S L I E K Y F S V E E
gaggaagatcaaaacgttgtaccagaaactacctctgaaggctacactttccaagttca
g
 E E D Q N V V P E T T S E G Y T F Q V Q
gatggggctcctgggacctttaacttt
 D G A P G T F N F

n) T25A

atggatgaccaacggaaaaaggcgagaaatacgcctttcaatatgctgaaacgcgagag
a
 M D D Q R K K A R N T P F N M L K R E R
aaccgcgtgtcggcagtacaacagctgacaaagagattctcacttggaatgctgcaggg
a
 N R V S A V Q Q L T K R F S L G M L Q G
cgaggaccattaaaactgttcatggccctggtggcgttccttcgtttcctaacaatccc
a
 R G P L K L F M A L V A F L R F L T I P
ccaacagcagggatactgaagagatggggaacaattaaaaaatcaaaagccattaatgt
t
 P T A G I L K R W G T I K K S K A I N V

```
ttgagagggttcaggaaagagattggaaggatgctggacatcttgaacaggagacgcag
a
 L  R  G  F  R  K  E  I  G  R  M  L  D  I  L  N  R  R  R  R
actgcaggcatgatcattatgctgattccaacagtgatggcg
 T  A  G  M  I  I  M  L  I  P  T  V  M  A
```

o) T30A

```
atggatgaccaacggaaaaaggcgagaaatacgcctttcaatatgctgaaacgcgagag
a
 M  D  D  Q  R  K  K  A  R  N  T  P  F  N  M  L  K  R  E  R
aaccgcgtgtcgactgtacaacagctggcaaagagattctcacttggaatgctgcaggg
a
 N  R  V  S  T  V  Q  Q  L  A  K  R  F  S  L  G  M  L  Q  G
cgaggaccattaaaactgttcatggccctggtggcgttccttcgtttcctaacaatccc
a
 R  G  P  L  K  L  F  M  A  L  V  A  F  L  R  F  L  T  I  P
ccaacagcagggatactgaagagatggggaacaattaaaaaatcaaaagccattaatgt
t
 P  T  A  G  I  L  K  R  W  G  T  I  K  K  S  K  A  I  N  V
ttgagagggttcaggaaagagattggaaggatgctggacatcttgaacaggagacgcag
a
 L  R  G  F  R  K  E  I  G  R  M  L  D  I  L  N  R  R  R  R
actgcaggcatgatcattatgctgattccaacagtgatggcg
 T  A  G  M  I  I  M  L  I  P  T  V  M  A
```

p) S34A

```
atggatgaccaacggaaaaaggcgagaaatacgcctttcaatatgctgaaacgcgagag
a
 M  D  D  Q  R  K  K  A  R  N  T  P  F  N  M  L  K  R  E  R
aaccgcgtgtcgactgtacaacagctgacaaagagattcgcacttggaatgctgcaggg
a
 N  R  V  S  T  V  Q  Q  L  T  K  R  F  A  L  G  M  L  Q  G
cgaggaccattaaaactgttcatggccctggtggcgttccttcgtttcctaacaatccc
a
 R  G  P  L  K  L  F  M  A  L  V  A  F  L  R  F  L  T  I  P
ccaacagcagggatactgaagagatggggaacaattaaaaaatcaaaagccattaatgt
t
 P  T  A  G  I  L  K  R  W  G  T  I  K  K  S  K  A  I  N  V
ttgagagggttcaggaaagagattggaaggatgctggacatcttgaacaggagacgcag
a
 L  R  G  F  R  K  E  I  G  R  M  L  D  I  L  N  R  R  R  R
actgcaggcatgatcattatgctgattccaacagtgatggcg
 T  A  G  M  I  I  M  L  I  P  T  V  M  A
```

q) T71A

```
atggatgaccaacggaaaaaggcgagaaatacgcctttcaatatgctgaaacgcgagag
a
 M  D  D  Q  R  K  K  A  R  N  T  P  F  N  M  L  K  R  E  R
aaccgcgtgtcgactgtacaacagctgacaaagagattctcacttggaatgctgcaggg
a
 N  R  V  S  T  V  Q  Q  L  T  K  R  F  S  L  G  M  L  Q  G
cgaggaccattaaaactgttcatggccctggtggcgttccttcgtttcctaacaatccc
a
 R  G  P  L  K  L  F  M  A  L  V  A  F  L  R  F  L  T  I  P
ccaacagcagggatactgaagagatggggagcaattaaaaaatcaaaagccattaatgt
t
 P  T  A  G  I  L  K  R  W  G  A  I  K  K  S  K  A  I  N  V
ttgagagggttcaggaaagagattggaaggatgctggacatcttgaacaggagacgcag
a
 L  R  G  F  R  K  E  I  G  R  M  L  D  I  L  N  R  R  R  R
actgcaggcatgatcattatgctgattccaacagtgatggcg
 T  A  G  M  I  I  M  L  I  P  T  V  M  A
```

r) T101A

```
atggatgaccaacggaaaaaggcgagaaatacgcctttcaatatgctgaaacgcgagag
a
 M  D  D  Q  R  K  K  A  R  N  T  P  F  N  M  L  K  R  E  R
aaccgcgtgtcgactgtacaacagctgacaaagagattctcacttggaatgctgcaggg
a
 N  R  V  S  T  V  Q  Q  L  T  K  R  F  S  L  G  M  L  Q  G
cgaggaccattaaaactgttcatggccctggtggcgttccttcgtttcctaacaatccc
a
 R  G  P  L  K  L  F  M  A  L  V  A  F  L  R  F  L  T  I  P
ccaacagcagggatactgaagagatggggaacaattaaaaaatcaaaagccattaatgt
t
 P  T  A  G  I  L  K  R  W  G  T  I  K  K  S  K  A  I  N  V
ttgagagggttcaggaaagagattggaaggatgctggacatcttgaacaggagacgcag
a
 L  R  G  F  R  K  E  I  G  R  M  L  D  I  L  N  R  R  R  R
gcagcaggcatgatcattatgctgattccaacagtgatggcg
 A  A  G  M  I  I  M  L  I  P  T  V  M  A
```

s) FLAG-tagged DENV C protein

Preprotrypsin leader sequence — FLAG

```
atgtctgcacttctgatcctagctcttgttggagctgcagttgctgactacaaagacgat
 M  S  A  L  L  I  L  A  L  V  G  A  A  V  A  D  Y  K  D  D
```

tag — FLAG tag

```
gacgacaagcttgactacaaagacgatgacgacaagggactagtaccgcgcggcagcatg
 D  D  K  L  D  Y  K  D  D  D  D  K  G  L  V  P  R  G  S  M
```

Thrombin Cleavage Site

```
aataaccaacggaaaaaggcgagaaatacgcctttcaatatgctgaaacgcgagagaaac
 N  N  Q  R  K  K  A  R  N  T  P  F  N  M  L  K  R  E  R  N
cgcgtgtcgactgtacaacagctgacaaagagattctcacttggaatgctgcagggacga
 R  V  S  T  V  Q  Q  L  T  K  R  F  S  L  G  M  L  Q  G  R
ggaccattaaaactgttcatggccctggtggcgttccttcgtttcctaacaatcccacca
 G  P  L  K  L  F  M  A  L  V  A  F  L  R  F  L  T  I  P  P
acagcagggatactgaagagatggggaacaattaaaaaatcaaaagccattaatgttttg
 T  A  G  I  L  K  R  W  G  T  I  K  K  S  K  A  I  N  V  L
agagggttcaggaaagagattggaaggatgctgaacatcttgaacaggagacgcagaact
 R  G  F  R  K  E  I  G  R  M  L  N  I  L  N  R  R  R  R  T
gcaggcatgatcattatgctgattccaacagtgatggcg
 A  G  M  I  I  M  L  I  P  T  V  M  A
```

t) Biotinylated DENV C protein

His Tag

```
atgggcagcagccatcatcatcatcacagcagcggcctggtgccgcgcggcagccat
 M  G  S  S  H  H  H  H  H  H  S  S  G  L  V  P  R  G  S  H
```

Thrombin Cleavage Site

```
atggctagctccggcctgaacgacatcttcgaggctcagaaaatcgaatggcacgaaggc
 M  A  S  S  G  L  N  D  I  F  E  A  Q  K  I  E  W  H  E  G
ggcgatgacgacgacaagagc
 G  D  D  D  D  K  S
```

Enterokinase Cleavage Site — Signal Peptide

```
                    atgaataaccaacgaaaaaaggcgagaaatacgcctttc
                     M  N  N  Q  R  K  K  A  R  N  T  P  F
aatatgctgaaacgcgagagaaaccgcgtgtcgactgtacaacagctgacaaagagattc
 N  M  L  K  R  E  R  N  R  V  S  T  V  Q  Q  L  T  K  R  F
tcacttggaatgctgcagggacgaggaccattaaaactgttcatggccctggtggcgttc
 S  L  G  M  L  Q  G  R  G  P  L  K  L  F  M  A  L  V  A  F
cttcgtttcctaacaatcccaccaacagcagggatactgaagagatggggaacaattaaa
 L  R  F  L  T  I  P  P  T  A  G  I  L  K  R  W  G  T  I  K
aaatcaaaagccattaatgttttgagagggttcaggaaagagattggaaggatgctgaac
 K  S  K  A  I  N  V  L  R  G  F  R  K  E  I  G  R  M  L  N
atcttgaacaggagacgcagaactgcaggcatgatcattatgctgattccaacagtgatg
 I  L  N  R  R  R  R  T  A  G  M  I  I  M  L  I  P  T  V  M
gcgtaa
 A  -
```

DENV C Protein

Biochemical and Biophysical Research Communications 389 (2009) 63–69

Contents lists available at ScienceDirect

Biochemical and Biophysical Research Communications

journal homepage: www.elsevier.com/locate/ybbrc

Specific interaction of capsid protein and importin-α/β influences West Nile virus production

Raghavan Bhuvanakantham, Mun-Keat Chong, Mah-Lee Ng *

Flavivirology Laboratory, Department of Microbiology, 5 Science Drive 2, National University of Singapore, Singapore 117597, Singapore

ARTICLE INFO

Article history:
Received 31 July 2009
Available online 25 August 2009

Keywords:
Capsid
Importin
Binding strength
Virus production

ABSTRACT

West Nile virus (WNV) capsid (C) protein has been shown to enter the nucleus of infected cells. However, the mechanism by which C protein enters the nucleus is unknown. In this study, we have unveiled for the first time that nuclear transport of WNV and Dengue virus C protein is mediated by their direct association with importin-α. This interplay is mediated by the consensus sequences of bipartite nuclear localization signal located between amino acid residues 85–101 together with amino acid residues 42 and 43 of C protein. Elucidation of biological significance of importin-α/C protein interaction demonstrated that the binding efficiency of this association influenced the nuclear entry of C protein and virus production. Collectively, this study illustrated the molecular mechanism by which the C protein of arthropod-borne flavivirus enters the nucleus and showed the importance of importin-α/C protein interaction in the context of flavivirus life-cycle.

Introduction

The *Flaviviridae* family consists of major disease causing pathogens such as West Nile virus (WNV), Dengue virus (DENV) and Yellow Fever virus (YFV). West Nile virus causes fever and encephalitic maladies in both avian and human hosts [1]. Its RNA genome encodes a single large polyprotein, which is processed by viral and host proteases into three structural proteins; capsid (C), membrane (M) and envelope (E) as well as seven non-structural proteins [2]. The virus RNA genome is packaged within a spherical nucleocapsid composed of multiple copies of C proteins. The nucleocapsid is further enwrapped by a modified lipid bilayer derived from host cellular membranes through insertion of virus E/M proteins [3].

The C proteins of various flaviviruses are localized in the cytoplasm and nuclei [4–7]. Wang and group [6] reported that when three copies of GFP were tagged with DENV C protein, it was able to enter nucleus. Although this suggested the presence of active transport system for C protein, the exact mechanism by which C protein of arthropod-borne flaviviruses enters the nucleus is unknown.

In this study, we investigated the molecular mechanism mediating the nuclear entry of WNV C protein by examining the involvement of importins. We showed that nuclear transport of arthropod-borne flavivirus C protein is mediated by importin-α/β complex and the interaction between C protein and importin-α is important for efficient nuclear localization of C protein and virus production.

Methods

Cells and viruses. Vero cells were grown in M199 (Sigma) at 37 °C in a humidified 5% CO_2 incubator. West Nile virus (Sarafend) and Dengue 2 virus (NGC), gifts from Emeritus E.G. Westaway (Sir Albert Sakzewski Virus Research Centre, Australia) were used.

Cloning. The cDNA coding sequences of WNV C protein were cloned into pcDNA3.1CT-GFP and pcDNA3.1TOPO-V5-His vectors (Invitrogen) to form pTCS and pV5CS, respectively. Truncated WNV C gene lacking 39 amino acids (aa) from carboxyl-terminus and the bipartite nuclear localization signal (NLS) motif of WNV C protein were cloned into pcDNA3.1CT-GFP to get pTCSΔ39 and pWNLS plasmids, respectively. The cDNA coding sequences of DENV full-length C or NLS regions were cloned into pcDNA3.1CT-GFP to get pDC or pDNLS, respectively.

The basic residues in the bipartite NLS sequence were mutated using QuikChange™ site-directed mutagenesis kit (Stratagene). The basic residues at positions 85/86 (M1), 97/98 (M2) and 85/86/97/98 (M1M2) of WNV C protein in pTCS were mutated to create pTCSM1, pTCSM2 and pTCSM1M2, respectively. Mutagenesis was also performed to obtain pTCSG42A, pTCSP43A and pTCSGP4243AA plasmids, which carried the mutations at aa 42 and/or 43 (4243) of C protein. The mutations M1, M2, M1M2 and 4243 were introduced into recombinant DENV C protein to obtain pDCM1/pDCM2/pDCM1M2/pDCGP4243AA plasmids.

* Corresponding author. Fax: +65 67766872.
E-mail address: micngml@nus.edu.sg (M.-L. Ng).

0006-291X/$ - see front matter © 2009 Elsevier Inc. All rights reserved.
doi:10.1016/j.bbrc.2009.08.108

Mutations were also introduced into C protein of full-length WNV infectious clone (pWNS, [8]) to obtain pWNSM1/pWNSM2/pWNSM1M2/pWNS4243 plasmids. In addition, we deleted the NLS region of C protein from pWNS clone to obtain pWNSΔNLS. The clones/mutants used in this study were shown in Supplementary Table S1.

Indirect immuno-fluorescence analysis (IFA). Vero cells (5×10^5) were infected with WNV or transfected with various mutated plasmids (WNV/DENV) and processed for IFA at the indicated timings as described earlier [8]. WNV C protein was detected with anti-WNVC (gift from Emeritus Prof. Westaway) and FITC/Texas Red-conjugated anti-rabbit IgG antibodies (Amersham Pharmacia). Optical immuno-fluorescence microscope (Olympus IX-81) was used to visualize the specimens. The images were taken at 100× magnification under oil immersion objective using Metamorph version 6 software (Universal Imaging Corporation).

Co-immunoprecipitation assay. Vero cells (5×10^5) were infected with WNV or electroporated with 20 μg of *in vitro* transcribed RNAs from pWNS/mutated pWNS plasmids as described earlier [8]. Various DENV C mutants were also transfected into Vero cells. At 14 h post-infection (p.i.) or 24 h post-transfection, cells were lysed using lysis buffer (Miltenyi Biotec) and cell lysates were pre-mixed with 2 μg of anti-GFP/anti-importin-α/anti-importin-β (Sigma) conjugated magnetic microbeads and purified using μMACs column (Miltenyi Biotec). Samples obtained from co-immunoprecipitation or transfected cell lysates were subjected to Western blotting using anti-importin-α/anti-importin-β/anti-GFP/anti-WNVC antibodies (Ab).

Mammalian two-hybrid (M2H) assay. Mammalian two-hybrid assays were performed as described by Bhuvanakantham and Ng [9]. Briefly, WNV/DENV C protein as well as mutated C proteins were amplified and joined to pSV40-GAL4 5′ element and SV40 pA 3′ element to create bait proteins of interest. Similarly, the prey protein (importin-α) was constructed using pSV40-VP16 5′ element and SV40 pA 3′ element. Co-transfection was performed using the DNA linear constructs generated from above along with pGAL/*lacZ* plasmid using Lipofectamine2000 (Invitrogen). At 12, 24 and 48 h post-transfection, β-galactosidase assay was performed as mentioned earlier [9] and the specific activity of the samples were calculated using the following formula: nmoles of ortho-nitrophenyl-β-D-galactopyranoside hydrolyzed/incubation-time/mg protein.

Far Western blotting. TNT quick-coupled transcription/translation system (Promega) was used to *in vitro* translate Myc-tagged C/E protein and importin-α/β at 30 °C for 1.5 h following manufacturer's instructions. The presynthesized Myc-tagged C, Myc-tagged E protein, importin-α and importin-β were purified using anti-Myc, anti-importin-α- or anti-importin-β-conjugated magnetic beads as mentioned earlier. Purified C/E/importin-α protein was fractionated on polyacrylamide denaturing gels and transferred onto PVDF membranes. Blots were blocked in binding buffer (20 mM HEPES KOH [pH 7.6], 75 mM KCl, 2.5 mM $MgCl_2$, 0.1 mM EDTA, 0.05% NP-40, 1 mM dithiothreitol, 1% BSA), followed by incubation at 4 °C overnight in binding buffer containing 20 nM of purified importin-α, importin-β or mixture of importin-α and importin-β. The C/E-bound importin-α, C/E-bound importin-β or importin-α-bound importin-β were detected using anti-importin-α or anti-importin-β Ab.

Virus growth kinetics. Vero cells (5×10^5) were transfected with 20 μg of purified RNA obtained from pWNS, pWNSΔNLS, pWNSM1, pWNSM2, pWNSM1M2, and pWNS4243 clones. At various time points post-electroporation, culture supernatant was collected to measure the growth characteristics of the resulting viruses by plaque assay.

Complementation analysis. Vero cells (5×10^5) were transfected with pV5CS plasmid using Lipofectamine2000. Twenty four hours post-transfection, electroporation was performed using 20 μg of RNAs transcribed from pWNS, pWNSΔNLS, pWNSM1, pWNSM2, pWNSM1M2 and pWNS4243 clones. At 12, 24, 36, 48 and 56 h post-electroporation, culture supernatants were sampled for plaque assay.

Results

Importin-mediated nuclear translocation of WNV C protein

Consistent with previous studies [7,10], we showed that WNV C protein entered the nucleus during infection and transfection (Supplementary Fig. S1A and B) using time series studies coupled with IFA. DENV C protein also localized to the nucleoli of the transfected cells (Supplementary Fig. S1C). Subsequently, we wanted to determine if importin-α/β played a role in mediating the nuclear translocation of WNV C protein. Vero cells were infected with WNV and at 14 h p.i., cell lysates were precipitated with anti-importin-α/β Ab and immunoblotted using anti-WNVC Ab. As shown in Fig. 1A(i and ii, Lane 3), the immuno-reactive band was observed only with WNV-infected cell lysates. This indicated that WNV C protein binds to the nuclear receptors, importin-α and importin-β.

Appropriate controls such as precipitation control [Fig. 1A(iii and iv)], input controls [Fig. 1A(v–vii)] and antibody isotype control [Fig. 1A(viii)] were included to demonstrate the specificity of interaction between WNV C protein and importin-α/β. Moreover, no interaction between importin-α and flavivirus E protein was detected (data not shown). Similarly, DENV C protein also interacted with importin-α (data not shown). This demonstrated that flavivirus C protein exploits importin-α/β complex for nuclear entry.

To reaffirm these results, M2H analysis was performed by co-transfecting C (bait), importin-α/β (prey) and the reporter plasmid encoding β-galactosidase gene. At 24 h post-transfection, cells were harvested for β-galactosidase assay. As shown in Fig. 1B, strong β-galactosidase activity was observed only with C protein and importin-α (C + Impa) and not with C protein and importin-β (C + Impb). This indicated that C protein interacted with importin-α and not with importin-β. Therefore, the C-importin–β interaction as suggested by co-immunoprecipitation [Fig. 1A(ii)], could be an indirect interaction mediated by importin-α.

To test this hypothesis, Far Western blotting was performed. Equal amounts of *in vitro* translated Myc-tagged C/E/importin-α protein [Fig. 1C(i, ii, and v)] was fractionated by SDS–PAGE and blotted to PVDF membrane. The blot was probed with importin-α (i), importin-β (ii,v) or mixture of importin-α and importin-β (iii). The formation of C/E-importin-α, C/E-importin-β or importin-α/β complex was then analyzed by immunoblotting with anti-importin-α (i) or anti-importin-β (ii,iii,v) Ab. The immuno-reactive bands were observed with C-importin-α [Lane 2, (i)], C-importin-α/β mixture [Lane 2, (iii)] and importin-α–importin-β (v). No bands were observed with E-importin-α [Lane 1, (i)] and C/E-importin-β [Lanes 1 and 2, (ii)]. Collectively, the absence of band with C-importin-β (ii) and the presence of band with C-importin-α/β mixture (iii) as well as importin-α–importin-β (v) confirmed that C protein interacted with importin-α directly and importin-α served as a bridge between C protein and importin-β.

NLS-mediated interaction between C protein and importin-α

Prosite scanning (http://ca.expasy.org/prosite) of WNV C protein revealed the presence of nuclear localization signal (NLS) between aa 85 and 101 (KKELGTLTSAINRRST). To verify the functionality of the predicted NLS motif, Vero cells were transfected with pWNLS/pTCSΔ39 and their cellular localization was visualized using IFA. Strong nucleolar localization [Fig. 2A (i)-arrows]

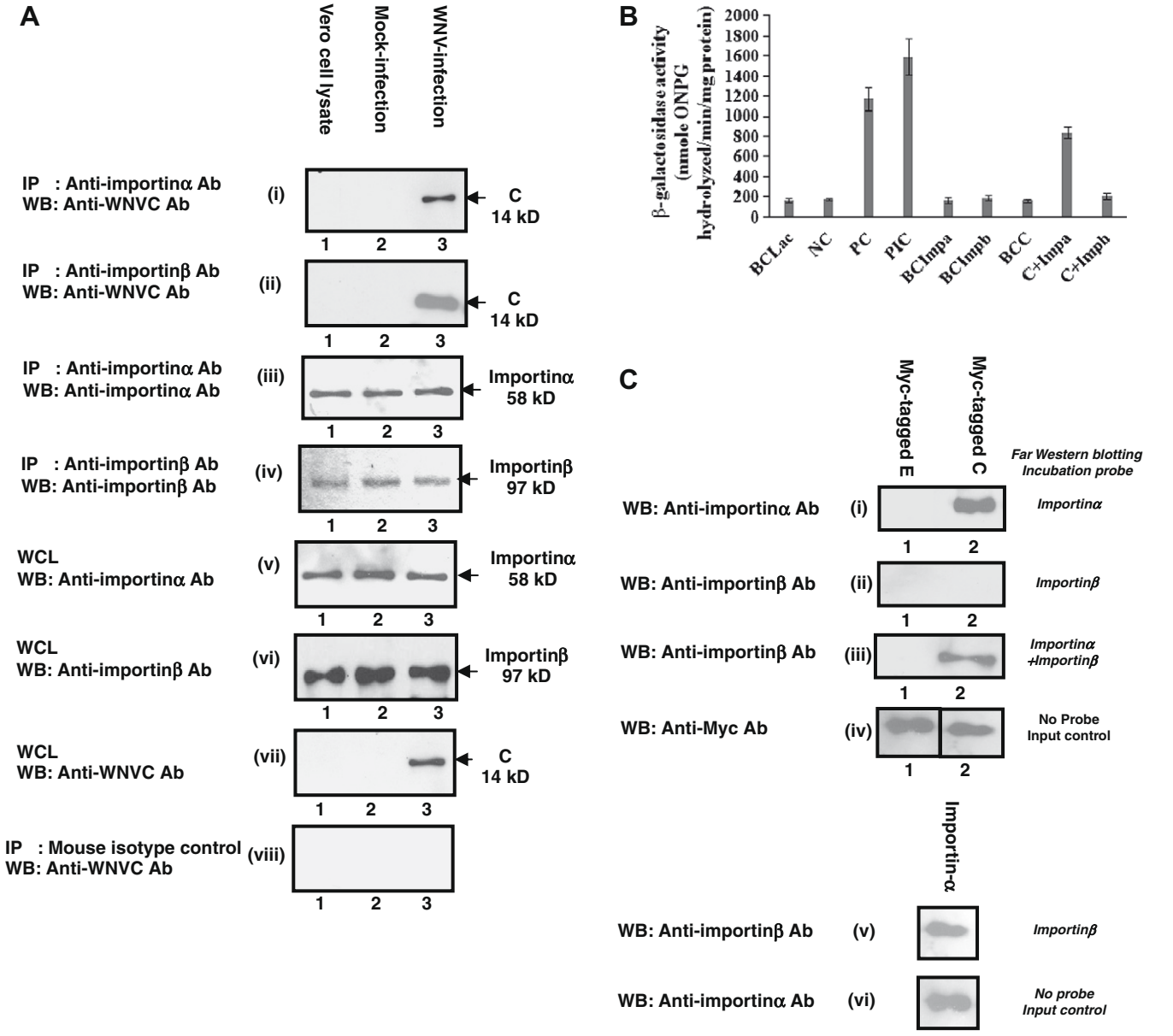

Fig. 1. Interaction between WNV C protein and importin-α. (A) Co-immunoprecipitation studies. Vero cells were infected with WNV and cell lysates were immunoprecipitated with anti-importin-α(i)/β(ii) Ab and immunoblotted with anti-C Ab. The presence of band in Lane 3 confirms C protein-importin-α/β binding in WNV-infected Vero cells. (iii and iv) Precipitation controls to ensure successful precipitation in all experimental groups. (v–vii) The amount of endogenous importin-α, importin-β and C protein in whole cell lysates (WCL) is detected using anti-importin-α/β and anti-C Abs (input controls). (viii) Mouse isotype Ab control to eliminate the possibility of non-specific precipitation. (B) M2H assay. BCLac and NC are negative controls. PC and PIC represent positive control and positive interaction control, respectively. bcc, BCImpa and BCImpb represent the background controls for bait protein (C) and prey proteins (importin-α/β, respectively. C + Impa/C + Impb represent the interacting partners. Strong interaction signal is only observed for C protein/importin-α (C + Impa) pairing. (C) Far Western blotting. *In vitro* translated Myc-C/Myc-E/importin-α was subjected to Western blotting. The blot was then incubated with importin-α and/or importin-β. The presence of C/E-importin-α or C/E-importin-β complexes is analyzed by immunoblotting with anti-importin-α (i) or anti-importin-β (ii and iii) Ab. The membrane-bound C/E/importin-α is also detected using anti-Myc/anti-importin-α Ab (iv and vi). The presence of importin-α–importin-β complex is analyzed by immunoblotting with anti-importin-β Ab (v).

was observed in pWNLS-transfected cells and predominant cytoplasmic distribution was observed in pTCSΔ39-transfected cells [Fig. 2A (ii)-arrows]. Similar results were obtained with DENV NLS motif (Supplementary Fig. S2). This confirmed that the predicted bipartite NLS motif of flavivirus C protein is functional.

Proteins containing NLS region generally interact with importin-α through their NLS motif. We thus deleted the entire NLS region on C protein from pWNS (pWNSΔNLS) to examine the requisite of NLS motif in mediating C-importin-α binding. The RNAs *in vitro* transcribed from pWNS and pWNSΔNLS were electroporated into Vero cells. Co-immunoprecipitation was performed using anti-importin-α Ab and immunoblotted with anti-WNVC Ab. The band was detected in pWNS-RNA-transfected cells [Lane 2, Fig. 2B (i)] and no band was observed in pWNSΔNLS-RNA-transfected cells [Lane 3, Fig. 2B (i)]. This confirmed that C protein–importin-α association is mediated by NLS motif.

Mutagenesis studies to determine the amino acids mediating importin-α/C protein binding

To define the residues mediating C protein–importin-α association, we performed site-directed mutagenesis on the consensus basic residues within the bipartite NLS motif of C protein in pWNS to generate pWNSM1, pWNSM2 and pWNSM1M2. Since Glycine42

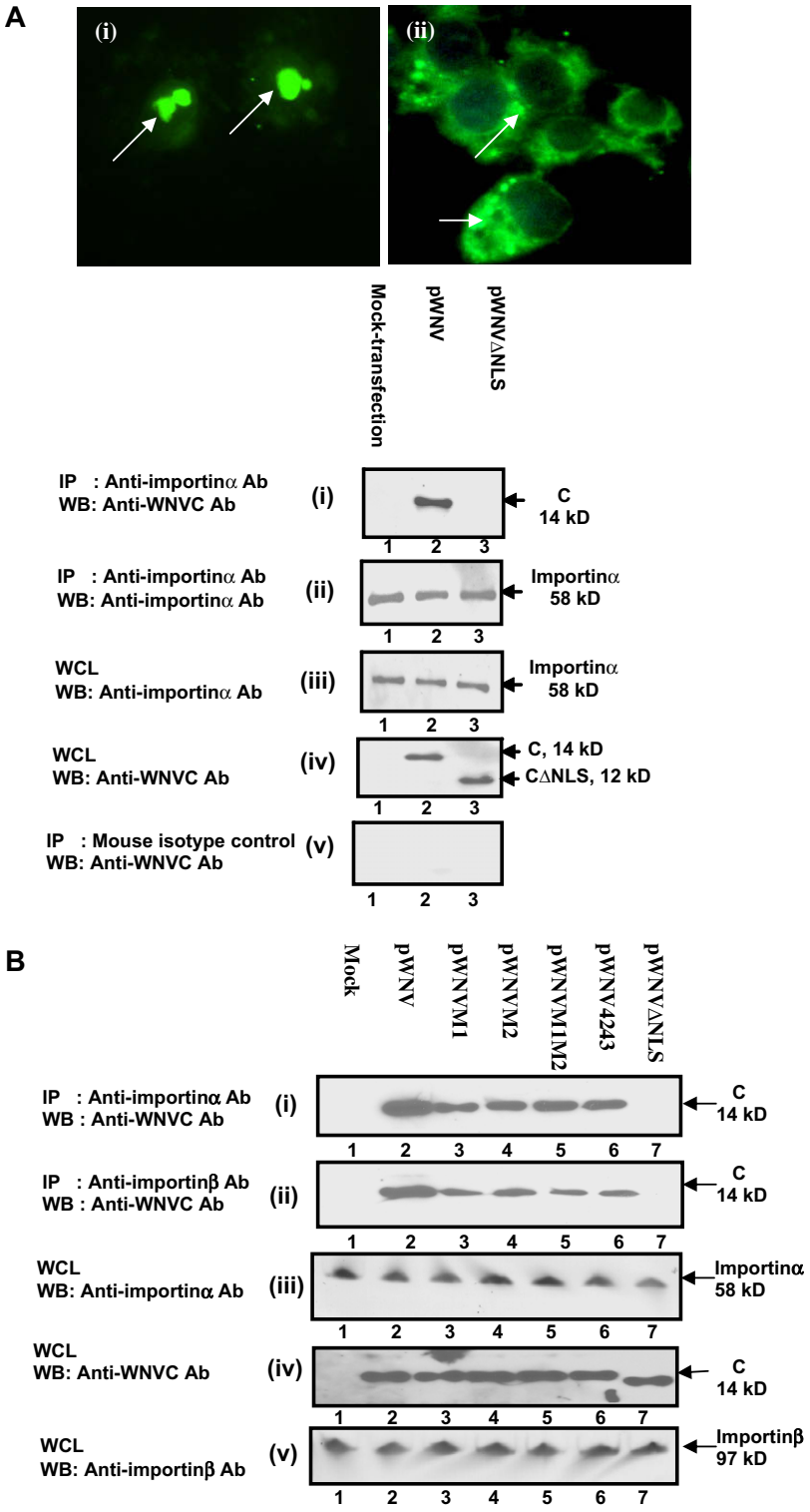

Fig. 2. NLS-mediated interplay between C protein and importin-α. (A) pWNLS transfected into Vero cells shows intense green fluorescence in the nucleoli region (arrows, i) in contrast to pTCSΔ39-transfected cells where only cytoplasmic fluorescence is observed even after 24 h post-transfection (arrows, ii). (B) Co-immunoprecipitation. Vero cells transfected with RNAs *in vitro* transcribed from pWNV/pWNVΔNLS were immunoprecipitated with anti-importin-α Ab and immunoblotted with anti-C Ab. The presence of band in Lane 2 and absence of band in Lane 3 confirm that C protein–importin-α binding is mediated by the NLS motif of C protein. (ii–v) Precipitation control, input controls and mouse isotype Ab controls. (C) Co-immunoprecipitation. Vero cells were transfected with RNA transcribed from pWNS/pWNSM1/pWNSM2/pWNSM1M2/pWNS4243/pWNSΔNLS plasmids. At 24 h post-transfection, immunoprecipitation was performed using anti-importin-α (i) or anti-importin-β (ii) Ab followed by immunoblotting using anti-WNVC Ab. The presence of bands in Lanes 2–6 and absence of bands in Lane 7 in anti-importin-α–β antibody-immunoprecipitated samples confirm the binding between importin-α/β and mutated C proteins except for pWNSΔNLS. (iii–v) Input controls.

and Proline43 of Japanese encephalitis virus (JEV) C protein influenced its nuclear translocation [4], these residues were also mutated to obtain pWNS4243 mutant. The RNAs transcribed from pWNS, pWNSM1, pWNSM2, pWNSM1M2, pWNS4243 and pWNSΔNLS were then electroporated into Vero cells and co-immunoprecipitation was performed using anti-importin-α/β Ab and

immunoblotted using anti-WNVC Ab. The interaction between importin-α/β and intact/mutated C protein was observed with all the introduced mutations except pWNSΔNLS [Fig. 2C (i and ii)], although the band intensity observed with pWNSM1, pWNSM2, pWNSM1M2, pWNS4243 mutants were lower (Lanes 3–6) compared to pWNS (Lane 2). The reduced band intensity on the immunoblot observed with M1, M2, M1M2 and 4243 mutations indicated that the basic residues of NLS motif and the residues 42/43 of C protein were important in modulating C-importin interaction.

Measuring the strength of interaction between importin-α and C protein

Since the above co-immunoprecipitation results [Fig. 2C (i and ii)] suggested altered binding efficiency between importin-α and M1/M2/M1M2/4243 mutants, we measured the strength of interaction between mutated C protein and importin-α using M2H analysis. The binding strength between importin-α and intact/mutated C protein varied significantly ($P < 0.05$, Fig. 3A). Moreover, the binding between mutated C and importin-α was significantly lower ($P < 0.05$) at 12 h post-transfection compared to 24 and 48 h post-transfection. Similar trends were observed with DENV C protein (Supplementary Fig. S3).

Cellular localization of mutated C protein

To investigate if the introduced mutations influence the nuclear localization pattern of C protein, IFA was performed in Vero cells transfected with pTCSM1/pTCSM2/pTCSM1M2 plasmids. At 12 h post-transfection [Fig. 3B (i, iv, vii)], intense fluorescence was

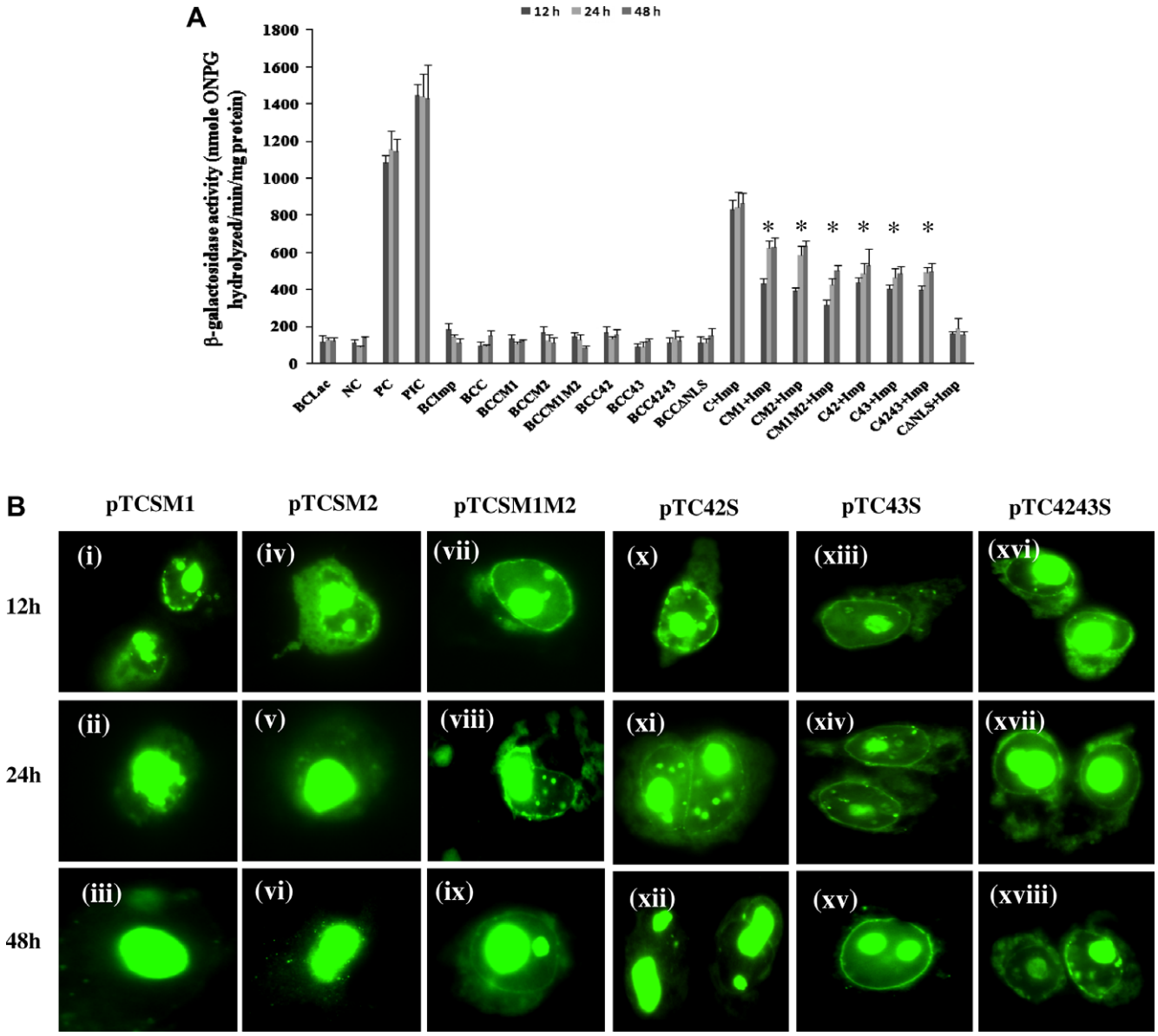

Fig. 3. Strength of interaction between WNV C protein and importin-α and its influence on nuclear translocation. (A) M2H assay. BCC, BCCM1, BCCM2, BCCM1M2, BCC42, BCC43, BCC4243 and BCCΔNLS represent the background controls for full-length/mutated/truncated C proteins (bait). BCImp represents the background control for the prey protein (importin-α C + Imp, CM1 + Imp, CM2 + Imp, CM1M2 + Imp, C42 + Imp, C43 + Imp, C4243 + Imp and CΔNLS + Imp represent the interacting partners. The binding strength is significantly higher for full-length C protein/importin-α pairing compared to other mutated C proteins/importin-α pairings while there is no detectable binding between CΔNLS and importin-α. *Represents $P < 0.05$. (B) IFA. Vero cells transfected with the different mutant plasmids, pTCSM1 (i–iii), pTCSM2 (iv–vi), pTCSM1M2 (vii–ix), pTCSG42A (x–xii), pTCSP43A (xiii–xv) and pTCSGP4243AA (xvi–xviii) were processed for IFA. The pTCSM1, pTCSM2, pTCSM1M2, pTCSG42A, pTCSP43A and pTCSGP4243AA mutants show strong fluorescence predominantly in nucleus and perinuclear regions at 12 h post-transfection compared to predominant nuclear staining at late timings (24/48 h post-transfection).

detected around the nuclear membrane and in the nuclei/nucleoli of mutated plasmids-transfected cells. At 24 [Fig. 3B (ii, v, viii)] and 48 h [Fig. 3B (iii, vi, ix)] post-transfection, peri-nuclear staining was not as prominent except for pTCSM1M2 [Fig. 3B (viii)]. Vero cells transfected with pTCSG42A/pTCSP43A/pTCSGP4243AA plasmids also showed strong fluorescence signal in the nucleoli with peri-nuclear staining [Fig. 3B (x–xviii)] at all time points. The kinetics of WNV C protein nuclear localization at 12/24/48 h post-transfection was also measured by enumerating 50 transfected cells displaying peri-nuclear and/or nuclear staining (Supplementary Fig. S4A). The kinetics of nuclear entry of mutant C proteins correlated with the binding efficiency of these mutants with importin-α at the respective timings (Fig. 3A).

Similar to WNV, the mutations introduced into DENV C protein also altered the nuclear localization pattern of C protein (Supplementary Fig. S4B and C). Collectively, these results implied that the mutations introduced on C protein led to reduced binding efficiency with importin-α, and thus interfered with the nuclear localization ability of arthropod-borne flavivirus C proteins.

Growth kinetics of pWNS mutants and trans complementation studies

To examine if virus replication is affected by the introduced mutations, virus growth characteristics in Vero cells transfected with pWNS-/pWNSM1-/pWNSM2-/pWNSM1M2-/pWNS4243-/pWNSΔNLS-RNA were measured (Fig. 4). The pWNSM1/pWNSM2/pWNSM1M2/pWNS4243 mutants showed 2–3 log units reduction in their virus titres at all timings compared to parental WNV (pWNS) (Fig. 4A, $P < 0.05$). The pWNSΔNLS mutant did not generate any viable virus even after 120 h post-transfection (Fig. 4A). The observed differences in growth characteristics of these mutant viruses correlated with the binding efficiency of the corresponding mutant C proteins with importin-α.

To ensure that the altered growth kinetics observed were not due to random second-site mutations, we performed complementation analysis using V5-tagged full-length C protein (pV5CS). This positive complementation restored the virus titre of pWNSM1/pWNSM2/pWNSM1M2/pWNS4243 mutants, comparable to pWNS (Fig. 4B). Viable, single-round infectious virus was also obtained from pWNSΔNLS-RNA transfected cells (Fig. 4B). The ability of full-length C protein to resuscitate the defective nature of pWNSΔNLS virus eliminated the possibility that the defective phenotype was caused by serendipitous inactivating mutations that may have occurred in other parts of the virus genome. Hence, this signifies that virus production was significantly compromised by all the introduced mutations and that the bipartite NLS motif in WNV C protein is vital for efficient virus production.

Discussion

Studies have demonstrated that C proteins of flavivirus were observed in both cytoplasm and nucleus [4–7]. However, the exact mechanism by which arthropod-borne flavivirus C protein enters the nucleus is unknown. Nuclear translocation of several proteins containing NLS motif is generally mediated by importins [11]. Since our study confirmed the presence of functional NLS motif

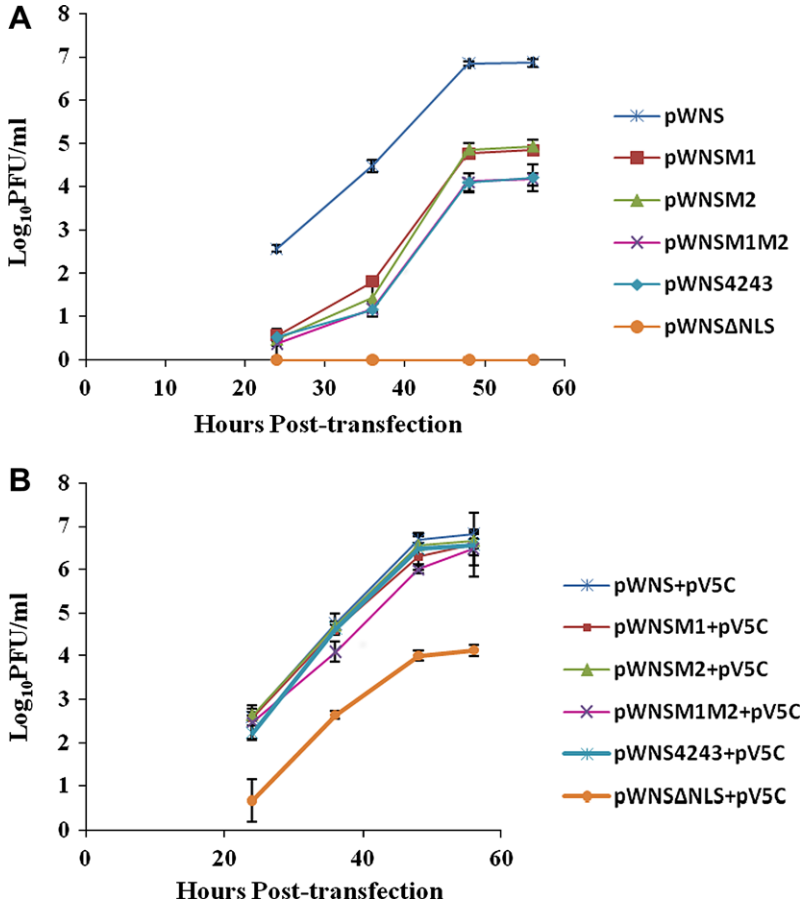

Fig. 4. Comparison of growth kinetics for parental WNV (pWNS) and various mutated pWNS. (A). All the mutants show reduced virus titre except pWNSΔNLS which failed to produce detectable levels of viable virus. (B) Complementation studies with pV5CS are able to restore virus production in various mutants-RNA transfected cells, comparable to pWNS, except for pWNSΔNLS where virus production is partially restored. The average value with standard deviation (±) is a representative from three independent experiments.

on WNV/DENV C protein (Fig. 2A and Supplementary Fig. S2), we investigated the role of importins in mediating the active transportation of flavivirus C protein into nucleus. Co-immunoprecipitation and M2H analyses confirmed that the nuclear translocation of WNV/DENV C protein occurs through importin-dependant pathway (Fig. 1). Using a combination of M2H analysis and Far Western blotting, we showed that C protein associated with importin-α directly and importin-α acted as an adaptor to bind with importin-β. This is the first study that unveils the role of importins in mediating the active transport of arthropod-borne flaviviruses C protein into nucleus.

Although the C protein of hepatitis C virus (HCV) also utilized importin-α for nuclear entry, the *in vitro* assays employed in an earlier study might not fully recapitulate the *in vivo* scenario since recombinant HCV C protein was used [5]. In contrast, our study employed full-length infectious clone of WNV with various mutations to study the authencity of WNV C protein/importin-α association.

Our study also demonstrated that the binding strength between C protein and importin-α is the rate-limiting step in controlling the kinetics of nuclear localization of flavivirus C protein. Using M2H analysis and IFA, we have shown that significantly lower binding strength between mutated C protein and importin-α at early timings led to predominant peri-nuclear staining besides nucleolar staining (Fig. 3 and Supplementary Fig. S4A).

The mutations introduced in this study affected the growth characteristics of the resulting viruses (Fig. 4). One might argue that the observed differences in growth characteristics of mutant viruses could result from inefficient ER anchoring or NS2B-NS3 cleavage. However, the domains assisting ER membrane association (aa 46–62, [12]) and NS2B-NS3 cleavage site (aa 104–106, [13]) were not mutated in this study. Thus, the introduced mutations should not have affected the membrane association/NS2B-NS3 cleavage. Patkar and colleagues [14] showed that deletion of NLS motif did not affect the packaging of YFV capsid protein. Thus, it is unlikely that the packaging of WNV is affected by the introduced mutations.

Many viruses utilize nuclear proteins such as PTB, nucleophosmin and hnRNPK for their efficient transcription and translation [15–17]. Similarly, WNV C protein could possibly exploit certain nuclear/nucleolar proteins and transcriptional regulators to establish a suitable environment for WNV replication. This could explain the observed differences in the growth characteristics of mutant viruses.

Our study also illustrated a positive correlation between nuclear localization and virus production. This finding is in agreement with JEV infection [4]. Mori and colleagues [4] reported a positive correlation between nuclear localization of JEV C protein and viral replication, although they did not address the interaction of C-importin-α and the influence of binding strength between these proteins on nuclear localization and virus production.

Overall, our findings unravelled the significance of importin-α/β/C protein association in mediating C protein nuclear translocation. We have also shown that nuclear entry of C protein is essential for efficient virus production. Understanding the precise molecular mechanism behind the association of importin-α/C protein and the influence of nuclear phase of C protein on the efficiency of virus replication will expand our current knowledge on the non-structural roles of C protein.

Acknowledgments

We thank Dr. Li Jun, Dr. Chu Jang Hann and Mr. Willis Chye for their help in this study. This work is supported by Grants from Biomedical Research Council, Singapore (BMRC/06/1/21/19/451) and National University of Singapore, Singapore (R-182-000-115-112).

Appendix A. Supplementary data

Supplementary data associated with this article can be found, in the online version, at doi:10.1016/j.bbrc.2009.08.108.

References

[1] E. Hayes, N. Komar, R. Nasci, S. Montgomery, D. O'Leary, G. Campbell, Epidemiology and transmission dynamics of West Nile virus disease, Emerg. Infect. Dis. 11 (2005) 1167–1173.
[2] T.J. Chambers, C.S. Hahn, R. Galler, C.M. Rice, Flavivirus genome organization, expression, and replication, Annu. Rev. Microbiol. 44 (1990) 649–688.
[3] S. Mukhopadhyay, R.J. Kuhn, M.G. Rossmann, A structural perspective of the flavivirus life cycle, Nat. Rev. Microbiol. 3 (2005) 13–22.
[4] Y. Mori, T. Okabayashi, T. Yamashita, Z. Zhao, T. Wakita, K. Yasui, F. Hasebe, M. Tadano, E. Konishi, K. Moriishi, Y. Matsuura, Nuclear localization of Japanese encephalitis virus core protein enhances viral replication, J. Virol. 79 (2005) 3448–3458.
[5] R. Suzuki, S. Sakamoto, T. Tsutsumi, A. Rikimaru, K. Tanaka, T. Shimoike, K. Moriishi, T. Iwasaki, K. Mizumoto, Y. Matsuura, T. Miyamura, T. Suzuki, Molecular determinants for subcellular localization of hepatitis C virus core protein, J. Virol. 79 (2005) 1271–1281.
[6] S.H. Wang, W.J. Syu, K.J. Huang, H.Y. Lei, C.W. Yao, C.C. King, S.T. Hu, Intracellular localization and determination of a nuclear localization signal of the core protein of dengue virus, J. Gen. Virol. 83 (2002) 3093–3102.
[7] E.G. Westaway, A.A. Khomykh, M.T. Kenney, J.M. Mackenzie, M.K. Jones, Proteins C and NS4B of the flavivirus Kunjin translocate independently into the nucleus, Virology 234 (1997) 31–41.
[8] J. Li, R. Bhuvanakantham, J. Howe, M.L. Ng, Identifying the region influencing the cis-mode of maturation of West Nile (Sarafend) virus using chimeric infectious clones, Biochem. Biophys. Res. Commun. 334 (2005) 714–720.
[9] R. Bhuvanakantham, M.L. Ng, Analysis of self-association of West Nile virus capsid protein and the crucial role played by Trp 69 in homodimerization, Biochem. Biophys. Res. Commun. 329 (2005) 246–255.
[10] W. Oh, M.R. Yang, E.W. Lee, K.M. Park, S. Pyo, J.S. Yang, H.W. Lee, J. Song, Jab1 mediates cytoplasmic localization and degradation of West Nile virus capsid protein, J. Biol. Chem. 281 (2006) 30166–30174.
[11] A. Cook, F. Bono, M. Jinek, E. Conti, Structural biology of nucleocytoplasmic transport, Annu. Rev. Biochem. 76 (2007) 647–671.
[12] L. Markoff, B. Falgout, A. Chang, A conserved internal hydrophobic domain mediates the stable membrane integration of the dengue virus capsid protein, Virology 233 (1997) 105–117.
[13] A.K. Bera, R.J. Kuhn, J.L. Smith, Functional characterization of cis and trans activity of the Flavivirus NS2B-NS3 protease, J. Biol. Chem. 282 (2007) 12883–12892.
[14] C.G. Patkar, C.T. Jones, Y.H. Chang, R. Warrier, R.J. Kuhn, Functional requirement of the yellow fever virus capsid protein, J. Virol. 81 (2007) 6471–6481.
[15] L. Jiang, H. Yao, X. Duan, X. Lu, Y. Liu, Polypyrimidine tract-binding protein influences negative strand RNA synthesis of dengue virus, Biochem. Biophys. Res. Commun. 385 (2009) 187–192.
[16] Y. Tsuda, Y. Mori, T. Abe, T. Yamashita, T. Okamoto, T. Ichimura, K. Moriishi, Y. Matsuura, Nucleolar protein B23 interacts with Japanese encephalitis virus core protein and participates in viral replication, Microbiol. Immunol. 50 (2006) 225–234.
[17] T.Y. Hsieh, M. Matsumoto, H.C. Chou, R. Schneider, S.B. Hwang, A.S. Lee, M.M. Lai, Hepatitis C virus core protein interacts with heterogeneous nuclear ribonucleoprotein K, J. Biol. Chem. 273 (1998) 17651–17659.

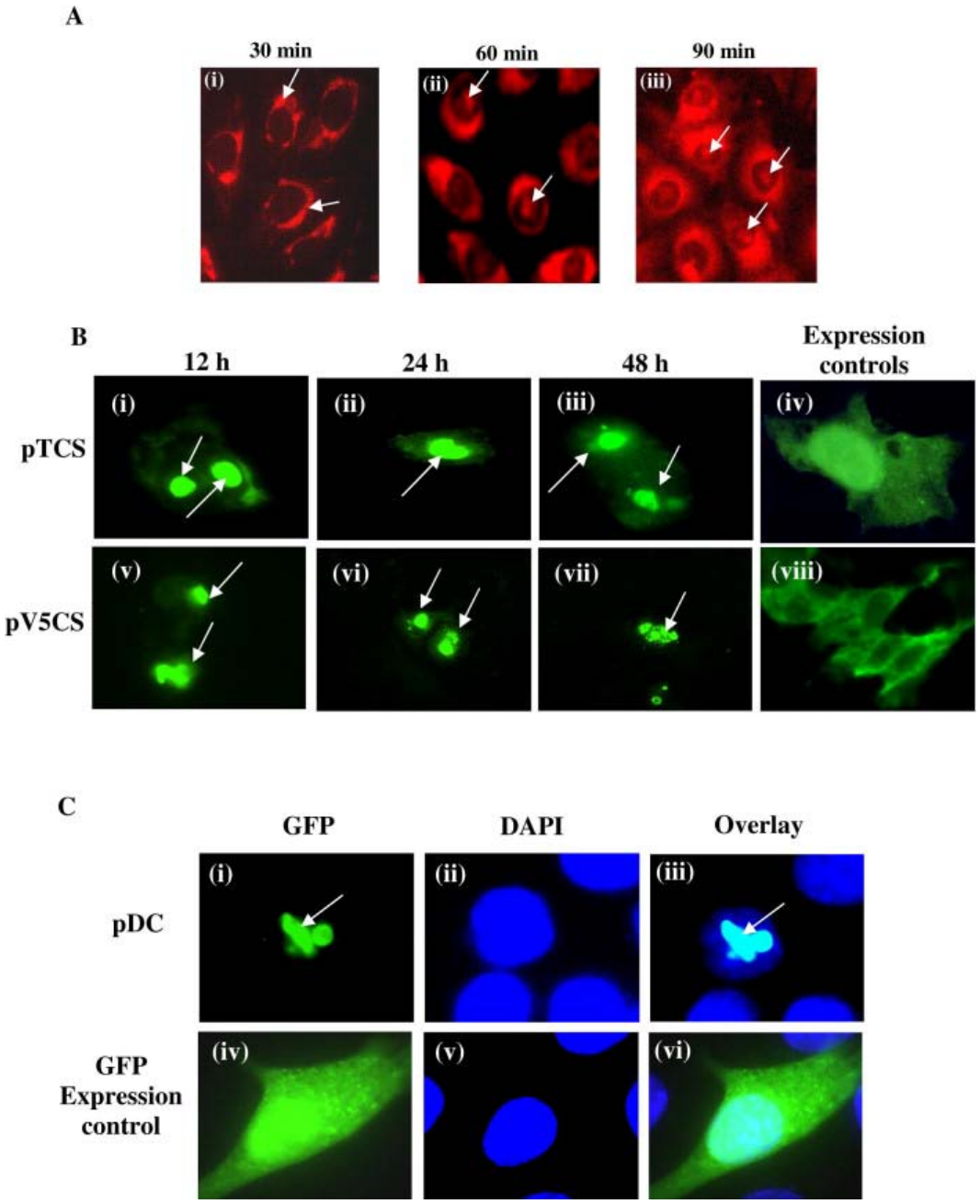

Supplementary 1. Nuclear localization of C proteins. (A) Nuclear localization of C protein during WNV infection. WNV-infected Vero cells were processed for IFA. The C protein was detected with anti-WNVC antibody followed by Texas red-conjugated secondary antibody. WNV C protein is detected predominantly in the cytoplasm and perinuclear region at 30 min p.i. (i). By 60min p.i. (ii), C protein is localized at the perinuclear and nuclear regions. Nucleolar translocation is more obvious at 90min p.i. (iii). (B) Nuclear localization of recombinant WNV C protein. Optical fluorescence microscopy images of pTCS/pV5CS-transfected Vero cells at 12 (i, v), 24 (ii, vi) and 48h (iii, vii) post-transfection. Arrows indicate intense fluorescence localized in the nucleoli/nuclei. Expression control plasmids [pcDNA3.1CT-GFP (iv)/lacZ-V5 (viii)]-transfected cell show diffuse fluorescence distribution in both nucleus and cytoplasm. (C) Recombinant GFP-tagged DENV C protein was transfected into Vero cells and processed for IFA. DENV C protein is able to localize into nucleoli (arrows) as indicated by the intense green fluorescence (i & iii). Cell nuclei are stained with DAPI (ii & v). Expression control is included to show the diffused fluorescence distribution pattern in both nucleus and cytoplasm (iv & vi).

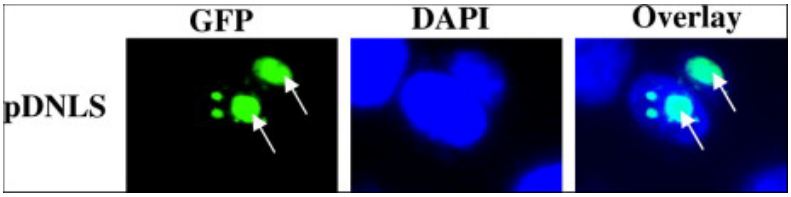

Supplementary 2. Nuclear localization of DENV NLS motif. pDNLS which contained only DENV NLS motif fused with GFP was transfected into Vero cells to examine its functionality. Intense green fluorescence is observed in the nuclei as indicated by the arrows. This shows that the NLS motif of DENV C protein is functional.

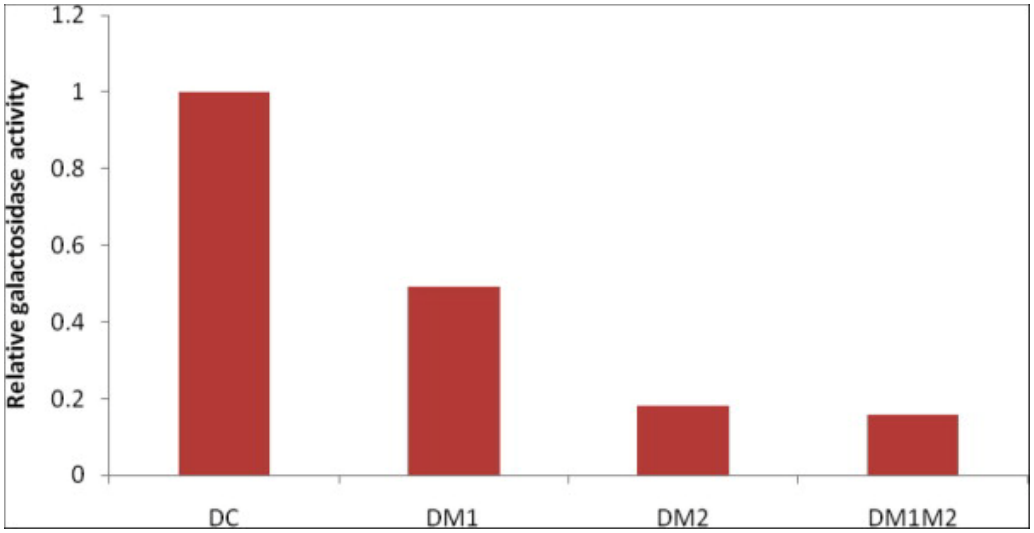

Supplementary 3. Binding efficiency of mutated DENV C protein with importin-α. The relative β-galactosidase activities of full-length DENV C protein and C protein mutants (M1, M2, and M1M2) were measured and plotted. An arbitrary value of 1 is set for the binding efficiency of full-length DENV C protein and importin-α association. The binding efficiency between C protein and importin-α is reduced up to 50% for M1 mutant and 80% for M2 and M1M2 mutants.

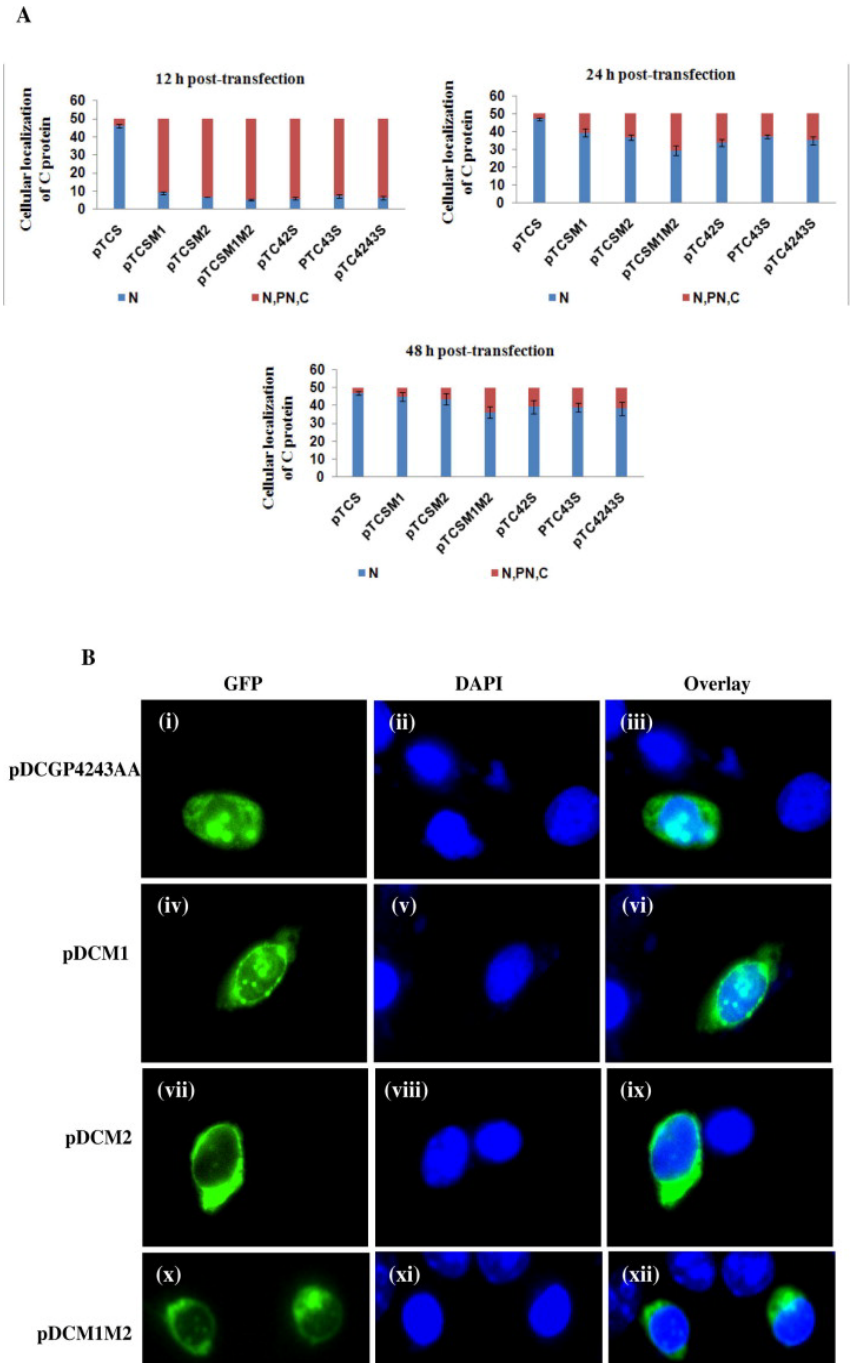

Supplementary 4. Optical fluorescence microscopy images of mutated DENV C protein and the kinetics of nuclear entry of mutant WNV/DENV C proteins. (A) The kinetics of nuclear entry of mutated WNV recombinant C protein noted in 50 transfected cells. (B) Recombinant GFP-tagged DENV C protein with different mutations (pDCGP4243AA, pDCM1, pDCM2, and pDCM1M2) were transfected into Vero cells and processed for IFA to examine the nuclear localization of these mutants. pDCGP4243AA (i-iii) and pDCM1 (iv-vi) mutants still show strong fluorescence in the 29 nucleoli with perinuclear staining. However, pDCM2 (vii-ix) and pDCM1M2 (x-xii) mutants show exclusively cytoplasmic staining after 24h post-transfection. (C) 50 transfected cells were counted and categorized into different cellular localization pattern. Most of the mutant C proteins are localized in the nuclei except when the second basic residue cluster (M2) is mutated to alanine. (N - Nucleus; N,PN,C - Nucleus, peri-nucleus, cytoplasm).

Protein Engineering, Design & Selection vol. 26 no. 5 pp. 377–387, 2013
Published online March 10, 2013 doi:10.1093/protein/gzs107

Optimized sequential purification protocol for *in vivo* site-specific biotinylated full-length dengue virus capsid protein

Mun Keat Chong[†], Krupakar Parthasarathy[†], Hui Yu Yeo and Mah Lee Ng[1]

Flavivirology Laboratory, Department of Microbiology, Yong Loo Lin School of Medicine, National University Health System, National University of Singapore, Singapore

[1]To whom correspondence should be addressed.
E-mail: micngml@nus.edu.sg

Received September 12, 2012; revised November 25, 2012; accepted December 13, 2012

Edited by Haruki Nakamura

Dengue virus (DENV) capsid (C) protein is one of the three structural proteins that form a mature virus. The main challenge impeding the study of this protein is to generate pure non-truncated, full-length C proteins for structural and functional studies. This is mainly due to its small molecular weight, highly positively charged, stability and solubility properties. Here, we report a strategy to construct, express, biotinylate and purify non-truncated, full-length DENV C protein. A 6× His tag and a biotin acceptor peptide (BAP) were cloned at the N-terminus of C protein using overlapping extension-polymerase chain reaction method for site-specific biotinylation. The final construct was inserted into pET28a plasmid and BL-21 (CodonPlus) expression competent cell strain was selected as there are 12% rare codons in the C protein sequence. Strikingly, we found that our recombinant proteins with BAP were biotinylated endogenously with high efficiency in *Escherichia coli* BL-21 strains. To purify this His-tagged C protein, nickel-nitriloacetic acid affinity chromatography was first carried out under denaturing condition. After stepwise dialysis and concurrent refolding, ion exchange-fast protein liquid chromatography was performed to further separate the residual contaminants. To obtain C protein with high purity, a final round of purification with size exclusion chromatography was carried out and a single peak corresponding to C protein was attained. With this optimized sequential purification protocol, we successfully generated pure biotinylated full-length DENV C protein. The functionality of this purified non-truncated DENV C protein was examined and it was suitable for structural and molecular studies.

Keywords: biotinylation/capsid protein/dengue virus/expression and purification

Introduction

Dengue virus (DENV) belongs to the Flavivirus genus within the *Flaviviridae* family. Other members of the Flavivirus genus include Yellow Fever virus, West Nile virus (WNV), Kunjin virus, Japanese Encephalitis virus and Tick-Borne Encephalitis virus, just to name a few. DENV infection encompasses a wide spectrum of severity ranging from mild asymptomatic dengue fever to critical and fatal dengue hemorrhagic fever/dengue shock syndrome. DENV caused about 15 000 deaths annually and it is estimated that more than 2.5 billion people are at risk of DENV infection in more than 100 countries (Gubler, 2002). However, anti-viral drug and vaccine are yet to be available in the market.

The whole mature virion particle is about 50 nm in diameter. Each virion contains a single positive-stranded RNA that is encapsulated by multiple copies of capsid (C) protein to form a spherical cage-like structure called nucleocapsid or core. The core is approximately 30 nm in diameter which can be seen as a dense particle under electron microscope (Hase *et al.*, 1987). Nucleocapsid is surrounded by a 10-nm-thick lipid bilayer derived from host cell membrane anchored with 180 membrane (M) protein and 180 envelope (E) protein (Zhang *et al.*, 2003).

DENV C protein is the first structural protein found in the open reading frame of its genome. Although the sequence homology of C proteins among other flaviviruses is poorly conserved (Fig. 1A and B), they are still structurally and functionally similar. The C-terminal hydrophobic signal sequence of full-length DENV C protein is cleaved by its NS2B-NS3 proteins to generate mature DENV C protein (Markoff, 1989; Amberg and Rice, 1999). DENV C protein has a molecular weight of about 12–15 kDa and is a highly basic protein that contains about 25% of lysine and arginine residues. The high basic-residue content confers its RNA-binding property to neutralize the negatively charged viral RNA. This explains the main function of C protein which is to encapsidate its viral RNA and form nucleocapsid.

Other than its structural function, DENV C protein is also known to carry non-structural functions. It is currently believed that multifunctional C protein is essential in the viral replication, assembly, RNA encapsidation, as well as pathogenesis. The role of C protein in inducing apoptosis by activating caspase-3 and caspase-9 leading to mitochondrial dysfunction was reported (Yang *et al.*, 2008). Recently, our laboratory also discovered that WNV and DENV C protein interact with human Sec3 exocyst protein (hSec3p) to antagonize the antiviral effect caused by hSec3p (Bhuvanakantham *et al.*, 2010). Moreover, DENV C protein was also known to localize in the nucleus of infected cells during replication (Tadano *et al.*, 1989). We found that C protein was transported into the nucleus by importain-α/β complex and the loss of the nuclear translocation ability affected virus replication (Bhuvanakantham *et al.*, 2009). However, the exact role of C protein in the nucleus still remains unclear and further investigation is warrant.

[†]Contributed equally in this project.

A

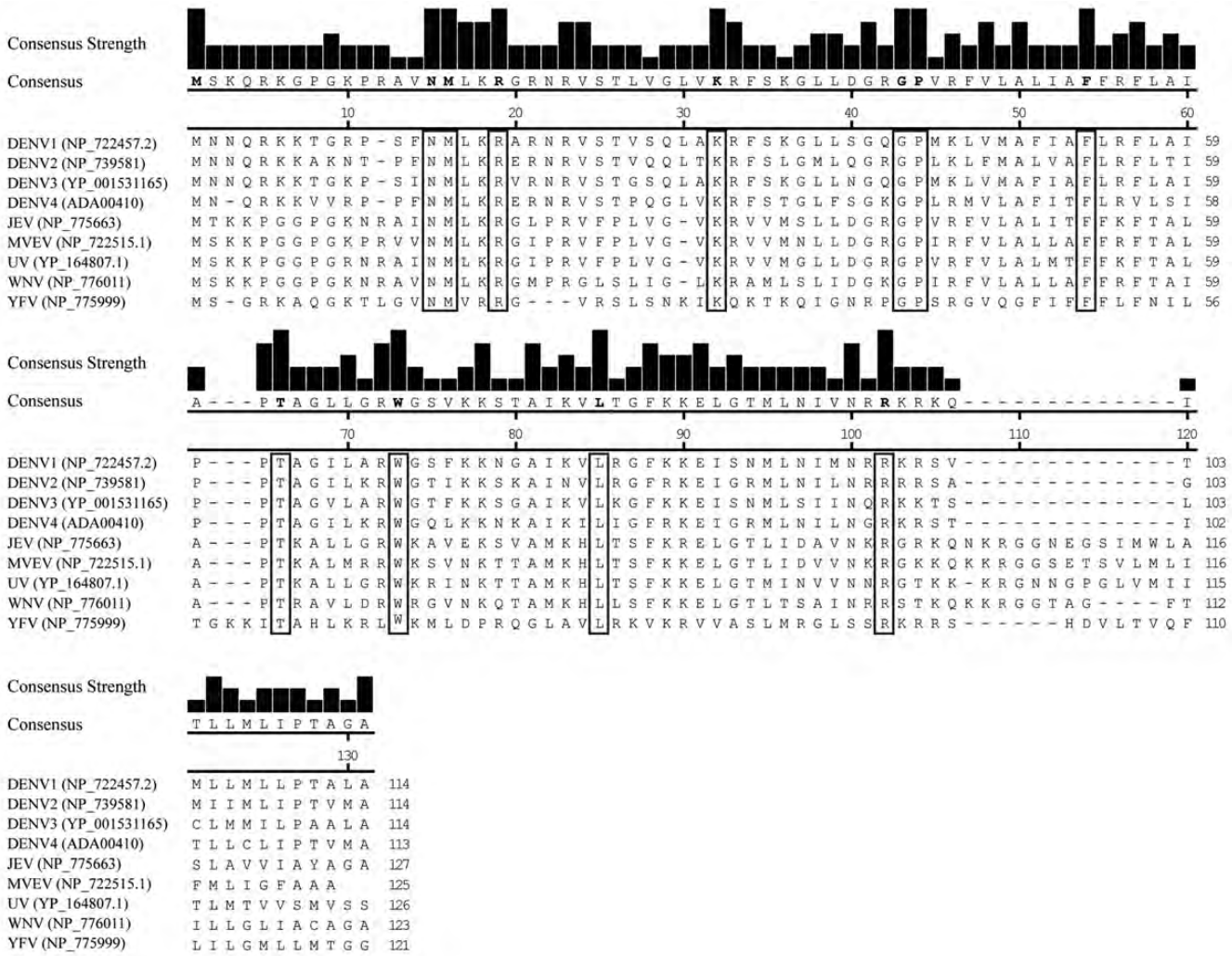

B

Percent Identity

	1	2	3	4	5	6	7	8	9		
1		69.3	82.5	68.1	35.4	36.9	36.3	38.9	27.3	1	DENV1 (NP_722457.2)
2	39.4		61.4	69.0	31.9	30.6	33.6	33.6	20.9	2	DENV2 (NP_739581)
3	20.0	53.7		58.4	37.2	37.8	36.3	38.9	27.3	3	DENV3 (YP_001531165)
4	41.4	39.9	59.9		36.6	35.5	40.2	37.5	22.7	4	DENV4 (ADA00410)
5	130.7	148.8	122.9	125.3		73.6	72.2	64.2	25.6	5	JEV (NP_775663)
6	123.8	156.0	120.0	130.5	32.6		71.8	66.1	26.1	6	MVEV (NP_722515.1)
7	126.7	139.4	126.7	110.8	34.7	35.4		58.2	23.1	7	UV (YP_164807.1)
8	115.6	139.4	115.6	121.4	48.3	44.9	60.3		24.8	8	WNV (NP_776011)
9	179.0	234.0	179.0	215.0	192.5	188.6	212.0	197.0		9	YFV (NP_775999)
	1	2	3	4	5	6	7	8	9		

Divergence

C

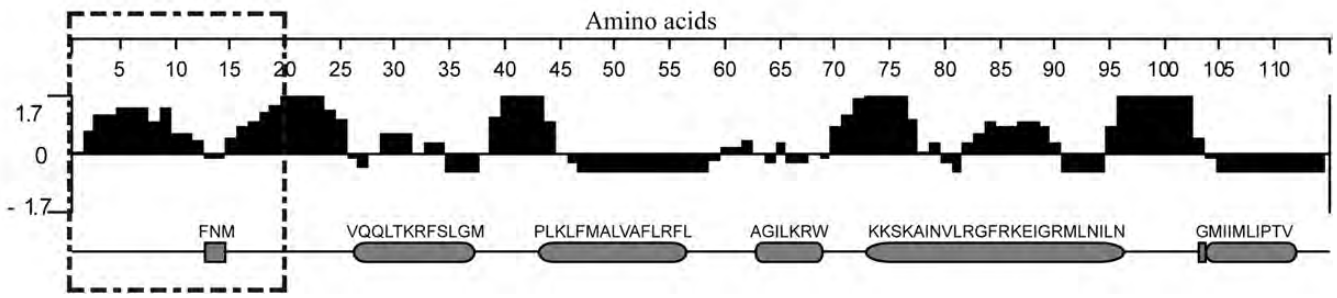

There is also a lack of information about the interaction of DENV C protein with either prM and E proteins or even its RNA genome. The binding of NS2B-NS3 protein with C protein and how it cleaves C-prM polyprotein is also unclear. This is mainly due to the difficulty of expressing and purifying full-length C protein for functional and structural studies. The NMR structure of DENV C protein studied thus far only encompasses 80 residues from the 21st to 100th amino acid (Ma *et al.*, 2004). The N-terminus is removed from the structural study because it is conformationally labile and unstable (Jones *et al.*, 2003). The hydrophobic C-terminus of DENV C protein is also excluded due to its solubility problem. Nevertheless, the N-terminus of C protein is found to be antigenic as predicted by bioinformatics analysis (Fig. 1C). This is also supported by Puttikhunt *et al.* (2009) that the N-terminus of DENV C protein was immunogenic in mice. Recently, Samsa *et al.* (2012) found that the first 18 amino acid residues from the N-terminus were essential for virus particle assembly. Taken together, these suggest that the N-terminus of DENV C protein have important roles in the pathogenesis and viral replication.

In this project, we aimed to express and purify full-length DENV C protein for structural and functional studies. Since biotinylation has been widely used to date for purification, detection, diagnostic, protein–protein interaction studies, imaging studies and other molecular studies (Chapman-Smith and Cronan, 1999*a*,*b*; de Boer *et al.*, 2003; Howarth and Ting, 2008; Postel *et al.*, 2011; Qi and Katagiri, 2011), a biotinylation site was engineered into C protein to ease further downstream experiments. Using our expression and purification strategy, we have successfully obtained functional biotinylated full-length DENV C protein.

Materials and methods

Construction of pET28aDENVBioCap plasmid

DENV C gene was amplified from cDNA synthesized from DENV-2 (NGC strain; accession number: M29095; nucleotide 100–438) RNA using SuperScript™ III First-Strand Synthesis System (Life Technologies, USA). Primers Biotin_F (5′-CTAGCTAGCTCCGGCCTGAACGAC-3′), Biotin_C_F (5′-GACGACGACAAGAGCATGAATAACCAA-3′), Biotin_C_R (5′-TTGGTTATTCATGCTCTTGTCGTCGTC-3′), and C_R (5′-CCGCTCGAGTTACGCCATCACTGT-3′) were used to join biotin acceptor peptide (BAP) gene (Cull and Schatz, 2000) containing an enterokinase cleavage site with DENV C gene via overlap extension polymerase chain reaction (OE-PCR). Gel-purified PCR products containing the joined fragments were subsequently inserted into expression vector, pET28a (Novagen, Germany) via *Nhe*I and *Xho*I cut sites. 6× His tag and thrombin cleavage site are at the N-terminus of signal peptide followed by enterokinase cleavage site and DENV C protein. DNA sequences of the constructs were confirmed by sequencing.

Competent cell strain screening

Transformed bacterial colonies of each strain [BL-21 (DE3) and BL-21-CodonPlus] (Agilent Technologies, USA) were picked and grown in 20 ml Luria-Bertani (LB) broth with 30 μg/ml kanamycin antibiotic. When the bacteria absorbance OD_{600nm} reached 0.65, protein expression was induced with 1 mM isopropyl β-D-thiogalactoside (IPTG) overnight at 28°C. After IPTG induction, the bacteria absorbance OD_{600nm} was measured again and 200 μl of equal bacteria density for both strains were used for expression level screening. Bacterial cells were pelleted down with centrifugation at 8000 rpm for 15 min at 4°C and resuspended with 100 μl 1× protein sample buffer containing β-mercaptoethanol. The samples were boiled for 10 min with constant vortexing at 1 min interval. Insoluble substances were pelleted down with centrifugation for 2 min at 20 000 g.

Protein expression and extraction

pET28aDENVBioCap plasmid was transformed into BL-21-CodonPlus expression competent cells (Agilent Technologies, USA) and grown on LB agar containing 30 μg/ml kanamycin. Selected clones were cultured in 1 l LB broth (30 μg/ml kanamycin) at 30°C until absorbance OD_{600nm} of 0.65. Expression of DENV C protein was induced with 1 mM IPTG overnight at 28°C. Bacterial cells were pelleted down with centrifugation at 8000 rpm for 15 min at 4°C. Pellet was then resuspended in 10 ml resuspension buffer (20 mM Tris, 300 mM NaCl, 0.2% Triton-X, pH 8.0) and pelleted down again at 8000 rpm for 15 min. The pellet was washed with wash buffer (20 mM Tris, 300 mM NaCl, pH 8.0) before it was resuspended in 30 ml lysis buffer (8 M urea, 20 mM Tris, 300 mM NaCl, 10 mM Imidazole, pH 8.0) containing EDTA-free protease inhibitor (Roche, Switzerland). The mixture was incubated at room temperature for 30 min and the lysate was subsequently clarified by centrifugation at 13 200 rpm for 20 min.

Nickel-nitriloacetic acid affinity chromatography

Bacterial lysate containing denatured DENV C protein was incubated with nickel-nitrilotriacetic acid resin (Bio-Rad, USA) for binding in a chromatography column overnight at 4°C. Ten column volume of wash buffer (8 M urea, 20 mM Tris, 300 mM NaCl, 20 mM Imidazole, pH 8.0) was used to wash away non-specific binding proteins. DENV C protein was eventually eluted out with elution buffer (8 M urea, 20 mM Tris, 300 mM NaCl, 500 mM Imidazole, pH 8.0) in 10 fractions. Next, all eluates were combined for refolding and dialysis to remove 8 M urea. Briefly, all eluates were

Fig. 1. Bioinformatics analysis of flavivirus C protein. (A) Multiple sequence alignment of mosquito-borne flavivirus C protein sequences using ClustalW method in MegAlign, DNASTAR Lasergene 7.2 software. Sequences with the highest consensus strength among the nine flavivirus C proteins are highlighted. (B) Sequence distances analysis using the ClustalV method shows that the protein sequence similarities among the nine flavivirus C proteins are mostly lower than 50% and the sequence divergence is more than 100%. The percent identity refers to the percentage of sequence similarity between two sequences whereas percent divergence is obtained by comparing two sequences in relation to their relative positions in the phylogenetic tree. (C) Antigenic plot of DENV2 C protein generated by Protean, DNASTAR Lasergene 7.2 software, using Jameson-Wolf methodology. The higher the antigenic index, the more likely the region will be recognized by immune system. The secondary structures are also shown in parallel with the antigenic plot. Alpha helices are shown in rounded rectangles while beta sheets are shown in regular rectangles. The high antigenicity of the first 20 amino acids is highlighted in dotted box. DENV1-4, dengue virus serotype 1-4; JEV, Japanese Encephalitis virus; MVEV, Murray Valley encephalitis virus; UV, Usutu virus; YFV, Yellow Fever virus. Accession number of the protein sequence is shown in the bracket.

pooled into a SnakeSkin dialysis membrane tubing, 3.5 k MWCO (Thermo Scientific, USA) and 0.5% of Tween-20 was added into the samples. The dialysis tubing was incubated in 1 l of 6 M urea for 6–12 h at 4°C and 250 ml of 25 mM Tris (pH 8.0) was added into the solution at every 6–12-h interval. When the final volume reached 3 L, the dialysis tubing was transferred into 2 L of 20 mM Tris (pH 8.0) for 6 h. Refolded DENV C proteins were collected from the dialysis tubing.

Ion exchange chromatography

Ion exchange chromatography column, Resource™ Q/S 1 ml-packed size column (GE Healthcare, UK), was connected to fast protein liquid chromatography (FPLC) system. The column was equilibrated with 10 column volumes of 20 mM Tris (pH 8.0) until the UV baseline and conductivity were stable. Refolded DENV C protein was injected into the column and the flow rate was set to 0.5 ml/min. After the sample passed through the column, 10 column volumes of 20 mM Tris (pH 8.0) was used to wash away all the unbound proteins. Ionically bound proteins were eluted out with increasing concentration of sodium chloride to a final concentration of 1 M (100%). All the fractions were analyzed via enzyme linked immunosorbent assay (ELISA) to determine the presence of biotinylated C protein.

Size exclusion chromatography

Superdex 75 10/300 GL chromatographic separation column (GE Healthcare, UK) was connected to the FPLC system. The column was washed with five column volumes of MilliQ™ water and then equilibrated with two column volumes of 1× phosphate-buffered saline (PBS) (pH 7.2). Samples were injected into the column and the flow rate was set to 0.25 ml/min. All the eluates were analyzed via ELISA to determine the presence of biotinylated C protein.

Enzyme-linked immunosorbent assay

To determine whether the expressed protein is biotinylated or not, 50 μl of samples were added into the wells of MaxiSorp plate (eBioscience, USA) in triplicate for coating overnight at 4°C. After washing with 1× 0.1% PBST, 150 μl blocking buffer (4% bovine serum albumin) was added into each well and incubated for another hour at room temperature. Next, 150 μl streptavidin-horseradish peroxidase (HRP) enzyme conjugates (1 : 5000 dilution) was added and incubated for 1 h. The plate was washed with 1× PBST three times to remove unbound conjugates and then 100 μl substrate solution, tetramethyl benzidine (TMB; Promega, USA), was added for development. To stop the reaction, 50 μl of 0.5 M H_2SO_4 solution was added. The absorbance was measured at 450 nm.

Product analysis

Samples collected from flow through, wash, and eluates were analyzed by sodium dodecyl sulphate-polyacrylamide gel electrophoresis (SDS-PAGE) and western blot. Twelve % Tris-tricine polyacrylamide denaturing gel was used to separate proteins in the samples and subsequently stained with Coomassie blue for detection. The presence of biotinylated DENV C protein was confirmed by western blot via two different approaches. First, the identity of DENV C protein was determined with anti-His antibody. Briefly, separated proteins were transferred from polyacrylamide gel onto a polyvinylidene difluoride (PVDF) membrane using iBlot® Dry Blotting System (Life Technologies, USA). Blocking was done with 5% skimmed milk for 1 h at room temperature. Next, the membrane was incubated with 0.1 μg/ml mouse anti-His antibody (Qiagen, Germany) overnight at 4°C. The membrane was then washed with 1× tris-buffered saline with Tween (TBST) and incubated with 0.1 μg/ml goat anti-mouse secondary antibody conjugated with HRP (Thermo Scientific, USA) for 1 h at room temperature. After washing with 1× TBST, the membrane was developed using SuperSignal® West Pico/Dura/Femto chemiluminescent substrate (Thermo Scientific, USA).

For the second approach, DENV C protein was detected directly using streptavidin conjugated with HRP. After transferring the samples onto a PVDF membrane, it was blocked with 4% bovine serum albumin (BSA) for 1 h at room temperature. The membrane was then incubated with HRP-conjugated streptavidin (Millipore, USA) for another hour at room temperature. Subsequently, the membrane was washed thoroughly with 1× PBST for 1 hr at room temperature and developed with chemiluminescent substrate.

Sample preparation for mass spectrometry

Purified protein was electrophoresed through SDS-PAGE using 12% Tris-tricine polyacrylamide denaturing gel and stained with Coomassie blue. The background of Coomassie-stained gel was removed with destaining solution (40% methanol, 10% glacial acetic acid, 50% distilled H_2O). DENV C protein-corresponding band was excised from the gel and kept in eppendorf tube containing distilled water. Samples were submitted to Dr Lim Yong Pin (Department of Biochemistry, NUS) for matrix-assisted laser desorption/ionization-time of flight (MALDI-TOF) mass spectrometry analysis.

Biotinylated protein-binding assay

The binding affinity of purified biotinylated DENV C protein was tested using streptavidin magnetic beads (GE Healthcare, UK) according to the manufacturer's protocol. Briefly, samples were mixed with the streptavidin magnetic beads and incubated for 1 h with gentle mixing at 4°C. Unbound proteins were removed with wash buffer while biotinylated proteins were eluted out with elution buffer provided in the kit. Eluted proteins were analyzed by ELISA to confirm the biotinylation.

DENV C protein functional assay

Pure Sec3 protein (Abnova, Taiwan; known interacting partner of flavivirus C protein; Bhuvanakantham *et al.*, 2010) was added into the wells of MaxiSorp plate (eBioscience, USA) for coating overnight at 4°C. After washing with 1× PBST, blocking buffer (4% bovine serum albumin) was added into each well and incubated for another hour. Purified DENV C protein was added into the well for binding at 37°C for 1 h. Next, streptavidin-HRP enzyme conjugates was added and incubated for another hour at 37°C. After washing three times with 1× PBS, 100 μl TMB substrate (Promega, USA) was added for development and 50 μl 0.5 M H_2SO_4 solution was added to stop the reaction when necessary. The absorbance was measured at 450 nm.

Results

Engineering of biotin acceptor peptide into full-length DENV capsid (C) plasmid, pET28aDENVBioCap

To avoid non-specific biotinylation, we engineered a BAP at the N-terminus of DENV C protein. Biotin is a very small molecule (molecular weight = 244.31) so it is unlikely to affect the structure and function of the protein. To ensure that the BAP will not result in any steric hindrance to the protein conformation, a secondary structure prediction was performed. As shown in Fig. 2A, the predicted secondary structures of DENV C protein with and without BAP do not differ from each other.

To clone the full-length DENV C protein, nucleotides 100 to 438 from DENV-2 genome (GeneBank accession number: **M29095**) were amplified, whereas the BAP sequence (Cull and Schatz, 2000) was synthesized together with an enterokinase cleavage site at the C-terminus. Both fragments were joined together through the OE-PCR method as illustrated in Fig. 2B. Schematic representations of the final recombinant gene and protein are shown in Fig. 2C and D, respectively.

The final ligated product was then cloned into bacterial expression vector, pET28 which consisted of a 6× His tag and a thrombin cleavage site in the upstream of the multiple cloning site. Hence, the recombinant full-length DENV C construct (pET28aDENVBioCap) contained two tags (6×

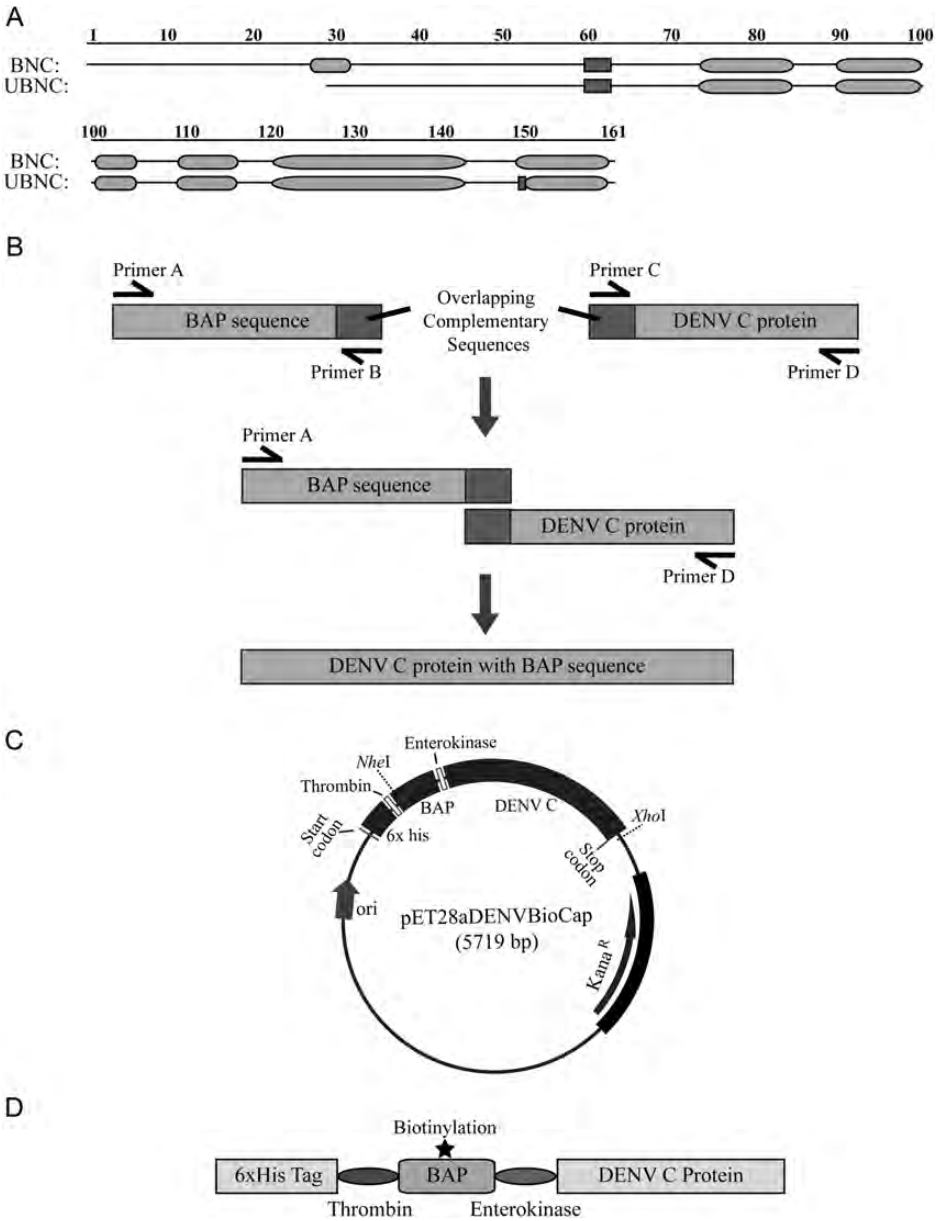

Fig. 2. Cloning strategies. (A) Secondary structure prediction of biotinylated C (BNC) and unbiotinylated C (UBNC) proteins shows that BAP insertion does not affect the overall secondary structure formation when it is added to the N-terminus of C protein. Alpha helices are represented in gray, rounded rectangles while beta sheets in black, regular rectangles. (B) Schematic diagram showing the OE-PCR technique. The 3′ overhang of BAP sequence is complementary to the 5′ overhang of DENV C protein sequence. As such, primers B and C are complementary to each other. Both fragments are joined together with primers A and D. (C) Plasmid vector map of pET28aDENVBioCap construct. (D) Final construct of recombinant protein generated. 6× His tag is at the N-terminal followed by thrombin cleavage site and BAP. Enterokinase cleavage site is included at the downstream of BAP. 6× His tag is used for affinity purification while BAP is the signal peptide for biotinylation.

His tag and BAP) at the N-terminus and two different enzyme cleavage sites (thrombin cleavage site and enterokinase cleavage site) for tag removal when necessary.

Five successfully transformed bacterial colonies were picked for colony PCR screening and DNA sequencing was performed to verify the constructs. The final DNA and protein sequence were shown in Supplementary Table S1. To further support our site-specific biotinylation strategy, WNV domain III (DIII) protein which has similar molecular weight as the C protein, was also engineered with a BAP concurrently via the same procedure. DENV C and WNV DIII proteins without BAP were also constructed for comparison purposes.

Optimal expression competent bacterial strain for DENV C protein

To express DENV C protein, an optimal expression competent bacterial strain is requisite. We detected 14 rare codons in the full-length DENV C protein DNA sequence (Supplementary Table S2). This raised a concern for protein expression because 12% of the total 115 codons are rare codons. To screen for the optimal bacterial expression competent cell, pET28aDENVBioCap plasmid was transformed into BL-21 (DE3) and BL-21-CodonPlus. BL-21 (DE3) is a common bacterial strain for high expression of recombinant proteins while BL-21-CodonPlus is a bacterial strain specifically engineered for expression of proteins with rare codons.

The expression of DENV C protein was indeed much higher in BL-21-CodonPlus strain. As indicated in Fig. 3, an obvious band corresponding to the recombinant full-length DENV C protein was detected in the lysate of IPTG-induced CodonPlus strain but not in the BL-21 (DE3) strain (Fig. 3Ai). Western blotting with anti-His antibody revealed that DENV C protein was expressed in both BL-21 (DE3) and BL-21-CodonPlus strains because C protein-corresponding bands were detected in the lysates of both strains (Fig. 3Aii). Nonetheless, the observed bands were much thicker in BL-21-CodonPlus strain as compared with BL-21 (DE3) strain. This demonstrated that DENV C protein expression level was much higher in BL-21-CodonPlus strain under the same condition. As for WNV DIII protein, the expression was good enough in normal BL-21 (DE3) strain (data not shown).

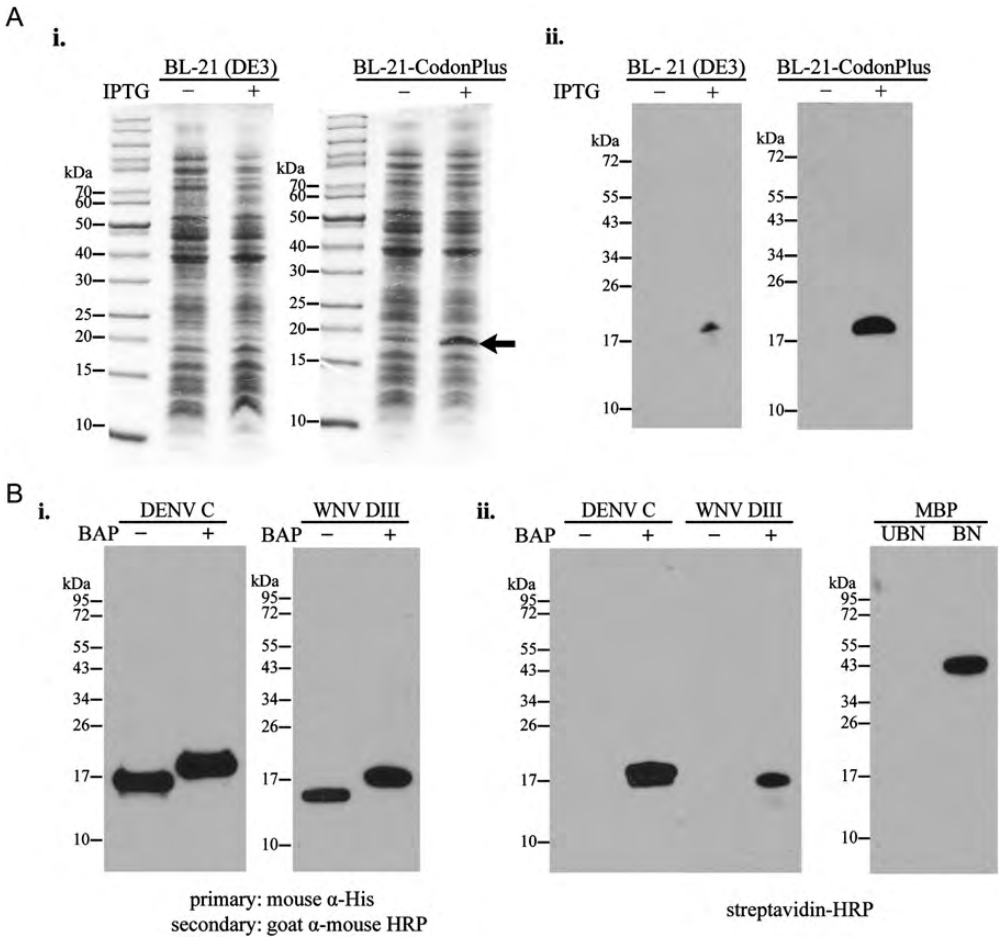

Fig. 3. Expression screening of bacterial clones with recombinant DENV C protein and detection of biotinylation. (A) Two expression competent cells are tested, namely BL-21 (DE3) and BL-21-CodonPlus. The presence of C protein band in the IPTG-induced bacterial cell lysate, as indicated by arrow, is detected via SDS-PAGE stained with Coomassie blue (i) and western blot (ii) using anti-His antibody. The expression of C protein is much higher in CodonPlus competent cells as the band intensity is much higher than normal BL-21 (DE) competent cells. (B) (i) The presence of His tag was detected using monoclonal mouse anti-His antibody and goat anti-mouse HRP-conjugated secondary antibody. Bands can be observed in both DENV C proteins with and without BAP. The molecular weight of C protein with BAP is higher than C protein without BAP. (ii) When western blot is performed using streptavidin-HRP secondary antibody, band is only observed in the DENV C and WNV DIII proteins lanes with BAP. Likewise, band is only observed in the biotinylated (BN) MBP and not unbiotinylated (UBN) MBP.

Discovery of endogenous biotinylation in BL-21 strains

As comparing DENV C protein with and without BAP via western blot using anti-His antibody, bands were observed in all the lanes for DENV C and WNV DIII proteins (Fig. 3Bi). As shown in Fig. 3Bi, recombinant proteins with BAP have higher molecular weight than those without BAP. This also indicated that all the DENV C and WNV DIII proteins with and without BAP were expressing well in the BL-21 strains.

Besides detecting the proteins of interest using anti-His antibody, streptavidin-HRP was also employed to detect the presence of biotinylated protein. Surprisingly, we found that our proteins of interest were biotinylated even before any *in vitro* biotinylation process. As shown in Fig. 3Bii, thick bands can be observed in the BAP-containing DENV C and WNV DIII proteins when streptavidin-HRP antibody was used. Similar bands were not detected in DENV C and WNV DIII proteins without BAP. Commercially available biotinylated and unbiotinylated maltose-binding protein (MBP; GeneCopoeia, USA) were used as positive and negative controls for biotinylation, respectively. Similarly, band was only seen in the biotinylated MBP lane. This result suggested that DENV C and WNV DIII proteins with BAP were biotinylated endogenously in BL-21 strains.

We postulated that bacterial BL-21 strains may contain biotin holoenzyme synthetase BirA gene that encodes for biotin ligase protein in their genome. To investigate the reason behind endogenous biotinylation, BirA gene sequence was analyzed using BLAST software and the result showed that BL-21 strains indeed possess BirA gene in their genome (Supplementary Table S3). It was also reported that biotin molecules were present in the LB broth (Tolaymat and Mock, 1989). As a result, proteins engineered with BAP could be directly expressed and biotinylated in BL-21 strains without the extra *in vitro* enzymatic biotinylation step.

Optimized sequential purification protocol for full-length C proteins

After confirming the expression and biotinylation of the protein of interest, large-scale production of bacterial culture was carried out. The initial attempt was to perform all the extraction and purification steps in native form so that the protein structure could be preserved without the need of refolding. However, the extraction of DENV C protein from the bacterial cells was not effective in native condition. There were still considerably large amounts of DENV C protein trapped in the pellet (data not shown). Therefore, 8 M urea was used to lyze the bacterial cells and affinity His-tag chromatography purification was first performed under denaturing condition.

The bacterial cell lysate with biotinylated DENV C protein was incubated with nickel-nitrilotriacetic acid resin to purify His-tagged proteins. Recombinant full-length DENV C protein contained 6× His tag at the N-terminus bound to the resin and unbound proteins were removed during washing with 20 mM imidazole. To ensure that most of the unbound proteins were washed away, 10 column volumes of wash buffer were used. The bound proteins were eluted out with 500-mM imidazole. However, many non-specific bands were still observed in the eluates of DENV C protein (Fig. 4A), especially in the second eluate fraction. Nonetheless, western blot result confirmed that most of the DENV C proteins were eluted out starting from fraction E2 until E10 (Fig. 4B and C).

Partially purified DENV C proteins from eluates E2 to E10 were pooled together for step-wise dialysis and concurrent refolding. Owing to its hydrophobic C-terminus, DENV C protein easily aggregated, resulting in major loss in amounts during refolding and dialysis. To prevent protein aggregation and to enhance efficient refolding, 0.05% of Tween-20 was added to the samples (Krupakar *et al.*, 2012). With this addition, protein aggregation was reduced significantly. No obvious precipitation was observed and the solution was clear after dialysis and refolding. This partially purified DENV C protein was then subjected to a second round of purification using ion exchange chromatography-fast protein liquid chromatography system (IEX-FPLC).

Theoretically, DENV C protein is a positively charged protein so cation-exchanger column, Resource MonoS, should be used. However, we found that biotinylated DENV C protein was not eluted out at a specific concentration of sodium chloride (NaCl). Miniature amount of the protein was eluted out slowly in an increasing gradient manner and it reached plateau at 70 mM of NaCl (Supplementary Fig. S1). This indicated that Resource MonoS column is not suitable for separating DENV C protein from the contaminants.

Counter intuitively, we were able to obtain better separation when we used anion-exchanger, Resource MonoQ, column (Fig. 5Ai). This could be due to the presence of BAP in the DENV C protein conferring its ability to bind to positively charged beads. As shown in Fig. 5A, biotinylated full-length DENV C protein bound perfectly to Resource MonoQ column as no biotinylated proteins were detected by ELISA in the flow although there was high UV absorbance detected in those fractions. During elution, one high peak was detected when the NaCl concentration reached approximately 350 mM (35%) while there was another small peak detected at the elution concentration of 100 mM of NaCl (10%). These peaks were confirmed to be biotinylated proteins as detected by ELISA using streptavidin-HRP antibody. This result showed that the second purification step managed to further separate most of the contaminants from DENV C protein.

To avoid any other contaminants that may have similar charge as biotinylated DENV C protein, eluates corresponding to the high UV absorbance peak after IEX-FPLC were injected into size exclusion chromatography (SEC), Superdex 75 10/300 GL column. It was previously reported that SEC could not be used to estimate the molecular weight of DENV C protein because there were many unspecific interaction between the gel matrix and C protein (Jones *et al.*, 2003). Nevertheless, it is still a good method to further isolate the proteins of interest from other possible residual contaminants based on the molecular weight differences. After SEC, three peaks were observed in the chromatogram (Fig. 5Bi). The first peak was identified to be the biotinylated DENV C protein as the fractions detected with high absorbance in ELISA using streptavidin-HRP antibody coincided with the first peak in the elution profile (Fig. 5Bii). The identity of this highly purified protein was further validated with matrix-assisted laser desorption/ionization-time of flight (MALDI-TOF) mass spectrometry analysis (Supplementary Table S4).

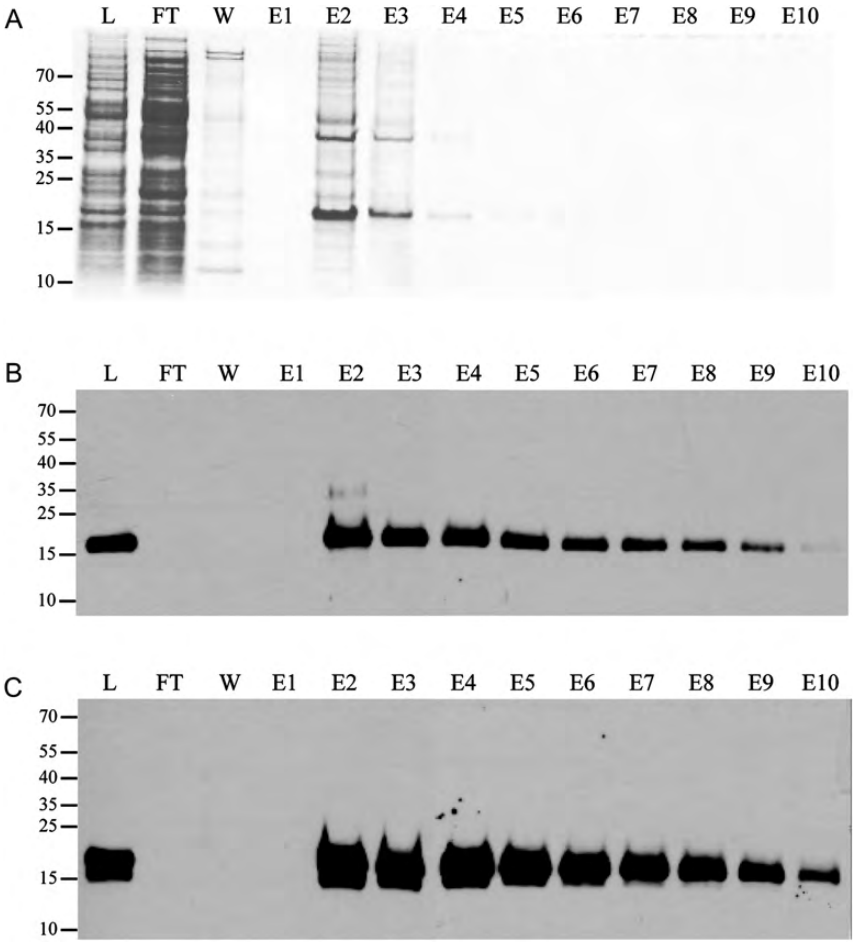

Fig. 4. Purification of biotinylated DENV C protein. IPTG-induced bacteria are lyzed in lysis buffer containing 8-M urea and the lysate (L) is incubated with nickel-charged resin overnight. Next, the resin is packed in a column and the flow through (FT) is kept for SDS-PAGE. 20 mM imidazole is used to wash away the unbound proteins (W) and 500 mM imidazole is used to elute the C protein in ten fractions (E1-10). SDS-PAGE is carried out and stained with Coomassie blue (A). Fraction E2 shows the most intense band but there are also many contaminants in the eluates. Western blot is also performed for the samples using anti-His antibody (B) and streptavidin-HRP secondary antibody (C). C protein-corresponding bands can be observed from fraction E2 until E10. The band intensity is the highest in fraction E2 and decreases until fraction E10. A faint C protein dimer-corresponding band can also be observed in fraction E2 as detected by anti-His antibody.

With this optimized sequential purification protocol, we were able to obtain 0.8–1.0 mg of highly purified biotinylated non-truncated, full-length DENV C protein from 1 l of IPTG-induced bacterial culture repeatedly.

High in vivo *biotinylation efficiency in BL-21 strains*

To compare the biotinylation efficiency of our strategy, the same amount of purified biotinylated DENV C, WNV DIII and MBP proteins were coated on the ELISA plate and streptavidin-HRP antibody was used for detection. Assuming that the coating efficiencies are the same among all three proteins, the absorbance detected via ELISA should be proportional to the number of coated proteins and inversely proportional to the power of two-third of its molecular size. Hence, the larger the protein, the lesser the proteins can be coated on the plate:

$$\text{Absorbance} \propto \frac{\text{Protein Concentration}}{\text{Protein Size}^{2/3}}$$

The molecular weight of MBP is approximately 42.5 kDa while DENV C and WNV DIII proteins have an approximate mass of 15.4 and 14 kDa, respectively. Assuming that one protein only carries one biotin which will bind to one streptavidin-HRP only, the absorbance of MBP should be roughly two times lower than our purified proteins for the same protein concentration. As shown in Fig. 6Ai, the absorbance of purified biotinylated DENV C and WNV DIII proteins indeed showed approximately two times higher the absorbance as compared with commercial biotinylated MBP. The same phenomenon was also observed when the biotinylated proteins were streptavidin captured by streptavidin-magnetic beads and detected via direct ELISA (Fig. 6Aii). The absorbance of eluted biotinylated DENV C protein and WNV DIII protein were two times higher than that of eluted biotinylated MBP. No significant absorbance was detected for unbiotinylated C and DIII proteins.

This result further supported that engineering an additional BAP on a protein could result in site-specific endogenous biotinylation with high efficiency in *Escherichia coli* BL-21 strains, without the need of an extra *in vitro* enzymatic or chemical conjugation step. Our strategy could produce biotinylated proteins that were as good quality as the manufactured biotinylated MBP.

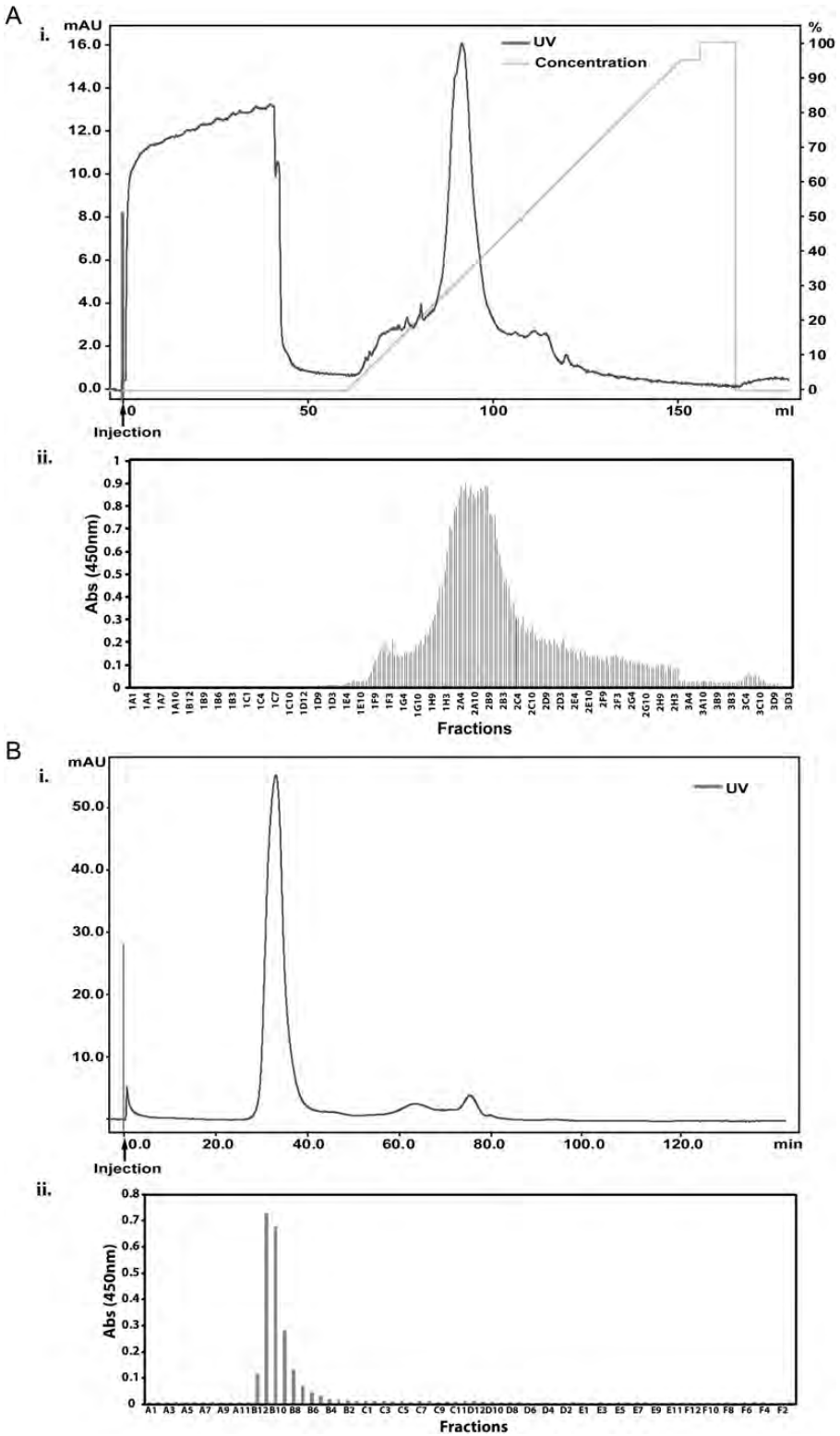

Fig. 5. Sequential purification of DENV C protein using the FPLC system after first round of affinity his-tag purification. Dialyzed and refolded DENV C protein from eluates E2 to E10 are injected into Resource MonoQ ion exchange chromatography column. Bound proteins are eluted out using increasing concentration of sodium chloride until final NaCl concentration of 1 M. One high peak can be observed when the sodium chloride concentration reaches 350 mM [A(i)]. The identity of the peak is confirmed to be C protein as detected by ELISA using streptavidin-HRP antibody [A(ii)]. The eluates from the peak are combined and inserted into size exclusion chromatography for further purification. One high peak is observed in the elution profile [B(i)] and this peak is identified to be C protein as confirmed by ELISA using streptavidin-HRP antibody [B(ii)].

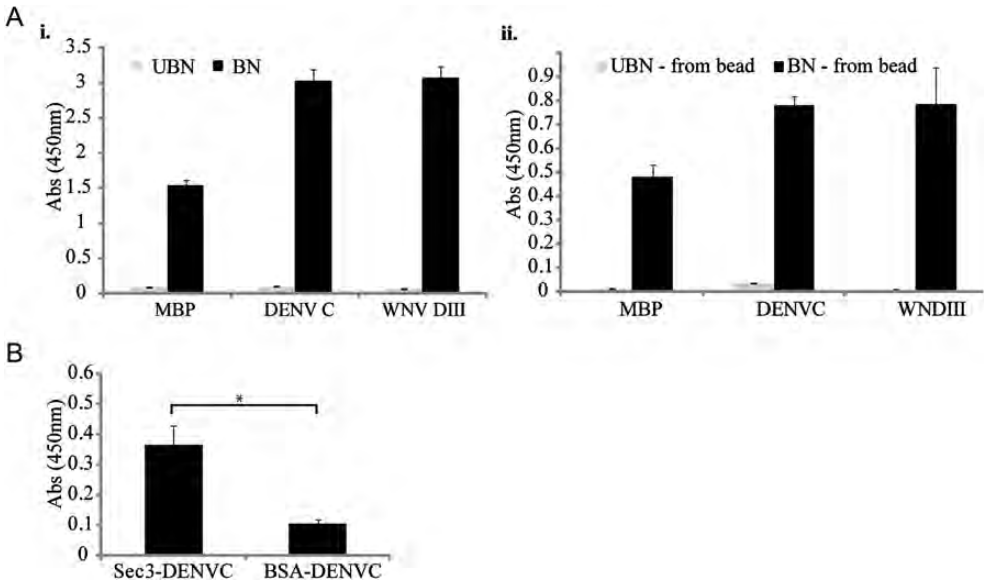

Fig. 6. Biotinylation efficiency and functional analysis of purified full-length DENV C protein. (A) (i) ELISA screening of 30 ng biotinylated (BN) and unbiotinylated (UBN) proteins. All three BN MBP, DENV C and WNV DIII proteins show high absorbance at 450 nm as compared with the protein without BAP. (ii) Biotin-streptavidin binding assay also shows that only BN proteins bind to streptavidin-magnetic beads and are detected in the eluates. (B) The functionality of DENV C protein is examined via a binding assay with Sec3 protein which is known to interact with C protein in host cells. Pure Sec3 protein is coated onto ELISA plate and purified full-length DENV C protein is added into the well for binding. Bovine serum albumin (BSA) is used as negative control. Significant absorbance is detected using streptavidin-horseradish peroxidase antibody in the wells with Sec3 protein coated (Sec3-DENVC) but not with BSA (BSA-DENVC). *$P < 0.05$.

Purified non-truncated, full-length DENV C protein is functional

It is essential to ensure that the purified proteins are functional before they are used for any further studies. According to our recent findings, WNV and DENV C proteins were found to interact with human Sec3 exocyst protein (Bhuvanakantham *et al.*, 2010). Thus, we examined the functionality of the purified DENV C protein by revisiting the interaction between biotinylated DENV C protein and Sec3 protein using ELISA. Pure Sec3 protein was coated overnight on ELISA plate and purified biotinylated DENV C protein was used as the probe. Bound DENV C proteins were detected with streptavidin-HRP antibody. As shown in Fig. 6B, statistically significant absorbance was detected in Sec3 protein-coated wells but not in BSA-coated wells. Thus, our purified DENV C protein did interact with Sec3 protein. This corroborated that our purified biotinylated full-length DENV C protein is functional and can be used for structural and molecular studies.

Discussion

Biotinylation is a popular process in protein engineering to ease detection and purification (Chapman-Smith and Cronan, 1999*a*,*b*; Cull and Schatz, 2000). Biotinylated hemagglutinin, for instance, was generated to develop a subtype-specific serological assay to diagnose influenza A virus in patients' sera (Postel *et al.*, 2011). One of the advantages of using biotinylated protein is that the detection sensitivity of the biotinylated protein is greatly enhanced by the high affinity and specificity between biotin and streptavidin (Bayer and Wilchek, 1990*a*,*b*). This advantage is exploited for techniques such as co-immunoprecipitation or library screening of interaction proteome (Markham *et al.* 2007; He *et al.*, 2009; Moreland *et al.*, 2010). Not only that, site-specific biotinylation was also developed as a means for molecular labeling and imaging (Howarth and Ting, 2008; Sueda *et al.*, 2011). As such, biotinylated DENV C protein is useful for various cellular, molecular, and imaging experiments because of the high detection limit while the function of the protein is still well preserved.

There are various approaches to biotinylate a protein, either chemically or enzymatically (Cull and Schatz, 2000). Various commercial kits are available in the market for chemical biotinylation by conjugating biotin molecules on proteins or antibodies that contain primary amines. However, chemical biotinylation may lead to non-specific and non-homogenous incorporation of biotin which might result in possible loss of activity of the protein (Bayer and Wilchek, 1990*a*,*b*). Moreover, another step of removing the excess biotin reagent will increase the chance of losing more proteins. To produce biotinylated proteins, we opted for site-specific biotinylation by engineering a biotin acceptor signal peptide (BAP) in the upstream of our proteins. To attach a biotin molecule onto BAP either *in vivo* or *in vitro*, bacterial biotin ligase BirA is required (Chapman-Smith and Cronan, 1999*a*,*b*; Cull and Schatz, 2000; Tan *et al.*, 2004; Yang *et al.*, 2004). Instead of performing this biotinylation step *in vitro*, we found that biotinylation of the BAP-containing proteins occurred endogenously in *Escherichia coli* BL-21 strains with high efficiency. As such, other proteins that require site-specific biotinylation may be produced easily by just simple OE-PCR and expression in *Escherichia coli* BL-21 strains without the need of an additional *in vitro* biotinylation step.

The purification of non-truncated, full-length DENV C protein was indeed challenging. Unlike DIII protein (Tan *et al.*, 2010), one single purification step was simply not adequate to produce pure DENV C protein. The presence of rare codons in the C protein sequence necessitates unique expression competent strain for its optimal protein expression.

Due to the hydrophobic C-terminus, aggregation easily occurred and most of the expressed proteins were trapped in the inclusion bodies. As such, we had to use 8 M urea to denature the proteins and perform affinity chromatography under denaturing condition. We also managed to solve the aggregation problem during dialysis and refolding by using non-ionic detergent. This is indeed critical in making this protein purification a success. To obtain highly purified DENV C protein, two more purification steps were included in our protocol, namely IEX and SEC. This sequential purification strategy can produce approximately 1 mg of purified full-length DENV C protein from 1 l of bacterial culture. This optimized sequential purification strategy may be useful for other proteins that have the similar properties.

This purified non-truncated, full-length DENV C protein is useful for various molecular and structural studies. For instance, it can be used to study the interaction of NS2B–NS3 serine proteinase and C protein. In order to produce mature C protein for encapsidation and assembly, full-length C protein has to be cleaved by NS2B–NS3 protein complex. Thus, it is crucial to identify the binding sites of NS2B–NS3 complex to full-length C protein, which is still unknown. It will in turn lead to the development of novel anti-viral drugs targeting the assembly of virus particles. Besides, it is also interesting to examine whether the cleaved C-terminus plays any unidentified role in the pathogenesis. The crystal structure of DENV NS2B–NS3 protein complex has been resolved (Erbel *et al.*, 2006). However, the crystal structure of full-length DENV C protein is still not yet available, although the NMR structure of partial DENV C protein was obtained (Ma *et al.*, 2004). We are now taking up the challenge to resolve the 3D structure of full-length DENV C protein using our purified protein.

Ma *et al.* (2004) proposed a model for the interaction between C protein and its viral genome using the partial DENV C protein. However, to date, this model is not validated and the exact mechanism of encapsidation is still unclear. Investigation of how DENV C protein interacts with its RNA and oligomerizes into nucleocapsid during maturation is vital for better understanding of the pathogenesis. Recent publications also demonstrated that N-terminus of DENV C protein was antigenic in mice study and the first 18 amino acid residues were involved in the virus assembly during maturation (Puttikhunt *et al.*, 2009; Samsa *et al.*, 2012). As a result, our purified non-truncated DENV C protein is absolutely desirable for delineating the whole process of encapsidation and virus assembly.

Another difficulty of studying DENV C protein is that anti-C antibody is yet to be available commercially. Most of the laboratories need to raise this antibody on their own before any further downstream experiments (Wang *et al.*, 2002; Puttikhunt *et al.*, 2009). Hence, pure full-length DENV C protein can be obtained simply by enterokinase cleavage and subsequently used to raise antibody in mice or rabbits for laboratory research usage and diagnostic tool. Both full-length DENV C protein and anti-DENV C antibody will be of commercial values.

In conclusion, we have developed an optimized protocol to engineer, express and purify the first biotinylated, full-length DENV C protein. This purified protein is useful for various molecular studies to further understand the underlying mechanism of C protein in pathogenesis. Only by stitching all these missing pieces of the puzzle together, novel antiviral strategies can be rationally designed.

Supplementary data

Supplementary data are available at *PEDS* online.

Funding

This work was supported by Exploit Technologies Pte Ltd, A*STAR Flagship grant (R182-000-164-592).

References

Amberg,S.M. and Rice,C.M. (1999) *J. Virol.*, **73**, 8083–8094.
Bayer,E.A. and Wilchek,M. (1990a) *Methods Enzymol.*, **184**, 174–187.
Bayer,E.A. and Wilchek,M. (1990b) *Methods Enzymol.*, **184**, 138–160.
Bhuvanakantham,R., Chong,M.K. and Ng,M.L. (2009) *Biochem. Bioph. Res. Co.*, **389**, 63–69.
Bhuvanakantham,R., Li,J., Tan,T.T.T. and Ng,M.L. (2010) *Cell. Microbiol.*, **12**, 453–472.
Chapman-Smith,A. and Cronan,J.E., Jr (1999a) *Trends Biochem. Sci.*, **24**, 359–363.
Chapman-Smith,A. and Cronan,J.E., Jr (1999b) *Biomol. Eng.*, **16**, 119–125.
Cull,M.G. and Schatz,P.J. (2000) *Methods Enzymol.*, **326**, 430–440.
de Boer,E., Rodriguez,P., Bonte,E., Krijgsveld,J., Katsantoni,E., Heck,A., Grosveld,F. and Strouboulis,J. (2003) *Proc Natl Acad Sci U S A*, **100**, 7480–7485.
Erbel,P., Schiering,N., D'Arcy,A., *et al.* (2006) *Nat. Struct. Mol. Biol.*, **13**, 372–373.
Gubler,D.J. (2002) *Arch. Med. Res.*, **33**, 330–342.
Hase,T., Summers,P.L., Eckels,K.H. and Baze,W.B. (1987) *Arch. Virol.*, **92**, 273–291.
He,Y.F., Bao,H.M., Xiao,X.F., Zuo,S., Du,R.Y., Tang,S.W., Yang,P.Y. and Chen,X. (2009) *Proteomics*, **9**, 5414–5424.
Howarth,M. and Ting,A.Y. (2008) *Nat. Protoc.*, **3**, 534–545.
Jones,C.T., Ma,L.X., Burgner,J.W., Groesch,T.D., Post,C.B. and Kuhn,R.J. (2003) *J. Virol.*, **77**, 7143–7149.
Krupakar,P., Ngo,A.M.L. and Ng,M.L. (2012) In Miguel,B. and Aguirre,V. (eds), *Protein Purification*. New York: Nova Science. pp. 147–170.
Ma,L., Jones,C.T., Groesch,T.D., Kuhn,R.J. and Post,C.B. (2004) *Proc Natl Acad Sci U S A*, **101**, 3414–3419.
Markham,K., Bai,Y. and Schmitt-Ulms,G. (2007) *Anal. Bioanal. Chem.*, **389**, 461–473.
Markoff,L. (1989) *J. Virol.*, **63**, 3345–3352.
Moreland,N.J., Tay,M.Y., Lim,E., Paradkar,P.N., Doan,D.N., Yau,Y.H., Geifman Shochat,S. and Vasudevan,S.G. (2010) *PLoS Negl. Trop. Dis.*, **4**, e881.
Postel,A., Letzel,T., Muller,F., Ehricht,R., Pourquier,P., Dauber,M., Grund,C., Beer,M. and Harder,T.C. (2011) *Anal. Biochem.*, **411**, 22–31.
Puttikhunt,C., Ong-Ajchaowlerd,P., Prommool,T., Sangiambut,S., Netsawang,J., Limjindaporn,T., Malasit,P. and Kasinrerk,W. (2009) *Arch. Virol.*, **154**, 1211–1221.
Qi,Y. and Katagiri,F. (2011) *Methods Mol. Biol.*, **712**, 21–30.
Samsa,M.M., Mondotte,J.A., Caramelo,J.J. and Gamarnik,A.V. (2012) *J. Virol.*, **86**, 1046–1058.
Sueda,S., Yoneda,S. and Hayashi,H. (2011) *Chembiochem*, **12**, 1367–1375.
Tadano,M., Makino,Y., Fukunaga,T., Okuno,Y. and Fukai,K. (1989) *J. Gen. Virol.*, **70** (Pt 6), 1409–1415.
Tan,L.C., Chua,A.J., Goh,L.S., Pua,S.M., Cheong,Y.K. and Ng,M.L. (2010) *Protein Expr. Purif.*, **74**, 129–137.
Tan,L.P., Lue,R.Y., Chen,G.Y. and Yao,S.Q. (2004) *Bioorg. Med. Chem. Lett.*, **14**, 6067–6070.
Tolaymat,N. and Mock,D.M. (1989) *J. Nutr.*, **119**, 1357–1360.
Wang,S.H., Syu,W.J., Huang,K.J., Lei,H.Y., Yao,C.W., King,C.C. and Hu,S.T. (2002) *J. Gen. Virol.*, **83**, 3093–3102.
Yang,J., Jaramillo,A., Shi,R., Kwok,W.W. and Mohanakumar,T. (2004) *Hum. Immunol.*, **65**, 692–699.
Yang,M.R., Lee,S.R., Oh,W., *et al.* (2008) *Cell Microbiol.*, **10**, 165–176.
Zhang,W., Chipman,P.R., Corver,J., *et al.* (2003) *Nat. Struct. Biol.*, **10**, 907–912.

Supplementary Figures and Tables

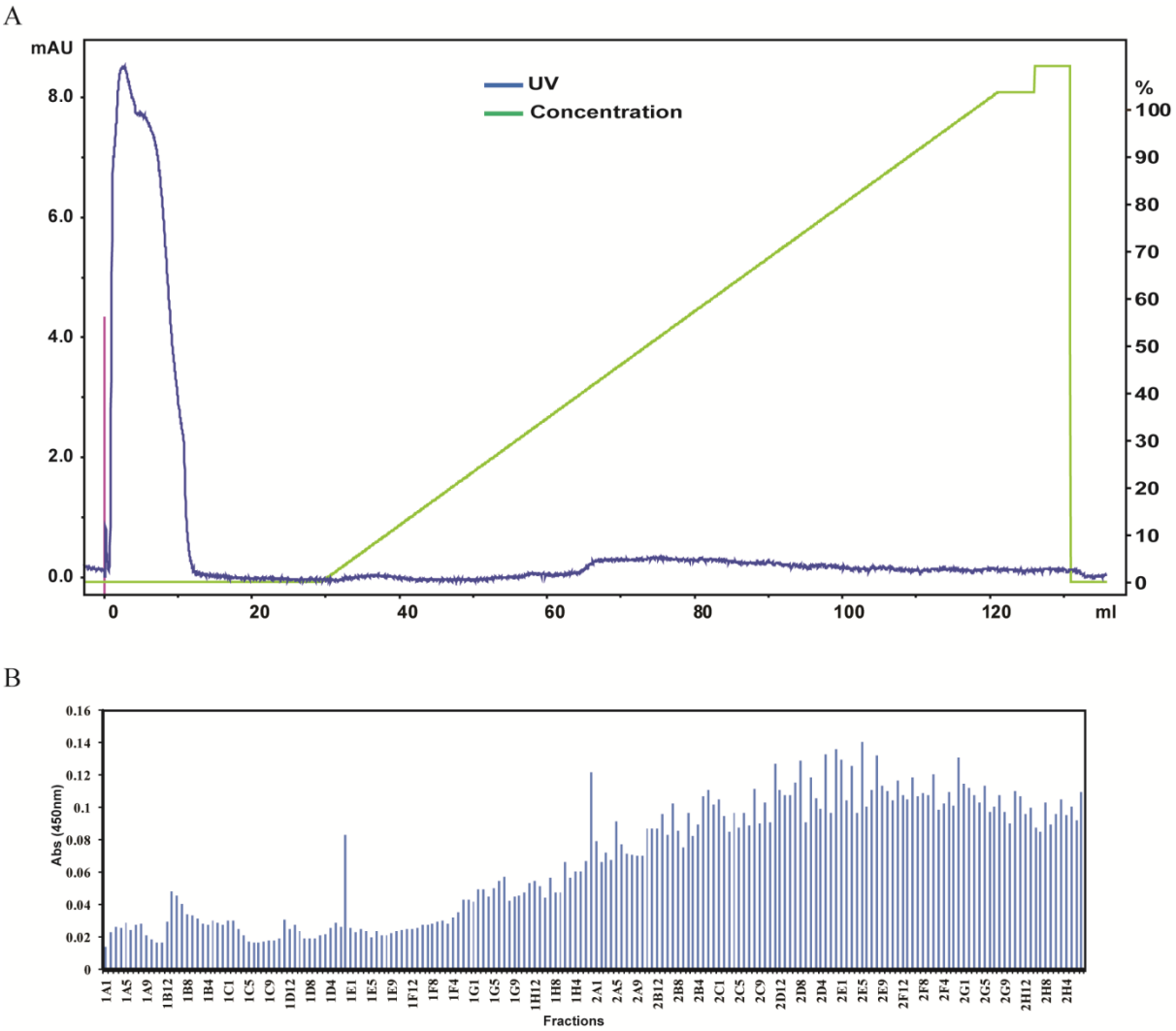

Suppl. Fig. 1. Cation exchange purification of DENV C protein using Resource MonoS column. (**A**) Dialysed and refolded DENV C proteins after affinity chromatography are injected into Resource MonoS ion exchange chromatography column. Bound proteins are eluted out using increasing concentration of sodium chloride until final concentration of 1 M. However, there is no obvious peak during the elution steps except a small increase of UV absorbance when the concentration of NaCl reaches 400 mM (40 %). (**B**) The presence of C protein is detected by ELISA using streptavidin-HRP antibody. An increasing amount of biotinylated DENV C protein is detected during elution and it reaches plateau at approximately 70 % of NaCl (700 mM NaCl).

Suppl. Table 1: DNA and protein sequences of full-length DENV C protein.

Constructs	DNA and Protein Sequences
Bacterial-Biotin-DENVC	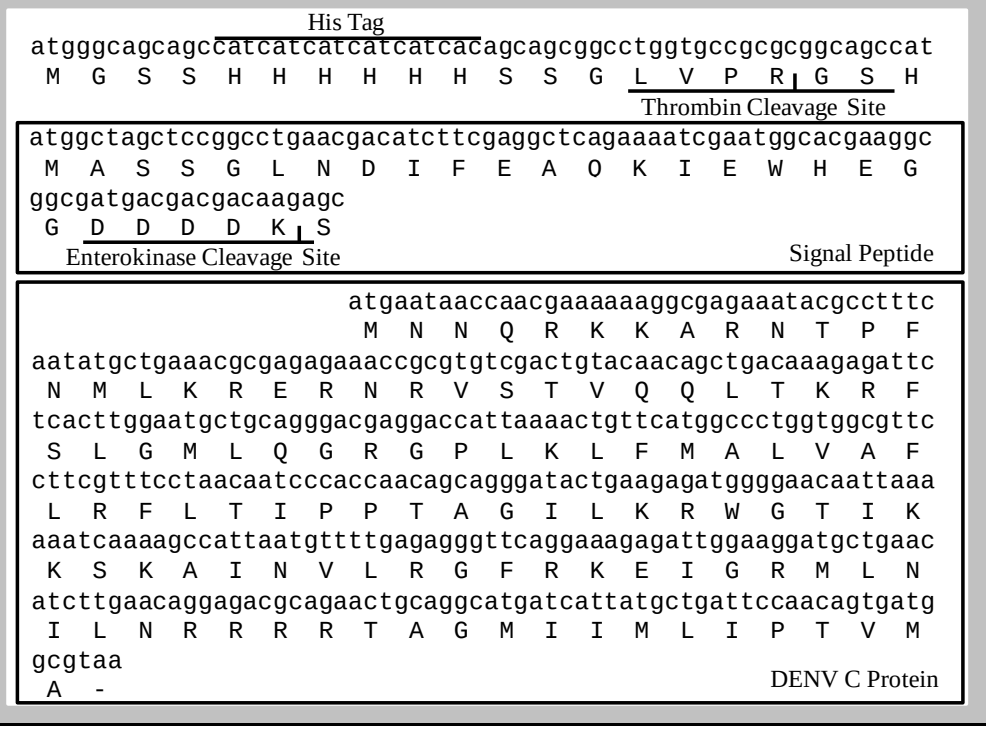

Suppl. Table 2. Rare codon analysis of full-length DENV C protein. Rare codons are in **BOLD** and underlined.

Rare Codon	Number
Arg (AGG, AGA, CGA)	12
Leu (CTA)	1
Ile (ATA)	1
Pro (CCC)	0

Full-length DENV C DNA sequence:

atg aat aac caa **cga** aaa aag gcg **aga** aat acg cct ttc aat atg
ctg aaa cgc gag **aga** aac cgc gtg tcg act gta caa cag ctg aca
aag **aga** ttc tca ctt gga atg ctg cag gga **cga** gga cca tta aaa
ctg ttc atg gcc ctg gtg gcg ttc ctt cgt ttc **cta** aca atc cca
cca aca gca ggg **ata** ctg aag **aga** tgg gga aca att aaa aaa tca
aaa gcc att aat gtt ttg **aga** ggg ttc **agg** aaa gag att gga **agg**
atg ctg aac atc ttg aac **agg** **aga** cgc **aga** act gca ggc atg atc
att atg ctg att cca aca gtg atg gcg taa

Suppl. Table 3: Competent cells identified through BLAST analysis of BirA gene.

Competent Cells	Accession Number	Features
BL-21 (DE3)	AM946981	Bifunctional biotin-[acetyl-CoA-carboxylase] ligase and transcriptional repressor
BL-21-CodonPlus	CP001665	Bifunctional BirA, biotin operon repressor/ biotin--acetyl-CoA-carboxylase ligase

Suppl. Table 4. MALDI-TOF mass spectrometry analysis of purified DENV C protein.

Identity	Fragment	Peptide Sequence	Calculated (Da)	Measure (Da)	Error (Da)
Dengue virus 2 core protein	81-89	FSLGMLQGR	1007.52	1007.49	-0.03
	104-116	FLTIPPTAGILKR	1425.87	1425.8	-0.07

IPOS
INTELLECTUAL PROPERTY
OFFICE OF SINGAPORE

Intellectual Property Office of Singapore
51 Bras Basah Road #04-01
Manulife Centre Singapore 189554
Tel: (65) 63398616 (General) Fax: (65) 63390252
(Patents) Fax: (65) 63399230
http://www.ipos.gov.sg

RF 101

In Reply Please Quote Our Reference

Your Ref	:	AFSTR.0216/EKC/MUZ
Our Ref	:	2012086021/121130/TMFMK/0966
Date	:	30/11/2012
Writer's Direct Line	:	63302749

Received	Date
P.O. Box	
Courier	3/12/12

ATMD BIRD & BIRD LLP
P.O. BOX 0643
RAFFLES CITY POST OFFICE
SINGAPORE 911722

Dear Sir/Madam,

Singapore Patent Application No.: 201208602-1
Title of invention: BIOTINYLATED PROTEIN
Applicant(s): NATIONAL UNIVERSITY OF SINGAPORE (SG)

ALLOCATION OF DATE OF FILING

Thank you for the documents that you have submitted in relation to your application for the grant of a patent which was received on 22/11/2012.

2. We are pleased to inform you that the application has been accorded a Date of Filing 22/11/2012.

3. The application number allocated to the application includes, at its end, a check digit. The full application number, including the check digit, should be quoted in all correspondences concerning proceedings in respect of the application up to the grant of the patent. When the application is published under section [27] of the Patents Act (Cap. 221), it will be accorded a seven-digit serial number. This number should be used only when seeking to identify patents after grant and to make enquiries concerning entries in the register.

4. If you have any further queries, please contact me.

Yours faithfully,

Fatehah Muhammad Khairuddin
for REGISTRAR OF PATENTS
INTELLECTUAL PROPERTY OFFICE OF SINGAPORE
Encl.

ANNEX

INFORMATION FOR APPLICANTS FOR NATIONAL PATENT APPLICATIONS (NON EXHAUSTIVE)

Date Of This Notification/Invitation: 30/11/2012	Application No.: 201208602-1

PAYMENT OF FILING FEES – RULE 19(2)

Where the filing fee is not paid within the same day of filing the application, the fee shall be paid within **1 month** from that day. Failure to pay the filing fee within the **1 month** period shall result in the application being treated as having been abandoned.

FILING OF PATENT CLAIMS – RULE 26(5)

Where claims have not been filed within the same day of filing the application, the application shall be treated as having been abandoned **unless** one or more claims are filed within:

(i) where there is no declared priority date, **12 months** from the date of filing of the application;

(ii) where there is a declared priority date, **12 months** from the declared priority date or **2 months** from the date of filing of the application, whichever expires later; or

(iii) where a new application has been filed under section 20 (3), 26 (11) or 47 (4), **2 months** from the date the new application was filed.

INVENTORSHIP – RULE 18

Where an applicant is not an inventor of the invention, a statement identifying the inventor(s) and indicating the derivation of the right of the applicant to be granted a patent on the invention must be filed on Patents Form 8 within **16 months** from the declared priority date or where there is no declared priority date, the date of filing of the application.

PRIORITY CLAIMS – RULE 9B(1)

Where a declaration claiming priority has been made at the time of filing the application, the applicant shall furnish to the Registry within **16 months** from the declared priority date the application or file number of each priority application specified in the declaration.

FILING A PATENT APPLICATION OUTSIDE SINGAPORE

- **National Security Check – Section 34**

If the Singapore application is the applicant's first application for the invention, an application for the same invention is **not** to be filed outside Singapore without first getting written authority from the Registry, unless **2 months** have lapsed since the filing of the Singapore application and no directions by the Registry have been given under Section 33.

- **Claiming priority on your Singapore application**

In general, if the applicant wishes to file a patent application outside Singapore claiming priority from the Singapore application, the overseas application would have to be filed within **12 months** from the date of filing of the Singapore application.

GENERAL

For details on how to proceed with your application, references should be made to the provisions found in the Patents Act and Rules.